Changes in rock lobster, demersal fish, and sessile benthic organisms in the Tasman Fracture Marine Park: comparisons between 2015 and 2021

Nicholas Perkins, Jacquomo Monk, Rachel Wong, Shenae Willis, Ashlee Bastiaansen and Neville Barrett

Institute for Marine and Antarctic Studies, University of Tasmania

UNIVERSITY of TASMANIA | IMAS INSTITUTE FOR MARINE & ANTARCTIC STUDIES

Enquiries should be addressed to:

Associate Professor Neville Barrett, Institute for Marine and Antarctic Studies, University of Tasmania.
Email: neville.barrett@utas.edu.au

Dr Nicholas Perkins, Institute for Marine and Antarctic Studies, University of Tasmania.
Email: nicholas.perkins@utas.edu.au

Dr Jacquomo Monk, Institute for Marine and Antarctic Studies, University of Tasmania.
Email: jacquomo.monk@utas.edu.au

Preferred Citation

Perkins N, Monk J, Wong R, Willis S, Bastiaansen A, Barrett N (2022). *Changes in rock lobster, demersal fish, and sessile benthic organisms in the Tasman Fracture Marine Park: comparisons between 2015 and 2021.* Report to the Parks Australia. Institute for Marine and Antarctic Studies, University of Tasmania. 141p.

Copyright

Acknowledgement

This work was undertaken for Parks Australia. Dr Cath Samson, Natalie Bool and Daniel Murphy from Parks Australia are thanked for their guidance. The IMOS AUV facility and Understand Marine Imagery sub-facility are thanked for deployment of the AUV '*Sirius*' and access to, and annotation of, resultant imagery. Both facilities are supported by Australia's Integrated Marine Observing System (IMOS) – IMOS is enabled by the National Collaborative Research Infrastructure Strategy (NCRIS). The skippers and crew of the vessels Chieftain and Odalisque.

Important Disclaimer

Contents

List of Figures

List of Tables

Executive Summary

The Tasman Fracture Marine Park (TFMP) is the southernmost Australian Marine Park that includes a no-take national park zone (NPZ). It is the only park within the South-east Marine Park Network (South-east Network) that has a NPZ on the continental shelf -a zone which prohibits all fishing activities. In 2014/15 initial baselines for rocky reef demersal fishes, rock lobster and sessile benthic invertebrates were established within the NPZ and contrasted with those observed in similar habitat in adjacent areas open to fishing (Monk et al., 2016). In the current study, we repeat these surveys to obtain an indication of temporal variability in these communities and assess the extent of any protection-related changes within the NPZ relative to adjacent fished reference area. This new survey involved a slight alteration to the sample design to improve the balance of reefs sampled at comparable depths inside/outside the NPZ on the basis of recently acquired additional mapping data.

Rock lobster

Overall, there was a significant rebuilding of the abundance and size structure of rock lobster both inside and outside the NPZ in the survey area over the period between the 2014 and 2021 surveys. This may reflect both successful recruitment events, perhaps prior to 2014, and the effect of a marked reduction in fishing pressure in response to quota reductions, changing market demand, and recent bans in importation of lobsters to China. Hence, while average size and abundance of lobsters has continued to increase in the NPZ between 2014 and 2021, and on a habitat-by-habitat basis is greater in the NPZ relative to adjacent fished reference areas, the difference is not as marked as would have been expected under historical fishing pressures. These findings therefore have relevance to both parks and fisheries management by documenting the changing nature of fishing pressure in this offshore region. While overall catch numbers between years may also be related to variation in rock lobster "catchability" between sampling events, the large changes in size structure, particularly larger, legal-sized individuals in fished reference areas, is clear evidence of changing fishing pressure and regional stock rebuilding.

Depth was an important predictor of lobster abundance, with a strong trend of lower abundance in deeper areas of the NPZ, particularly on reef below 100 m. Model estimates show an approximate three-fold increase in abundance of rock lobster in the shallowest depths surveyed (60-70 m) compared to the deepest depths (140-150 m). As the distribution of reef within the NPZ is heavily skewed towards depths below 100 m, catch rates in the zone are typically well below that found in adjacent areas where the fishery operates, as deep reef (below 100 m) is rare outside the NPZ.

Habitat complexity is another known driver of species distributions and is particularly important for rock lobsters, which rely on refuge provided by complex habitat to avoid predation. Rugosity, a proxy for habitat complexity derived from multibeam mapping, was shown to be an effective (positive) predictor of abundance, average male size and the sex-ratio (negatively correlated with the proportion of males) in this region.

As predicted based on the extent of protection, bycatch of species likely to be impacted by fishing operations were higher in the NPZ than adjacent fished reference sites. Conger eels (*Conger Verreauxi*) were around twice as abundant inside the NPZ compared to outside, and roughly doubled in abundance between 2014 and 2021, both inside and outside the NPZ. As conger eels were often used by fishermen for bait, it is likely that the recovering abundances of conger eels are an indicator of both recovery from previous fishing pressure through protection (inside the NPZ) and the recent reduction in offshore fishing pressure in areas still open to fishing. For bycatch species, overall levels

during both the 2014 and 2021 surveys were relatively low in the region compared to elsewhere in South-eastern Australia (Leon et al. 2019). Presumably this may be at least partly related to the composition and abundance of species recorded here being driven by the deeper depth distribution of the reefs surveyed compared to those predominantly targeted in the rock lobster fishery in Tasmanian waters.

Demersal fishes

The 2021 fish survey of shelf reefs in the TFMP and adjacent fished reference areas has provided the first time-step in an ongoing monitoring program, following an initial baseline survey in 2015. At this point in time there are no marked differences in reef-associated fish assemblages between fished and protected locations, either at the broad assemblage level or for particular targeted species such as jackass morwong or striped trumpeter. It is likely that these patterns are the result of both the park being located in a remote region away from most recreational fishing pressures, and a low (and reduced) level of overall commercial fishing effort in this offshore location in recent years. The significant increase in rock lobster numbers and sizes outside the park between 2015 and 2021 recorded in our associated rock lobster study, suggests a major reduction in fishing effort occurred over that period in response to substantial market and quota changes. As rock lobster fishers also constitute the main line-fishing effort in this region (undertaken jointly while lobster fishing), we can anticipate that there would be a corresponding increase in the abundance of target and bycatch species over this time-period, and indeed, this pattern was seen here. While these trends in fishing effort can mask traditional analysis of MPA "effectiveness", our overall results suggest a general trend between the 2015 and 2021 surveys towards increased abundance and size of target and bycatch species in the NPZ, in line with expectations of NPZ performance. Overall, the results show the benefit of establishing a marine park in remote areas as there is currently little in the way of obvious pressure on park boundaries such as poaching and other enforcement issues.

The southern Tasmanian/Australian location of this park means that it is likely the last cool water refuge for many shelf-associated species with cool-water affinity, and as such, provides a vital climate refuge for climate-threatened species. A marked highlight of the survey was the sighting of a pink handfish (*Brachiopsilus dianthus*) in BRUV (Baited Remote Underwater Video) footage from reef habitat in approximately 120 m. Subsequent examination of AUV (Autonomous Underwater Vehicle)-derived imagery from the benthic cover survey has discovered additional pink handfish as well as several likely confirmed sightings of Ziebell's handfish (*Brachiopsilus ziebelli*), both being reef-associated listed threatened species of significant conservation interest. These sightings markedly extend the known depth distribution of both of these species, from 20 m to 140 m, as well as extending their known spatial extent, from localised inshore SE Tasmania to the offshore SW coast. In addition, a number of other handfish, potentially Australian handfish (*Brachionichthys australis*), a soft-sediment associated species, and warty handfish (*Thymichthys verrucosus*), have been found at depths of 120-140 m, and overall, at least 70 handfish (many of insufficient resolution to identify to species) have been seen in AUV-derived imagery examined to date with more imagery yet to be examined. A future dedicated survey of the habitats within the park where handfish have been recorded is recommended to determine population size and status of the listed handfish species, as well as provide improved resolution imagery (via use of ROVs) for species identification, coupled with eDNA sampling to further confirm identification.

This survey also recorded the presence of the Collar seahorse (*Hippocampus jugumus*) in the park, the first sighting of this species in Australian continental waters, the only recorded sighting of a live individual and only the third sighting of this species ever. The remaining records are specimens

collected from Lord Howe Island, and the Poor Knights Islands in New Zealand. While this widespread distribution and wider thermal range indicates that this species may not be as vulnerable to warming as the handfish, its extreme rarity means that it is an almost automatic classification as a rare and endangered species on the basis of its rarity alone. Hence it ideally should be treated as such until a formal listing is prepared.

Seabed benthos

Ongoing surveys using autonomous underwater vehicles (AUVs) across the South-east AMP Network are providing valuable information about the spatial distribution of the kinds of benthic (seabed) plants and sessile animals (sponges, bryozoans, corals etc) present. These can often be identified to morphospecies (the finest level able to separate groups by imagery alone), and annotation at that level has allowed us to examine the temporal changes that have occurred in these groups through time (2015-21), as well as the spatial distribution of these with depth and location throughout the TFMP. This information is crucial to underpinning effective long-term monitoring of mesophotic to rariphotic habitats and the biota within them across the region. Understanding where morphospecies occur, their natural variability and whether they may have responded to pressures helps with the selection of indicators for ongoing monitoring. The 2021 survey provided extensive coverage of the spatial extent and depth coverage of reef systems within the TFMP, allowing the distribution of key benthic biota to be reliably quantified. Like similar surveys in other shelf reef systems in the region, no single morphospecies was present at greater than 2% average coverage on reefs within the park, with the vast majority having much lower overall coverage, thus presenting a challenge around the extent of future sampling required for ongoing monitoring. However, at the community level, the benthic assemblage present in the TFMP was markedly different that that observed in other parks sampled within the SE AMP network, confirming the bioregional significance of the TFMP. Currently, only one repeat survey has been conducted in the TFMP (and was restricted to comparison only with a small set of locations able to be sampled in the truncated 2015 survey), thus, the monitoring component of this study is somewhat restricted and in early stages of our understanding of the drivers of variability in benthic cover species in mesophotic to rariphotic depths. However, surveys to date have revealed that these depths, as well as being biodiverse with rare and unique morphospecies, are more dynamic than previously assumed. Trends observed between 2015 and 2021 show a marked decline in a number of iconic octocoral morphospecies in the TFMP. Whether this is the result of shorter-term natural variation, or a longer-term trajectory should be the focus of future survey work given that the abundance of soft corals in the TFMP represent a key cool-water fauna that differentiates the shelf fauna in this park from that found elsewhere in the SE AMP network.

1 General introduction

The Tasman Fracture Marine Park (TFMP) is the southernmost Australian Marine Park (AMP) that includes continental shelf habitats. Established as part of the South-east Marine Parks Network (South-east Network), the first phase of AMP proclamation, the TFMP has been established for over 15 years. The TFMP is the only park in the South-east Network that includes a national park zone (i.e., fully protected from fishing activity) on the continental shelf. In 2015/16 initial baselines for demersal fishes, rock lobster and sessile invertebrates were established (Monk et al. 2016). The recommended re-survey period to build a time series for measuring the condition and trend of park values to inform management effectiveness evaluation was 5 years (Monk et al. 2016). It is expected that the results of this work will inform the review of the management plan for the South-east Network which is currently underway.

The current study aimed to repeat survey previously sampled sites for rock lobster and demersal fishes, as well as repeat and extend the AUV coverage for characterising the seabed benthic community. A slight alteration to the sample design was done to improve the balance in comparable depths outside the national park zone. This was in response to a key recommendation from the 2014/15 work for the need to find additional reef in comparable depths outside the national park zone. This reef was identified using the additional multibeam sonar mapping to the north-west of the multiple-use zone by IMAS and CSIRO in 2019 (https://marlin.csiro.au/geonetwork/srv/eng/catalog.search#/metadata/17a94733-becb-493e-849c-945dfcc80e1e).

Objectives for this study were:

1. Contrast the rock lobster population structure between the AMP and adjacent fished reference areas based on potting surveys and assess their change since 2014.

2. Contrast demersal fish population structure between the AMP and adjacent fished reference areas based on baited remote underwater stereo video stations (stereo BRUVS) and assess their change since 2015.

3. Improve the spatial and temporal understanding of seabed benthic community diversity and cover based on imagery obtained using Australia's Integrated Marine Observing System (IMOS) autonomous underwater vehicle (AUV) '*Sirius*'. This included collecting additional new transects not achieved in 2015 due to poor weather to provide better spatial coverage across reef habitats within TFMP.

2 Population trends in rock lobster

Following establishment of the TFMP in 2007, habitats in the Marine National Park Zone (NPZ) where fishing is prohibited had the potential to demonstrate a range of changes in the abundance of commercially targeted species once fishing ceased, including southern rock lobsters (*Jasus edwardsii*). An initial survey of rock lobster populations in the NPZ and at adjacent fished reference areas was undertaken in 2014, approximately 7 years after the park was established. Here, we further examine the trajectory of changes that have occurred in the abundance, size structure and population demographics of rock lobsters between the initial survey in 2014 and the latest survey in 2021. This allowed estimation of the extent of changes in the rock lobster population in the NPZ following initial protection in 2007, as well as providing insights into the trajectory of rock lobster populations in the adjacent fished areas.

Analysis of the 2014 survey data (Monk et al. 2016) showed that depth was an important factor for the abundance of rock lobster in the survey area, with markedly higher abundance on shallower reefs in the park (70 m) vs the deeper reef margins (at around 140 m). In the 2014 study, the depth distribution versus surface area of available reef in the reserve (based on extensive multibeam mapping) led to a higher density of sampling of deeper reef in the reserve compared to adjacent fished reference areas, as reef below 100 m depth was exceedingly rare outside of the park. To rectify this depth imbalance in the experimental design, additional multibeam mapping was undertaken in the vicinity of the TFMP to define the location of suitable reef to sample in the 100 - 140 m depth range for incorporation into subsequent spatially and depth-balanced sampling. The additional deeper reefs utilised here were immediately to the west of the NPZ, allowing for close spatial comparability and simplified logistics of deployment, with a total of 20 pots deployed on this section of reef. These pots were redeployed from the 20 shallowest locations as SE Cape and South Cape (Fig. 1) that were typically shallower than reef found in the TFMP and therefore removed from the 2021 survey. The remaining 180 pots of the 200 total were deployed at the same locations as the initial survey (Figure 1), with a total of 100 pots inside the marine park and 100 pots outside in the fished reference area. The initial 180 pots were located on mapped reef habitat using Generalised Random Tessellated Sampling outlined in Monk et al. (2016), with the additional 20 new pot locations being selected using Balanced Adaptive Sampling outlined in Foster et al. (2020), targeting reefs between 100-140 m to add extra replication in a depth class previously unsampled in the fished reference area in the 2015 survey.

All pots deployed were research pots, with no escape gaps. Therefore, the size classes caught are unlikely to exactly represent what is caught in commercial pots, with an over-representation of sub-legal-size classes. Also, bycatch composition is likely to reflect higher catch rates of smaller individuals and smaller species than would be caught in the commercial fishery where escape gaps would allow some of these smaller bycatch species to escape.

The 2014 survey was conducted between 29th November and the 3$^{rd\ of}$ December 2014, and the 2021 survey between the 18th to 21st March 2021. While ideally, we would have matched survey months between the 2014 and 2021 surveys, delays in contracting, vessel, and pot availability, as well as weather suitability resulted in deferral until the first window of opportunity. All catch data has been lodged with IMAS managed CrayBase database, with raw data available upon request.

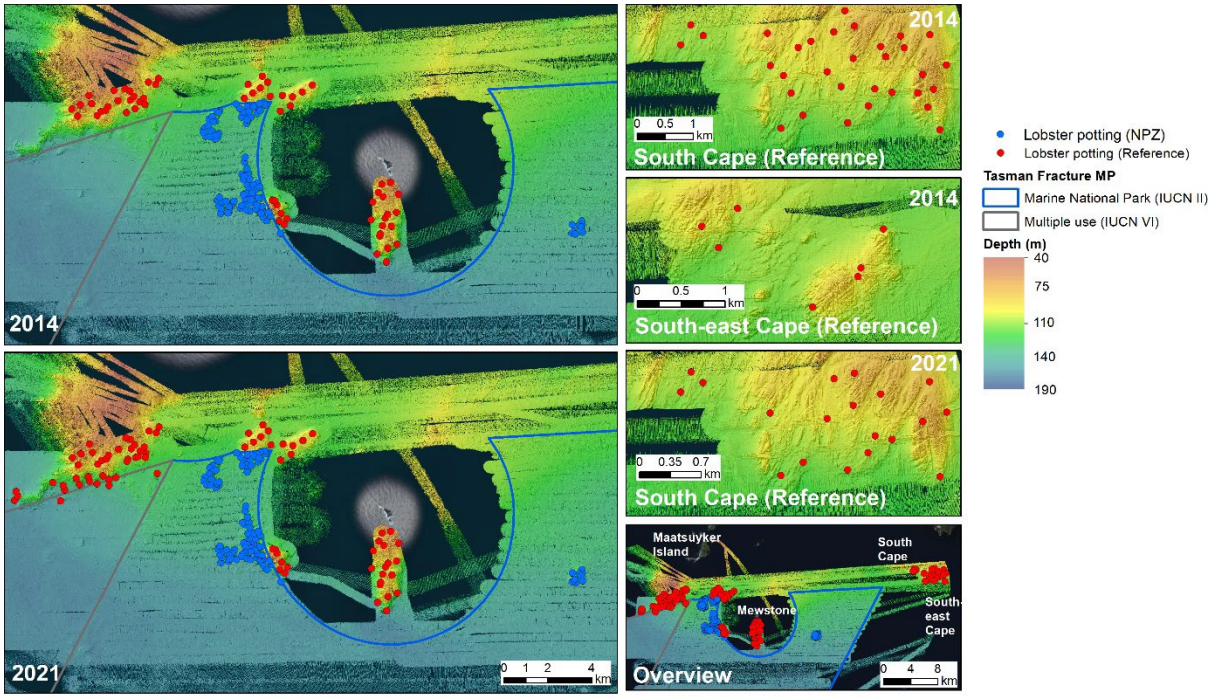

Figure 1. Rock lobster potting locations from 2014 and 2021 sampling of Tasman Fracture and surrounding fished reference areas

2.1 Descriptive patterns in rock lobster abundance, biomass, and size structure

2.1.1 Abundance

A total of 2588 rock lobsters were caught in the 2021 survey, with 1841 caught outside the reserve in fished reference areas and 747 caught inside. The total abundance was more than double the 1277 rock lobsters caught in 2014, reflecting a recovery in stocks in fished locations as well as a potential change in catchability between survey years and months. This is despite the 20 shallowest and highest catch locations from the 2015 sampling in fished reference areas being swapped and replaced by deeper reef samples (between 100-140 m) with lower catch rates, in the 2021 survey.

The pattern of lower catch rates of rock lobsters inside the reserve relative to fished locations that was reported in 2014 was also found in the 2021 survey, with an average of 7.4 rock lobsters per pot lift inside the NPZ in 2021 versus 18 in fished reference areas. However, both catch rates were higher in 2021 compared to 2014 (3.5 and 9.2 rock lobsters per pot lift inside and in fished reference areas respectively in 2014). Also, catch rates varied markedly across the survey region with significantly higher abundance per pot lift in the reef outside the NPZ to the north-east (Figure 2). Presumably much of this spatial variation throughout the region and between fished and unfished areas relate to differences in overall reef complexity and habitat suitability for rock lobsters, although other factors, such as increasing abundance of bycatch species such as conger eels in the NPZ may also play a role if their presence in a pot deters lobsters from entering.

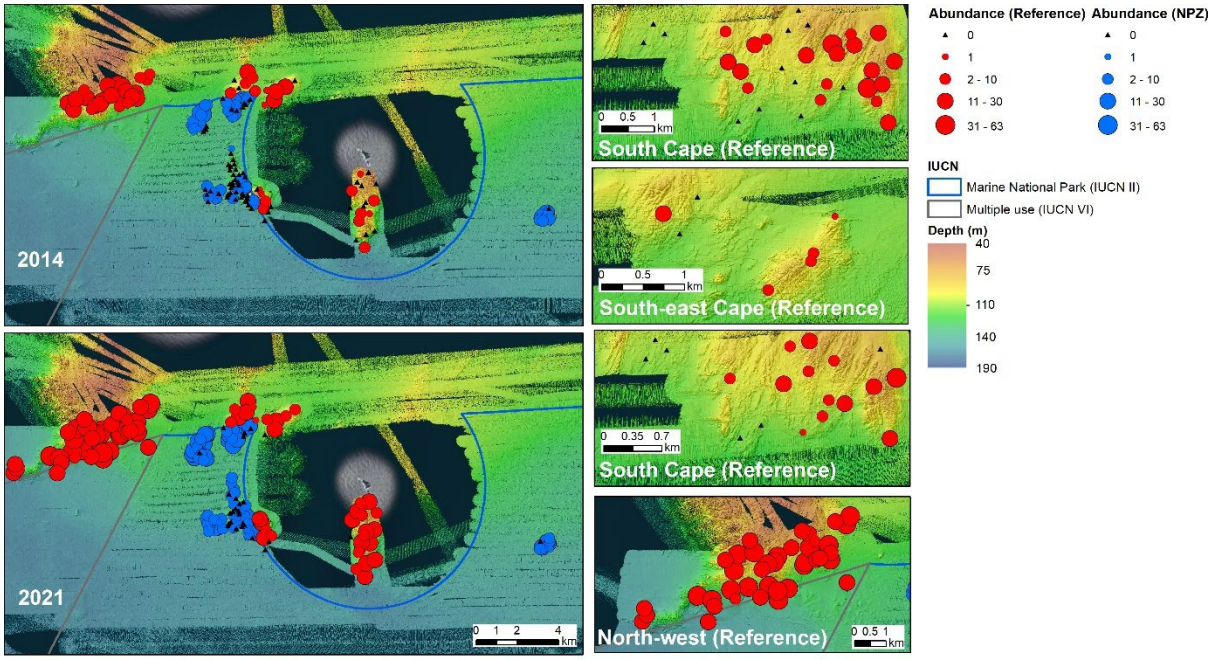

Figure 2. Spatial distribution of rock lobster abundance between sampling periods

2.1.2 Biomass

Length data was converted to biomass by the following formulae, provided by Rafael Leon (IMAS), based on length-to-weight relationships for rock lobsters in Tasmania (see Appendix, Figure A1):

$$Females: weight = 0.00048 * length^{3.02}$$

$$Male: weight = 0.00052 * length^{2.99}$$

The total biomass of rock lobsters caught in the NPZ increased by 3 times, from 161.5 kg in 2014 to 481.2 kg caught in 2021. The total biomass of rock lobsters in the fished reference areas increased by 2.5 times, from 387.2 kg in 2014 to 980.5 kg in 2021, with general increases in pots to the south and west of the Mewstone (Figure 3). The biomass of legal sized rock lobsters caught in the NPZ increased by 4.7 times, from 70.8 kg in 2014 to 333.6 kg in 2021. The biomass of legal sized rock lobsters caught in the fished reference areas increased by 6.1 times, from 81.3 kg in 2014 to 495.7 kg in 2021.

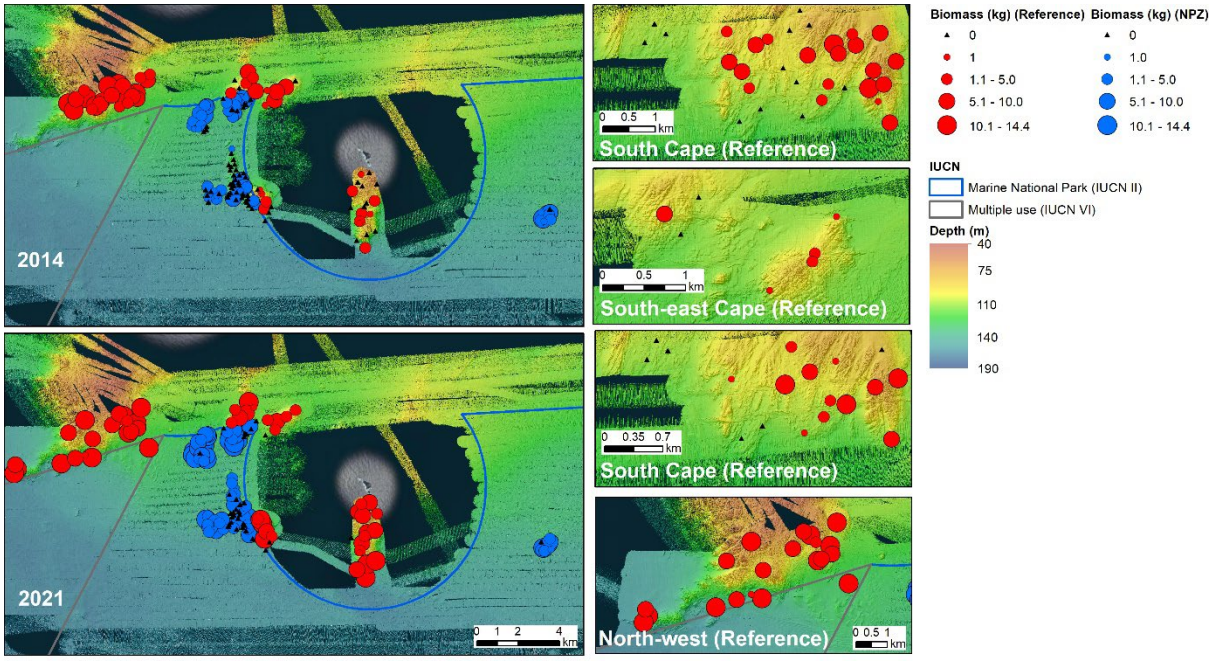

Figure 3. Spatial distribution of rock lobster total biomass per pot between sampling periods

2.1.3 Size structure

There was a clear shift in size structure of rock lobsters both inside and outside the NPZ between 2014 and 2021, with a significant increase in the larger size classes in 2021 relative to 2014 (Figure 4). This shift is particularly apparent in the NPZ, where abundances in the largest size classes were much higher in the 2021 survey. This is indicative of a filling in of sizes classes of a previously truncated size structure due to prior fishing of rock lobsters above the legal-size limit before the park was established. A building of larger size classes was also observed in the fished reference areas over this period, with a much larger proportion of the total population being over the legal size in the fished reference area in 2021 relative to 2014. This implies there has been a significant decrease in fishing effort in the fished reference area between survey times. The largest size classes of male rock lobsters (> 140 mm carapace length) were still relatively uncommon in the 2021 fished reference area data compared to the NPZ data, indicative of no fishing pressure in the NPZ (compared to reduced fishing pressure outside the NPZ) and the 15 years since the NPZ came into effect (compared with reduced fishing effort since 2015).

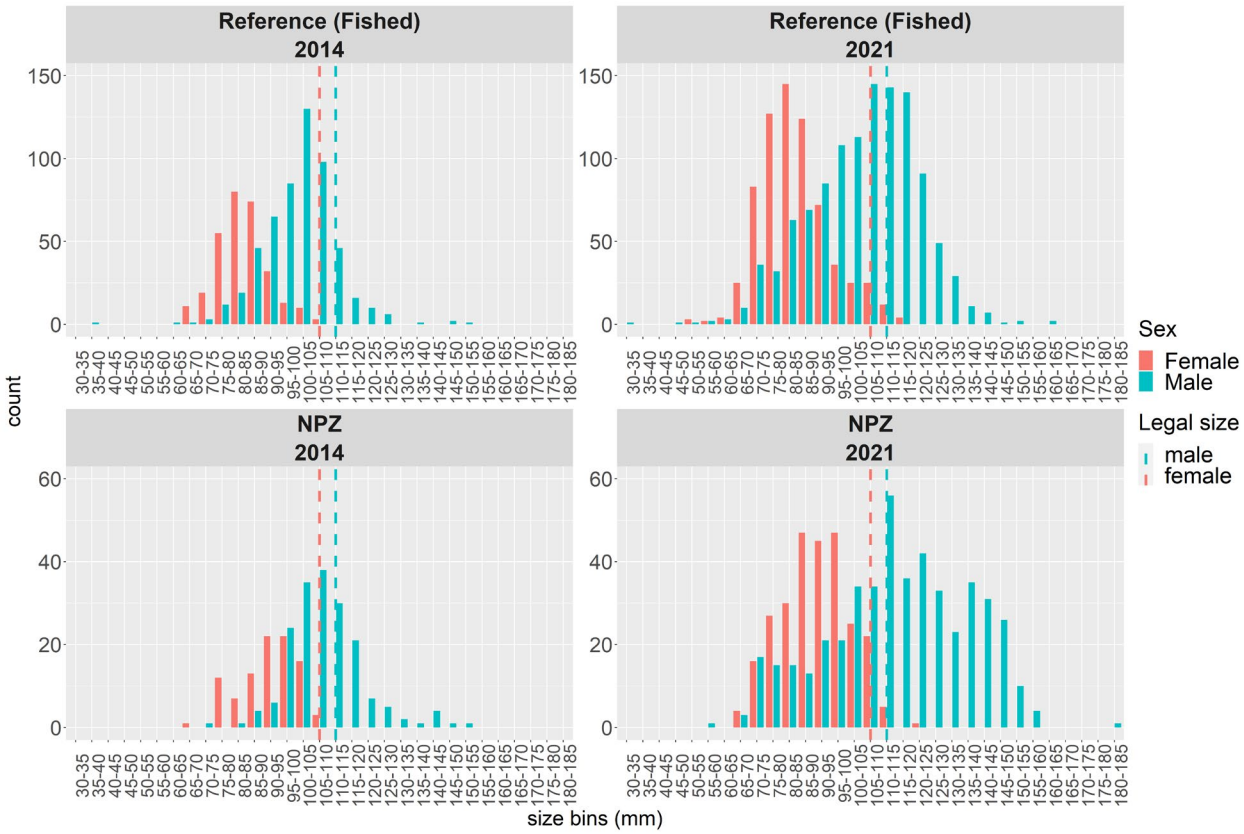

Figure 4. Size frequency of rock lobsters caught inside the marine national park (NPZ) and in fished reference areas in the 2014 and 2021 surveys. Note the different y-axis scale used for the fished reference areas and marine park, reflecting differences in overall catch between the marine park zone and fished reference areas.

2.2 Detailed analysis

2.2.1 Methods

Bayesian spatial models were used to quantify several metrics between pots deployed inside and outside of the NPZ in 2014 and 2021. These models provide a flexible means of incorporating important covariates that may influence the catch rates as well as accounting for spatial autocorrelation in the data. Covariates such as the depth of available reef, habitat complexity (quantified here as rugosity) and the abundance of rock lobster predators vary between the NPZ and adjacent fished reference areas and therefore need to be considered. For example, modelling of the initial survey data (2014) showed that depth was an important factor, and that surveyed reef within the NPZ was generally much deeper than surveyed reef outside the NPZ. While additional deep reef outside the NPZ was included to help balance this aspect in the 2021 survey, as was the removal of the shallowest reef surveyed in the fished reference area surveyed in 2014 that was shallower than any NPZ reef, there was still a difference in the balance of depths surveyed between fished and NPZ locations (Appendix, Figure A2), with fished locations on average being shallower than NPZ locations. While this could have been rectified by adding greater sampling of deeper fished reefs to the survey design, the logistics of travelling greater distances to these systems (e.g., off SW Cape) meant that extra days would need to be allocated to sampling, adding significant cost. Hence, it was decided to instead address this imbalance via a model-based analysis rather than add the additional cost of extra field days.

In addition to depth factors, spatial autocorrelation is likewise important to consider in sample comparisons, as pots deployed across a reef area are unlikely to be independent random samples and modelling spatial autocorrelation allows incorporation of how the data is correlated in space. For example, a pot deployed close to other pots that have high catch rates is likely to also have a relatively high catch. If the covariates used in the model are unable to explain this difference (e.g., there is better quality habitat not captured by depth or rugosity) then the spatial component of the model accounts for this.

Detailed Bayesian modelling was conducted for the following metrics across the two survey times:

i. Abundance
ii. Proportion of legal male rock lobsters
iii. Proportion of all legal rock lobsters
iv. Average male size
v. Average female size
vi. Sex-ratio

These metrics were chosen to allow an exploration of the changes both inside and outside the NPZ through time, and any effect that the NPZ is having on rock lobster abundance and size structure. For testing the effect of the NPZ (the “NPZ” effect) it was hypothesised that the primary effect would be on the size structure, with the no-take regulations allowing the rebuilding of larger size classes, in particular legal-sized rock lobsters. Also, as the abundance of legal-sized female rock lobsters is extremely low in this region, a significant proportion of females would be subjected to fishing mortality through repeated risk of predation in pots and when being returned to the water, or due to handling. Therefore, differences in the sex ratio could indicate the impacts of fishing on the population. Changes in abundance and average size are explored in order to report on the general status of the stock and to examine detectable changes in size structure. However, it should be noted that the timing of recruitment events and the emergence of smaller size cohorts will also affect these metrics and should be considered when interpreting the results.

Covariates included in the models were: the NPZ effect, year of survey, the interaction between AMP and year, depth, depth-squared, rugosity with a 50 metre and 500 metre buffers around pot locations, and the count of the bycatch of predatory species in pots. The “NPZ effect” tests for a significant difference in the metric for the first survey (2014). A significant interaction effect (NPZ*Year) indicates that there is a different rate of the metric between the NPZ and fished reference areas, with a positive effect meaning there is a positive rate of change for the NPZ compared to the fished reference area, and a negative value indicating there is a negative rate of change compared to the fished reference area. Depth-squared was included to account for any non-linear effects of depth, for example if mid-range depths had higher (or lower) catch rates. Rugosity was calculated from the 2 m resolution bathymetric maps across the survey area. The vector rugosity measure (VRM) and the standard deviation of depth were calculated in the benthic terrain modeller plug-in in ArcGIS software. Each metric was then averaged within 50, 100 and 500 metre buffers around pot deployment sites. Data exploration showed that these measures were highly correlated within each buffer distance and between the two measures, except at the largest distances (50 and 500 metres). Therefore, only rugosity at 50 metres and 500 meters were included in the final model. It is known that the presence of certain bycatch species such as octopus and eels in pots is likely to result in low (or no) catch of rock lobster as these species prey upon rock lobsters. These species are also often kept by fishermen to use as bait (eels) or sell as by-product (octopus) (Leon et al. 2019). Thus, abundances of these are likely to be higher in no-fishing areas and may influence the catch rates of rock lobsters. This factor was included as a covariate in the analysis by including the observed combined count of octopus and conger eels. All covariates were scaled prior to analysis by subtracting the mean and dividing by the standard deviation. Scaling was done to allow comparison between different covariates whose raw values span different ranges of values.

All modelling was conducted using the Integrated Nested Laplace Approximation (INLA) approach in R statistical software (RStudio version 4.1.3, 2022). A stepwise approach was taken, whereby all covariates were used and then sequentially removed from the model until a “best model” fit was achieved using a subset of all the covariates. Best model fit was assessed using the Deviance Information Criterion (DIC), with a threshold difference of two or more being used to determine improved model fits. Priors for the spatial component of the model were set using the PC priors approach (Fuglstad et al. 2018), with the probability that the spatial range was < 50 m set at 0.1, and the probability that the spatial standard deviation was > 1 set at 0.1. The default priors were used for all fixed effects. For abundance data a Poisson distribution was used, for all proportion-based models and sex-ratio a binomial distribution was used, and for average sizes a gaussian distribution was used. As model outputs are Bayesian, inference is done through interpreting the posterior distribution of each effect. Posteriors that are distributed further from zero have stronger evidence of an effect, while those that include zero would generally be considered non-significant (i.e., $p > 0.05$) in a frequentist analysis. Effect magnitudes on the linear predictor scale can be calculated by taking the exponent of the effect (i.e., $\exp(\beta)$); however, care should be taken in interpreting main effects when there is an interaction effect.

The overall trends for each metric were explored by taking 5000 joint posterior sample draws for the fixed effects of each best-fitting model. These posterior samples were then applied to the relevant models, with effects quantified at the mean values for the continuous variables (depth, rugosity, bycatch), and the spatial effects set to zero. In this way the overall average trends for each metric could be explored while accounting for differences in important covariates between the NPZ and fished reference areas. Plots are provided showing the mean effects for each metric at each survey time, the trend between survey times and the 95% credible intervals for the mean estimates. It should be noted that by setting the spatial effects to zero, areas of higher or lower abundance (for

example) are ignored. The calculated averages and credible intervals will therefore not encompass the full range of abundance seen in the raw data. Additionally, for each metric where there were significant covariates for depth, rugosity and bycatch, the effects were explored over the range of each covariate for the 2021 survey data.

2.2.2 Results

2.2.2.1 Abundance

The abundance of rock lobsters increased, both inside and outside of the NPZ, between the surveys in 2014 and 2021. Model estimates for the year effect indicated an approximate doubling in abundance over the seven years between surveys (i.e. exp(0.710) = 2; Table 1; Figure 5), with the interaction effect between NPZ and year providing evidence for a slightly larger increase in abundance inside the reserve of approximately 2.6 times compared to fished reference areas. The abundance of rock lobsters inside the reserve was lower in 2014 than fished reference areas (negative NPZ effect; Table 1; Figure 5).

Important covariates kept in the best model fit for abundance were depth, bycatch, and rugosity with a 50 m buffer (Table 1). A negative association with depth indicates that abundance generally decreased with depth (Figure 6). The lack of inclusion of the depth-squared term shows that the depth relationship with abundance is largely captured with a linear effect. Catch rates at >140 m (the deepest depths surveyed) were approximately 3 times lower than catch rates at 60-70 m (the shallowest depths surveyed; Figure 6). Rugosity within a 50 m buffer had a positive effect on rock lobster abundance (Figure 7), with more complex habitat being associated with higher abundance. The count of predatory bycatch species was negatively associated with abundance (Figure 8), with higher counts of conger eels and octopus leading to lower abundance of rock lobsters in pots.

Table 1. Estimates of the model fixed effects for abundance of rock lobsters. Effects highlighted in red indicate evidence for a negative effect for that effect, while those highlighted in green indicate evidence for a positive effect.

Effect	mean	sd	0.025 quantile	0.975 quantile
intercept	1.379	0.181	1.023	1.735
NPZ	-0.827	0.362	-1.538	-0.118
Year	0.710	0.049	0.615	0.806
NPZ*Year	0.264	0.088	0.093	0.437
Depth	-0.326	0.134	-0.590	-0.063
Bycatch	-0.144	0.036	-0.215	-0.074
Rugosity 50 m	0.250	0.087	0.080	0.420

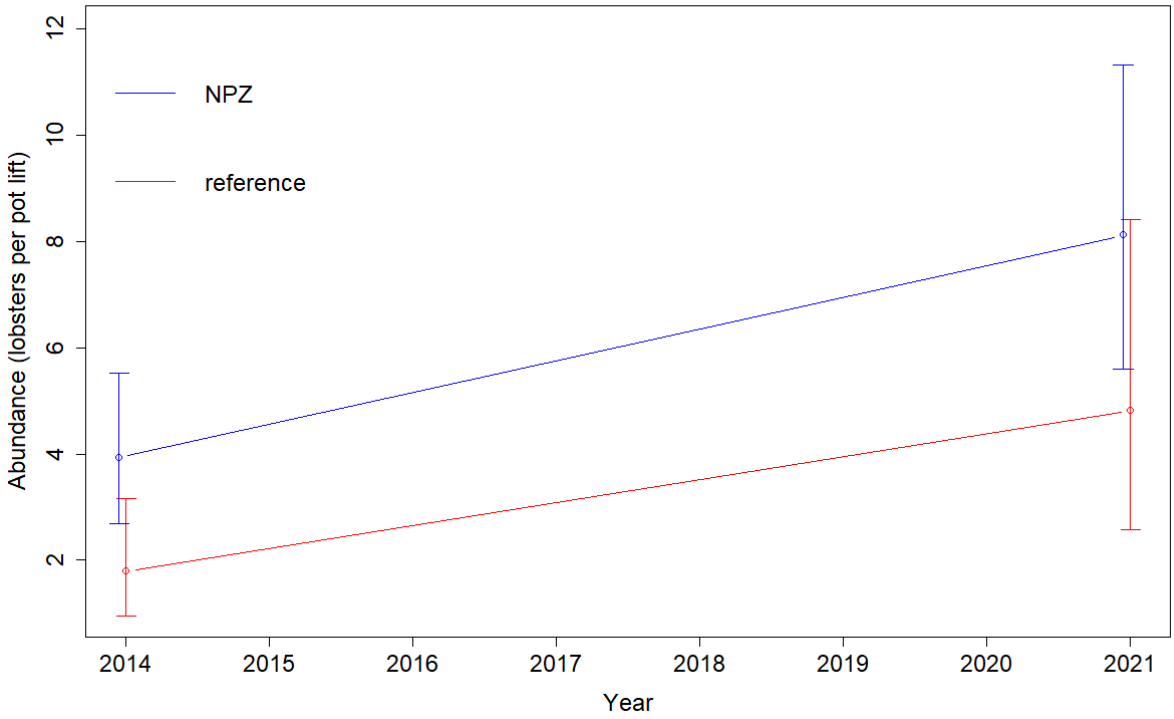

Figure 5. Model-based estimates of the trends in abundance (expressed as mean number of rock lobsters per pot lift) for the national park zone (NPZ) and fished reference areas between 2014 and 2021. Estimates were made at the mean values for depth, rugosity, and bycatch across the survey area. Error bars are the 95% credible intervals of the estimate

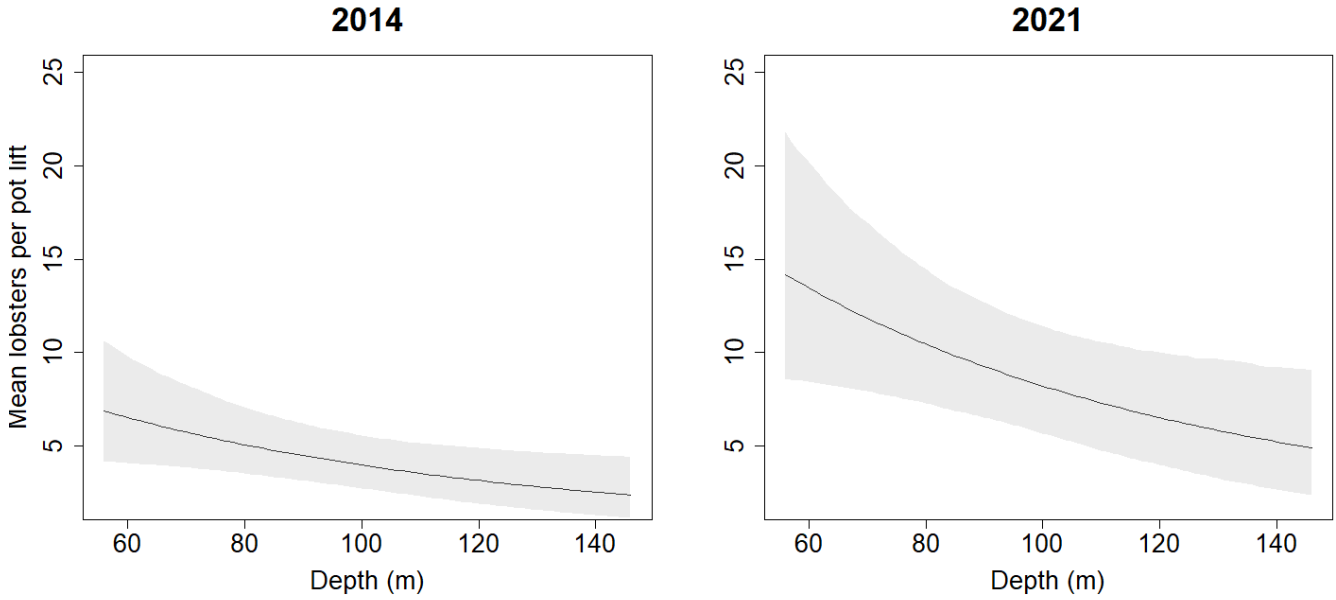

Figure 6. Relationship between abundance (mean rock lobsters per pot lift) and depth from model-based estimates and for 2021. Estimates were made at the mean rugosity and bycatch levels across the data set for the 2014 and 2021 surveys. Line shows mean response in the absence of spatial effects. Shading shows 95% credible intervals.

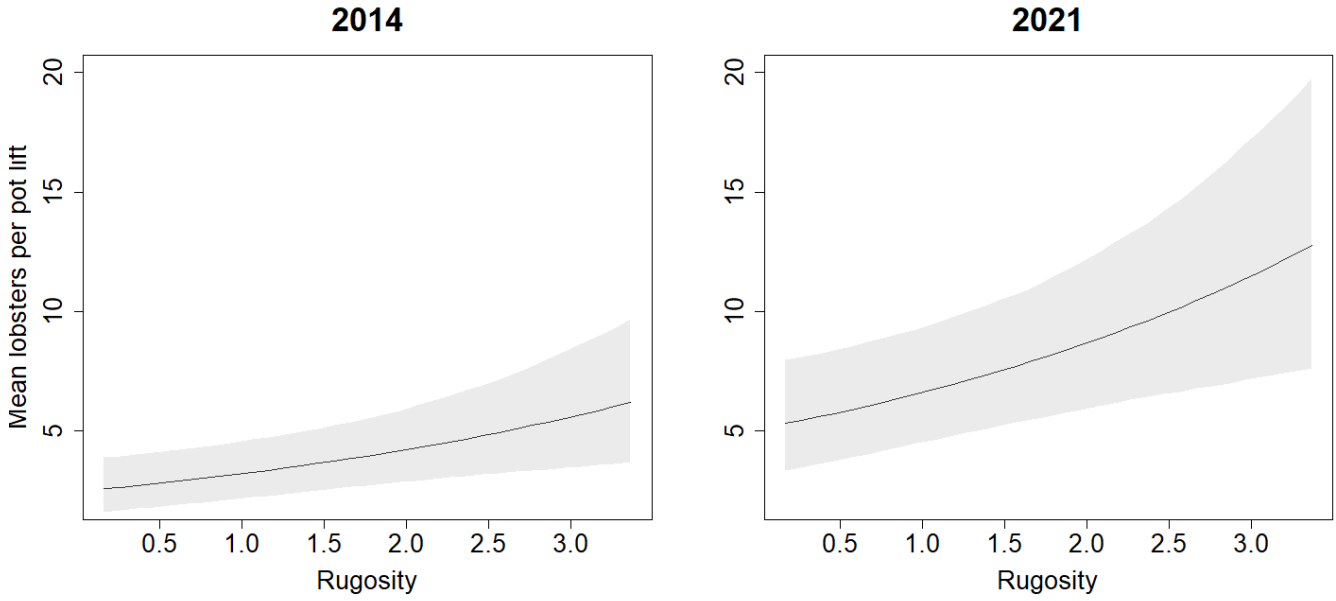

Figure 7. Relationship between abundance (mean rock lobsters per pot lift) and rugosity from model-based estimates. Estimates were made at the mean depth and bycatch levels across the data set for the 2014 and 2021 surveys. Line shows mean response in the absence of spatial effects. Shading shows 95% credible intervals.

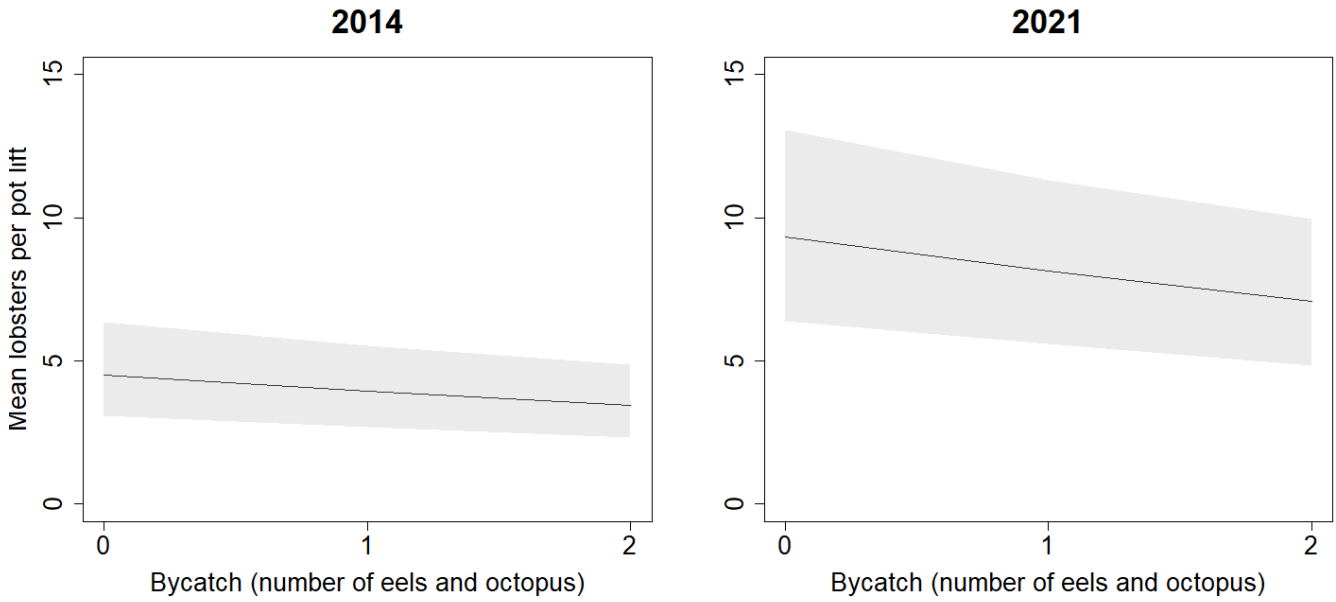

Figure 8. Relationship between abundance (mean rock lobsters per pot lift) and bycatch of rock lobster predators (conger eels and octopus) from model-based estimates. Estimates were made at the mean depth and rugosity levels across the data set for the 2021 survey. Line shows mean response in the absence of spatial effects. Shading shows 95% credible intervals.

2.2.2.2 Proportion of legal male rock lobsters

The proportion of legal-sized male rock lobsters increased both inside and outside the NPZ between 2014 and 2021 (positive Year effect; Table 2 ; Figure 9), indicating a rebuilding of the size structure of the population of male rock lobsters. Model results also suggested there was an overall positive effect of protection on the proportion of legal-sized male rock lobsters in 2014, with the odds of a male rock lobster being legal-sized in the NPZ 2.13 times more likely compared to in fished reference areas in the initial survey; however, this effect would not be considered statistically significant. The increase in the proportion of legal-sized males between the two surveys was greater in fished reference areas than in the NPZ (negative AMP*Year effect; Table 2 ; Figure 9). Spatial patterns in proportion of legal male rock lobster reflected a similar pattern to total biomass, with general increases in pots to the south and (north) west of the Mewstone (Figure 10).

There was a small increase in the proportion of legal sized males with depth and with increased rugosity at 50 m, but the evidence for these effects is not strong (overlap of posterior distribution includes zero; Table 2).

Table 2. Estimates of the model fixed effects for the proportion of legal-sized male rock lobsters. Effects highlighted in red indicate evidence for a negative effect for that effect, while those highlighted in green indicate evidence for a positive effect.

Effect	mean	sd	0.025 quantile	0.975 quantile
intercept	-1.029	0.227	-1.476	-0.584
NPZ	0.757	0.388	-0.004	1.518
Year	1.351	0.153	1.055	1.654
NPZ*Year	-0.541	0.250	-1.032	-0.051
Depth	0.080	0.127	-0.170	0.330
Rugosity 50 m	0.134	0.084	-0.030	0.299

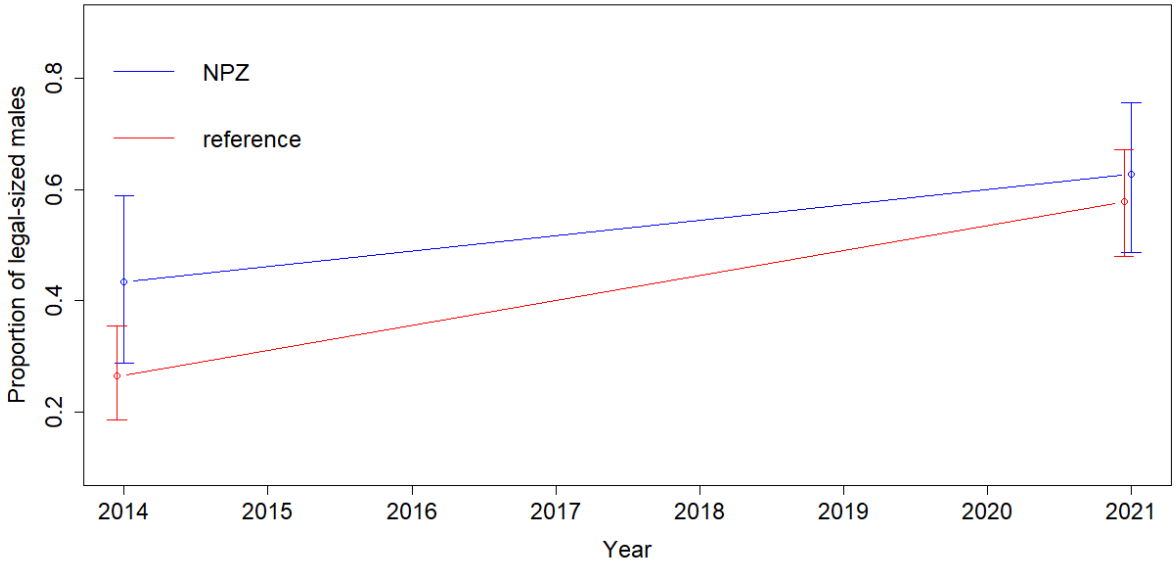

Figure 9. Model-based estimates of the trends in the proportion of legal-sized male rock lobsters for the national park zone (NPZ) and fished reference areas between 2014 and 2021. Estimates were made at the mean values for depth and rugosity across the survey area. Error bars are the 95% credible intervals of the estimate

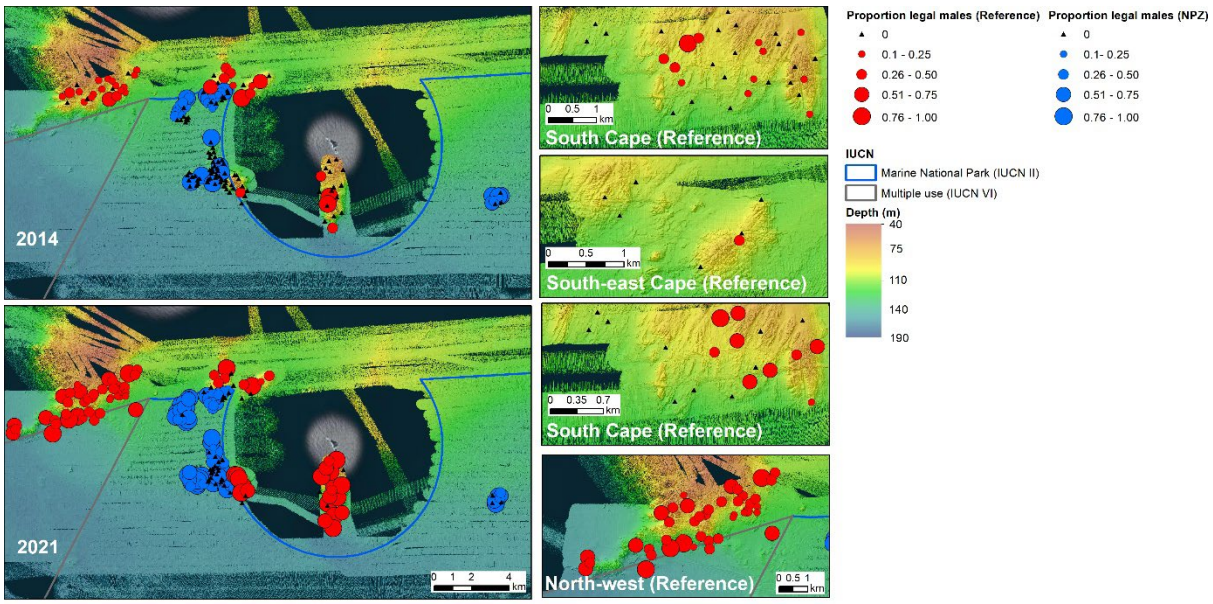

Figure 10. Spatial distribution of the proportion of legal sized male rock lobster per pot between sampling periods

2.2.2.3 Proportion of all legal rock lobsters

The proportion of all legal-sized rock lobsters showed similar trends to the proportion of legal sized male rock lobsters, as legal sized females make up a relatively small proportion of the total population. The proportion of legal sized rock lobsters increased both inside and outside the NPZ between 2014 and 2021 (positive Year effect; Table 3; Figure 11), indicating a rebuilding of the size structure of the entire population. Model results suggest there was a positive effect of protection on the proportion of legal-sized rock lobsters in 2014, with the overall odds of a rock lobster being legal-sized in the NPZ 1.9 times more likely compared to fished reference areas. However, the increase in the proportion of legal-sized rock lobsters was greater in fished reference areas (negative NPZ*Year effect; Table 3; Figure 11) than in the NPZ between the two survey times, with the protection effect size being smaller in 2021 than in 2014 (Figure 11).

There was a small increase in the proportion of legal sized males with depth and positive effect of depth squared, indicating that mid-depths surveyed had a lower proportion of legal sized rock lobsters relative to shallow and deep depths surveyed (Figure 12).

The spatial patterns in proportion of all legal rock lobster exhibited general increases in pots to the south and (north) west of the Mewstone (Figure 13).

Table 3. Estimates of the model fixed effects for the proportion of legal-sized rock lobsters. Effects highlighted in red indicate evidence for a negative effect for that effect, while those highlighted in green indicate evidence for a positive effect.

Effect	mean	sd	0.025 quantile	0.975 quantile
intercept	-1.691	0.231	-2.146	-1.240
NPZ	0.649	0.341	-0.021	1.319
Year	1.076	0.139	0.806	1.353
NPZ*Year	-0.522	0.211	-0.937	-0.107
Depth	0.146	0.112	-0.074	0.365
Depth squared	0.161	0.073	0.018	0.305

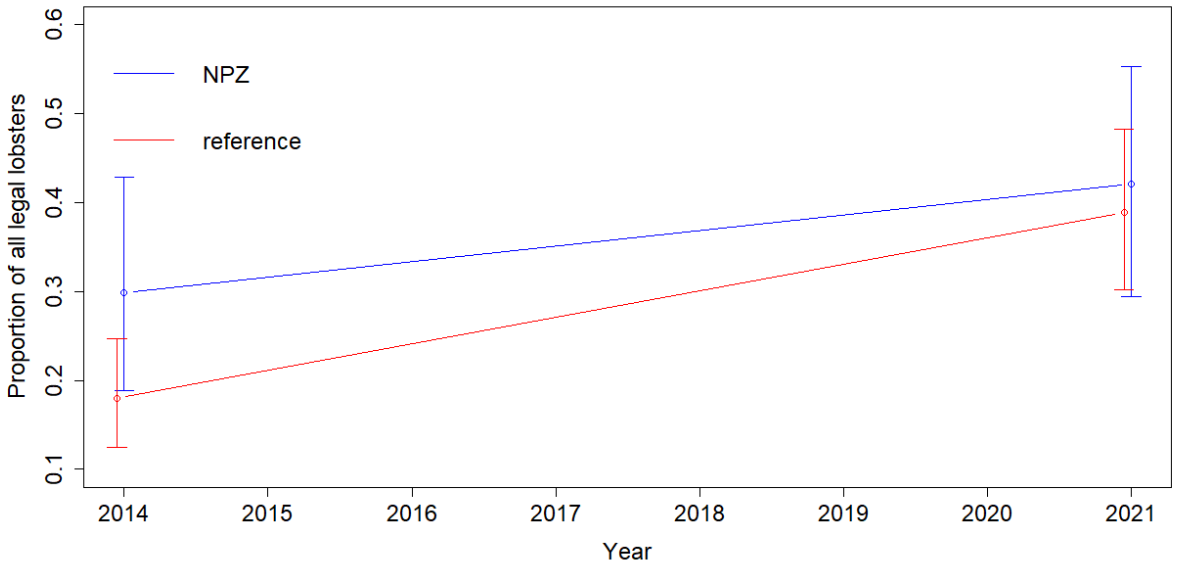

Figure 11. Model-based estimates of the trends in the proportion of all legal-sized rock lobsters for the national park zone (NPZ) and fished reference areas between 2014 and 2021. Estimates were made at the mean values for depth and depth-squared across the survey area. Error bars are the 95% credible intervals of the estimate

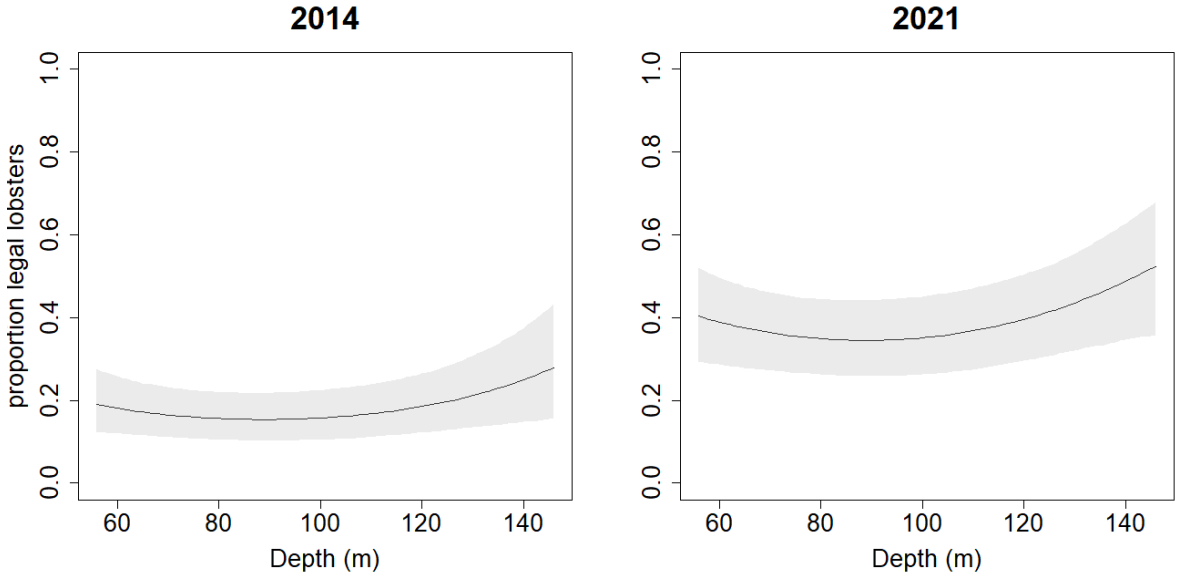

Figure 12. Relationship between the proportion of all legal rock lobsters with depth from model-based estimates for 2021. Estimates were made for the 2014 and 2021 survey data. Line shows mean response in the absence of spatial effects. Shading shows 95% credible intervals

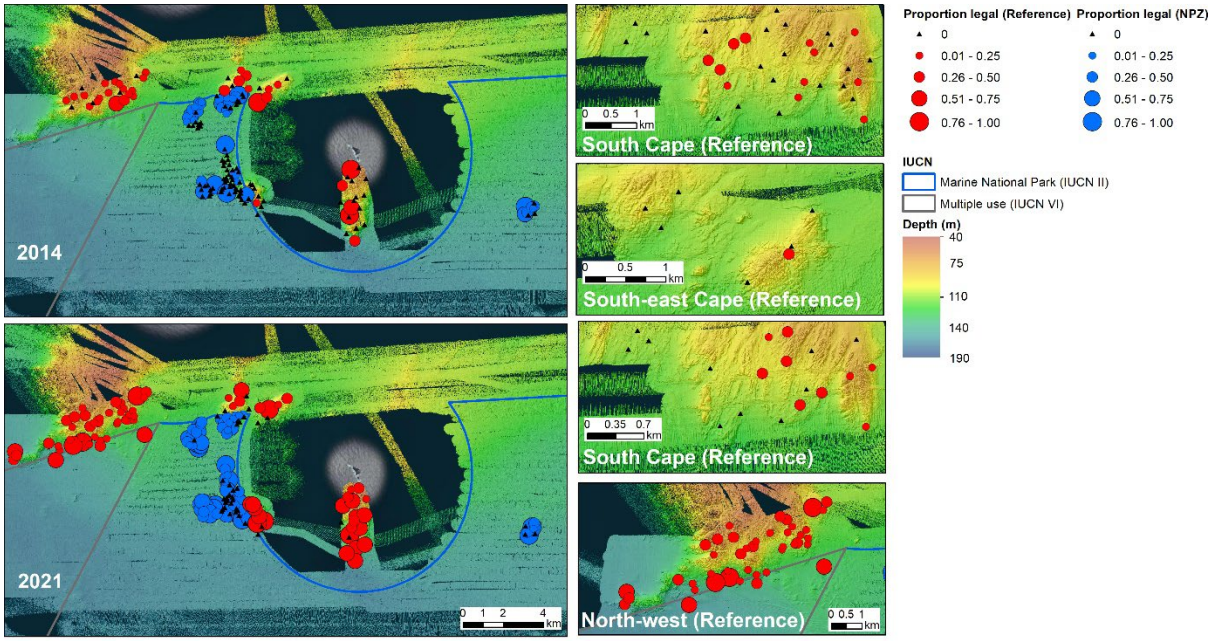

Figure 13. Spatial distribution of proportion of legal sized rock lobster per pot between sampling periods

2.2.2.4 Average male size

The average size of male rock lobsters increased both inside and outside the NPZ between the two surveys (positive Year effect; Table 4), but a larger increase was seen inside the NPZ (strong NPZ*Year effect; Table 4). On average, male rock lobsters had a carapace length of 105.5 mm in fished reference areas in 2014, with male rock lobsters being 1.7 mm larger in the NPZ (Table 4). The average size of male rock lobsters increased by 3.2 mm between 2014 and 2021. However, there was a strong interaction effect between protection and time (NPZ*Year effect; Table 4; Figure 14), with male rock lobsters being on average 11.4 mm larger in the NPZ compared to fished reference areas in 2021.

There was a small increase in size of male rock lobsters with depth, but evidence for this effect is small. Rugosity with a 50 m buffer was positively correlated with average male size (Figure 15), indicating larger rock lobster tend to occupy more rugose habitat.

The spatial patterns in average size of male rock lobster exhibited general increases in pots to the south and (north) west of the Mewstone (Figure 16).

Table 4. Estimates of the model fixed effects for the average size of male rock lobsters. Effects highlighted in red indicate evidence for a negative effect for that effect, while those highlighted in green indicate evidence for a positive effect.

Effect	mean	sd	0.025 quantile	0.975 quantile
intercept	105.751	1.786	102.243	109.255
NPZ	1.713	2.759	-3.703	7.125
Year	3.270	1.744	-0.153	6.690
NPZ*Year	6.422	2.622	1.275	11.565
Depth	1.820	0.951	-0.047	3.686
Rugosity 50 m	1.903	0.706	0.516	3.289

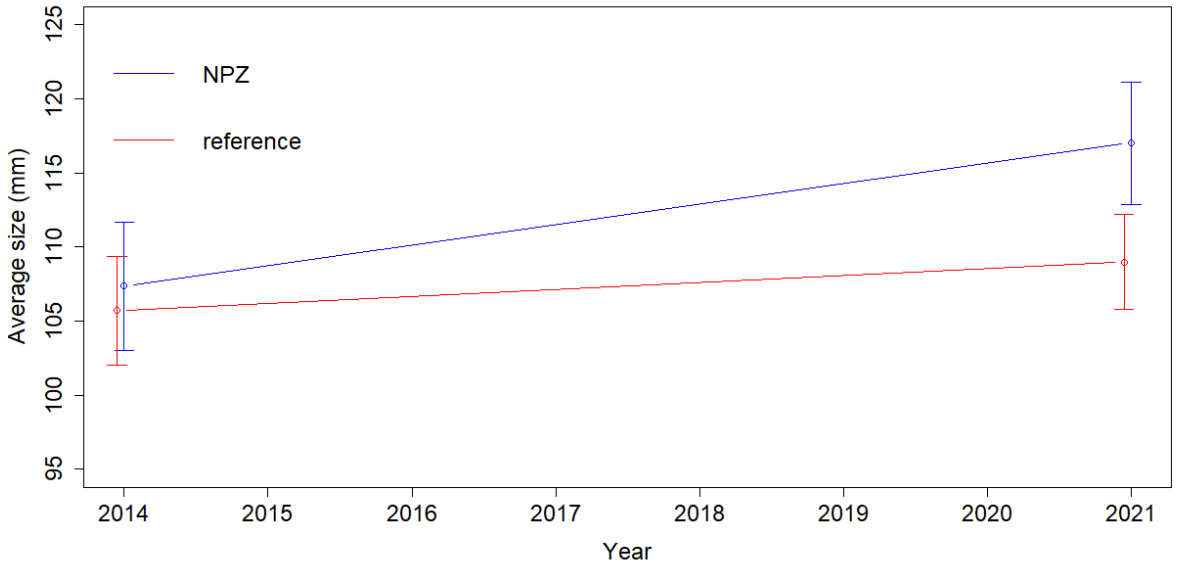

Figure 14. Model-based estimates of the trends in the average size for male rock lobsters for the NPZ and fished reference areas between 2014 and 2021. Estimates were made at the mean values for depth and rugosity across the survey area. Error bars are the 95% credible intervals of the estimate.

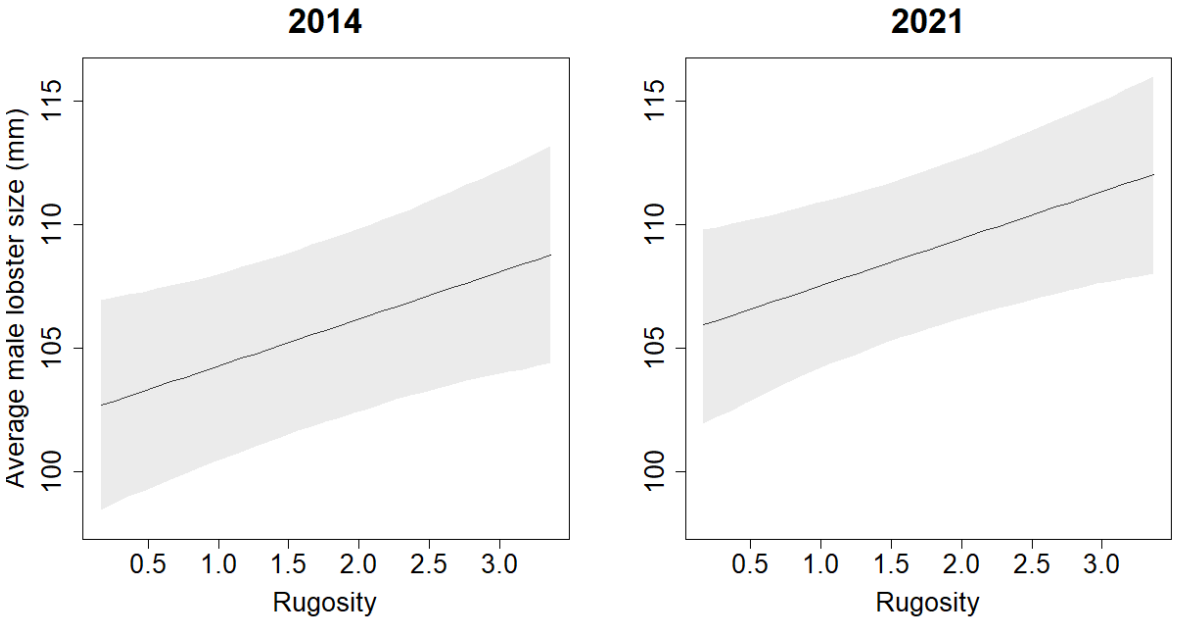

Figure 15. Relationship between the average male rock lobster carapace length (mm) with rugosity from model-based estimates for the 2014 and 2021 survey data. Line shows mean response in the absence of spatial effects. Shading shows 95% credible intervals.

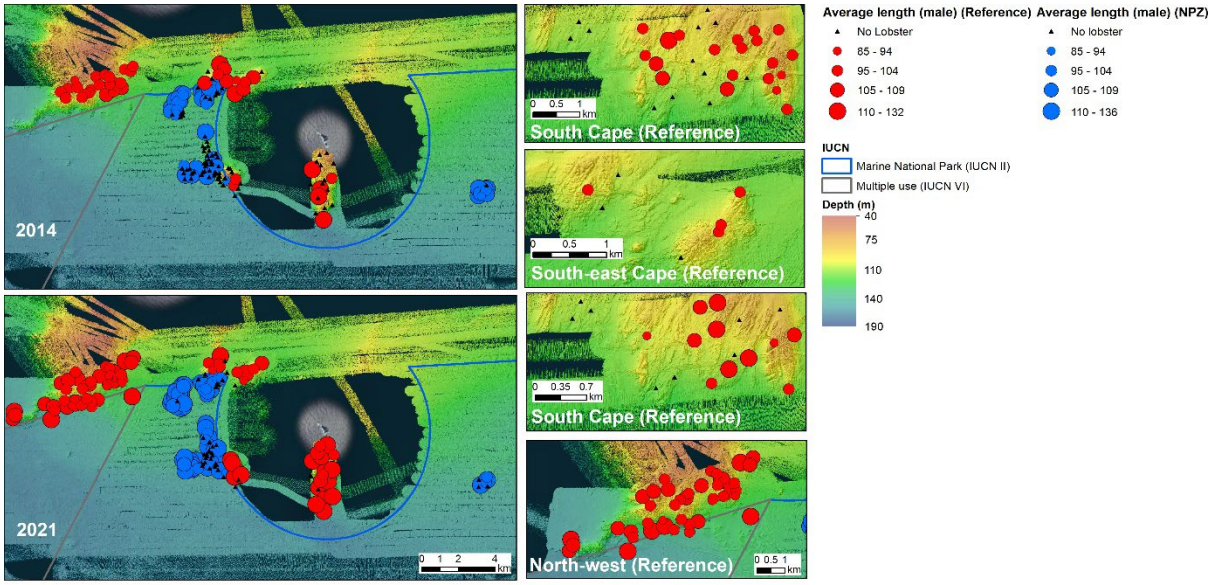

Figure 16. Spatial distribution of average length (mm) of male rock lobster per pot between sampling periods

2.2.2.5 Average female size

Model estimates suggest an overall decrease in the average female size between 2014 and 2021 (negative Year effect; Table 5; Figure 17), with a slightly larger decrease for fished reference areas compared to the NPZ (postive NPZ*Year interaction; Table 5; Figure 17). The average female size increased marginally with depth. However, there was not strong evidence for any of these effects, with posterior distributions for all effects including zero (Table 5).

The spatial patterns in average size of female rock lobster exhibited general increases in pots to the south and (north) west of the Mewstone (Figure 18).

Table 5. Estimates of the model fixed effects for the average size of female rock lobsters. Effects highlighted in red indicate evidence for a negative effect for that effect, while those highlighted in green indicate evidence for a positive effect.

Effect	mean	sd	0.025 quantile	0.975 quantile
intercept	88.881	2.207	84.900	92.858
NPZ	0.433	2.125	-3.740	4.602
Year	-1.296	1.000	-3.258	0.665
NPZ*Year	1.668	1.522	-1.321	4.655
Depth	0.447	0.703	-0.934	1.826

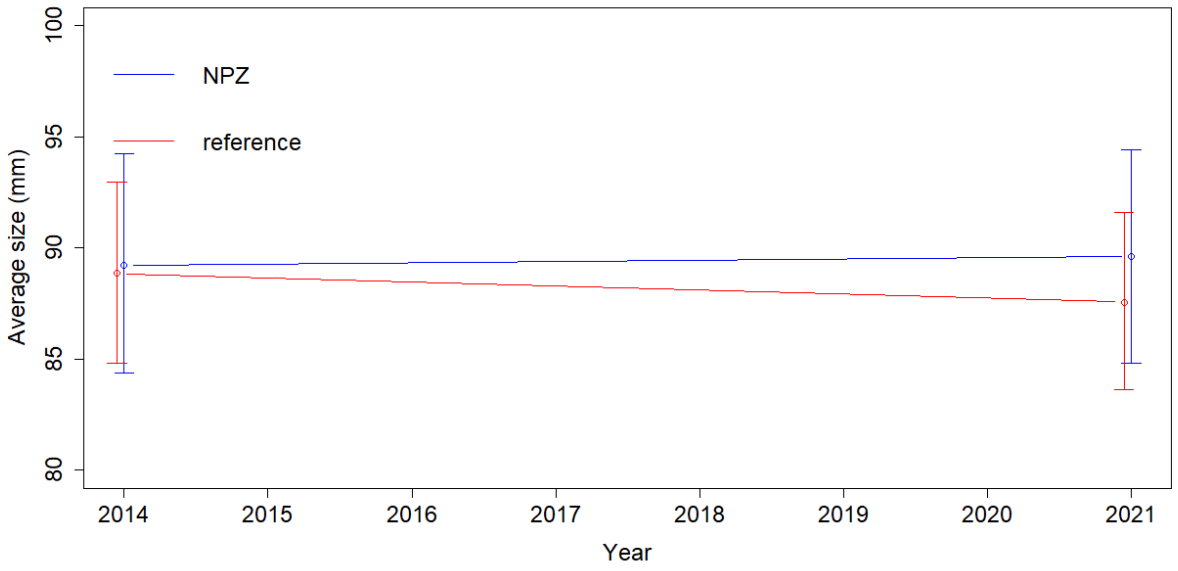

Figure 17. Model-based estimates of the trends in the average size of female rock lobsters for the NPZ and fished reference areas between 2014 and 2021. Estimates were made at the mean values for depth across the survey area. Error bars are the 95% credible intervals of the estimate.

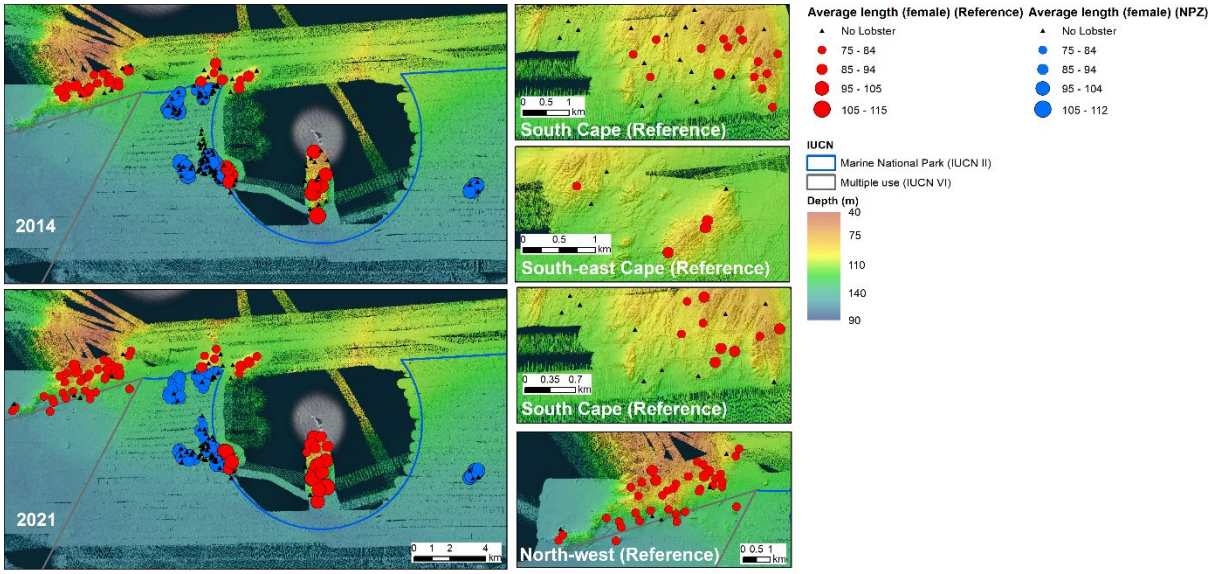

Figure 18. Spatial distribution of average length (mm) of female rock lobster per pot between sampling periods

2.2.2.6 Sex-ratio

The sex-ratio (proportion of males to females) decreased both inside and outside of the NPZ between 2014 and 2021 (negative Year effect; Table 6; Figure 19). The proportion of males to females was also slightly lower inside the NPZ, indicating a higher proportion of females in the population inside the NPZ, although there is not strong evidence for this effect.

There was a negative association between rugosity at 50 m and the sex ratio, indicating that the proportion of females increased in more complex habitat (Figure 20). There was a positive effect of depth-squared, pointing to a decreased proportion of males in mid-depths surveyed (Figure 21).

The spatial patterns in sex-ratio of rock lobster exhibited general increases in pots to the south and (north) west of the Mewstone (Figure 22)

Table 6. Estimates of the model fixed effects for the sex ratio (male: female) rock lobsters. Effects highlighted in red indicate evidence for a negative effect for that effect, while those highlighted in green indicate evidence for a positive effect.

Effect	mean	sd	0.025 quantile	0.975 quantile
intercept	0.768	0.163	0.663	1.226
NPZ	-0.038	0.277	-0.594	0.481
Year	-0.272	0.110	-0.482	-0.051
NPZ*Year	-0.096	0.199	-0.488	0.296
Depth	0.224	0.100	-0.035	0.326
Bycatch	0.119	0.061	0.000	0.242
Rugosity 50 m	-0.223	0.071	-0.359	-0.079
Depth-squared	0.163	0.071	0.027	0.314

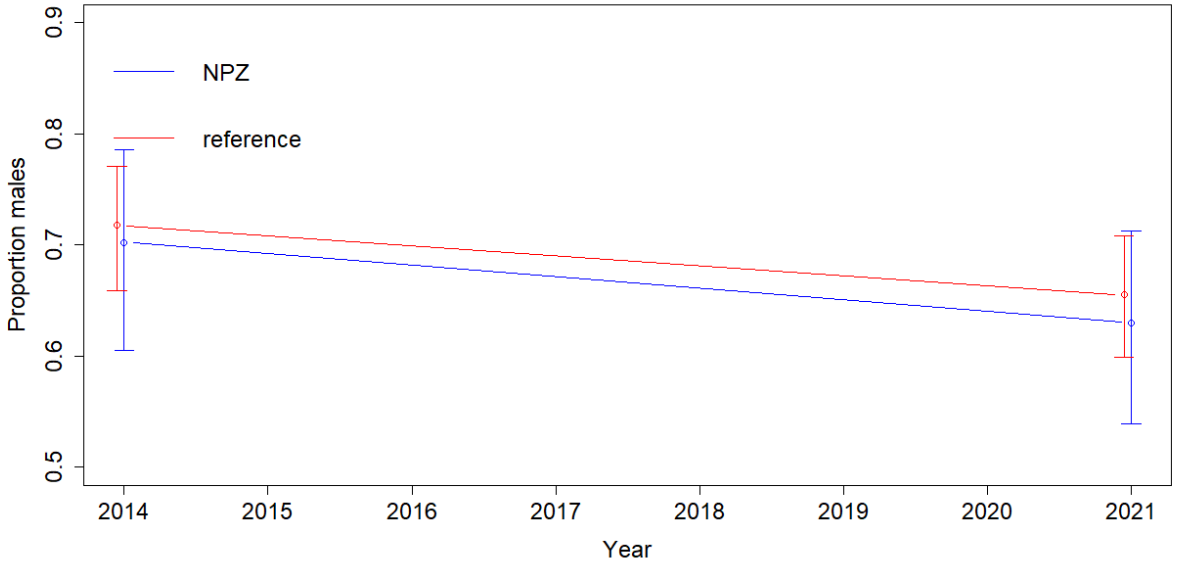

Figure 19. Model-based estimates of the sex ratio of rock lobsters (males: females) for the NPZ and fished reference areas between 2014 and 2021. Estimates were made at the mean values for depth, depth-squared, bycatch and rugosity across the survey area. Error bars are the 95% credible intervals of the estimate

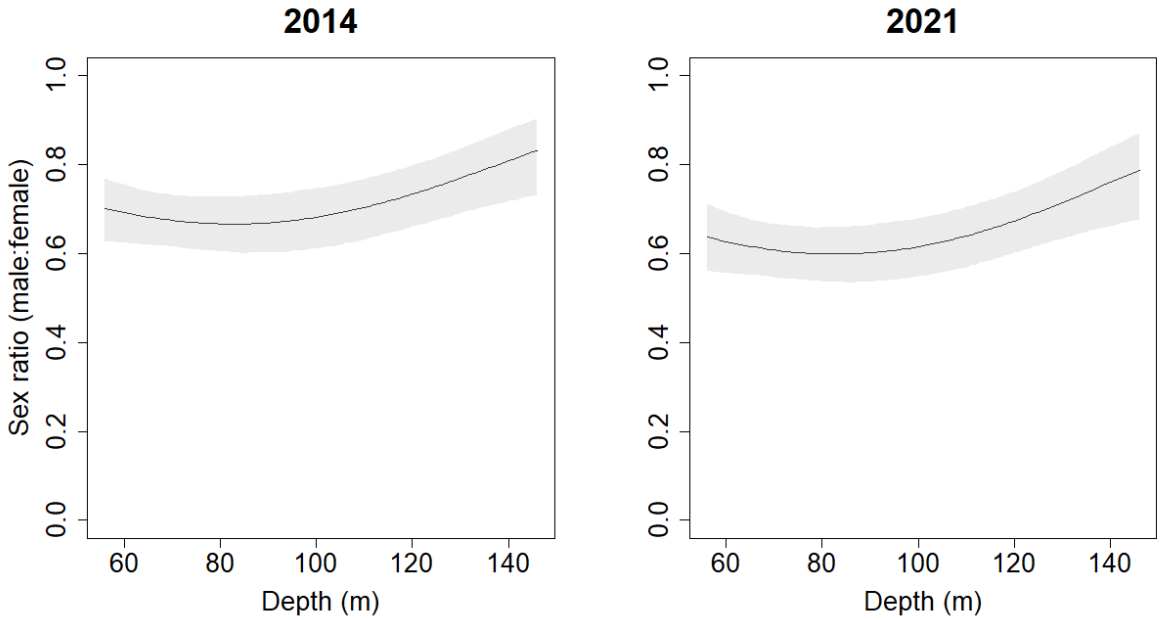

Figure 20. Relationship between the proportion of male to female rock lobsters with depth from model-based estimates for the 2014 and 2021 survey data. Line shows mean response in the absence of spatial effects. Shading shows 95% credible intervals.

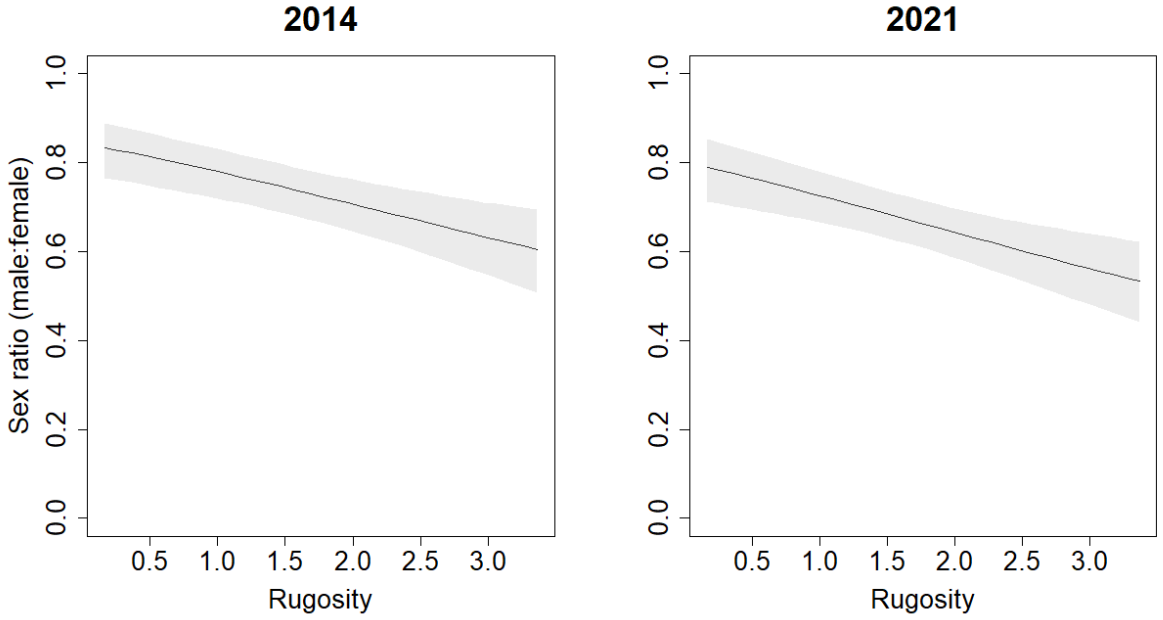

Figure 21. Relationship between the proportion of male to female rock lobsters with rugosity from model-based estimates for the 2014 and 2021 survey data. Line shows mean response in the absence of spatial effects. Shading shows 95% credible intervals.

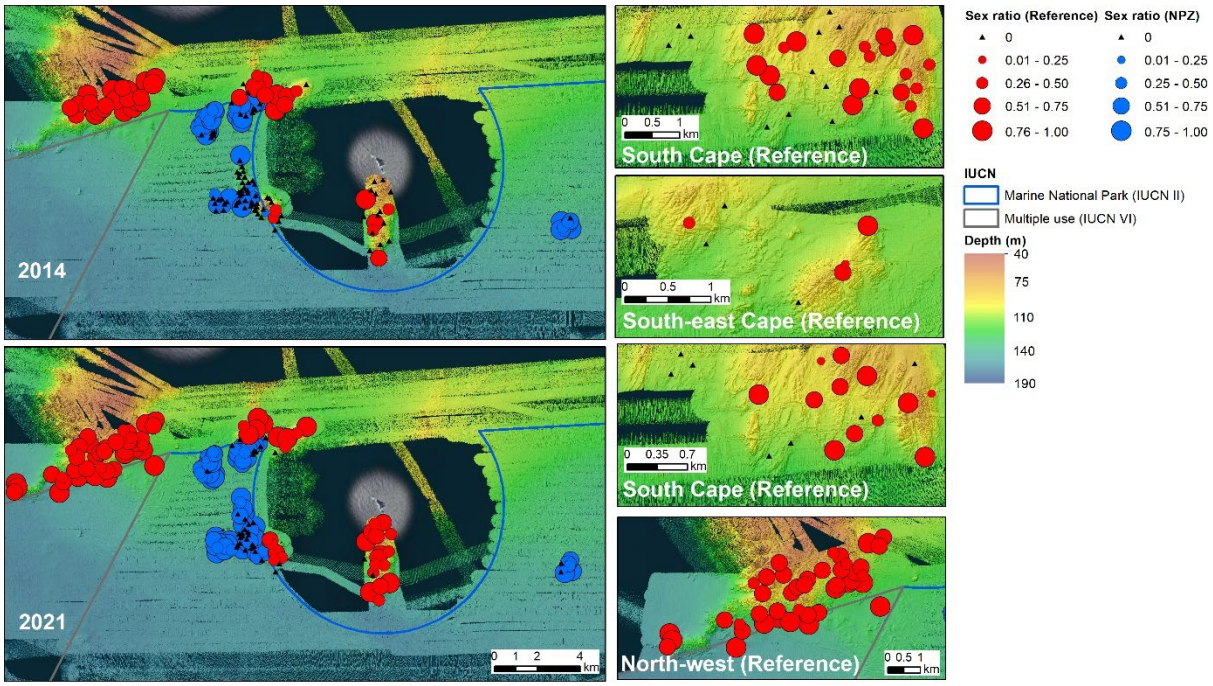

Figure 22. Spatial distribution of sex-ratio of rock lobsters per pot between sampling periods

2.2.2.7 Bycatch in rock lobster pots

The diversity of bycatch species did not alter drastically between the two survey periods; however there were some notable shifts in the abundance of some species (Table 7). Draughtboard sharks (*Cephaloscyllium laticeps)* were a dominant portion of the bycatch over the entire survey period, but with an increase in the numbers caught in 2021 inside the NPZ and a decrease in numbers caught outside. There was a notable decline in the bycatch of ocean perch (*Helicolenus percoides*) with 58 and 7 individuals being caught inside and outside respectively in 2014, but only a single individual caught in 2021 inside the NPZ. Bycatch of conger eels (*Conger verreauxi*) increased both inside and outside the NPZ in 2021, with overall higher abundances recorded inside the NPZ. Other notable changes in bycatch were a larger number of jackass morwong (*Nemadactylus macropterus*) caught inside the NPZ in 2021, and an increase in the catch of giant crab (*Pseudocarcinus gigas*) from 2 inside the NPZ in 2014 to 9 in 2021. However, the giant crab caught in the 2021 survey were noted to be small juveniles compared to the larger individuals caught in 2014.

Table 7. Bycatch species from rock lobster pot sampling

Taxa	NPZ 2014	NPZ 2021	Reference 2014	Reference 2021
Cephaloscyllium laticeps (Draughtboard Shark)	20	39	50	29
Asymbolus rubiginosus (Orange spotted cat shark)	0	4	1	7
Conger verreauxi (Conger eel)	11	27	7	13
Helicolenus percoides (Ocean Perch)	58	1	7	0
Octopus maorum (Maori Octopus)	0	4	2	2
Octopus spp	2	0	0	0
Latris lineata (Striped trumpeter)	1	0	0	0
Nemadactylus macropterus (Jackass morwong)	1	19	0	0
Pseudophycis spp (Red cod and Bearded Cod combined)	11	7	0	3
Nectocarcinus spp (Red velvet crab)	0	2	11	8
Pseudolabrus rubicundus (Rosy wrasse)	0	1	2	0
Strigopagurus strigimanus (Hermit crab)	37	102	51	63
Pseudocarcinus gigas (Giant crab)	2	9	1	1
Caesioperca rasor (Barber Perch)	0	0	0	3
Caesioperca lepidoptera (Butterfly Perch)	0	0	0	2
Unidentified Decorator Crab	3	4	4	1
Plagusia chabrus (Red Bait Crab)	0	2	0	1
Leptograpsus variegatus (Speedy Crab)	0	0	0	1
Leptomithrax gaimardii (Spider Crab)	0	1	0	1
Gymnothorax prasinus (Green Moray Eel)	0	1	0	0
Neosebastes scorpaenoides (Red Gurnard Perch)	0	1	0	0
Ranella australasia (Whelk)	0	0	1	0
Brittle Star (Ophiuroidea)	25	0	0	0

3 Population trends in demersal fishes between 2015 and 2021

Demersal fish populations both inside and outside of the Marine National Park Zone (NPZ) of the TFMP were surveyed in both 2015 and again in 2021 using baited remote underwater stereo video stations (stereo BRUVs). The survey design replicated that used for the rock lobster potting surveys (but utilising a subset of the rock lobster sites due to time-constraints involved with this method), with a subset of the same sites surveyed across both survey years and some additional deeper fished reference sites added in the 2021 survey to create a more balanced survey across depth. Initial results from 2015 suggested that some targeted fish species had higher abundances and/or size structures inside the NPZ compared to the fished reference area, and that this may be early evidence of a protection effect. However, in the absence of a baseline survey at the time of initial protection, it was not possible to reliably determine if observed patterns were due to protection or habitat/sampling effects. A time-series of observations was recommended to track potential changes and protection effects. The central aim of the current study was to undertake the first step in that time-series and explore the trajectory of these populations since the baseline survey in 2015, to establish whether ongoing protection from fishing effort is having an effect relative to changes in adjacent and similar fished habitats. The core focus is on key targeted species such as striped trumpeter and jackass morwong, which are known to be targeted by a range of fishing practices and kept by fishers as either market fish or to be used as bait, and hence, are more likely to show a contrast between fished and unfished areas. However, the entire demersal fish community is also quantified and contrasted here, providing a useful baseline of fish communities in deeper shelf waters in this region for assessing longer term-changes in response to a range of pressures, including ocean warming.

All BRUV deployments followed standardised protocols outlined in NESP Hub guidelines (Langlois et al. 2020), with one hour deployments using ~ 800 g of pilchards for bait. A total of 92 deployments were achieved in 2015, and 113 in 2021 (Figure 23). The parameter MaxN was used as the abundance measure for all subsequent abundance analyses and summaries. MaxN is the maximum number of fish of a given species seen in one segment of video where all fish can be identified as different individuals. This prevents repeated counting of the same individual and provides a relative index of abundance to allow comparison between sites and times. All individuals comprising the MaxN frames were also measured using the stereo imagery in EventMeasure software and quality check using CheckEM (https://globalarchive.shinyapps.io/checkem/). Stereo BRUVs data is deposited in https://globalarchive.org/geodata/data/project/get/148.

The composition of fish species observed on the BRUV surveys between the 2015 and 2021 surveys consisted of the same predominant species, with a few notable exceptions (Table 8). Of particular note was the observation of a single pink handfish (*Brachiopsilus dianthus*) inside the park Multiple Use Zone (MUZ) in 2021, a species that was recently listed on the endangered species list and had not been observed in the wild for over 22 years. Following this discovery, AUV-derived imagery collected for benthic cover studies was additionally searched for the presence of handfish, finding at least one other specimen of this species (detailed in the Seabed Benthos section). Three Australian handfish (*Brachionichthys australis*) and a single spiny pipehorse (*Solegnathus spinosissimus*) were also observed in the BRUV imagery from 2021, within the NPZ. Dominant species include high abundances of butterfly perch (*Caesioperca lepidoptera*), mackerel species (*Trachurus spp.)*, splendid perch (*Callanthias australis*), jackass morwong *(Nemadactylus macropterus*), morid cod species

(*Pseudophycis spp.*), ocean perch (*Helicolenus percoides*) and rosy wrasse (*Pseudolabrus rubicundus*). Total abundances (all species combined) were higher in the fished reference area compared to the NPZ, with small declines between 2015 and 2021 for both the NPZ and fished reference areas. However, this is likely to reflect random sampling of more abundant species (e.g., butterfly perch) or pelagic species (e.g., mackerel) rather than changes in resident reef species which mostly showed increases (Table 8).

Of the reef resident species, notable increases were seen both inside and outside the NPZ for morid cod (Moridae) species, draughtboard sharks (*Cephaloscyllium laticeps*), jackass morwong *(Nemadactylus macropterus*), striped trumpeter (*Latris lineata*) and ocean perch (*Helicolenus percoides*). All these species are either targeted by fisheries or caught as bycatch in the rock lobster fishery (draughtboard sharks, morid cod and ocean perch). However, all these species showed larger increases in abundance in the fished reference areas compared to the NPZ, indicating that recent fishing pressure is likely to be low in the fished reference area. The trends in both abundance and size of these species is explored in the detailed modelling and size frequency distribution sections below.

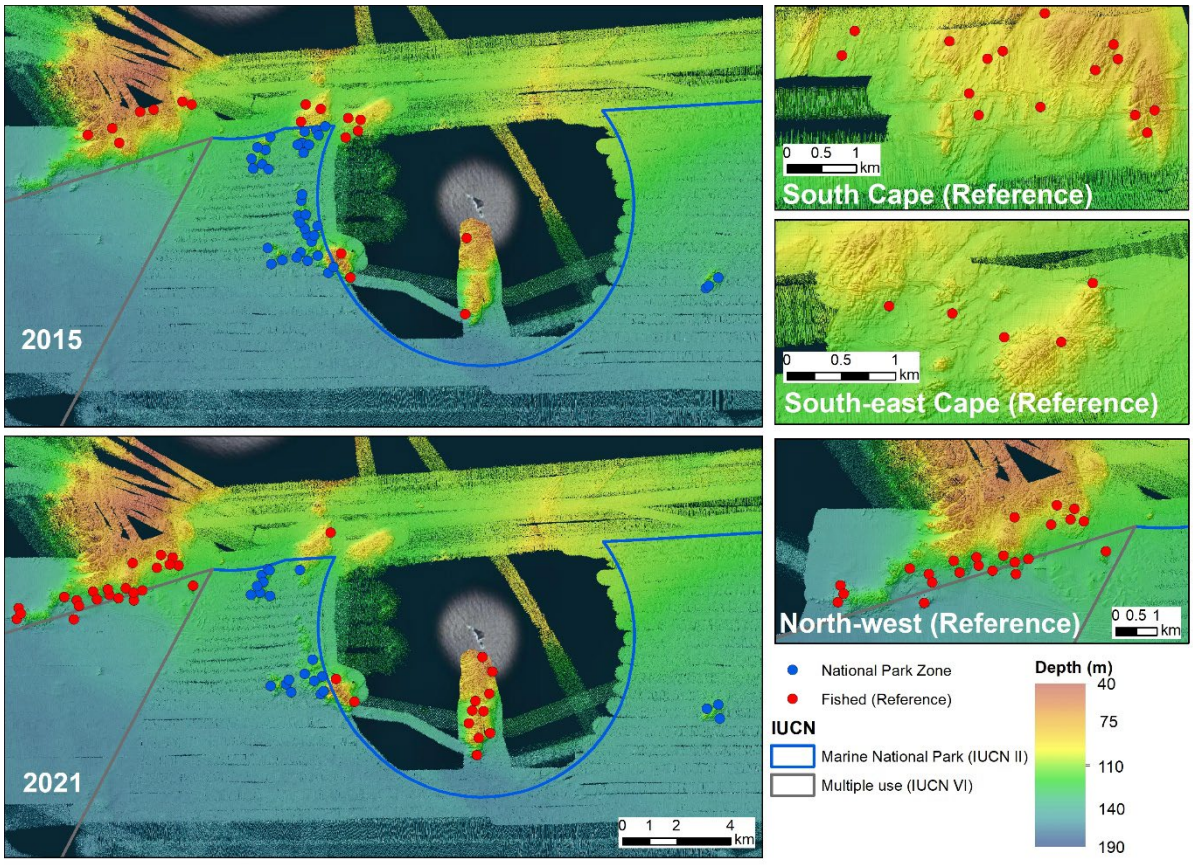

Figure 23. Map of BRUV deployments conducted in the NPZ and adjacent fished reference areas in 2015 and 2021.

Table 8. Abundance (total of MaxN) of fish species recorded in surveys of the Tasman Fracture Marine Park NPZ in 2015 and 2021 and in similar habitat in adjacent fished reference areas, including the TFMP MUZ. Baitfishes (order Clupeiformes) were not included in this table. Note that a larger number of stereo BRUVs were deployed in 2021 (113 vs 92 in 2015) and the survey design was changed to incorporate more deeper sites in the fished reference area in 2021.

Family	Scientific name	Common name	Reference 2015	Reference 2021	NPZ 2015	NPZ 2021	Habitat preference	Trophic group
Number of successful BRUV drops			48	53	46	60		
Berycidae	*Centroberyx spp*	Redfish	1	0	0	0	Reef/Pelagic	Demersal carnivore
Brachionichthyidae	*Brachionichthys australis*	Australian handfish	1	0	0	3	Reef	Demersal carnivore
	Brachiopsilus dianthus	Pink handfish	0	1	0	0	Reef	Demersal carnivore
Callanthiidae	*Callanthias australis*	Splendid perch	265	214	59	70	Reef/Pelagic	Demersal planktivore
Callorhinchidae	*Callorhinchus milii*	Elephantfish	0	1	0	0	Reef/Soft sediment	Demersal carnivore
Carangidae	*Pseudocaranx spp*	Trevally spp	0	5	0	0	Reef/Pelagic	Pelagic planktivore
	Trachurus declivis	Jack mackerel	745	0	430	0	Pelagic	Pelagic carnivore
	Trachurus spp	Mackerel spp	1331	2683	60	25	Pelagic	Pelagic carnivore
Centrolophidae	*Seriolella brama*	Blue warehou	2	1	0	0	Reef/Pelagic	Pelagic planktivore
Cheilodactylidae	*Nemadactylus macropterus*	Jackass morwong	103	214	214	285	Soft sediment	Demersal invertivore
Congridae	*Conger verreauxi*	Conger eel	0	2	2	1	Reef/Soft sediment	Demersal carnivore
Cyttidae	*Cyttus australis*	Silver dory	8	14	74	3	Reef/Soft sediment	Demersal invertivore
Dasyatidae	*Dasyatis brevicaudata*	Smooth stingray	1	0	0	0	Reef/Soft sediment	Demersal invertivore
Gempylidae	*Thyrsites atun*	Barracouta	8	0	0	0	Pelagic	Pelagic carnivore
Hexanchidae	*Notorynchus cepedianus*	Broadnose sevengill shark	2	4	0	1	Pelagic	Pelagic carnivore
Labridae	*Pseudolabrus rubicundus*	Rosy wrasse	106	110	26	29	Reef	Demersal invertivore
	Pseudolabrus spp	Wrasse spp	0	0	0	1	Reef	Demersal carnivore
	Notolabrus tetricus	Bluethroat wrasse	1	0	0	0	Reef	Demersal invertivore
Latridae	*Latris lineata*	Striped trumpeter	19	41	13	28	Reef/Soft sediment	Demersal invertivore
Macroramphosidae	*Notopogon lilliei*	Crested bellowsfish	0	71	5	59	Reef	Demersal invertivore
Monacanthidae	*Eubalichthys gunnii*	Gunn's leatherjacket	0	1	0	0	Reef	Browsing herbivore
	Meuschenia australis	Brownstriped leatherjacket	3	3	0	0	Reef	Browsing herbivore
	Meuschenia scaber	Cosmopolitan leatherjacket	150	71	11	11	Reef	Demersal invertivore
	Meuschenia spp	Leatherjacket spp	0	1	0	0	Reef	Demersal invertivore
	Thamnaconus degeni	Degen's leatherjacket	21	0	0	0	Reef	Demersal invertivore
Moridae	*Lotella rhacina*	Rock cod	1	4	0	1	Reef	Demersal carnivore
	Pseudophycis bachus	Red cod	65	232	59	156	Reef	Demersal carnivore
	Pseudophycis barbata	Southern codling	6	22	8	18	Reef	Demersal carnivore
	Pseudophycis spp	Cod spp	0	7	2	7	Reef	Demersal carnivore
Narcinidae	*Narcine tasmaniensis*	Tasmanian numbfish	0	0	1	0	Soft sediment	Demersal invertivore
Neosebastidae	*Neosebastes scorpaenoides*	Common gurnard perch	8	5	1	3	Reef	Demersal invertivore
Ophidiidae	*Genypterus tigerinus*	Rock ling	0	0	1	0	Reef/Soft sediment	Demersal invertivore
Ostraciidae	*Aracana aurita*	Shaw's cowfish	1	1	0	0	Reef	Demersal invertivore

Paraulopidae	*Paraulopus nigripinnis*	Blacktip cucumberfish	1	0	1	1	Soft sediment	Demersal invertivore
Pinguipedidae	*Parapercis allporti*	Barred grubfish	28	66	76	126	Soft sediment	Demersal invertivore
Platycephalidae	*Platycephalus spp*		1	0	0	0	Soft sediment	Demersal carnivore
Rajidae	*Dentiraja lemprieri*	Thornback skate	0	0	1	1	Soft sediment	Demersal carnivore
	Spiniraja whitleyi	Melbourne skate	4	2	2	0	Soft sediment	Demersal carnivore
Scombridae	*Thunnus spp*	Tuna spp	88	36	1	0	Pelagic	Pelagic carnivore
Scorpaenidae	*Scorpaena papillosa*	Southern red scorpionfish	1	10	3	8	Reef	Demersal invertivore
Scyliorhinidae	*Asymbolus rubiginosus*	Orange spotted catshark	3	3	7	10	Reef	Demersal carnivore
	Asymbolus spp	Catshark spp	0	2	0	0	Reef	Demersal carnivore
	Cephaloscyllium laticeps	Draughtboard shark	15	53	10	45	Reef	Demersal carnivore
Sebastidae	*Helicolenus percoides*	Ocean perch	75	203	192	262	Reef	Demersal carnivore
Serranidae	*Caesioperca lepidoptera*	Butterfly perch	2242	884	467	231	Reef	Pelagic planktivore
	Caesioperca rasor	Barber perch	5	1	5	0	Reef	Pelagic planktivore
	Caesioperca spp	Perch spp	31	18	4	31	Reef	Pelagic planktivore
	Hypoplectrodes maccullochi	Halfbanded seaperch	0	1	0	0	Reef	Demersal invertivore
	Lepidoperca pulchella	Eastern orange perch	0	7	8	16	Reef/Pelagic	Pelagic planktivore
	Plectranthias maculicauda	Spot-tail perchlet	0	0	0	1	Reef/Pelagic	Pelagic planktivore
Syngnathidae	*Hippocampus jugumus*	Collared seahorse	0	1	0	0	Reef/Pelagic	Benthic invertivore
	Solegnathus spinosissimus	Spiny pipehorse	0	0	0	1	Reef	Pelagic planktivore
Trachichthyidae	*Paratrachichthys macleayi*	Sandpaper fish	17	10	11	4	Reef	Demersal carnivore
Triakidae	*Mustelus antarcticus*	Gummy shark	0	7	0	4	Reef/Soft sediment	Demersal carnivore
Triglidae	*Pterygotrigla polyommata*	Latchet	0	0	0	1	Soft sediment	Demersal
Urolophidae	*Urolophus cruciatus*	Banded stingaree	2	1	3	1	Soft sediment	Demersal invertivore
	Urolophus paucimaculatus	Sparsely spotted stingaree	2	1	0	0	Soft sediment	Demersal invertivore
	Urolophus spp	Stingaree spp.	0	1	0	0	Soft sediment	Demersal invertivore
	Totals		5363	5015	1757	1444		

3.1 Size frequency distributions and abundance maps

Length-frequency plots and abundance maps are shown below for fish species that are potentially affected by fishing pressure and where sufficient numbers were seen and able to be measured from the stereo imagery. These included jackass morwong (*Nemadactlyus macropterus*), ocean perch (*Helioclenus percoides*), Morid cods (*Moridae* species), striped trumpeter (*Latris lineata*) and draughtboard shark (*Cephaloscyllum laticeps*), a bycatch species in the rock lobster fishery.

There were increases in the mean size of all species inside the NPZ between 2015 and 2021, with the exception of striped trumpeter which remained relatively stable between surveys, with just a small decrease in the mean size (Table 9), although the measured sample size was likely too low to give confidence in this trend. Of particular note was the increase in mean size of jackass morwong of > 7 cm between 2015 and 2021 in the NPZ, presumably related to a large number of juveniles seen in 2015, that had subsequently grown. In the fished reference area, mean sizes of most species remained relatively stable, but with a notable decrease in mean size of jackass morwong. Despite that, the average size in the fished reference area remained above that of the NPZ.

Table 9. Mean lengths, range of lengths, number measured, and proportion measured for selected targeted fish species.

Species	No. (propn.) measured	Reference 2015	No. (propn.) measured	Reference 2021	No. (propn.) measured	NPZ 2015	No. (propn.) measured	NPZ 2021
Cephaloscyllium laticeps	6 (40%)	576 (369-774)	38 (72%)	661 (414-1669)	5 (45%)	388 (309 - 466)	38 (84%)	608 (316-917)
Helicolenus percoides	41 (53%)	219 (78-337)	151 (74%)	200 (36-310)	85 (41%)	181 (42 - 307)	197 (75%)	202 (92-342)
Latris lineata	15 (79%)	609 (488-936)	31 (76%)	637 (487-917)	6 (46%)	616 (515 - 743)	18 (64%)	609 (352-734)
Nemadactylus macropterus	31 (30%)	298 (99-584)	142 (66%)	234 (89-443)	115 (54%)	137 (40 - 334)	178 (62%)	215 (103-362)
Moridae	50 (68%)	320 (78-467)	184 (69%)	311 (143-521)	52 (68%)	224 (85 - 592)	150 (82%)	297 (135-441)

3.1.1 Jackass morwong

The abundance of jackass morwong increased in both the NPZ and fished reference areas between 2015 and 2021, at least in part reflecting some of the changes in survey location, with a larger increase occurring in the fished reference area, including significant numbers in the new, deeper sample sites to the NW of the NPZ and south of the Mewstone (Figure 24). Hotspots of abundance remained mostly consistent between 2015 and 2021 surveys at sites sampled on both occasions (Figure 24).

An increase in the proportion of larger individuals can be seen in the length frequency distribution of jackass morwong between 2015 and 2021 (Figure 25), with the large cohort of juveniles (< 150 mm) observed in 2015 (especially in the NPZ) being absent in 2021. This likely reflects the growth of this cohort into adult-sized fish between surveys. It appears that only small amounts of recruitment have occurred between surveys, with a much smaller proportion of smaller-sized fish being apparent in 2021 relative to 2015.

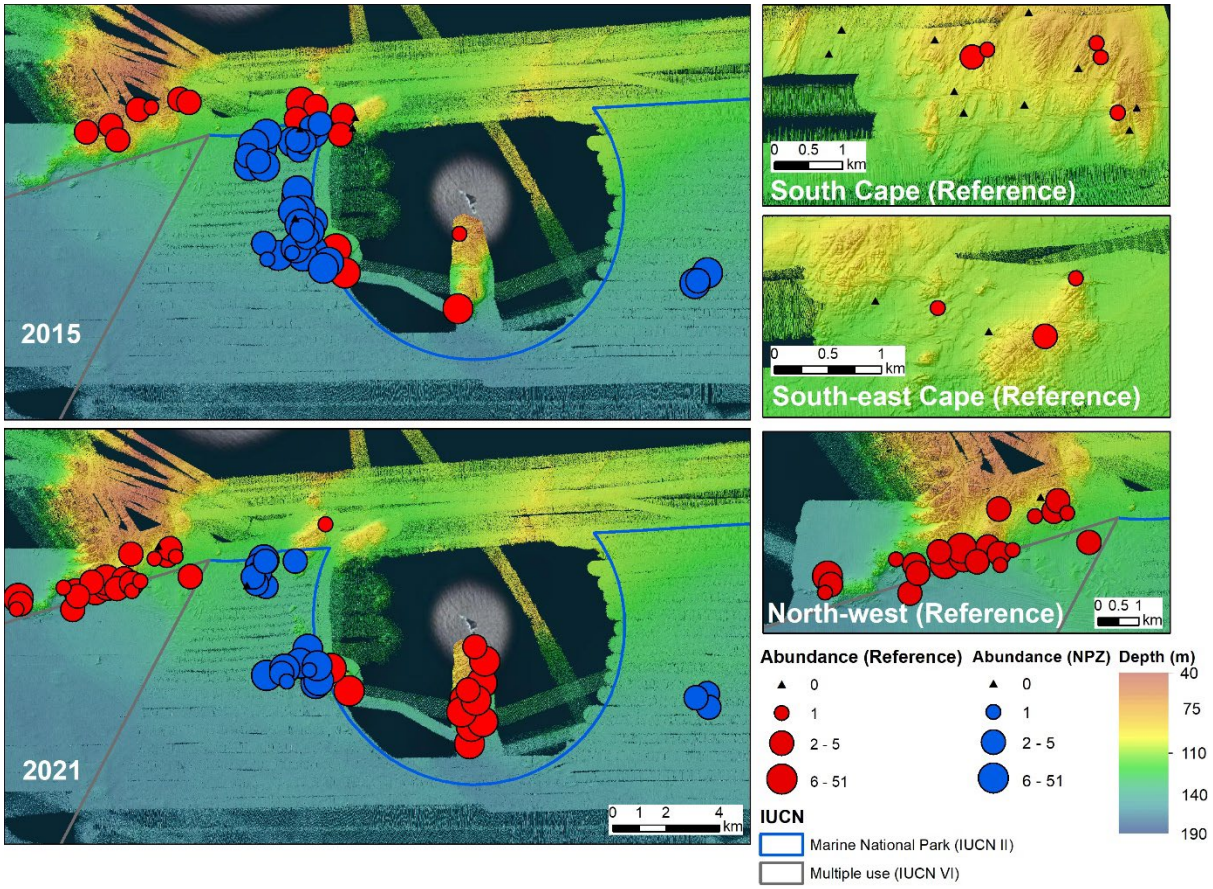

Figure 24. Abundance map of jackass morwong observations in the 2015 and 2021 stereo BRUV surveys.

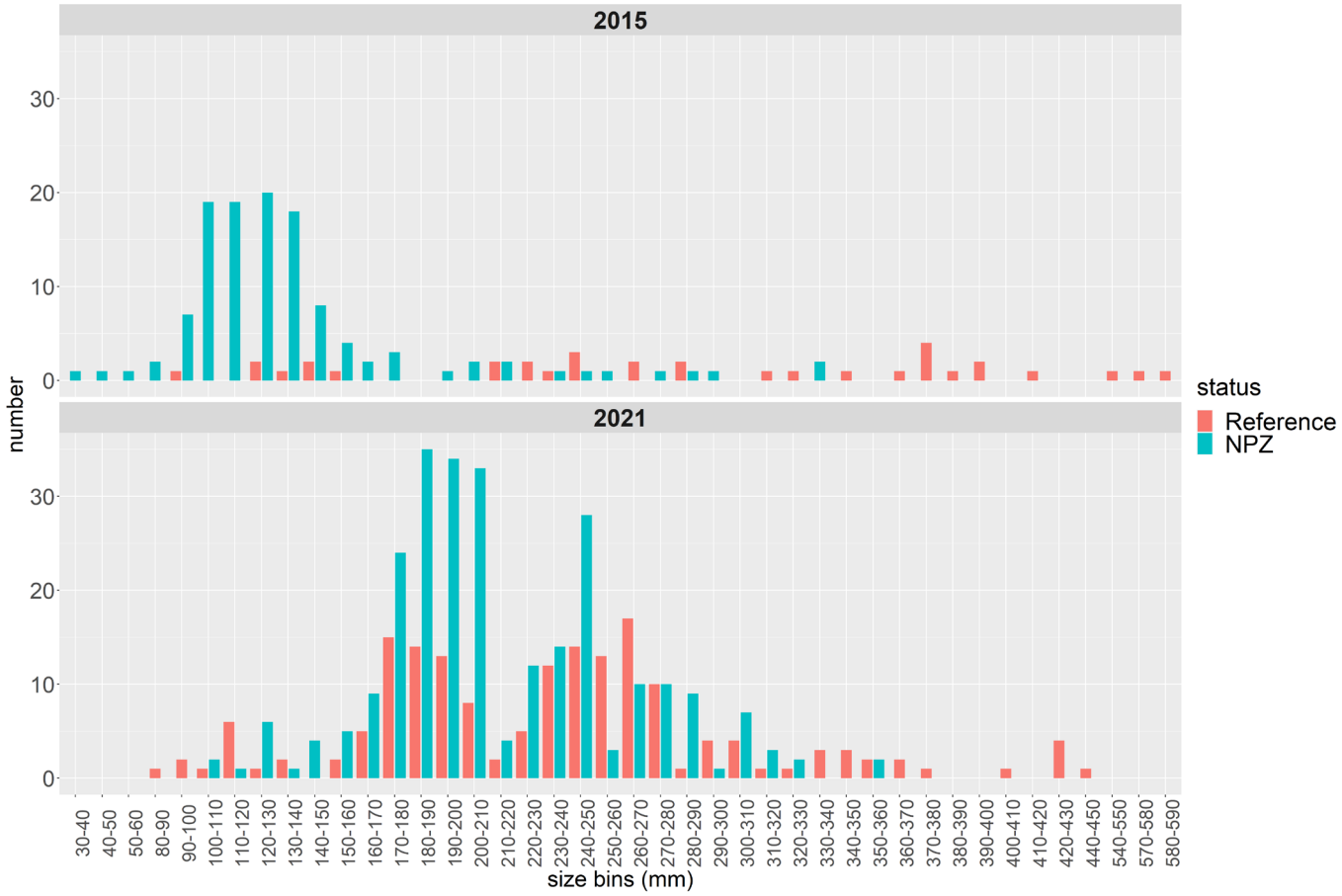

Figure 25. Length-frequency distribution of jackass morwong inside the NPZ and fished reference area between 2015 and 2021. Note that a different proportion of individuals were measured between the surveys (Table 9).

3.1.2 Ocean perch

The abundance of ocean perch increased in the NPZ and fished reference areas between 2015 and 2021, with a larger increase occurring in the fished reference area (Figure 26). However, at least in part, that increase reflected some of the changes in survey locations in the fished reference area between the 2015 and 2021 surveys (Figure 23) where this species was particularly abundant in some of the newer and deeper sites to the NW of the NPZ and south of the Mewstone. Hotspots of abundance remained mostly consistent between surveys at the sites surveyed in both periods (Figure 26).

There was no marked change in the length frequency distribution of ocean perch between 2015 and 2021 or between areas, with the size distribution observed in 2015 being similar to that in 2021, albeit with increases in abundance across all size classes (Figure 27).

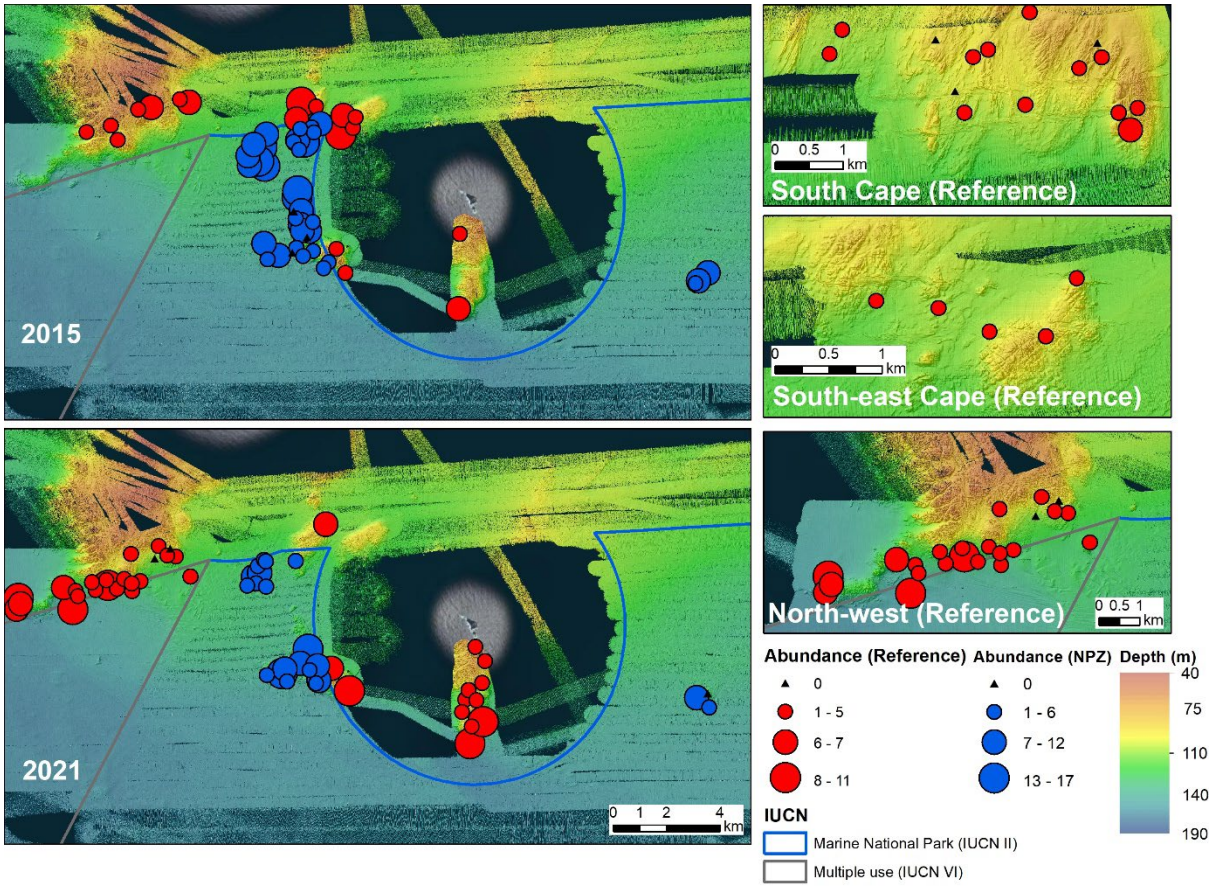

Figure 26. Abundance map of ocean perch observations in the 2015 and 2021 stereo BRUV surveys.

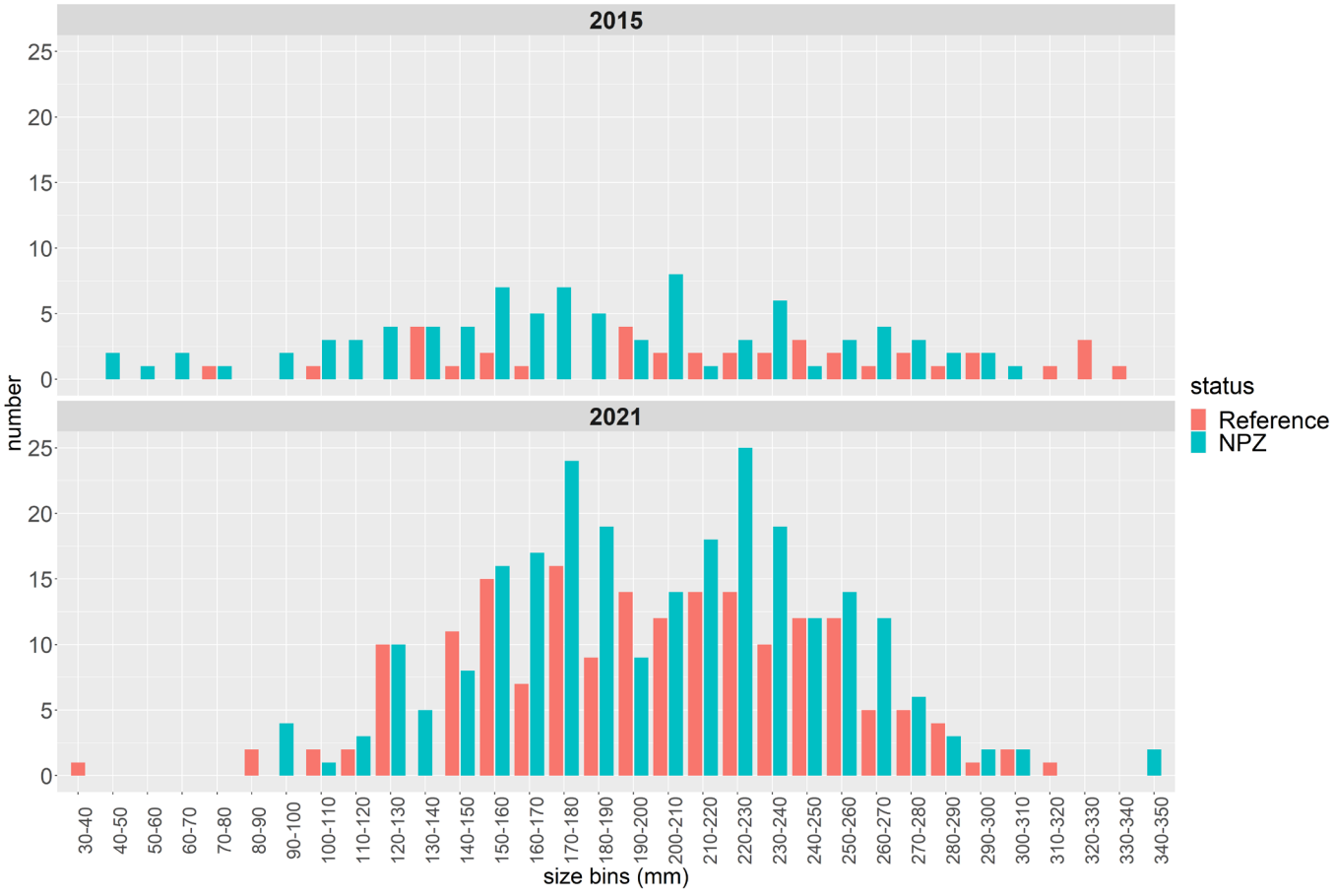

Figure 27. Length-frequency distribution of jackass morwong inside the NPZ and fished reference area between 2015 and 2021. Note that a different proportion of individuals were measured between the surveys (Table 9).

3.1.3 Morid cods

The abundance of morid cods increased in the NPZ and fished reference areas between 2015 and 2021 (Figure 28) although hotspots of abundance remained mostly consistent between surveys. The increase in sites with cod present in the fished reference area to the NW of the NPZ and to the south of the Mewstone mostly reflected some of the changes in survey locations between 2015 and 2021 (Figure 23).

There was a decrease in the proportion of smaller individuals in the length frequency distribution of morid cod between 2015 and 2021, with the cohort of the smallest size classes observed in 2015 being largely absent in 2021, and an overall increase in the frequency of all other size classes reflecting the increase in abundance (Figure 29).

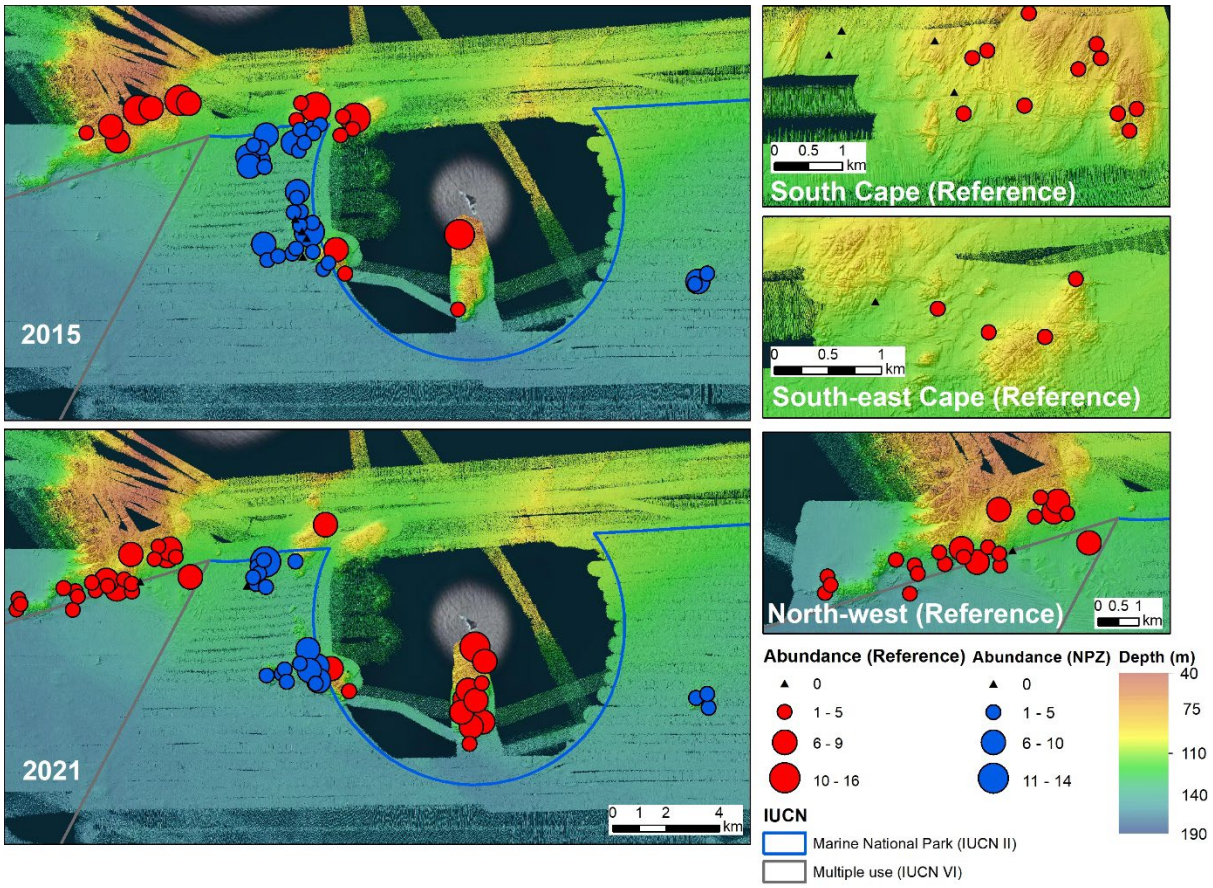

Figure 28. Abundance map of morid cod observations in the 2015 and 2021 stereo BRUV surveys.

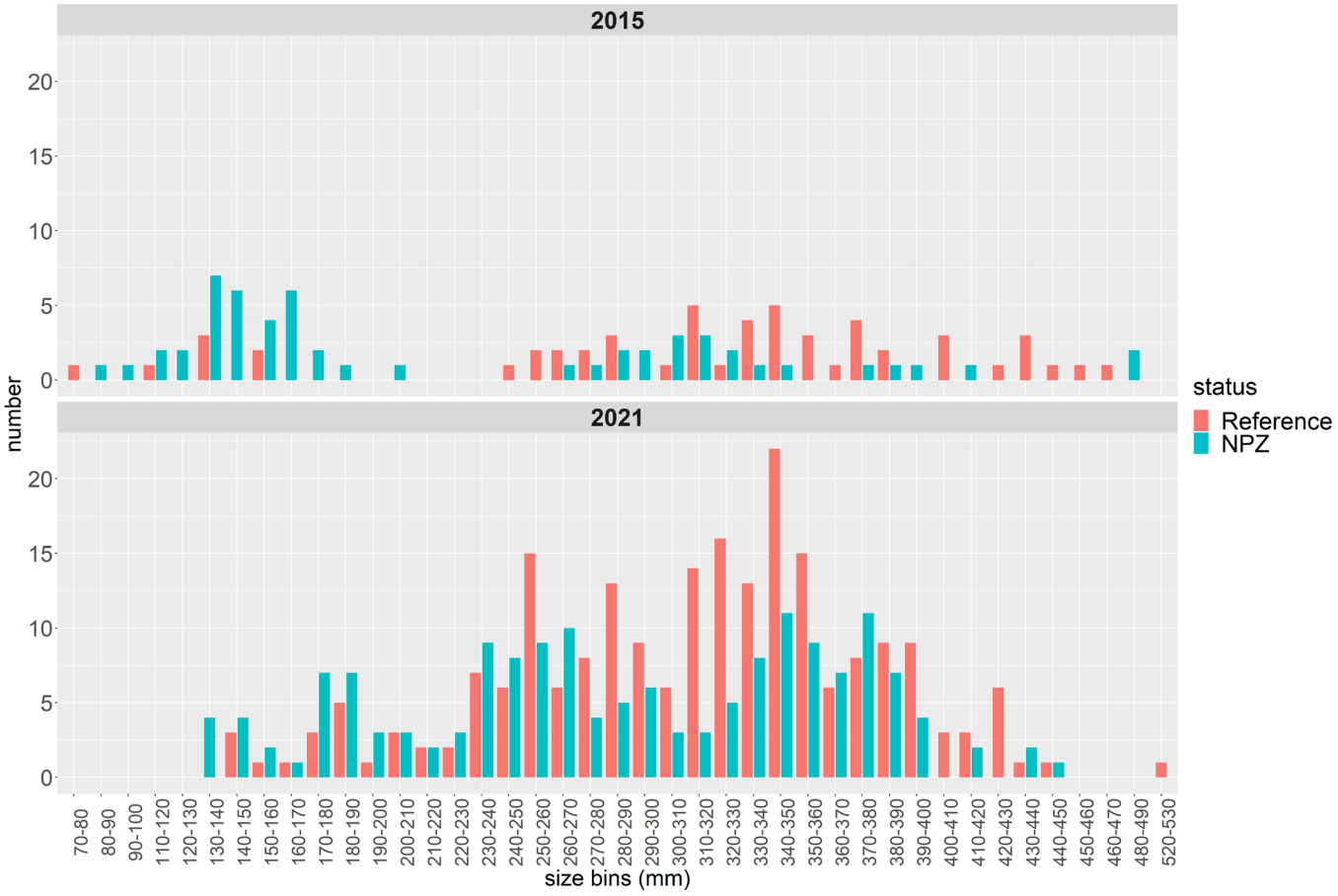

Figure 29. Length-frequency distribution of morid cod inside the NPZ and fished reference area between 2015 and 2021. Note that a different proportion of individuals were measured between the surveys (Table 9).

3.1.5 Striped trumpeter

The abundance of striped trumpeter increased in the NPZ and fished reference areas between 2015 and 2021 (Figure 30). Hotspots of abundance remained mostly consistent between surveys, with the exception of the fished reference area south of the Mewstone, which was a hotspot in 2021 but was absent of fish in 2015. However, this in part reflected some of the changes in survey locations between 2015 and 2021 (Figure 23), with addition of extra sites in this area.

There were insufficient numbers of observed individual striped trumpeter to make meaningful length-frequency plots.

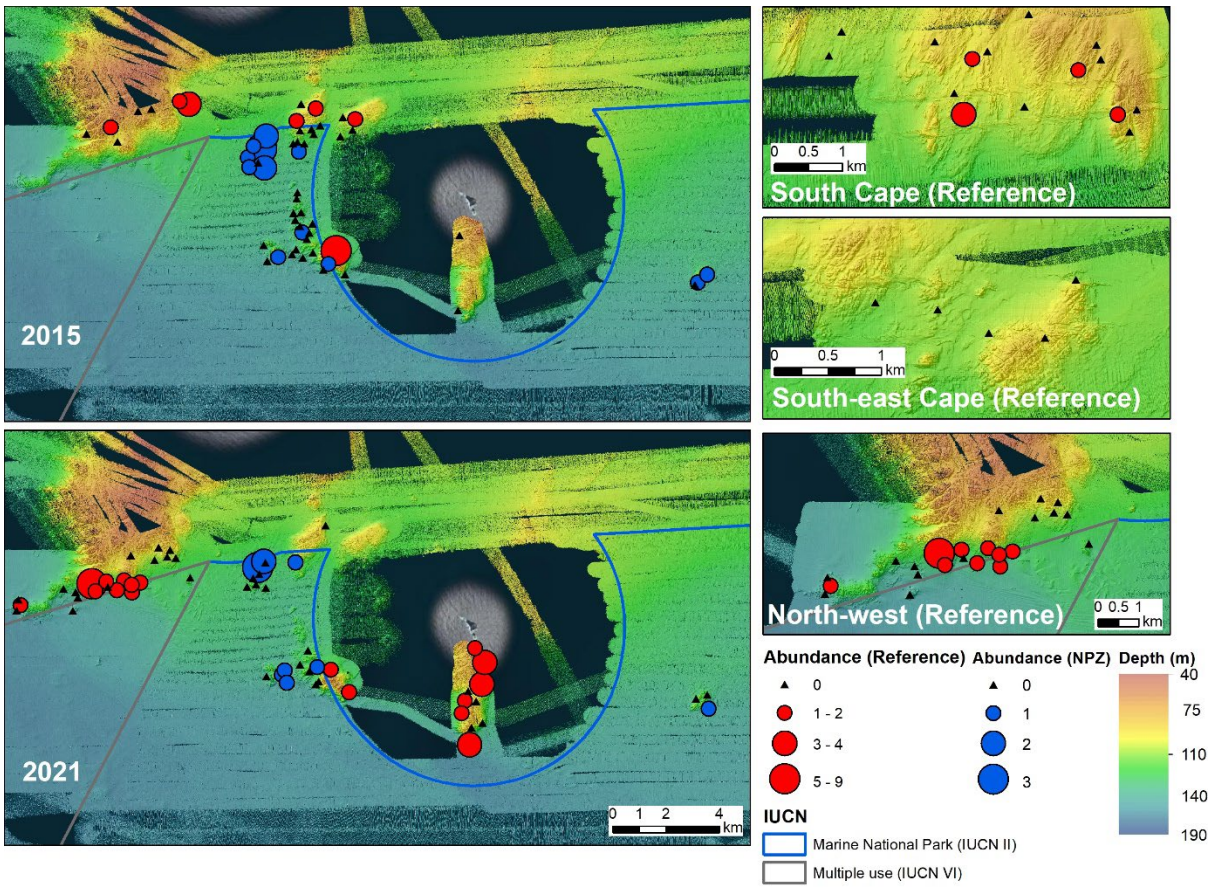

Figure 30. Abundance map of striped trumpeter observations in the 2015 and 2021 stereo BRUV surveys.

3.1.6 Draughtboard sharks

The abundance of draughtboard sharks increased in the NPZ and fished reference areas between 2015 and 2021 (Figure 31). Hotspots of abundance remained mostly consistent at sites repeated between surveys, however, the notable catches in the fished reference area south of the Mewstone and along the NW park boundary reflected some of the additions in survey locations between 2015 and 2021 (Figure 23).

There were insufficient numbers of observed individual draughtboard sharks to make meaningful length-frequency plots.

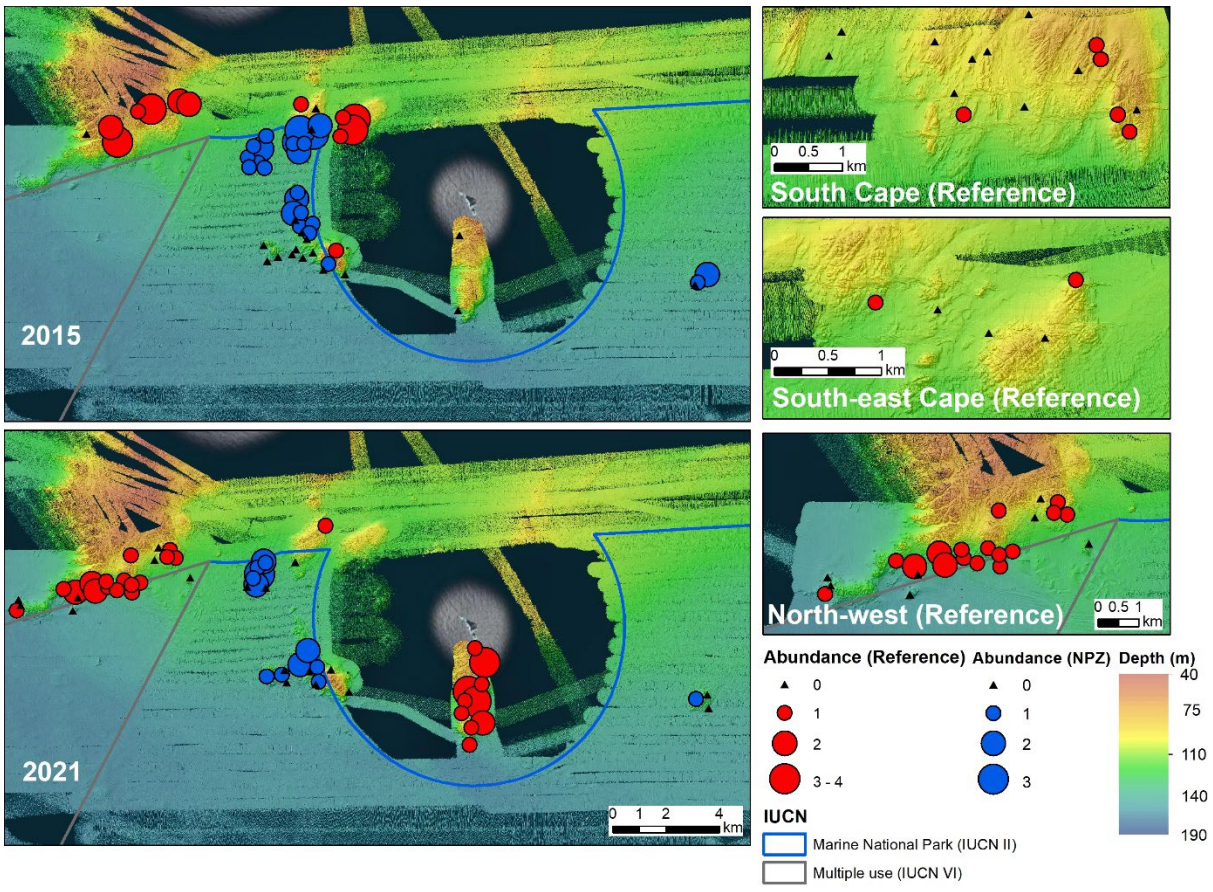

Figure 31. Abundance map of draughtboard shark observations in the 2015 and 2021 stereo BRUV surveys.

3.2 Detailed modelling of demersal fishes

Following on from previous modelling conducted on the initial 2015 survey data, analysis was conducted for the same subset of key species and the same metrics to assess changes that had occurred between 2015 and 2021. The key species modelled were jackass morwong, ocean perch, morid cods, striped trumpeter, and draughtboard sharks. These species were chosen as they had sufficient data to model and are species commonly targeted in fisheries or are important bycatch species in the rock lobster fishery. Metrics modelled were: (i) abundance, (ii) average size, and (iii) abundance of legal-sized fish for jackass morwong and striped trumpeter. For (iii) these two species were selected as they are target species and have specified size-limits. Therefore, fishing is expected to reduce the abundance of fish above the legal-size limits. For jackass morwong, the legal size is 25 cm, and for striped trumpeter the legal-size limit is 55 cm.

The same Bayesian model-based approach used in modelling the rock lobster potting data was used with the same environmental covariates of depth, depth-squared (to capture non-linear effects) and rugosity derived from multibeam data at scales of 50- and 500-metres. A stepwise model fitting approach was used and only covariates in the best-fitting model were retained in the final reported models.

3.2.1 Jackass morwong

3.2.1.1 Abundance

No overall effect of protection, or protection through time (the NPZ*Year interaction) were found for the abundance of jackass morwong in the BRUV data (Table 10 and Figure 32), with posterior distributions of coefficients including zero. Results suggest an increase in abundance of jackass morwong in the NPZ and fished reference areas between 2015 and 2021, although the effect is small and once again would not be considered statistically significant.

Positive effects of increasing depth and rugosity at 500 m scale were found for the abundance of jackass morwong, indicating a preference for complex habitat at deeper depths in the surveyed area (Figure 33 and Figure 34).

Table 10. Model-based estimates for the abundance (MaxN per stereo BRUV drop) of jackass morwong. Effects highlighted green indicate evidence for a positive effect whereas effects highlighted red indicate there is evidence for a negative effect. Estimates are on the linear predictor (log) scale.

Effect	mean	sd	0.025 quantile	0.975 quantile
intercept	0.873	0.165	0.546	1.195
NPZ	-0.036	0.267	-0.560	0.488
Year	0.089	0.140	-0.185	0.365
NPZ*Year	0.009	0.168	-0.322	0.339
Depth	0.584	0.114	0.361	0.807
Rugosity 500 m	0.470	0.093	0.288	0.652

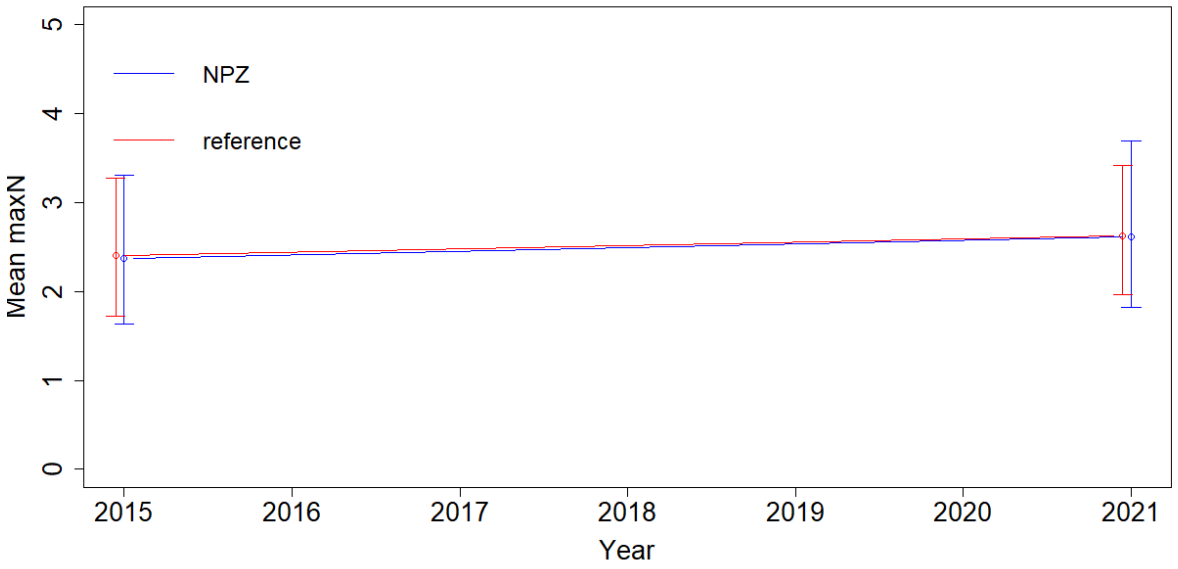

Figure 32. Model-based estimate of trends in relative abundance (MaxN per stereo BRUV drop) for jackass morwong inside the NPZ and in the fished reference areas between 2015 and 2021. Error bars represent 95% credible intervals. Estimates are made at mean depth and rugosity values over the survey area.

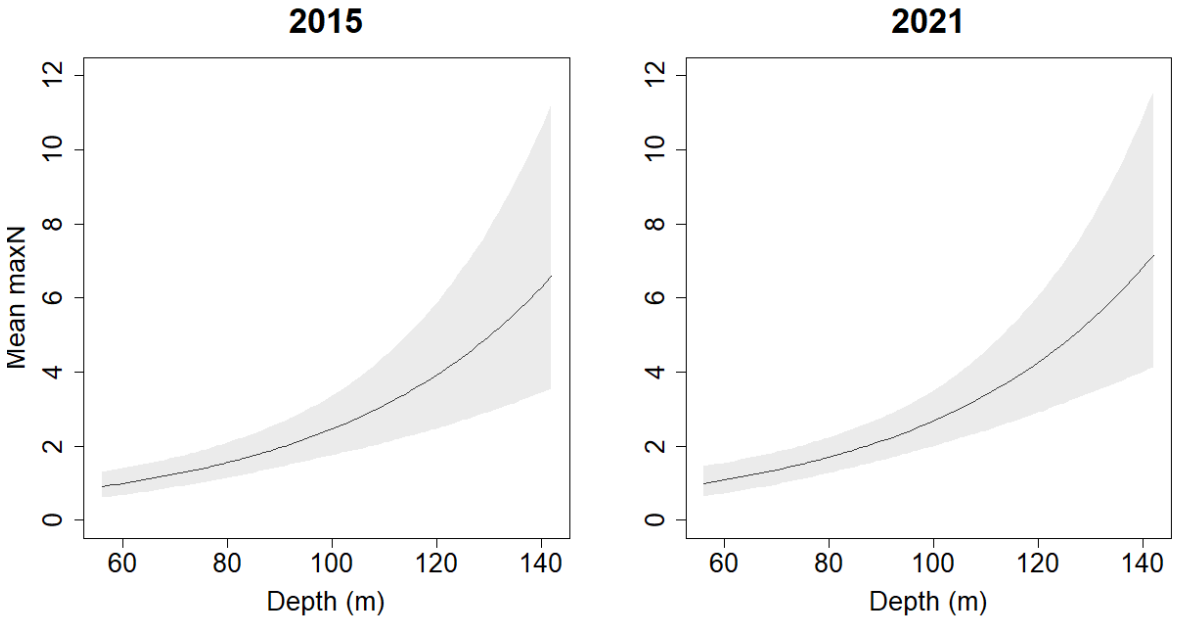

Figure 33. Model-based estimate of the relationship between abundance (MaxN) and depth for jackass morwong based on the 2015 and 2021 data. Line shows the mean response and shading shows 95% credible intervals.

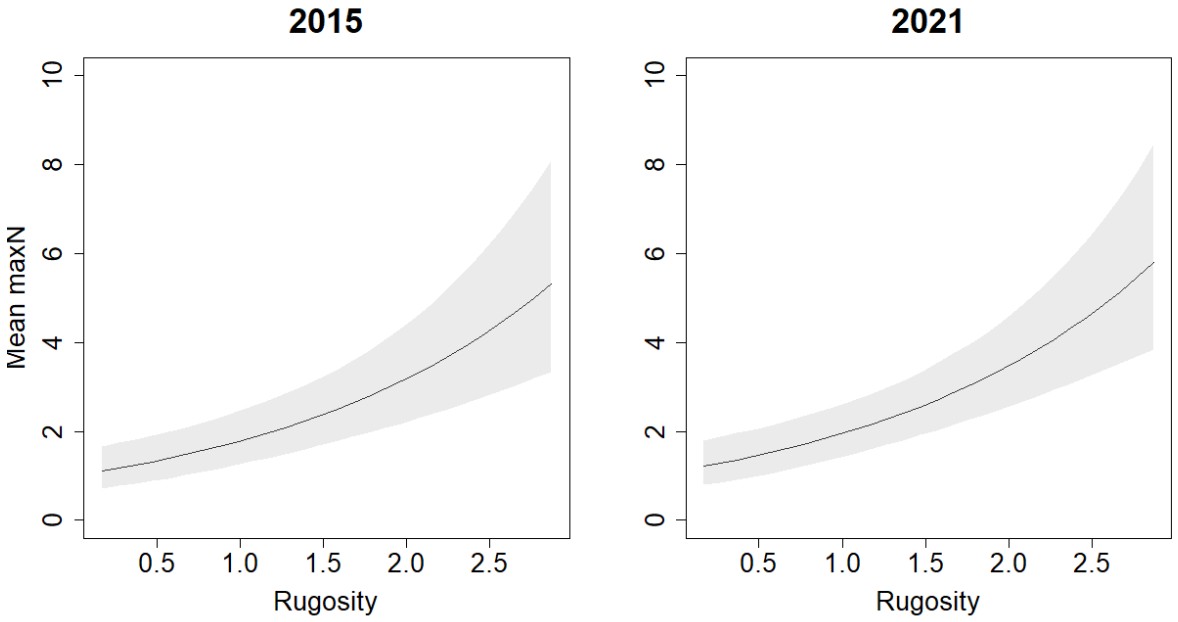

Figure 34. Model-based estimate of the relationship between abundance (MaxN) and rugosity at 500 m for jackass morwong from the 2015 and 2021 survey data. Line shows the mean response and shading shows 95% credible intervals.

3.2.1.2 Average size

The mean size of jackass morwong across the entire survey area and both surveys was 28.6 cm (Table 4). A lower mean size of jackass morwong was found for the NPZ in 2015, with fish on average 8 cm smaller in the NPZ (Table 11). No significant overall change in average size was observed between 2015 and 2021. However, a positive interaction between protection and year indicates that the average size increased more in the NPZ than the adjacent fished reference area between 2015 and 2021 (Table 11 and Figure 35).

Negative relationships were found for both depth and rugosity at a 500 m scale, indicating that larger jackass morwong prefer shallower and less complex habitat at a 500 m scale across the surveyed area (Figure 36 and Figure 37).

Table 11. Model-based estimates for the mean size of jackass morwong. Effects highlighted green indicate evidence for a positive effect whereas effects highlighted red indicate there is evidence for a negative effect. Estimates are in centimetres.

Effect	mean	sd	0.025 quantile	0.975 quantile
intercept	28.587	2.592	23.498	33.672
NPZ	-8.278	2.769	-13.715	-2.846
Year	-3.366	2.208	-7.702	0.966
NPZ*Year	9.422	2.727	4.069	14.771
Depth	-3.808	0.892	-5.560	-2.058
Rugosity 500 m	-1.490	0.724	-2.911	-1.490

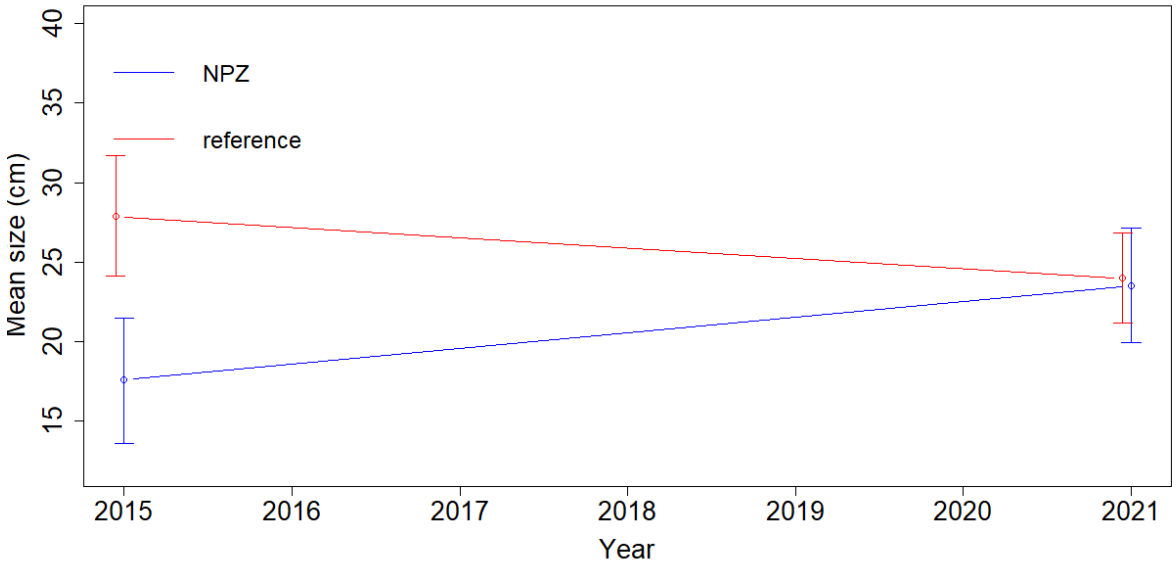

Figure 35. Model-based estimate of trends in mean size for jackass morwong inside the NPZ and in the fished reference areas between 2015 and 2021. Error bars represent 95% credible intervals. Estimates are made at mean depth and rugosity values over the survey area.

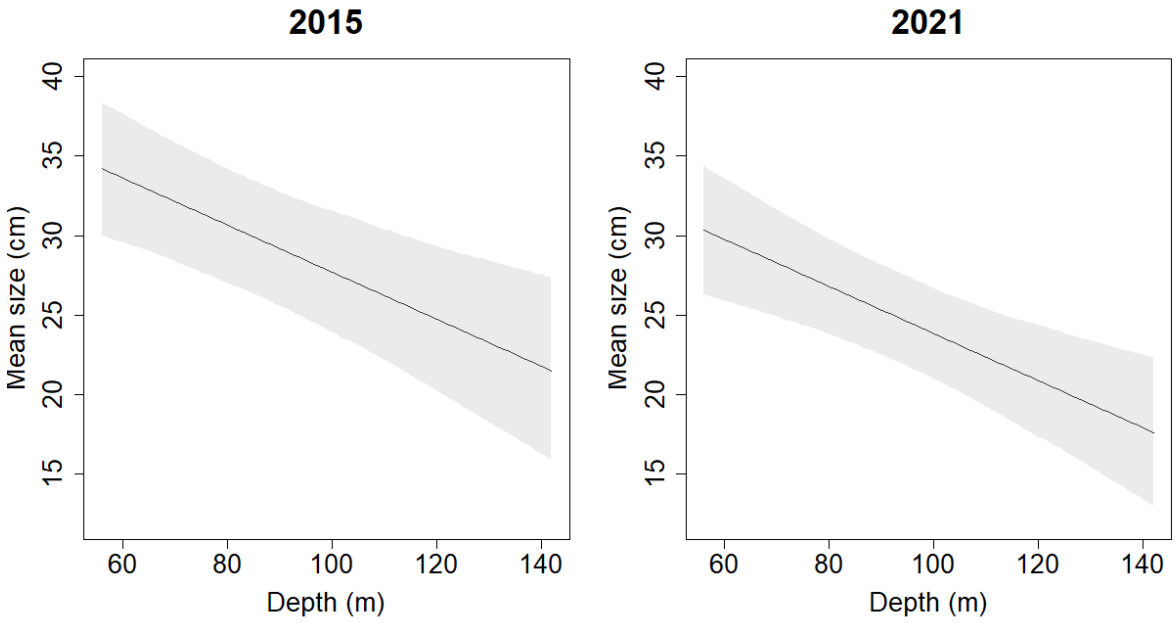

Figure 36. Model-based estimate of the relationship between mean size and depth for jackass morwong. Line shows the mean response and shading shows 95% credible intervals.

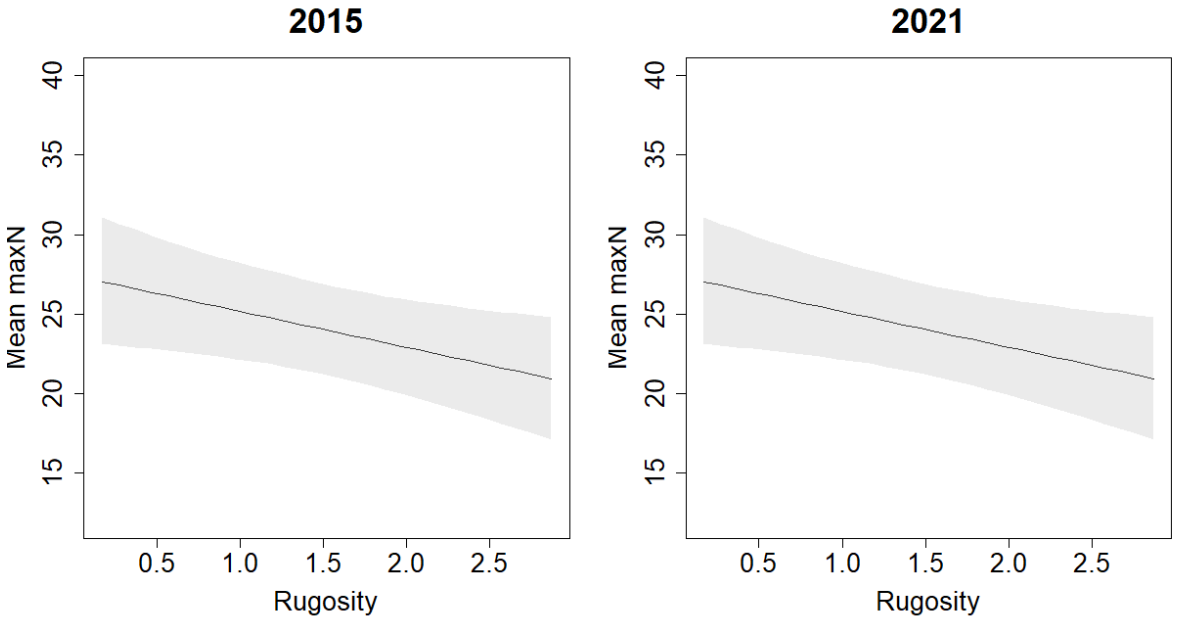

Figure 37. Model-based estimate of the relationship between mean size and rugosity at 500 m for jackass morwong for the 2015 and 2021 survey data. Line shows the mean response and shading shows 95% credible intervals.

3.2.1.3 Abundance of legal-sized

An overall increase in legal-sized jackass morwong was observed, in the NPZ and fished reference areas, between 2015 and 2021 (year effect, Table 12). There is no evidence for a strong effect of protection or the interaction of protection through time on the abundance of legal-sized individuals (Figure 38). There were also no strong correlations between environmental covariates of depth and rugosity on the abundance of legal-sized jackass morwong.

Table 12. Model-based estimates for the abundance of legal-sized (> 25 cm) jackass morwong per stereo BRUV drop. Effects highlighted green indicate evidence for a positive effect whereas effects highlighted red indicate there is evidence for a negative effect. Estimates are on the linear predictor (log) scale.

Effect	mean	sd	0.025 quantile	0.975 quantile
intercept	-1.407	0.348	-2.107	-0.740
NPZ	-0.846	0.647	-2.148	0.392
Year	0.764	0.318	0.155	1.404
NPZ*Year	0.383	0.561	-0.678	1.525
Depth	-0.184	0.195	-5.568	0.198

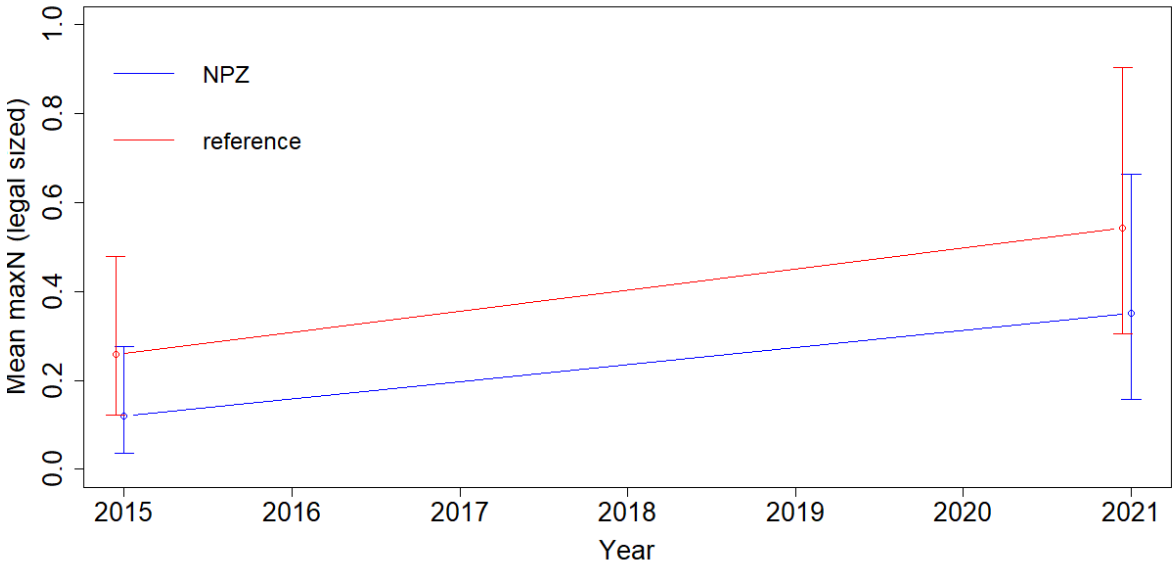

Figure 38. Model-based estimate of trends in the abundance of legal-sized jackass morwong (> 25 cm) inside the NPZ and in the fished reference areas between 2015 and 2021. Error bars represent 95% credible intervals. Estimates are made at mean depth and rugosity values over the survey area.

3.2.2 Striped trumpeter

3.2.2.1 Abundance

No effects of protection or time were found for the abundance of striped trumpeter (Table 13 and Figure 39), with abundances remaining relatively stable between survey times and protection levels.

A positive effect of rugosity at a 50 m scale was found (Figure 40) indicating striped trumpeter have a preference for complex habitat at a 50 m scale.

Table 13. Model-based estimates for the abundance (MaxN per BRUV drop) of jackass morwong. Effects highlighted green indicate evidence for a positive effect whereas effects highlighted red indicate there is evidence for a negative effect. Estimates are on the linear predictor (log) scale.

Effect	mean	sd	0.025 quantile		0.975 quantile
intercept	-1.532	0.362	-2.260		-0.838
NPZ	-0.610	0.611	-1.814		0.583
Year	0.417	0.335	-0.230		1.085
NPZ*Year	-0.084	0.483	-1.028		0.868
Depth	0.026	0.223	-0.412		0.463
Rugosity 50 m	0.416	0.153	0.115		0.714

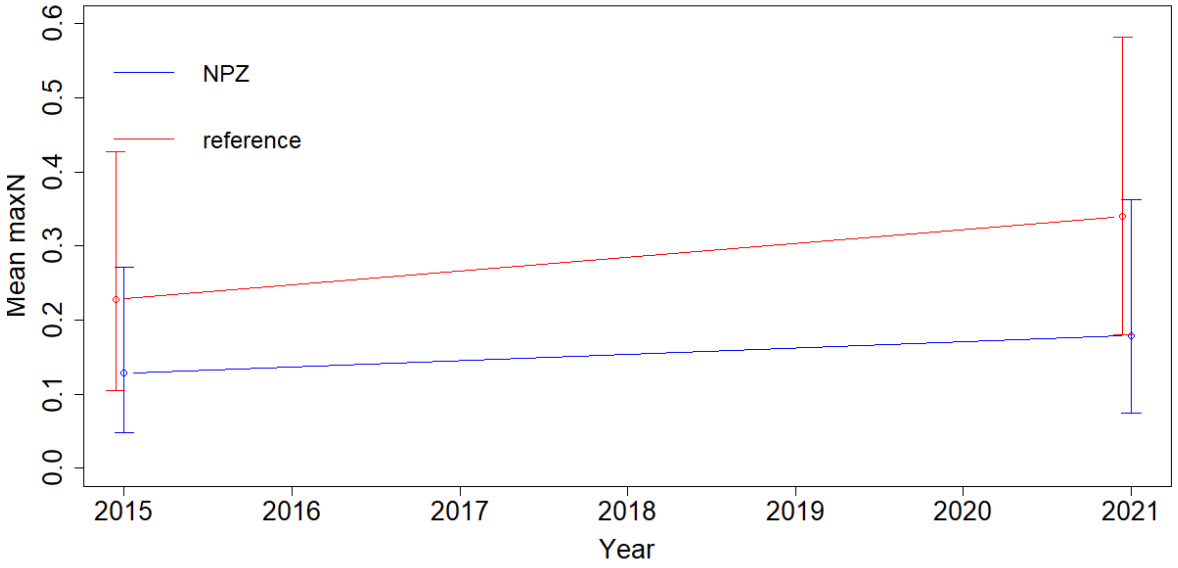

Figure 39. Model-based estimate of trends in relative abundance (MaxN per BRUV drop) for striped trumpeter inside the NPZ and in the fished reference areas between 2015 and 2021. Error bars represent 95% credible intervals. Estimates are made at mean depth and rugosity values over the survey area.

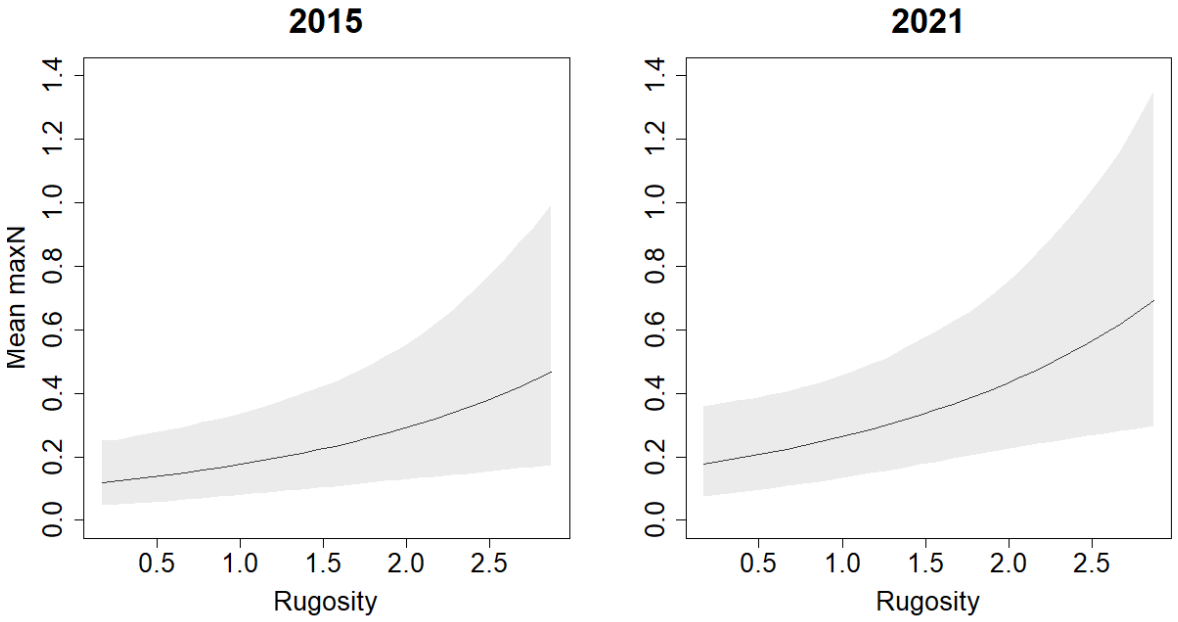

Figure 40. Model-based estimate of the relationship between abundance (MaxN) and rugosity at 50 m for striped trumpeter for the 2015 and 2021 data. Line shows the mean response and shading shows 95% credible intervals.

3.2.2.2 Average size

The mean size of striped trumpeter across the entire survey area and both surveys was 64.9 cm (Table 14), a value somewhat above the minimum legal size of 55 cm. No effects of protection or time were found for the average size of striped trumpeter (Table 14 and Figure 41), with sizes remaining relatively stable between survey times and protection levels. Also, no relationships were found between environmental covariates of rugosity and depth and the size of striped trumpeter.

Table 14. Model-based estimates for the mean size of striped trumpeter. Effects highlighted green indicate evidence for a positive effect whereas effects highlighted red indicate there is evidence for a negative effect. Estimates are in centimetres.

Effect	mean	sd	0.025 quantile	0.975 quantile
intercept	64.962	3.812	57.478	72.440
NPZ	-6.540	6.323	-18.955	5.864
Year	0.774	4.234	-7.569	9.051
NPZ*Year	-0.354	6.868	-13.839	13.119
Depth	2.327	1.871	-1.345	5.997

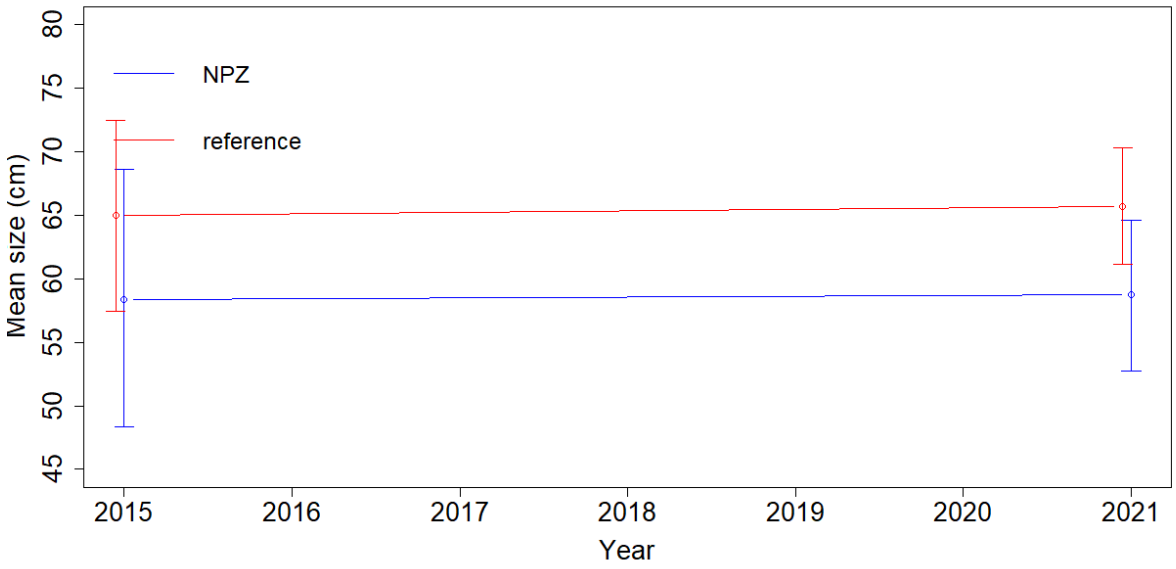

Figure 41. Model-based estimate of trends in mean size of striped trumpeter inside the NPZ and in the fished reference areas between 2015 and 2021. Error bars represent 95% credible intervals. Estimates are made at mean depth and rugosity values over the survey area.

3.2.2.3 Abundance of legal-sized individuals

Evidence was found for a positive effect of year on the abundance of legal-sized striped trumpeter (Table 15 Figure 42), indicating an overall increase. This increase was larger in the fished reference area, although the difference was not found to be significantly different to the NPZ.

Table 15. Model-based estimates for the abundance of legal-sized (> 55 cm) striped trumpeter per stereo BRUV drop. Effects highlighted green indicate evidence for a positive effect whereas effects highlighted red indicate there is evidence for a negative effect. Estimates are on the linear predictor (log) scale.

Effect	mean	sd	0.025 quantile	0.975 quantile
intercept	-2.739	0.539	-3.863	-1.745
NPZ	-0.017	0.847	-1.700	1.627
Year	1.421	0.553	0.394	2.567
NPZ*Year	-0.734	0.810	-2.307	0.871
Depth	-0.117	0.245	-0.599	0.364

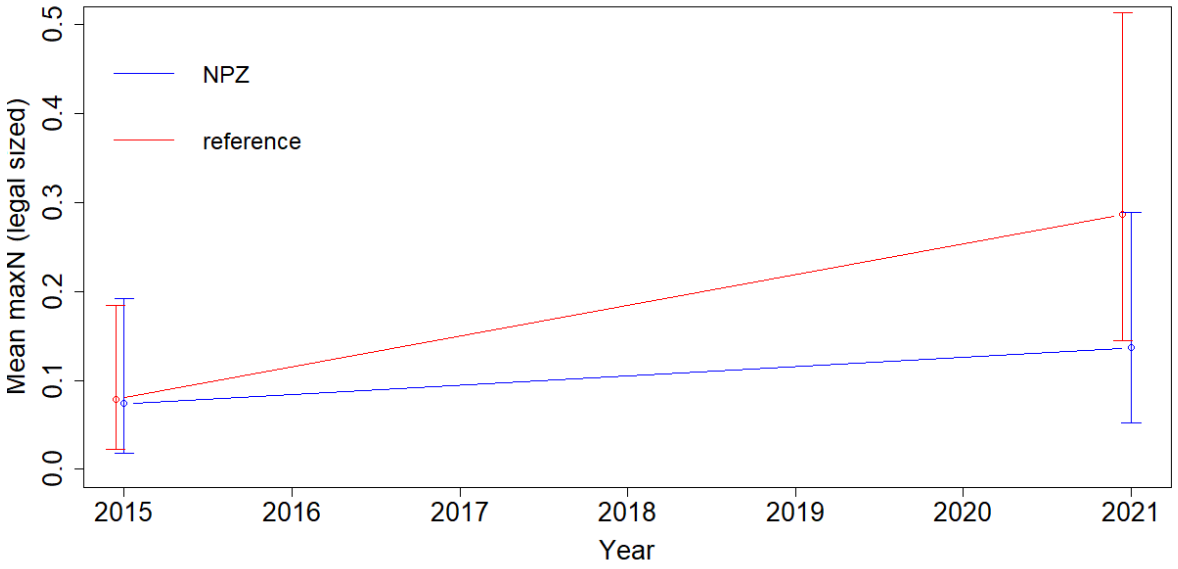

Figure 42. Model-based estimate of trends in the abundance of legal-sized striped trumpeter (> 55 cm) inside the NPZ and in the fished reference areas between 2015 and 2021. Error bars represent 95% credible intervals. Estimates are made at mean depth and rugosity values over the survey area.

3.2.3 Morid cod

3.2.3.1 Abundance

Evidence was found for an initial higher abundance of morid cod in the NPZ and an overall increase in the abundance of morid cod between survey times (NPZ effect, Table 16, and Figure 43). However, there was a larger increase in the abundance of morid cod in the fished reference area compared to the NPZ (negative NPZ*Year interaction, Table 16 and Figure 43).

A negative correlation between depth and abundance of morid cod was found (Figure 44) indicating a preference for shallow depths in the survey region.

Table 16. Model-based estimates for the abundance (MaxN per BRUV drop) of morid cod. Effects highlighted green indicate evidence for a positive effect whereas effects highlighted red indicate there is evidence for a negative effect. Estimates are on the linear predictor (log) scale.

Effect	mean	sd	0.025 quantile	0.975 quantile
intercept	-0.032	0.142	-0.318	0.241
NPZ	0.555	0.207	0.150	0.961
Year	1.423	0.143	1.149	1.709
NPZ*Year	-0.752	0.204	-1.152	-0.353
Depth	-0.377	0.062	-0.500	-0.256
Rugosity 500 m	-0.071	0.052	-0.173	0.029

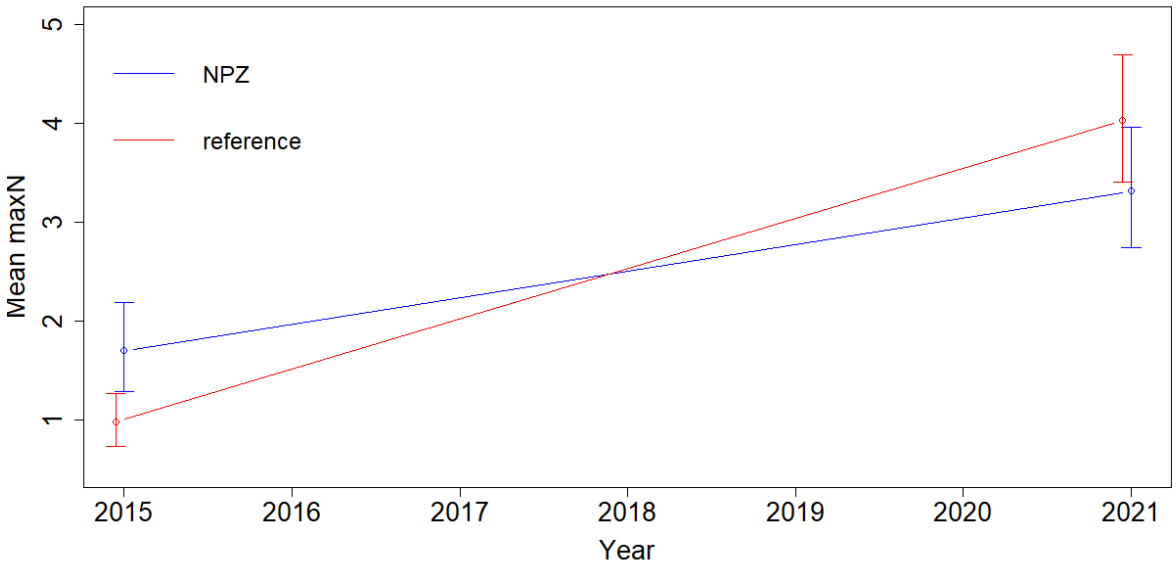

Figure 43. Model-based estimate of trends in relative abundance (MaxN per BRUV drop) for morid cod inside the NPZ and in the fished reference areas between 2015 and 2021. Error bars represent 95% credible intervals. Estimates are made at mean depth and rugosity values over the survey area.

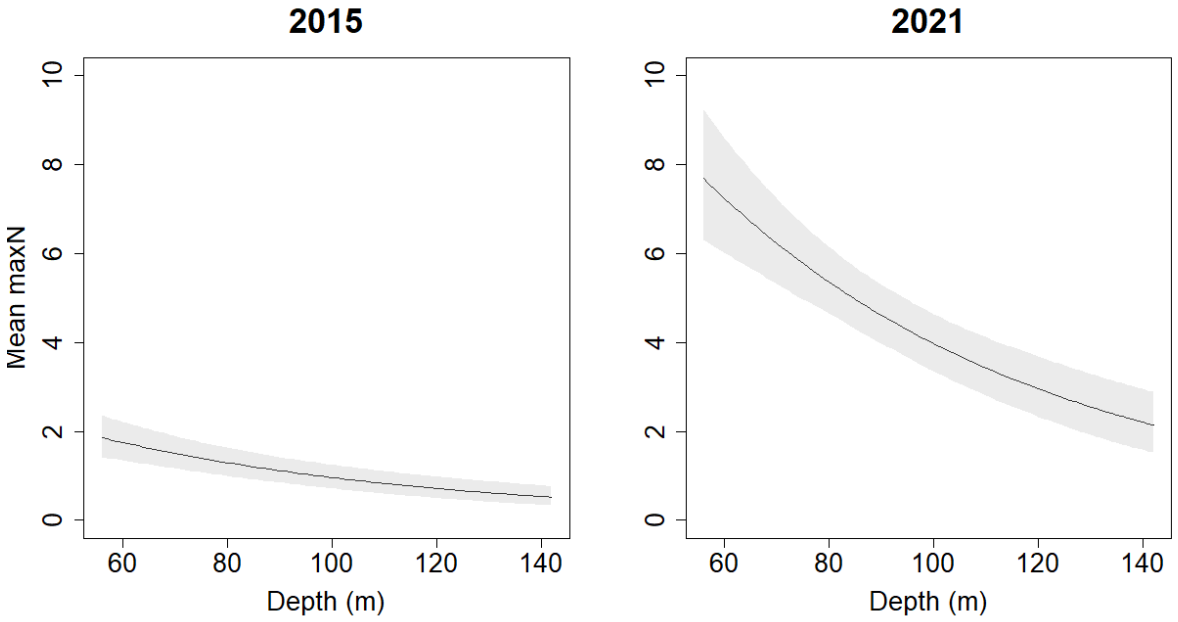

Figure 44. Model-based estimate of the relationship between abundance (MaxN) and depth for morid cod from the 2015 and 2021 data. Line shows the mean response and shading shows 95% credible intervals.

3.2.3.2 Average size

The mean size of morid cod across the entire survey area and both surveys was 29.4 cm (Table 17). The average size of morid cod was found to be significantly smaller in the NPZ in 2015, with fish an average of 5.5 cm smaller (NPZ effect Table 17 and Figure 45). Analysis suggests that the mean size increased inside the NPZ, but that this effect was not significant, with mean sizes being roughly equal between the NPZ and the fished reference area in 2021 (Figure 45).

Negative association between depth and rugosity at 500 m were found (Figure 46 and Figure 47), indicating that larger morid cod preferred shallower less complex habitat at the 500 m scale across the survey area.

Table 17. Model-based estimates for the mean size of morid cod. Effects highlighted green indicate evidence for a positive effect whereas effects highlighted red indicate there is evidence for a negative effect. Estimates are in centimetres.

Effect	mean	sd	0.025 quantile	0.975 quantile
intercept	29.387	1.631	26.185	32.587
NPZ	-5.530	2.462	-10.364	-0.700
Year	1.053	1.939	-2.754	4.857
NPZ*Year	4.792	2.695	-0.500	10.080
Depth	-1.990	0.910	-3.778	-0.205
Rugosity 500 m	-1.812	0.699	-3.185	-0.440

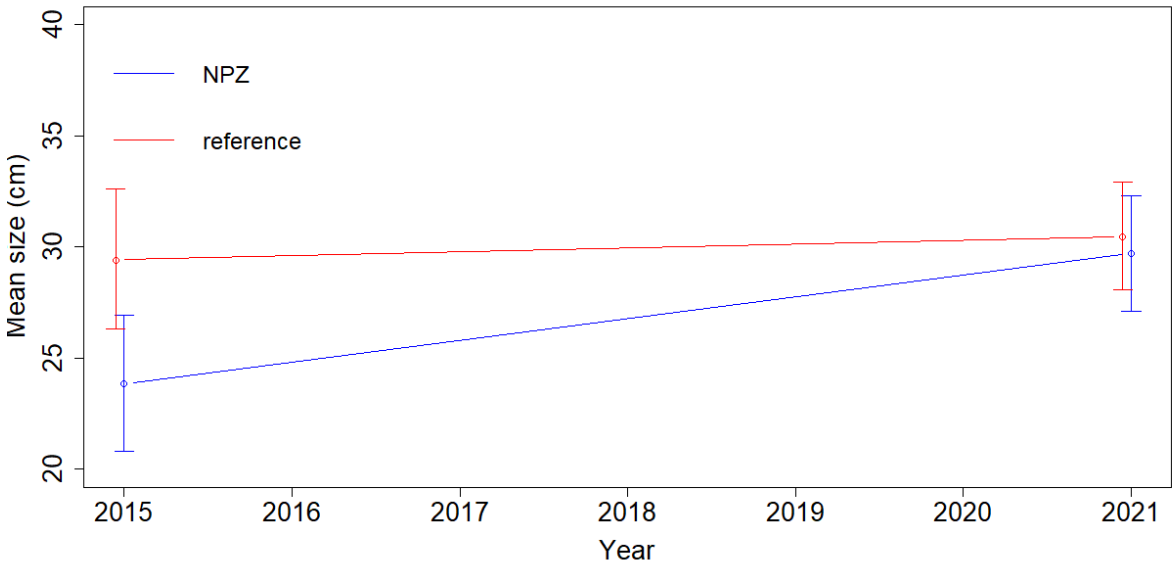

Figure 45. Model-based estimate of trends in mean size of morid cod inside the NPZ and in the fished reference areas between 2015 and 2021. Error bars represent 95% credible intervals. Estimates are made at mean depth and rugosity values over the survey area.

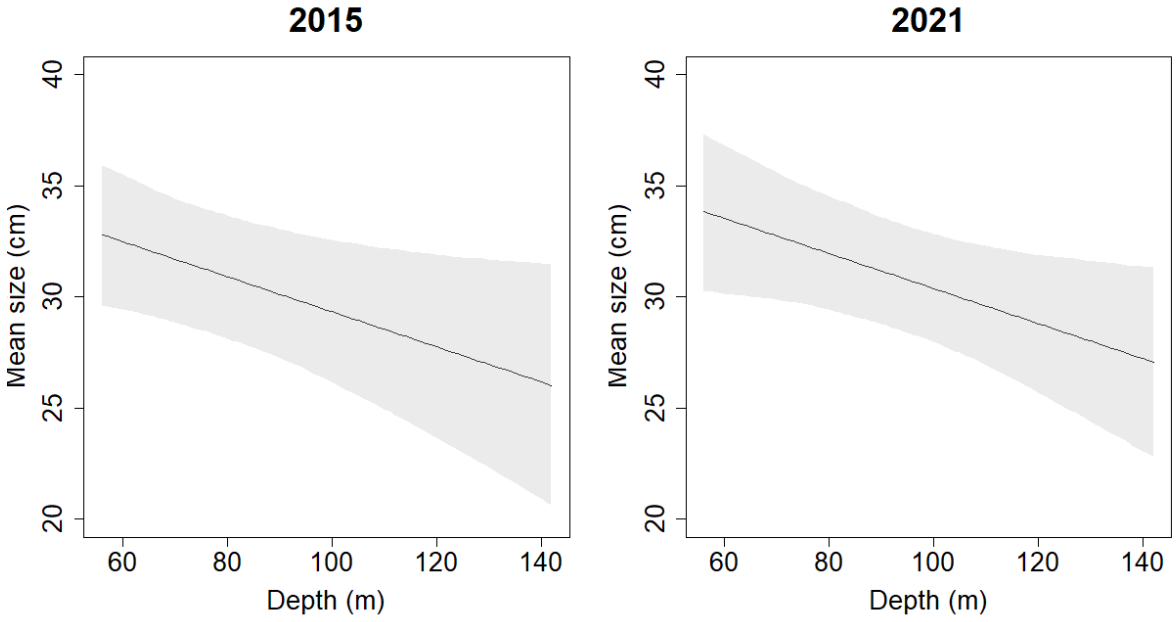

Figure 46. Model-based estimate of the relationship between mean size and depth for morid cod. Line shows the mean response and shading shows 95% credible intervals.

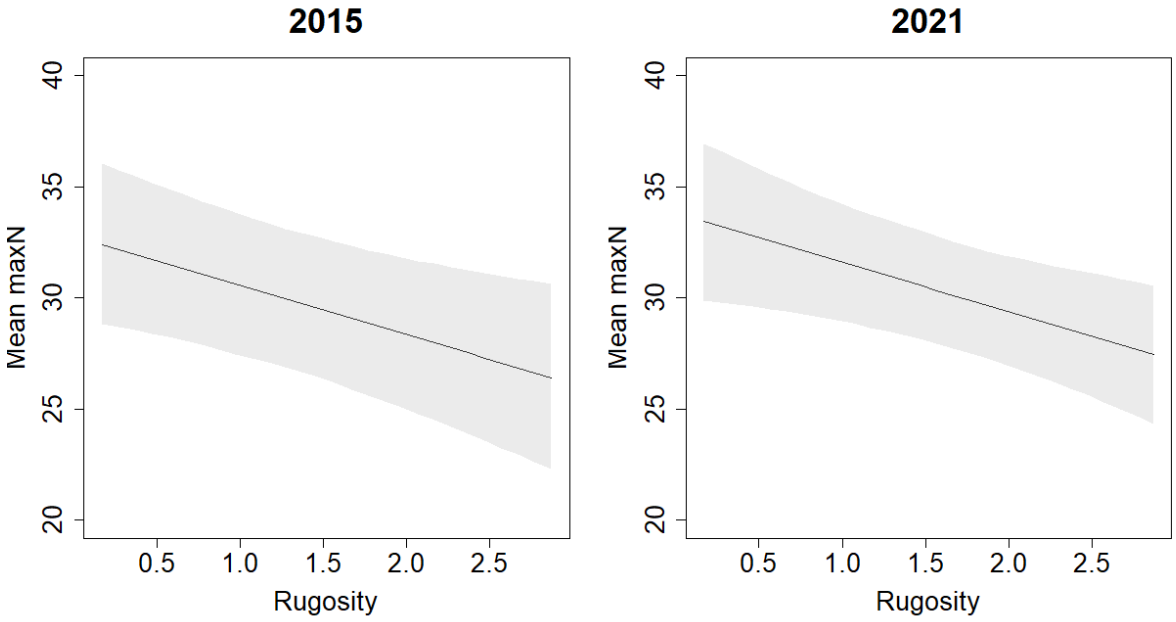

Figure 47. Model-based estimate of the relationship between mean size and rugosity at 500 m for morid cod. Line shows the mean response and shading shows 95% credible intervals.

3.2.4 Ocean perch

3.2.4.1 Abundance

In 2015 the abundance of ocean perch in the NPZ was higher than the adjacent fished reference areas (NPZ effect, Table 18), with the overall abundance increasing in time both inside and outside the NPZ between surveys (positive year effect, Table 18). However, the abundance in the fished reference area increased at a markedly greater rate than the NPZ between surveys (Negative NPZ*year interaction Table 18, Figure 48).

A postive correlation was found for increased depth and abundance of ocean perch (Figure 49), indicating a preference for deeper depth in the surveyed region.

Table 18. Model-based estimates for the abundance (MaxN per BRUV drop) of ocean perch. Effects highlighted green indicate evidence for a positive effect whereas effects highlighted red indicate there is evidence for a negative effect. Estimates are on the linear predictor (log) scale.

Effect	mean	sd	0.025 quantile	0.975 quantile
intercept	0.600	0.150	0.301	0.888
NPZ	0.601	0.214	0.184	1.022
Year	0.731	0.158	0.425	1.044
NPZ*Year	-0.728	0.186	-1.096	-0.365
Depth	0.213	0.079	0.058	0.368
Rugosity 50 m	0.056	0.062	-0.066	0.176

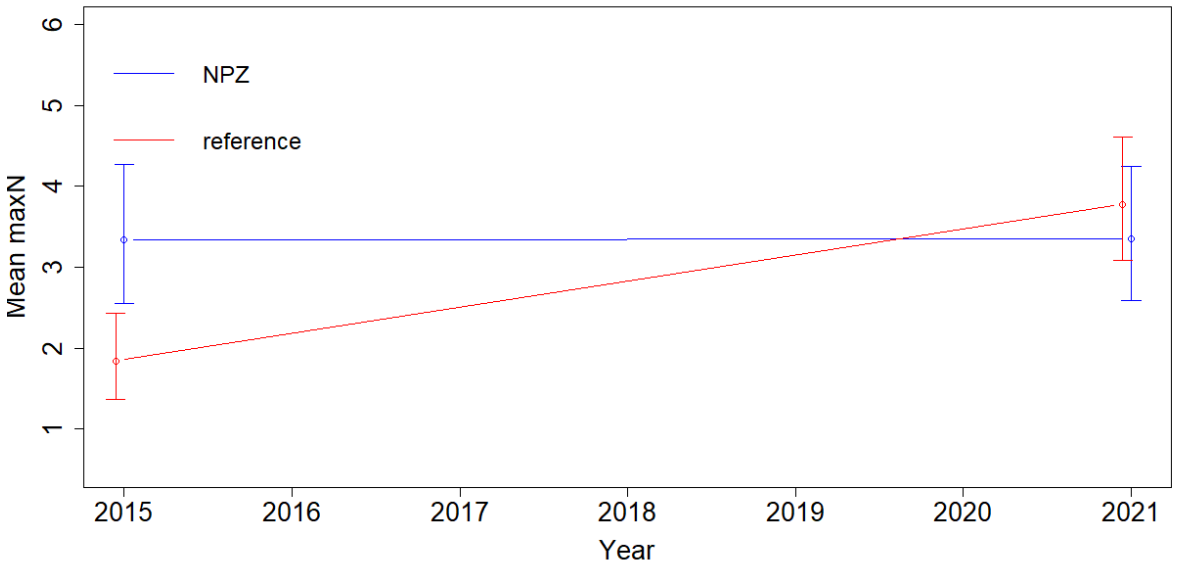

Figure 48. Model-based estimate of trends in relative abundance (MaxN per BRUV drop) for ocean perch inside the NPZ and in the fished reference areas between 2015 and 2021. Error bars represent 95% credible intervals. Estimates are made at mean depth and rugosity values over the survey area.

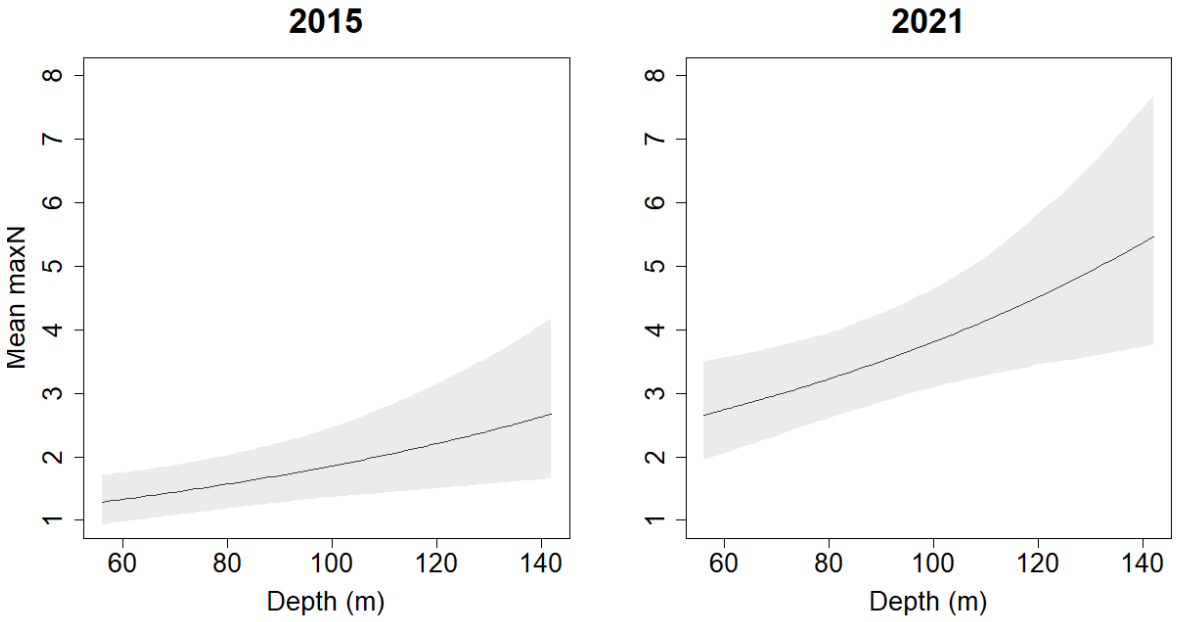

Figure 49. Model-based estimate of the relationship between abundance (MaxN) and depth for ocean perch. Line shows the mean response and shading shows 95% credible intervals.

3.2.4.2 Average size

The mean size of ocean perch across the entire survey area and both surveys was 20.9 cm (Table 19). No clear effects of protection or time were found for the mean size of ocean perch, with results indicating a larger increase in mean size in the NPZ (Figure 50), but that that this change was not significantly different to the fished reference area.

Table 19. Model-based estimates for the mean size of ocean perch. Effects highlighted green indicate evidence for a positive effect whereas effects highlighted red indicate there is evidence for a negative effect. Estimates are in centimetres.

Effect	mean	sd	0.025 quantile	0.975 quantile
intercept	20.919	2.969	15.090	26.744
NPZ	-0.481	1.797	-4.008	3.044
Year	1.980	1.564	-1.092	5.048
NPZ*Year	0.623	1.885	-3.079	4.322
Depth	-0.574	0.519	-1.594	0.445

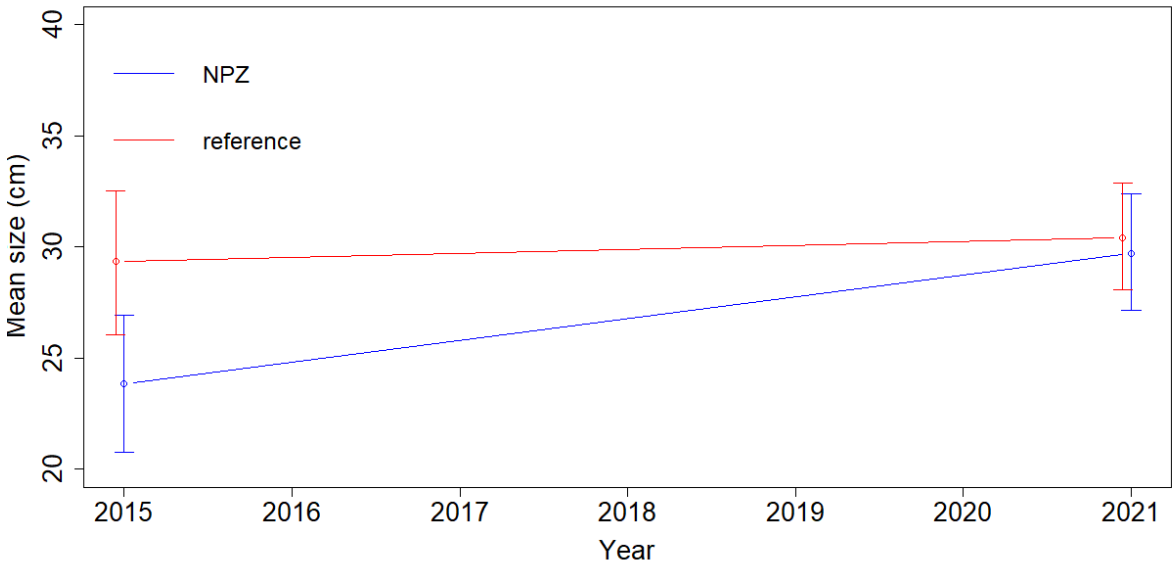

Figure 50. Model-based estimate of trends in mean size of ocean perch inside the NPZ and in the fished reference areas between 2015 and 2021. Error bars represent 95% credible intervals. Estimates are made at mean depth and rugosity values over the survey area.

3.2.5 Draughtboard sharks

3.2.5.1 Abundance

Model results showed evidence for an increase in abundance of draughtboard sharks, both inside and outside the NPZ, over the survey period (Year effect, Table 20 and Figure 51). There was no evidence for any effect of protection for draughtboard sharks.

Negative associations with depth and depth-squared were found for draughtboard sharks (Table 20 and Figure 52) indicating a preference for shallower depths over the survey area for this species.

Table 20. Model-based estimates for the abundance (MaxN per BRUV drop) of draughtboard sharks. Effects highlighted green indicate evidence for a positive effect whereas effects highlighted red indicate there is evidence for a negative effect. Estimates are on the linear predictor (log) scale.

Effect	mean	sd	0.025 quantile	0.975 quantile
intercept	-1.328	0.295	-1.935	-0.778
NPZ	0.146	0.449	-0.750	1.012
Year	1.331	0.297	0.773	1.938
NPZ*Year	-0.112	0.459	-0.999	0.803
Depth	-0.473	0.141	-0.760	-0.205
Depth-squared	-0.201	0.090	-0.385	-0.030

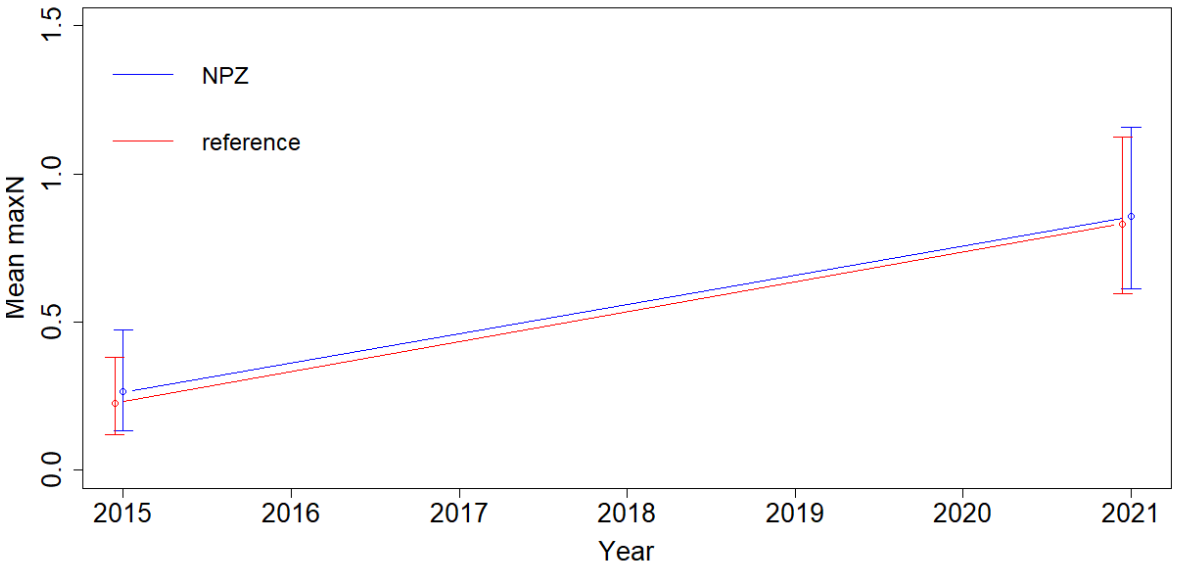

Figure 51. Model-based estimate of trends in relative abundance (MaxN per BRUV drop) for draughtboard sharks inside the NPZ and in the fished reference areas between 2015 and 2021. Error bars represent 95% credible intervals. Estimates are made at mean depth and rugosity values over the survey area.

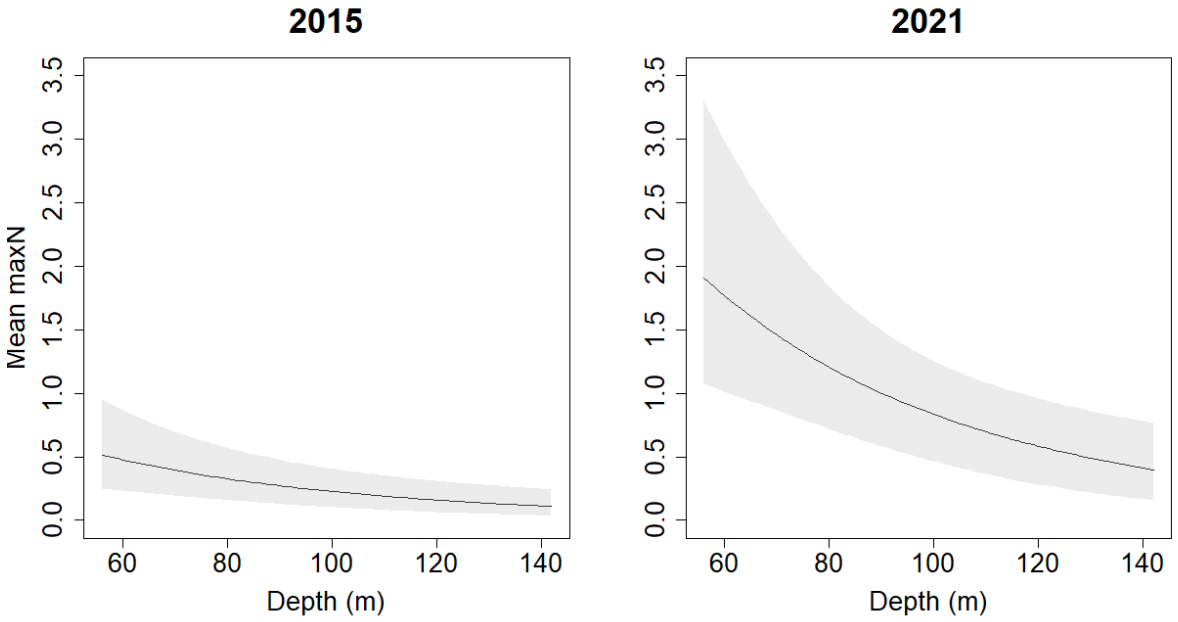

Figure 52. Model-based estimate of the relationship between abundance (MaxN) and depth for draughtboard sharks. Line shows the mean response and shading shows 95% credible intervals.

3.2.5.2 Average size

The mean size of draughtboard sharks across the entire survey area and both surveys was 54.1 cm (Table 21). Model results indicate that the mean size was significantly smaller inside the NPZ in 2015 relative to adjacent fished reference areas (causing a negative NPZ effect, Table 21 and Figure 53), with draughtboards sharks an average of 17.8 cm smaller inside the NPZ in 2015. However, mean sizes in 2021 were similar between the fished reference area and the NPZ (Figure 53). Despite this the overall changes in mean sizes not being found significant over the survey period (i.e., no significant NPZ*year effect). As these results are based on a small number of length measurements able to be made in 2021, it is likely they lacked sufficient statistical power to detect and describe overall trends, hence should be treated with caution. No significant effect of the depth or rugosity covariates were found for mean size of draughtboard sharks.

Table 21. Model-based estimates for the mean size of draughtboard sharks. Effects highlighted green indicate evidence for a positive effect whereas effects highlighted red indicate there is evidence for a negative effect. Estimates are in centimetres.

Effect	mean	sd	0.025 quantile	0.975 quantile
intercept	54.131	5.447	43.436	64.818
NPZ	-17.766	8.772	-34.989	-0.557
Year	9.189	5.876	-2.348	20.716
NPZ*Year	16.338	9.144	-1.615	34.276
Depth	-2.816	2.293	-7.317	1.682

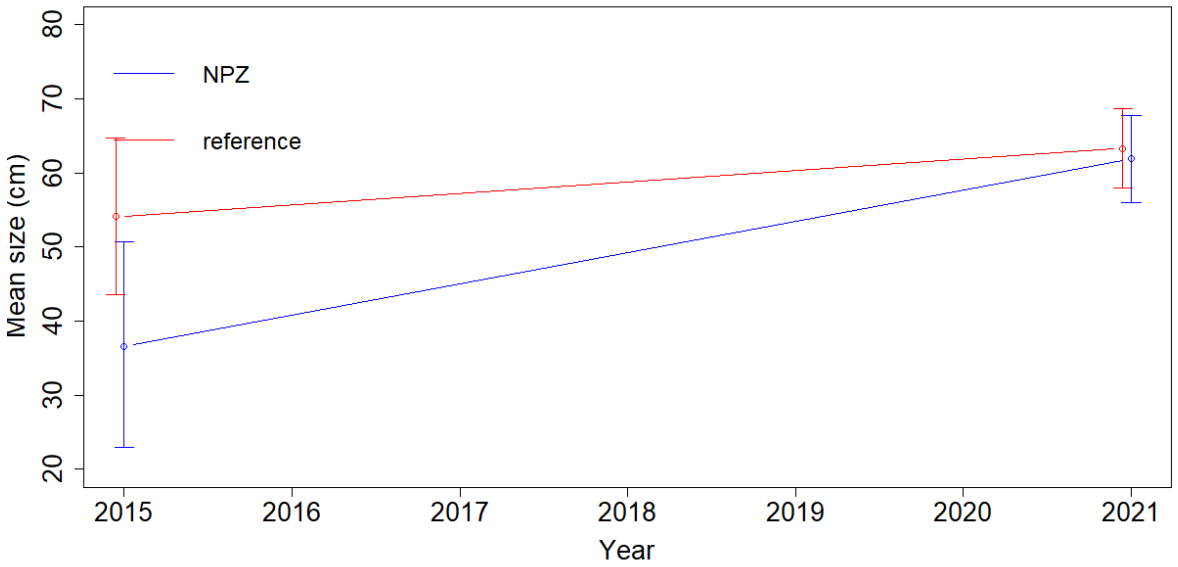

Figure 53. Model-based estimate of trends in mean size of draughtboard sharks inside the NPZ and in the fished reference areas between 2015 and 2021. Error bars represent 95% credible intervals. Estimates are made at mean depth and rugosity values over the survey area.

4 Spatial and temporal patterns in seabed benthos

4.1 Background and methods

A total of 11 IMOS AUV '*Sirius'* missions were completed on rocky reef systems within the TFMP and adjacent fished reference areas between 14th to 17th June 2021. This included repeat surveys of two transects in the NPZ previously surveyed on 1st March 2015 (Monk et al. 2016), 5 new surveys within the NPZ to maximise representation of depths and habitats, 2 new surveys within the MUZ to comprehensively cover reefs found there, and 2 new surveys on reefs adjacent to the park to provide representation of reefs in the region shallower than found within the TFMP (Figure 54). These later surveys were designed to allow for better understanding of the depth distribution relationships of species found within the park itself, as well as combining with the MUZ sites for future examination of any ecosystem-wide effects of fishing (such as changing sponge cover) relative to the NPZ.

The annotation of AUV imagery collected during the 2021 survey followed protocols developed under the National Environment and Science Program (NESP; Monk et al. 2020). Image sub-sampling within each transect was conducted using systematic sampling along the length of the transect, with the spacing of samples ensuring that a minimum of 100 images were scored in each transect (Table 22). Of note is the shallower depth distribution of the two transects within the reference areas compared to the transects conducted within the TFMP. All annotation was conducted within the Squidle+ online scoring platform (https://squidle.org/), with a random allocation of 25 points superimposed on each image. All annotation was completed to the lowest taxonomic resolution possible, which was typically the "morphospecies" level where morphologically distinct taxa are used as the basis for scoring. An extended CATAMI (Collaborative and Automated Tools for Analysis of Marine Imagery- https://github.com/catami/classification) catalogue known as the Australian Morphospecies Catalogue (AMC), which has been advocated as a standardised schema for AUV imagery within AMPs, was used for this purpose so that cover and diversity is readily comparable between AMPs in the future. All annotations are available via Squidle+ in the publicly visible Tasman Fracture AMP group (ID:152), as are links to the AMC schema.

*Table 22. Depth range, within transect sampling levels and total number of images scored for each transect in the 2021 survey. * denotes the two transects repeated*

Transect	Min. Depth (m)	Max. Depth (m)	Sampling	No. images scored 2015	No. images scored 2021
NPZ_01*	109	133	Every 30th image; 25 random points	115	127
NPZ_02*	100	137	Every 30th image; 25 random points	100	138
NPZ_03	90	148	Every 45th image; 25 random points		150
NPZ_04	95	142	Every 40th image; 25 random points		139
NPZ_06	96	130	Every 40th image; 25 random points		186
NPZ_07	90	127	Every 35th image; 25 random points		125
NPZ_08	123	134	Every 40th image; 25 random points		248
MUZ_01	131	153	Every 40th image; 25 random points		164
MUZ_02	135	157	Every 40th image; 25 random points		158
Ref_C_1	39	69	Every 40th image; 25 random points		98
Ref_N_1	63	114	Every 40th image; 25 random points		108

Statistical analyses presented here include descriptive summaries of the dominant biota across each transect and zone within the TFMP and detailed modelling of the changes between the 2015 and 2021 surveys for a subset of dominant species. Prior to calculating percent cover, all images that were completely sand were excluded so that only images that contained a proportion of reef were used in calculations. In these deep offshore habitats, there is often no clear distinction at the image-scale, of reef vs sand, as most reefs at such depths tend to be low-profile and are therefore sand-inundated to some extent.

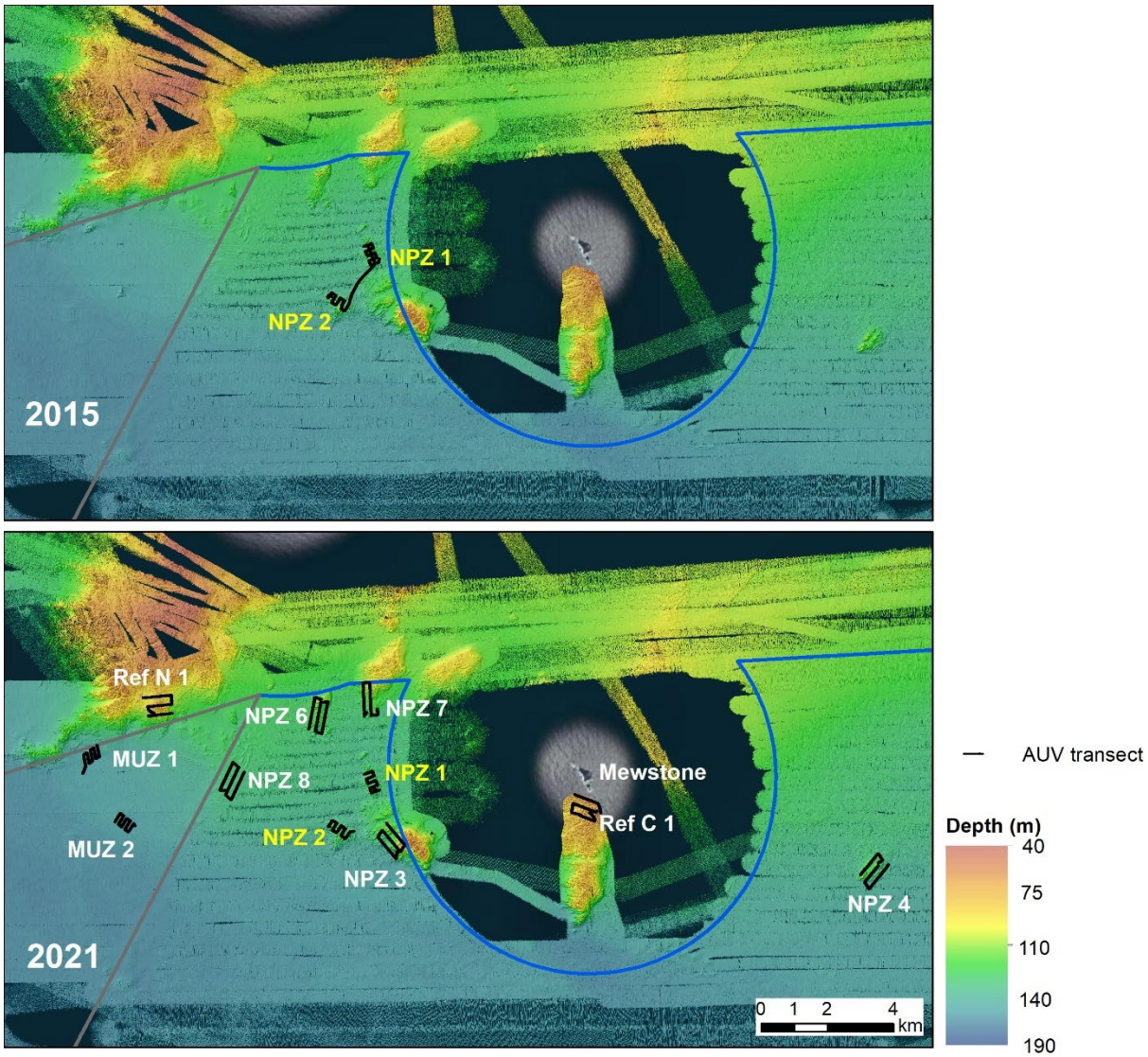

Figure 54. Location of AUV transects completed in and around Tasman Fracture Marine Park.

4.2 Broad habitat patterns

Patterns in the proportion of sand, rock and biota (both distinguishable biota and biological matrix categories) across the TFMP and associated external areas revealed different proportions of rocky reef and associated biota across transects (Figure 55), in part reflecting the sand-covered nature of these deep-reef systems, but also at some locations, reflecting the limited extent of reef relative to the scale of standard-length AUV transects (typically 1 km). This was particularly the case in the MUZ where reefs were deep, rare, small, and isolated, hence sand cover was high. Whereas the external sites Ref_C_1 and Ref_N_1 were shallower, large, and continuous (as a result of greater swell influence) so had relatively low sand cover. When sampled on reef habitat, the low proportion of bare rock across all transects reflects the high biological cover on available rocky substrate in the surveyed area.

Transects within the MUZ were sand dominated, with > 90% of each transect being sand interspersed with small sections of reef. MUZ_01 had a larger amount of reef than MUZ_02 but cover of reef was still relatively low compared to other transects within the TFMP. Transects within the NPZ were also sand dominated but had higher proportions of rocky reef than the MUZ transects, except for NPZ_08 which had < 1% biological cover. This site was predominantly examining sediment habitat rather than reef to ascertain the extent of biotic cover on sediment systems here, so not surprisingly, there was no emergent biota rather than a fine cover of biological matrix, given the swell-influenced dynamic nature of sediments in this region. NPZ_01 and NPZ_02 had the highest biological cover of all sites surveyed with in the TFMP, with approximately 36% and 30% respectively. By contrast, both fished reference area transects had much higher biological cover than transects within the TFMP, with ~80% in Ref_C_1 and ~58% in Ref_N_1, likely as a result of shallower depths and associated reduction in sand-inundation.

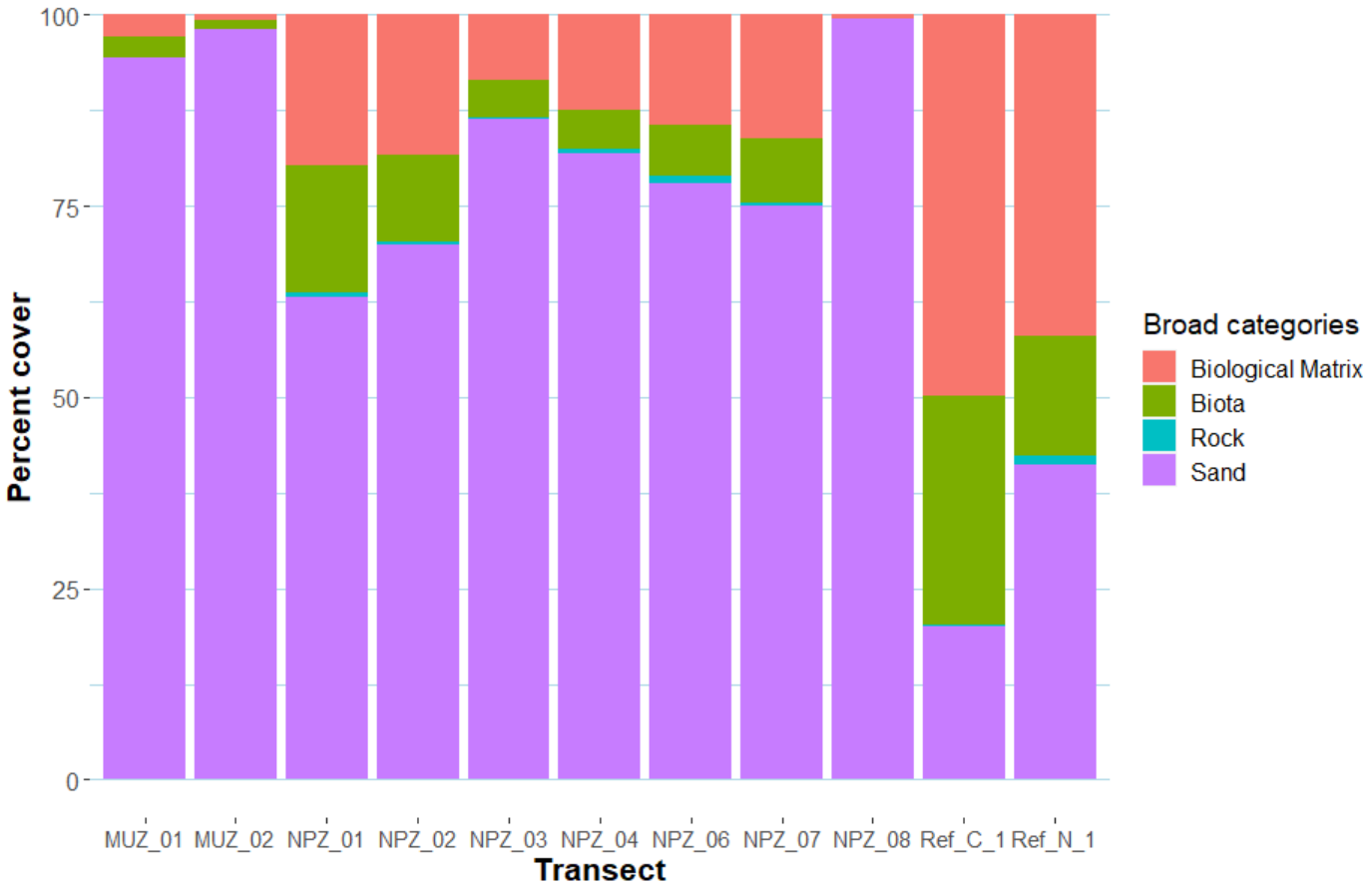

Figure 55. Proportions of sand, bare rock, discernible biota, and biological matrix based on point scoring of imagery across each transect in the TFMP and externally sampled fished reference areas.

4.3 Detailed description of dominant seabed organisms within each AUV transect

4.3.1 National Park Zone transect 1

This transect is located to the west of the Mewstone just inside the NPZ (Figure 54). The transect covers a mixture of low-profile boulder habitat interspersed with rippled sediments and high-profile consolidated reefs (Figure 57) that range in depth from ~109 to 133m. Dominant morphospecies include red *Pteronisis* gorgonian coral (top image in Figure 58), a variety of soft bryozoa, a high diversity of sponges including encrusting orange, yellow, and white sponge morphospecies, simple white rough massive sponges, as well as the conspicuous white cup morphospecies (Figure 57). Sea whips, lace bryozoa and a variety of hydroids were also observed relatively frequently. Ophiuroids (brittle stars) were observed in high abundances in both 2015 and 2021 imagery sets (approximately 2.1% cover in 2021) and were seen climbing on sponges, presumably to improve access to passing particulates (Figure 58). Soft corals were also present across the transect, but not high enough in cover to contribute to the top 30 morphospecies.

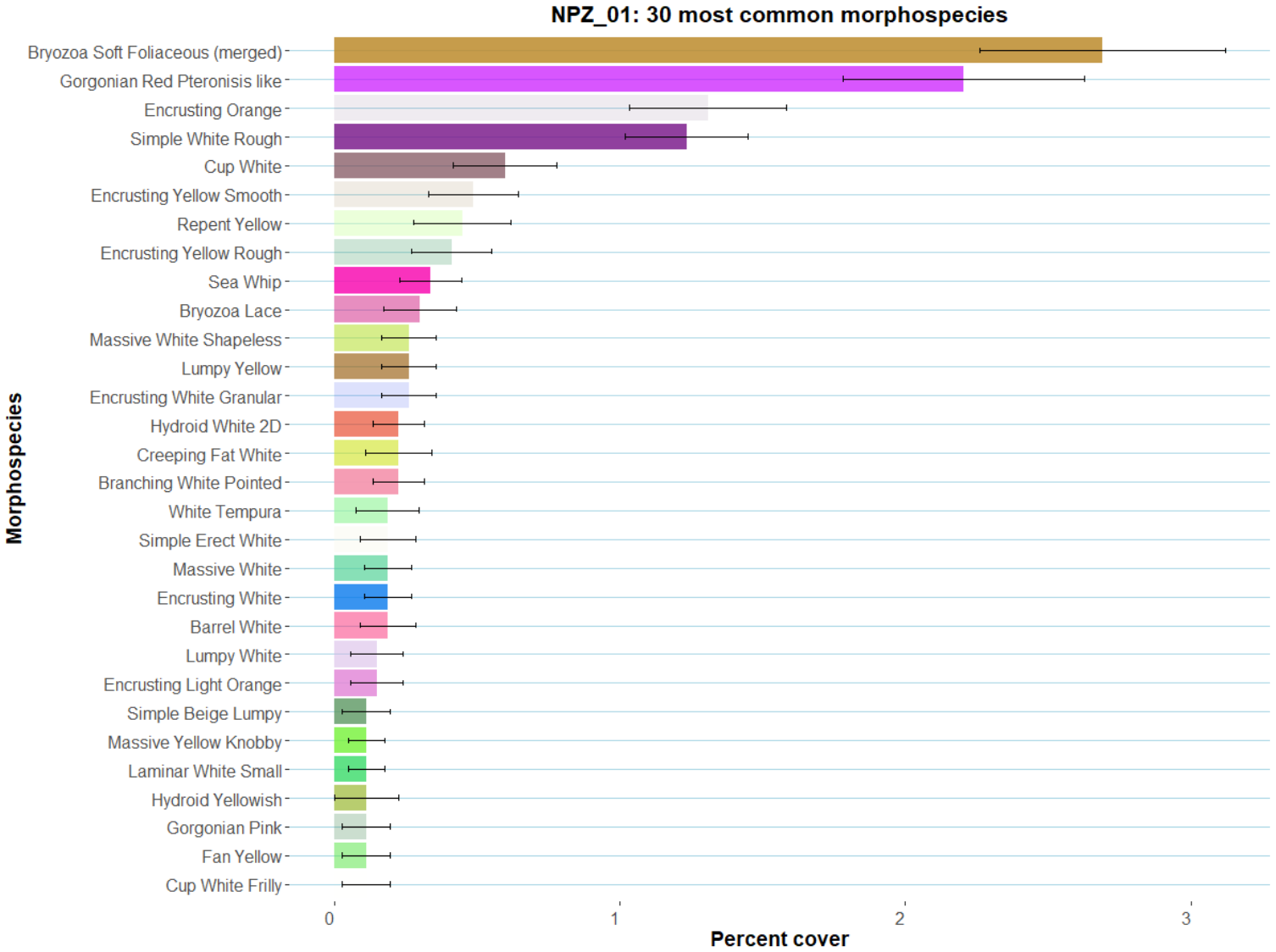

Figure 56. The 30 most dominant morphospecies across NPZ transect 1 in terms of percent cover. Error bars show standard error of percent cover estimates. Physical substrate categories, mobile species and biological matrix categories have been removed.

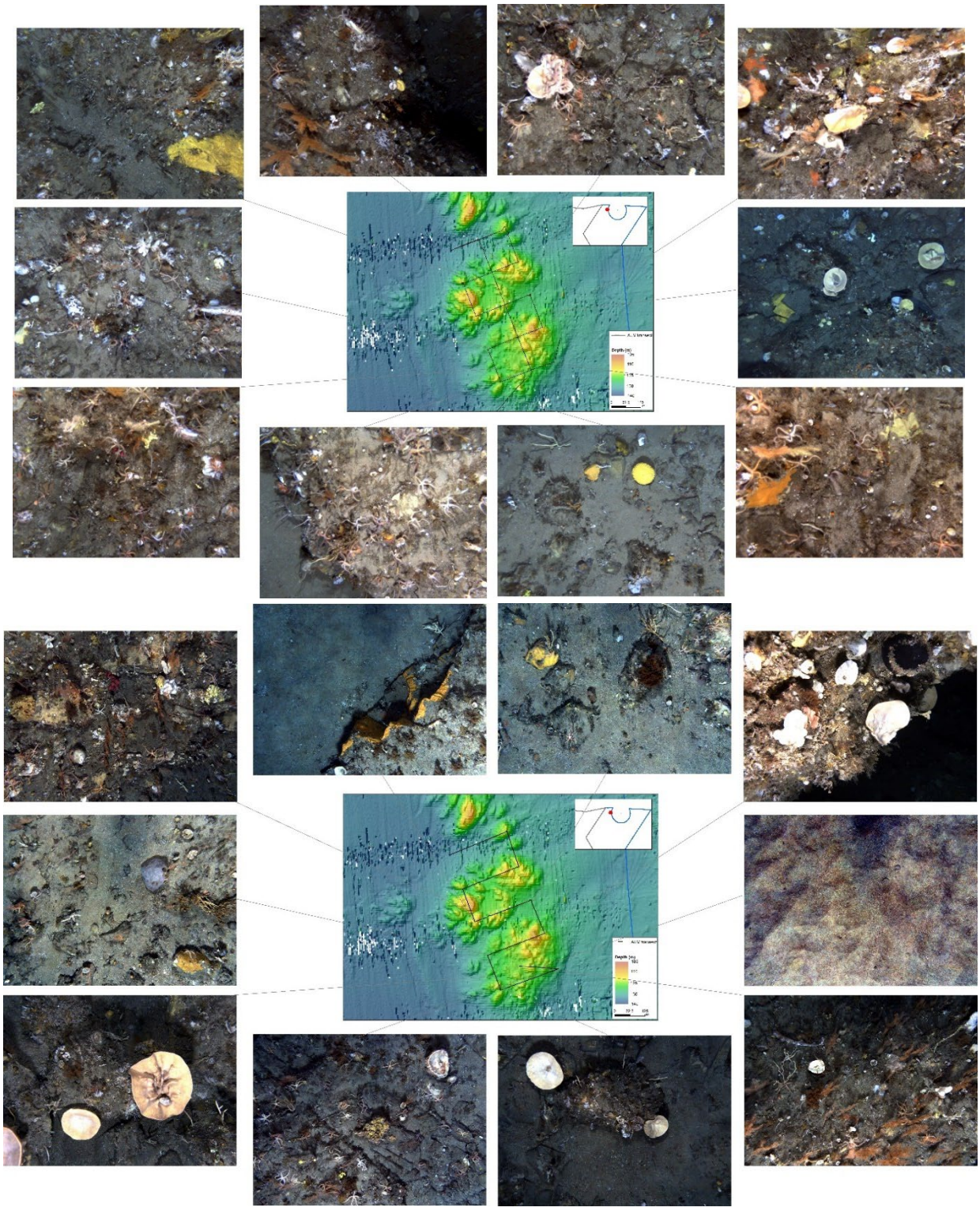

Figure 57. NPZ 1 transect sampled 2015 (top) repeated in 2021 (bottom) showing the diversity of morphospecies and substratum types present in this region of the Tasman Fracture Marine Park. Common morphospecies include white cup sponges (bottom and right images in 2021), encrusting orange sponge (top right images in 2021), encrusting yellow sponge (top left 2015 images) and red Pteronisis bamboo coral (bottom right images both years). Examples of morphospecies are shown in more detail in Figs 107-118 in the Appendix.

Figure 58. Examples of red Pteronisis bamboo coral (top image) and ophiuroids (brittle stars, bottom image) observed in high abundances in both 2015 and 2021 imagery sets, often climbing on sponges.

4.3.2 National Park Zone transect 2

This transect is located to the south-west of the Mewstone and ~ 2km south-west of NPZ 1 transect (Figure 54). The transect covers a mixture of large boulder/slab high-profile habitat interspersed with rippled sediments that range in depth from ~100 to 137m (Figure 60). Dominant species were similar to NPZ_01 transect, with soft bryozoans and the red *Pteronisis* gorgonian coral being the two most common morphospecies followed by a wide range of sponges including encrusting morphospecies such as yellow smooth, yellow rough, and orange; massive forms such as simple white rough and lumpy white; and cup (e.g. cup white Figure 60) and erect fan and erect branching species. Hydroids, lace bryozoans and soft corals were also present, such as the soft purple octocoral and the fleshy branching octocoral *Soft Capnella Like* (bottom images in Figure 60). Ophiuroids (brittle stars) were observed in high abundances in both 2015 and 2021 imagery sets (approximately 1.9% cover in 2021) and were seen climbing on sponges, presumably to improve access to passing particulates.

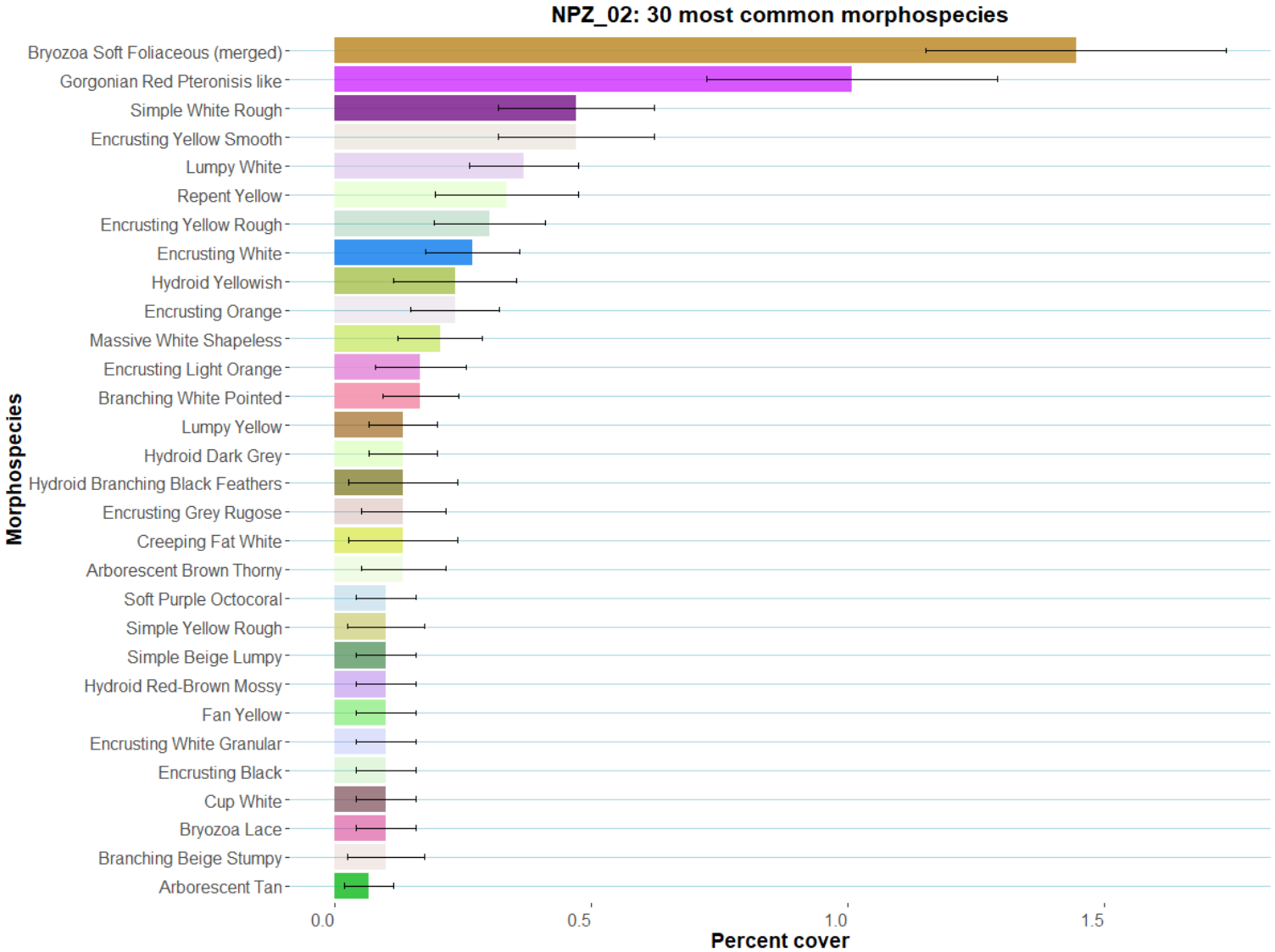

Figure 59. The 30 most dominant morphospecies across NPZ transect 2 in terms of percent cover. Error bars show standard error of percent cover estimates. Physical substrate categories, mobile species and biological matrix categories have been removed.

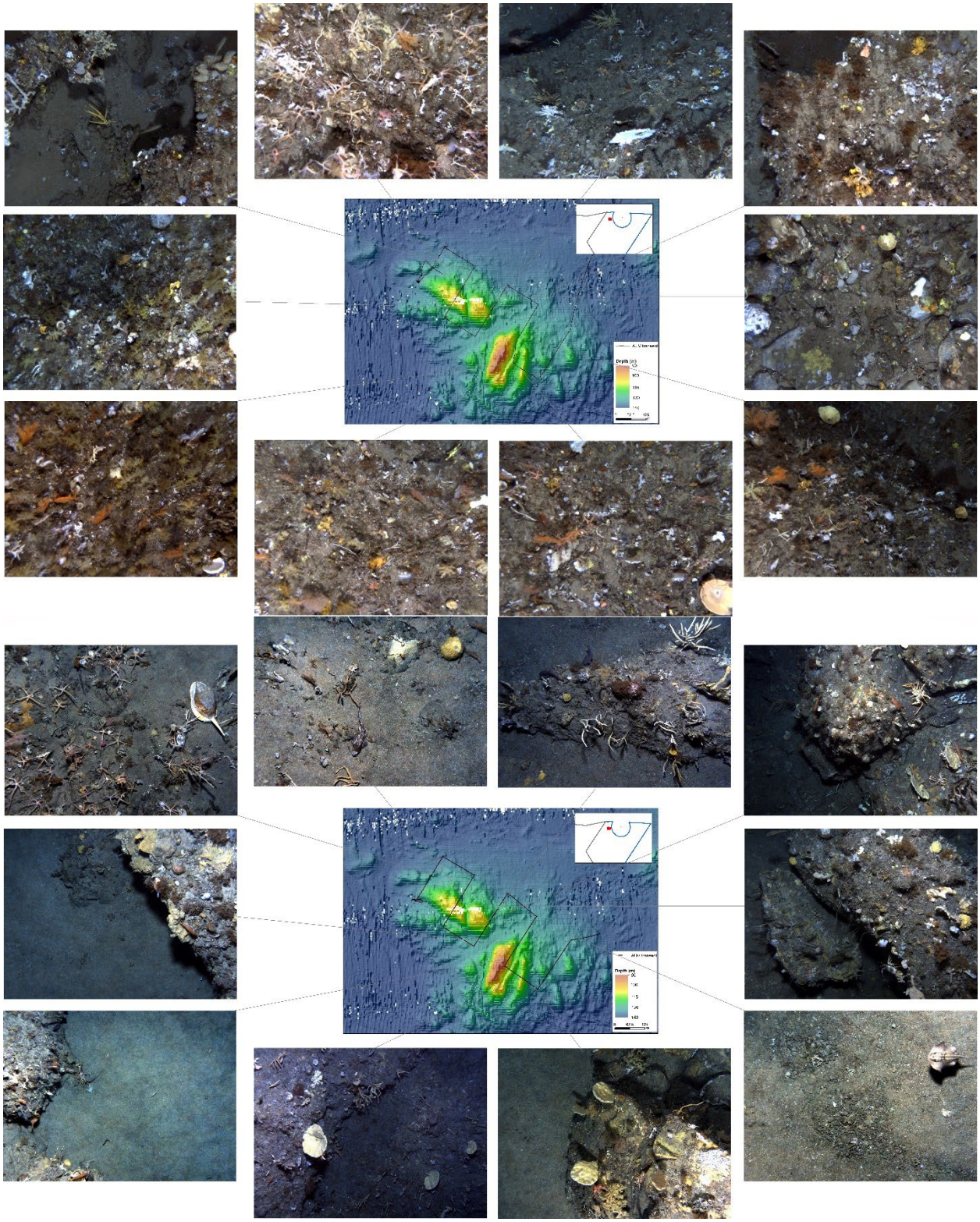

Figure 60. NPZ 2 transect and representative imagery, sampled 2015 (top) repeated in 2021 (bottom) showing key habitat features and dominant morphospecies. Common morphospecies include red Pteronisis bamboo coral (bottom images in 2015), branching white pointed (upper right image in 2021), yellow fans (bottom images in 2021), and repent yellow sponges (top left image in 2015). Examples of morphospecies are shown in more detail in Figs 107-118 in the Appendix.

4.3.3 National Park Zone transect 3

This transect is located to the south-west of the Mewstone and ~ 2km south of NPZ 1 transect (Figure 54). The transect covers a mixture of large boulder/slab high-profile habitat interspersed with rippled sediments that range in depth from ~90 to 148m (Figure 62). Overall biological cover was lower than NPZ_01 and NPZ_02 transects, with a higher proportion of sand images (Figure 55). Dominant species included soft bryozoans, the red *Pteronisis* gorgonian coral, and sea whips (Figure 61). A wide variety of sponge morphospecies were present including encrusting morphospecies such as orange and white granular; a variety of laminar and fan morphospecies; massive forms such as massive white shapeless and lumpy yellow; and white cup sponges. Hydroids, lace bryozoans and soft corals were also present, such as the bramble coral *Asperaxis karenae*. Ophiuroids (brittle stars) were observed in high abundances (approximately 0.2% total cover) and were seen climbing on sponges, presumably to improve access to passing particulates.

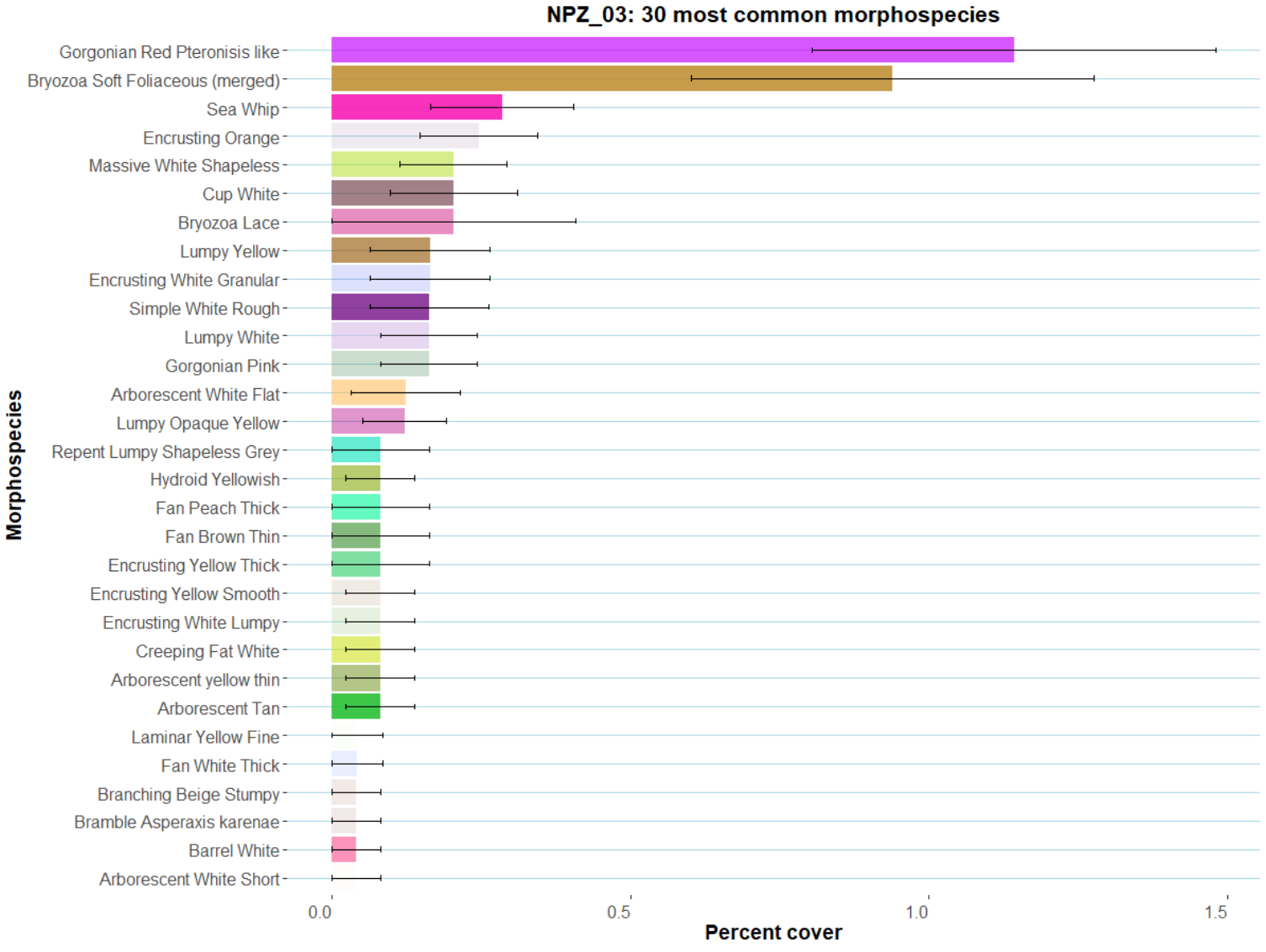

Figure 61. The 30 most dominant morphospecies across NPZ transect 3 in terms of percent cover. Error bars show standard error of percent cover estimates. Physical substrate categories, mobile species and biological matrix categories have been removed.

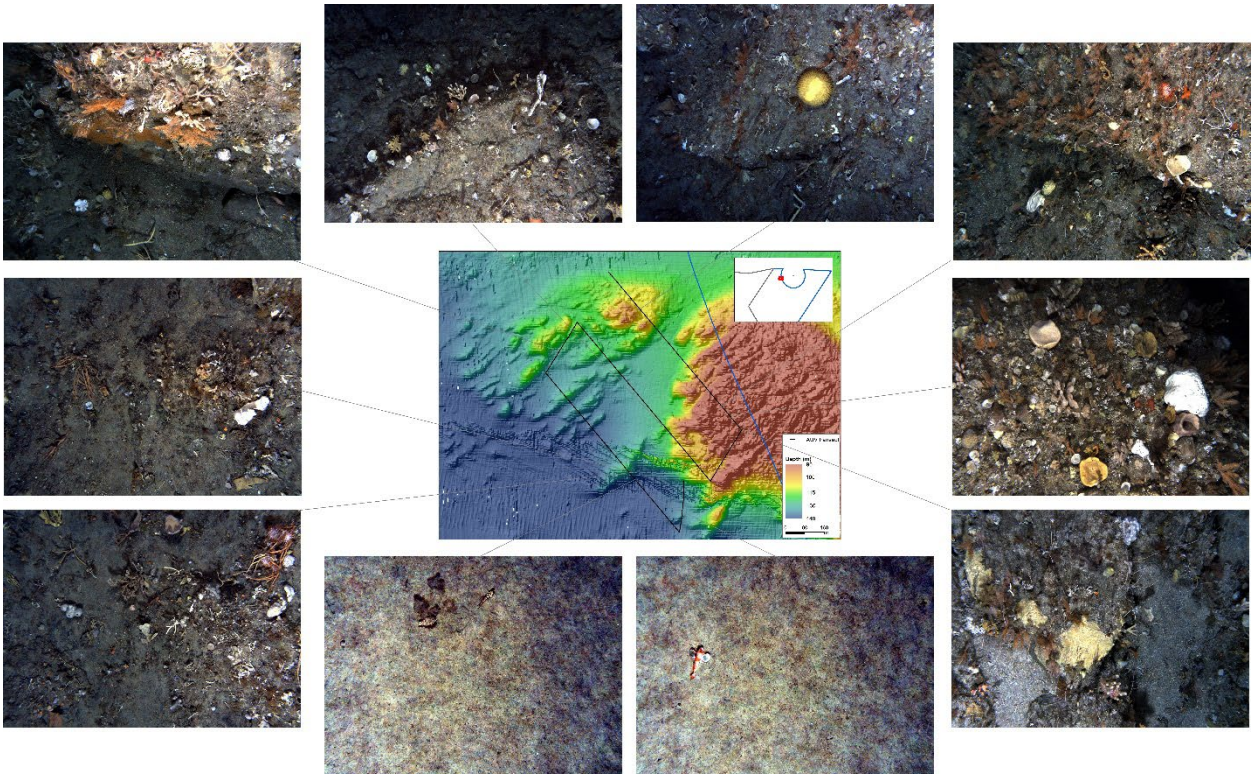

Figure 62. NPZ 3 transect and representative imagery showing key habitat and broad morphospecies distribution across the surveyed transect lines. Common morphospecies include red Pteronisis bamboo coral (top left image), encrusting yellow smooth sponge (bottom right image), white cup sponges (top left image), and massive white shapeless sponges (right centre image). Examples of morphospecies are shown in more detail in Figs 107-118 in the Appendix.

4.3.4 National Park Zone transect 4

This transect is located approximately 8 km to the south-east of the Mewstone (Figure 54). The transect covers a mixture of large boulder/slab high-profile habitat interspersed with rippled sediments and patchy reef that ranges in depth from ~95 to 142m (Figure 65). Overall biological cover was lower than NPZ_01 and NPZ_02 transects, but higher than NPZ_03 (Figure 55). Dominant species included soft bryozoans, the red *Pteronisis* gorgonian coral (Figure 64). A wide variety of sponge morphospecies were present including encrusting morphospecies such as yellow smooth and black; erect forms such as simple erect cream, arborescent white, and fan white thick; massive forms such as massive white shapeless and lumpy white; and white cup sponges. Hydroids, lace bryozoans and soft corals were also present, such as gorgonian pink, soft white octocoral, bramble *Acabaria sp*., and bramble coral *Asperaxis karenae*.

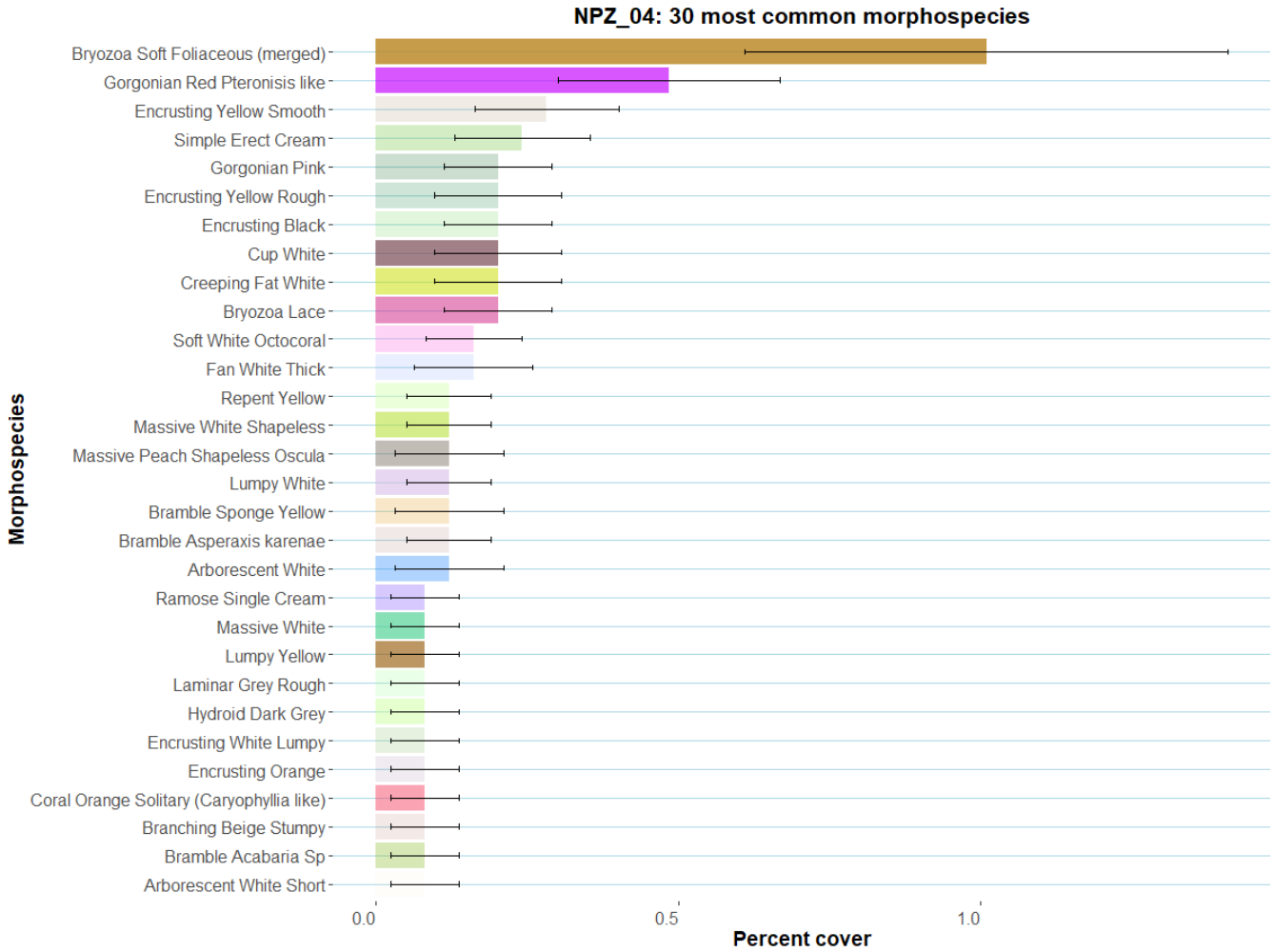

Figure 63. The 30 most dominant morphospecies across NPZ transect 4 in terms of percent cover. Error bars show standard error of percent cover estimates. Physical substrate categories, mobile species and biological matrix categories have been removed.

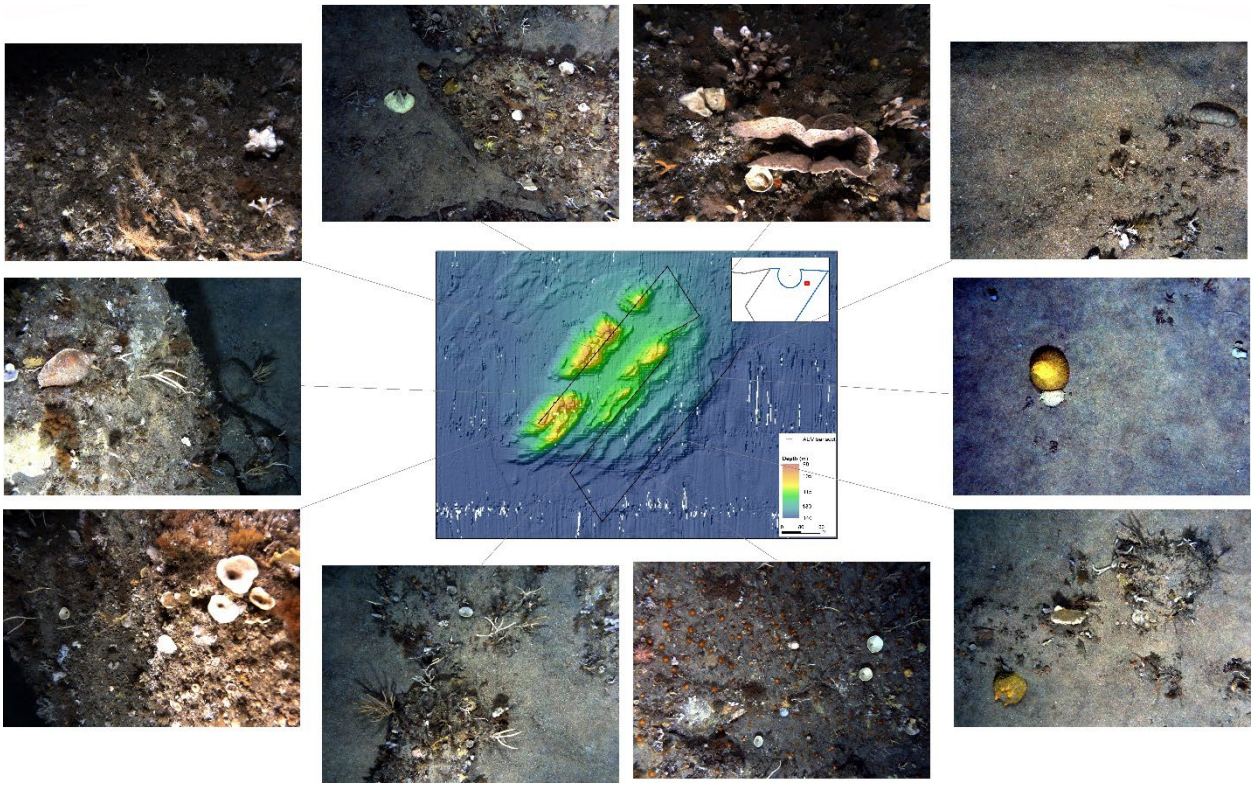

Figure 64. NPZ 4 transect and representative imagery showing key habitat features and common or unusual morphospecies. Common morphospecies include soft bryozoans (left bottom image) and white cup sponges (top left image and bottom right image). Examples of morphospecies are shown in more detail in Figs 107-118 in the Appendix.

4.3.5 National Park Zone transect 6

This transect is located approximately 8 km to the north-east of the Mewstone (Figure 54). The transect covers a mixture of large boulder/slab high-profile habitat interspersed with rippled sediments and patchy reef that ranges in depth from ~96 to 130m (Figure 67). Overall biological cover was lower than NPZ_01 and NPZ_02 transects, but higher than NPZ_03 and NPZ_04 (Figure 55). Dominant species included soft bryozoans and encrusting sponges such as orange, yellow and light orange morphospecies (Figure 66). A wide variety of other sponge morphospecies were also present including other encrusting forms; massive forms such as lumpy white; erect forms such branching white pointed, arborescent tan, and branching yellow thick pointed; and white cup sponges. Hydroids, lace bryozoans, orange cup corals, and soft corals were also present, such as red gorgonians, soft white octocoral, and bramble *Acabaria sp*. There was also a reasonably high number of brittle stars present across the transect.

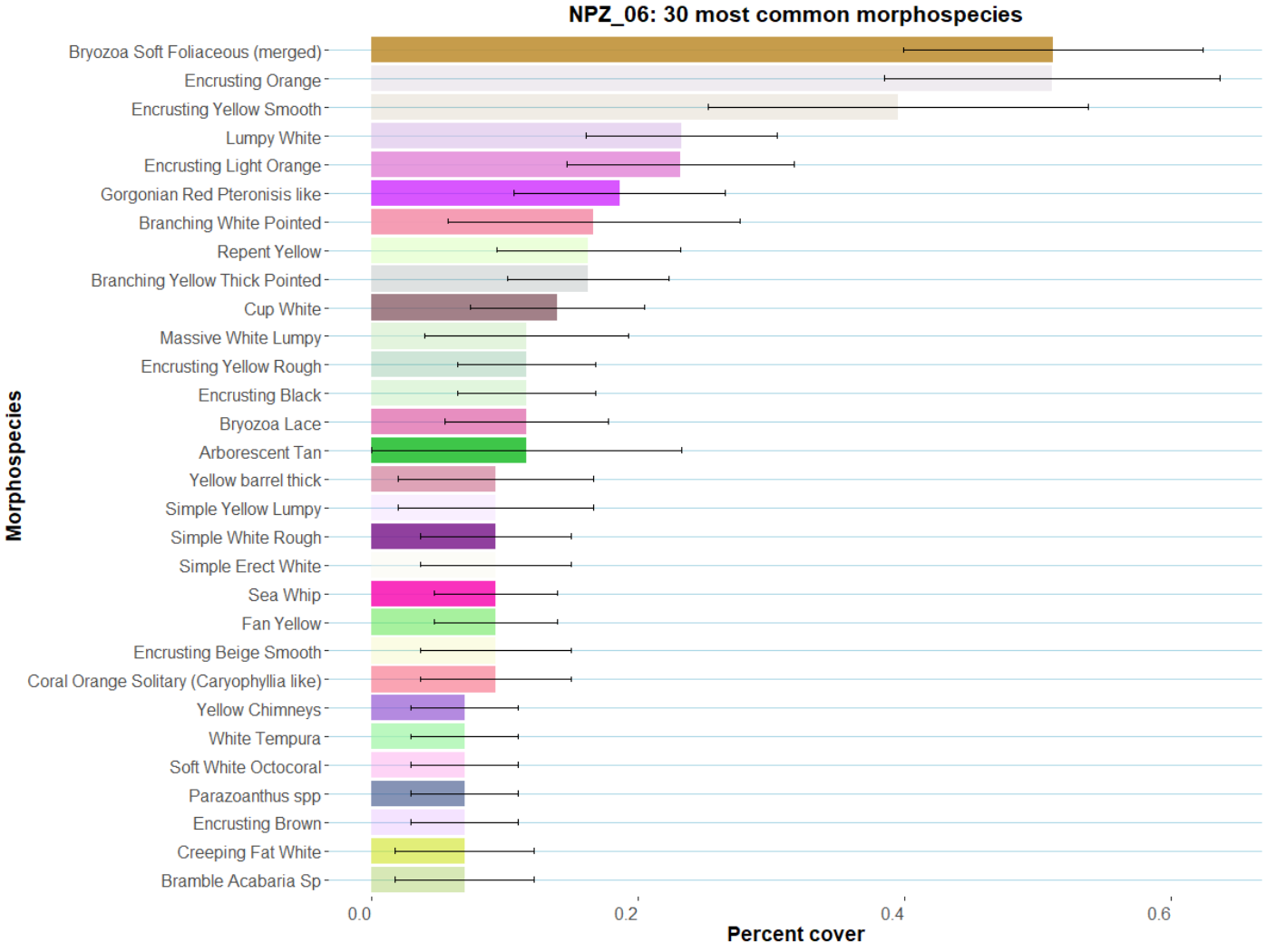

Figure 65. The 30 most dominant morphospecies across NPZ transect 6 in terms of percent cover. Error bars show standard error of percent cover estimates. Physical substrate categories, mobile species and biological matrix categories have been removed.

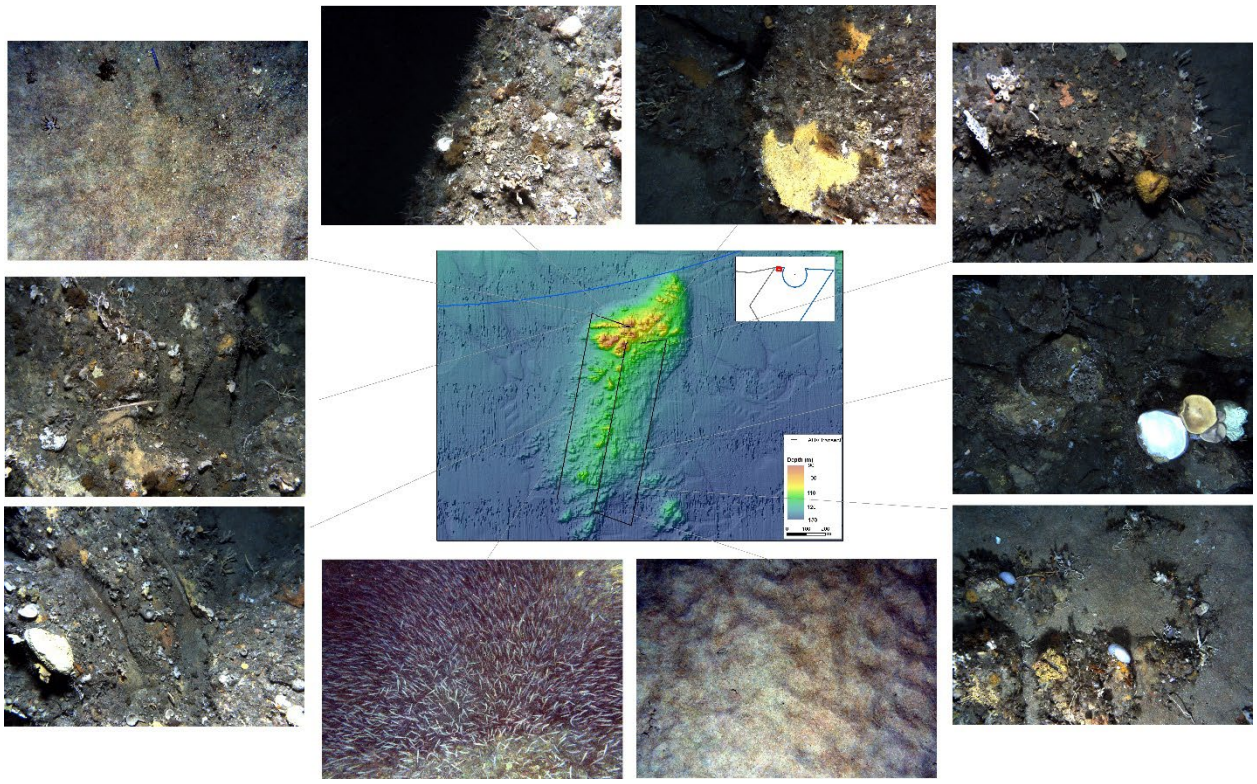

Figure 66. NPZ 6 transect and representative imagery showing key habitat features and common or unusual morphospecies. Common morphospecies include encrusting yellow smooth sponge (top right image), white and yellow cup sponges (centre right image), and massive white lumpy sponge(bottom left image). Examples of morphospecies are shown in more detail in Figs 107-118 in the Appendix.

4.3.6 National Park Zone transect 7

This transect is located approximately 6 km to the north-east of the Mewstone and approximately 2 km to the east of NPZ_06 (Figure 54). The transect covers a mixture of large boulder/slab high-profile habitat interspersed with rippled sediments and patchy reef that ranges in depth from ~90 to 127m (Figure 69). Overall biological cover was lower than NPZ_01 and NPZ_02 transects, and roughly the same as NPZ_06 (Figure 55). Dominant species included soft bryozoans and the red *Pteronisis* gorgonian coral (Figure 68). A wide variety of sponge morphospecies were present including encrusting forms such as encrusting orange, yellow smooth, and yellow rough; massive forms such as simple white rough; erect forms such branching white pointed, arborescent yellow, and arborescent tan; and white cup sponges. Hydroids, solitary orange cup corals and octocorals were also present, such as soft white octocoral, and bramble coral *Asperaxis karenae*. Handfish (4 to date) have also been found in whole of image searches in the NPZ_07 transect (top transect in Figure 63), although they are not clearly identifiable to species to the AUV-derived imagery, and only a subset of images has been examined to date.

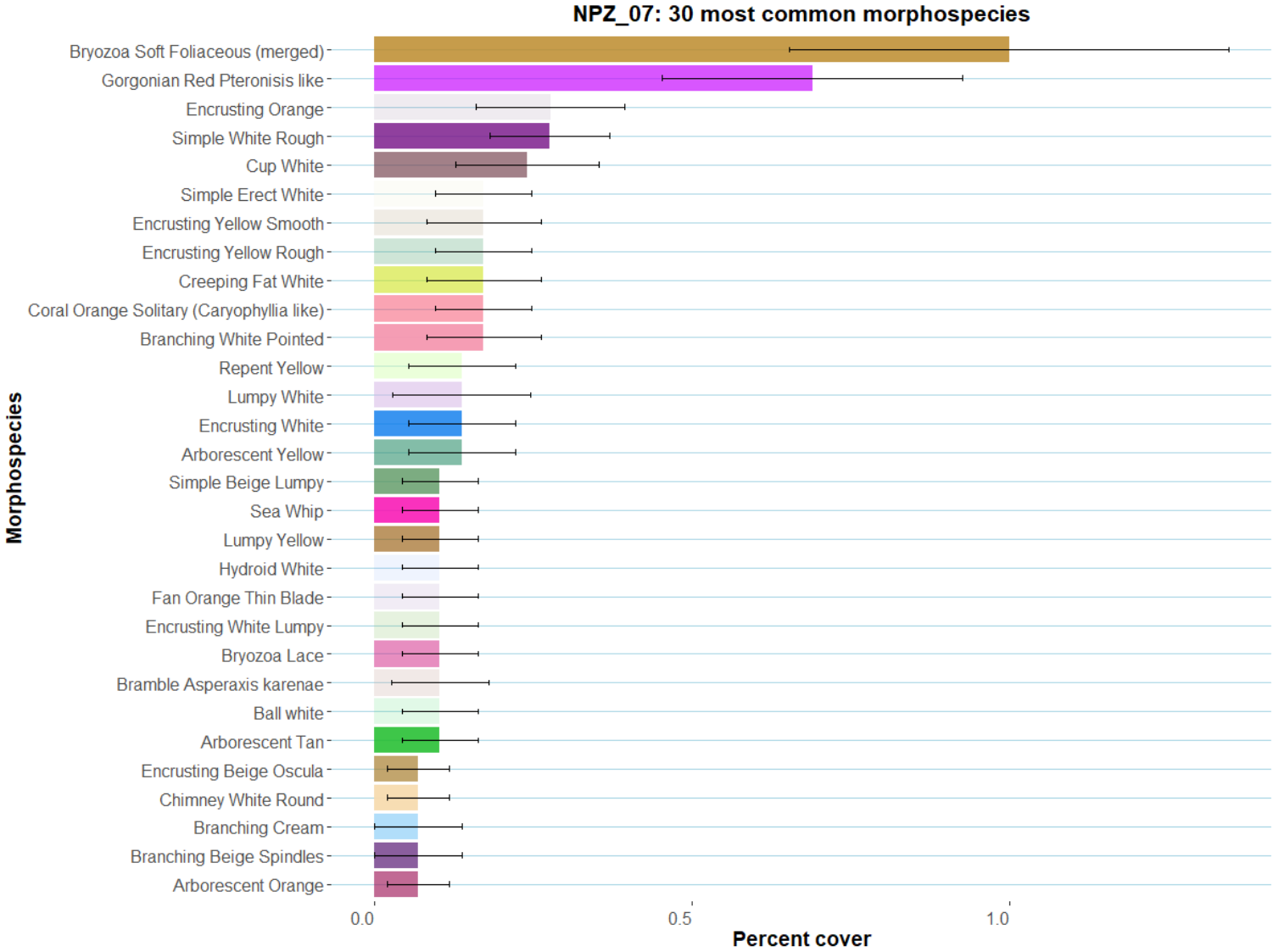

Figure 67. The 30 most dominant morphospecies across NPZ transect 7 in terms of percent cover. Error bars show standard error of percent cover estimates. Physical substrate categories, mobile species and biological matrix categories have been removed.

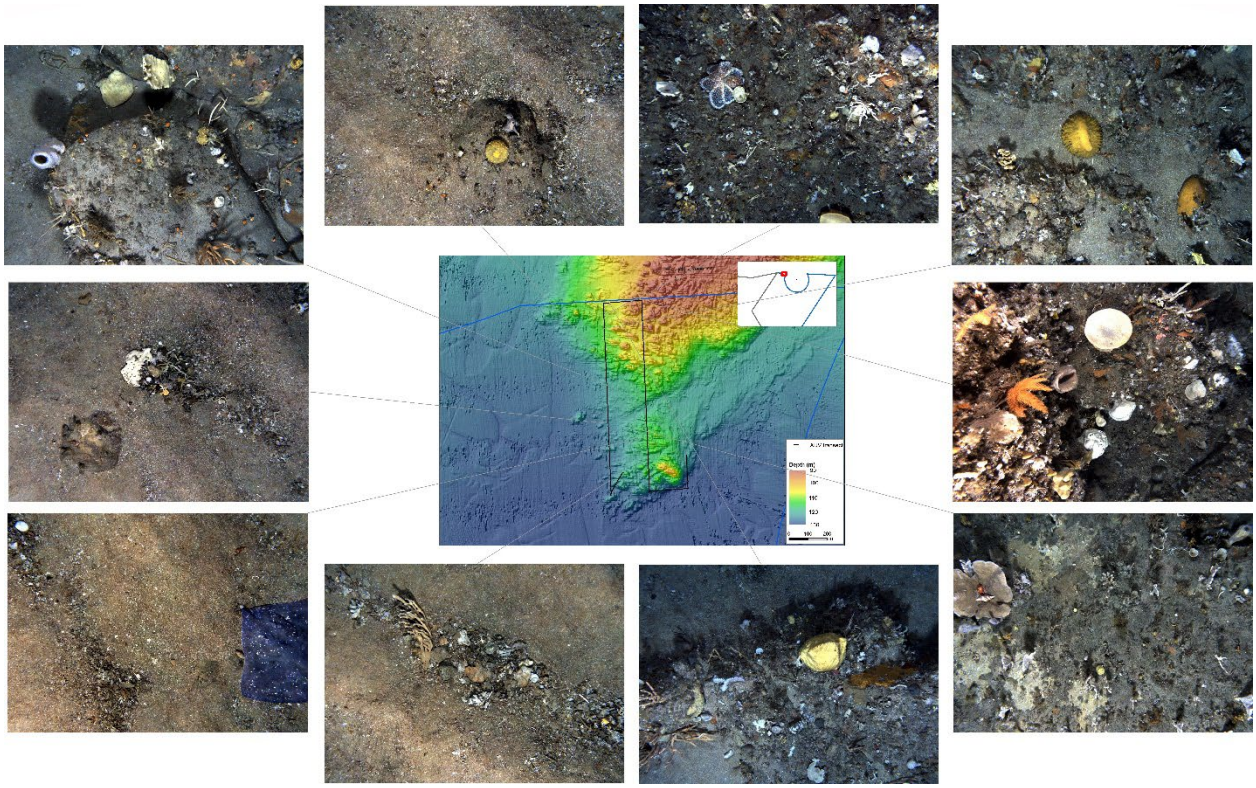

Figure 68. NPZ 7 transect and representative imagery showing key habitat features and common or unusual morphospecies. Common morphospecies include encrusting white sponge (bottom right image), red Pteronisis bamboo coral (centre right image), and cup white sponge (centre right image). Examples of morphospecies are shown in more detail in Figs 107-118 in the Appendix.

4.3.7 National Park Zone transect 8

This transect is located approximately 10 km to the west of the Mewstone (Figure 54) and was primarily designed to explore and describe the habitat and emergent fauna of a soft-sediment dominated region of the park, rather than reef-based features. Hence the transect is sand dominated with a small low profile patchy reef on the eastern flank of the transect, ranging in depth from ~123 to 134m (Figure 71). Overall biological cover on this reef system was very low (<0.2% cover) and was entirely restricted to the small number of sampled images that contained rocky reef features (Figure 55). Further sampling of reef images in this transect is flagged for future work. Only 7 morphospecies were scored across the reef component of the transect, comprising sponges, hydroids, and red gorgonians (Figure 70). The remaining sand habitat had no emergent sessile fauna, presumably due to regular disturbance of sediments in large swells.

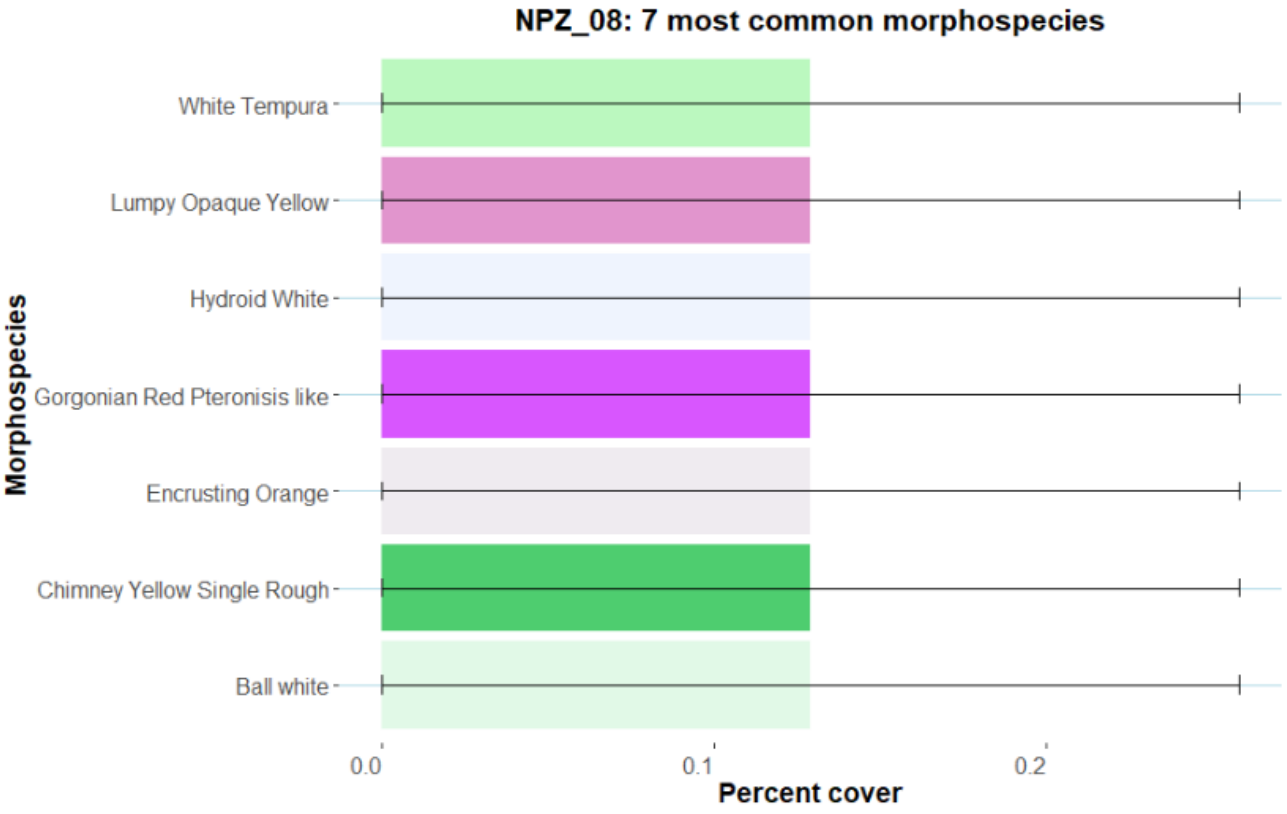

Figure 69. The 7 most dominant morphospecies across NPZ transect 8 in terms of percent cover. Error bars show standard error of percent cover estimates. Physical substrate categories, mobile species and biological matrix categories have been removed. Note that only 7 morphospecies were annotated in this transect.

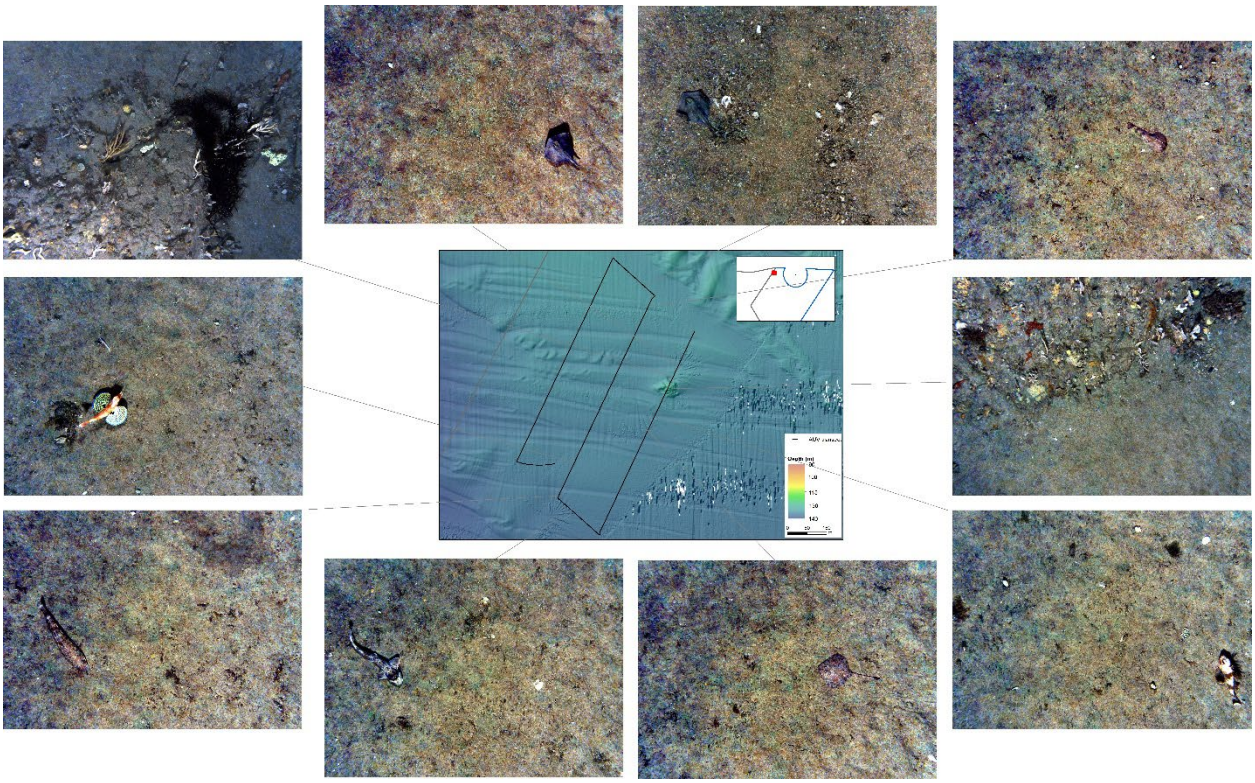

Figure 70. NPZ 8 transect and representative imagery showing key habitat features and common morphospecies. Common invertebrate morphospecies are difficult to discern and are typically low cover on sediment inundated reef as seen in the top left and right centre image. Fish associated with soft sediment and reef margins such as gurnard (centre left) and ocean perch (bottom right) are also shown. Examples of morphospecies are shown in more detail in Figs 107-118 in the Appendix.

4.3.8 Multi-Use Zone transect 1

This transect is located in the northern part of the MUZ close to the AMP boundary (Figure 54). The transect covers a mixture of large boulder/slab high-profile habitat interspersed with sediments and patchy reef that ranges in depth from ~131 to 153m (Figure 73). Overall biological cover on images including a reef component was lower than all transects in the NPZ except for NPZ_08, with no individual morphospecies exceeding 0.25% cover (Figure 55 and Figure 72). Dominant species included soft bryozoans and encrusting sponge morphospecies such as yellow smooth, white lumpy and orange beige morphospecies (Figure 72). A wide variety of other sponge morphospecies were present including ramose and creeping sponges such as ramose single cream and white tempura; erect forms such as arborescent white flat and branching white pointed; and massive forms such as ball pink oscula and ball yellow papillate irregular. Hydroids, lace bryozoans, solitary orange cup corals and octocorals were also present, such as black fine-branching octocoral, and orange bushy octocoral. MUZ_01 also had a large number of brittle stars and also hermit crabs with anemones attached to their shells (bottom right image in Figure 73).

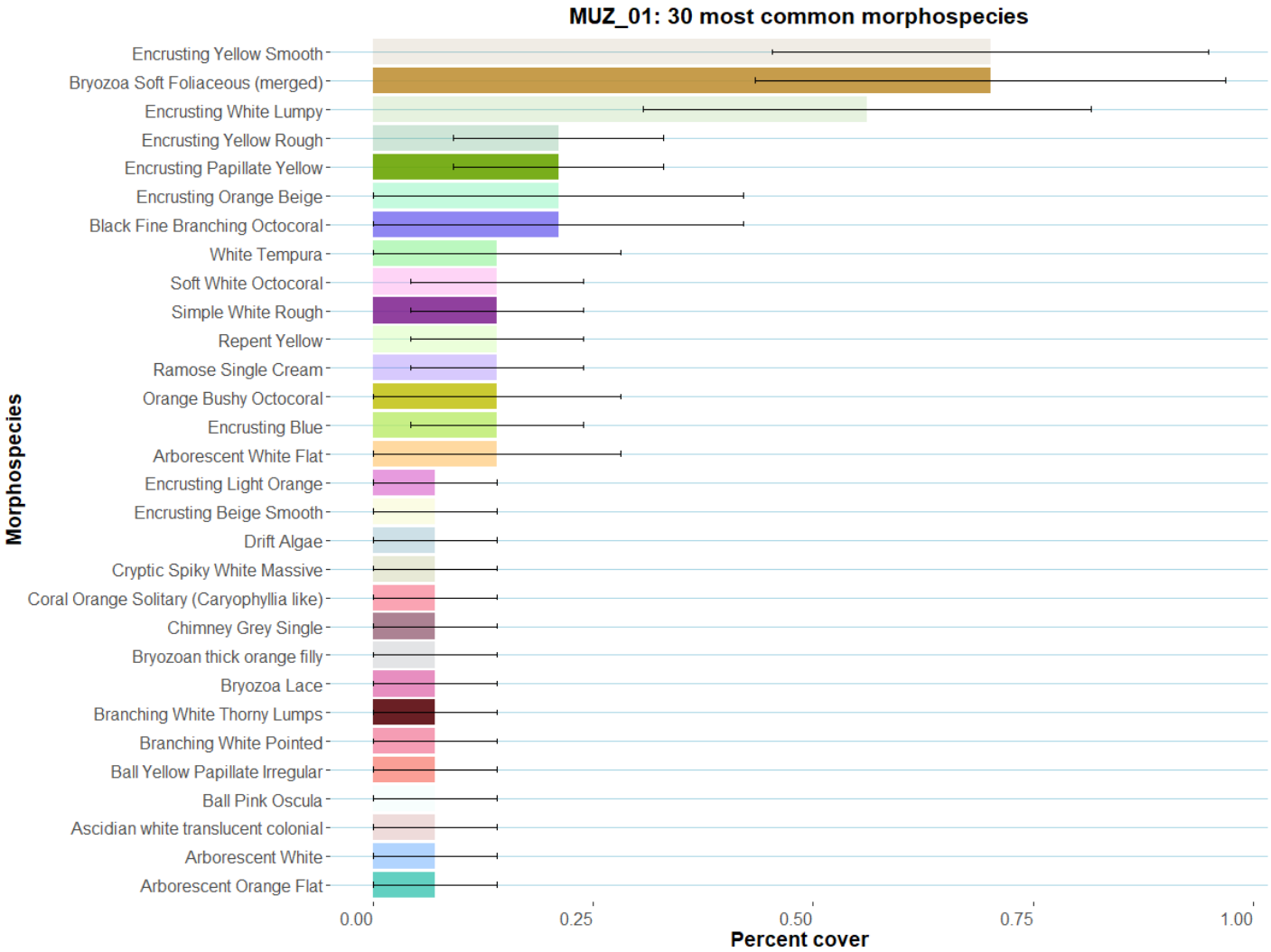

Figure 71. The 30 most dominant morphospecies across MUZ transect 1 in terms of percent cover. Error bars show standard error of percent cover estimates. Physical substrate categories, mobile species and biological matrix categories have been removed.

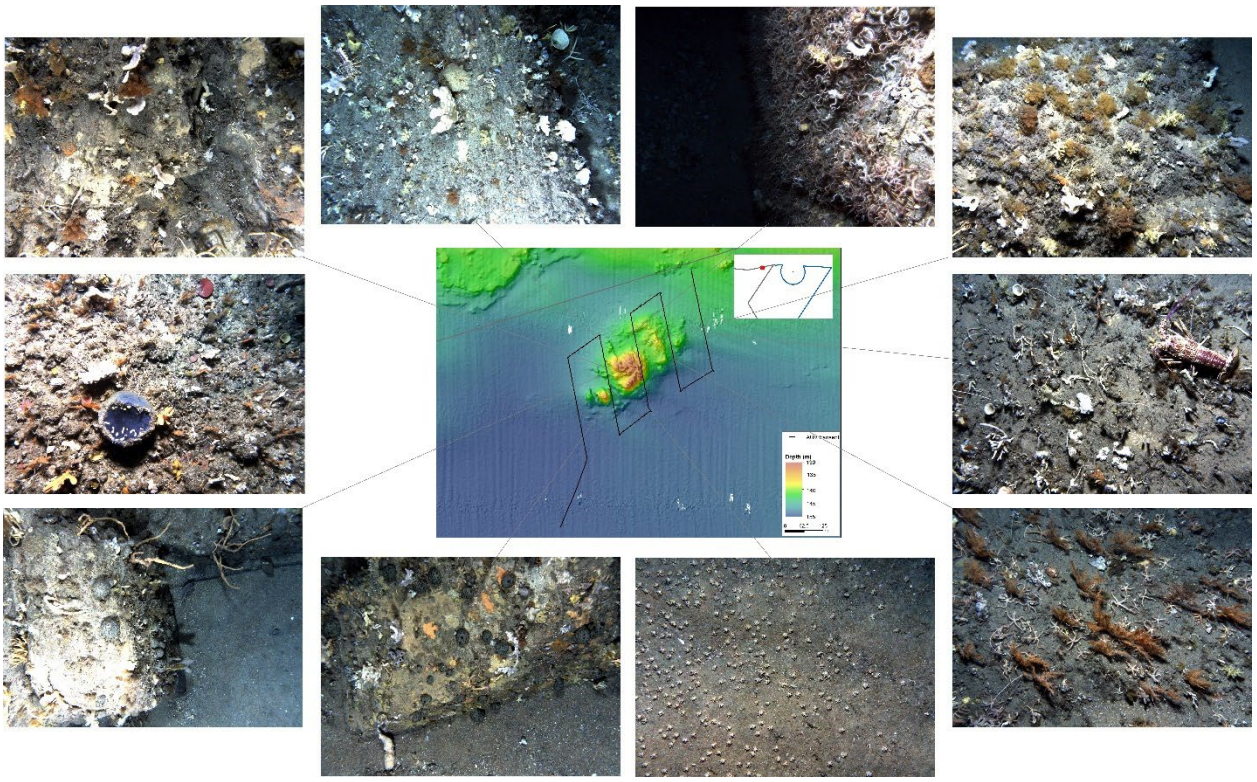

Figure 72. MUZ 1 transect and representative imagery showing key habitat features and common morphospecies. Common morphospecies include red Pteronisis bamboo coral (bottom right image) and soft bryozoans (top right image). Rock lobster (centre right image) and hermit crabs (bottom right image) are also shown. Examples of morphospecies are shown in more detail in Figs 107-118 in the Appendix.

4.3.9 Multi-Use Zone transect 2

This transect is located in the MUZ approximately 4 km south of the MUZ_01 transect (Figure 54). The transect is predominantly sand dominated with a small reef system occupying approximately 15% of the transect. This reef was composed of occasional large boulder/slab high-profile habitat and patchy reef that ranges in depth from ~135 to 157m and included the deepest known shelf reef outcrop in the park (Figure 75). Overall biological cover was lower than all transects in the NPZ except for NPZ_08, with the most abundant morphospecies (soft bryozoans) only comprising 0.1% cover (Figure 55 and Figure 74). Dominant species included soft bryozoans and encrusting sponge morphospecies such as yellow smooth and orange morphospecies (Figure 74). Other sponge morphospecies, hydroids, ascidians, and the octocorals bramble *Acabaria sp*. and *Asperaxis karenae*. were also present. MUZ_02 also had a large number of brittle stars (approximately 0.3% cover).

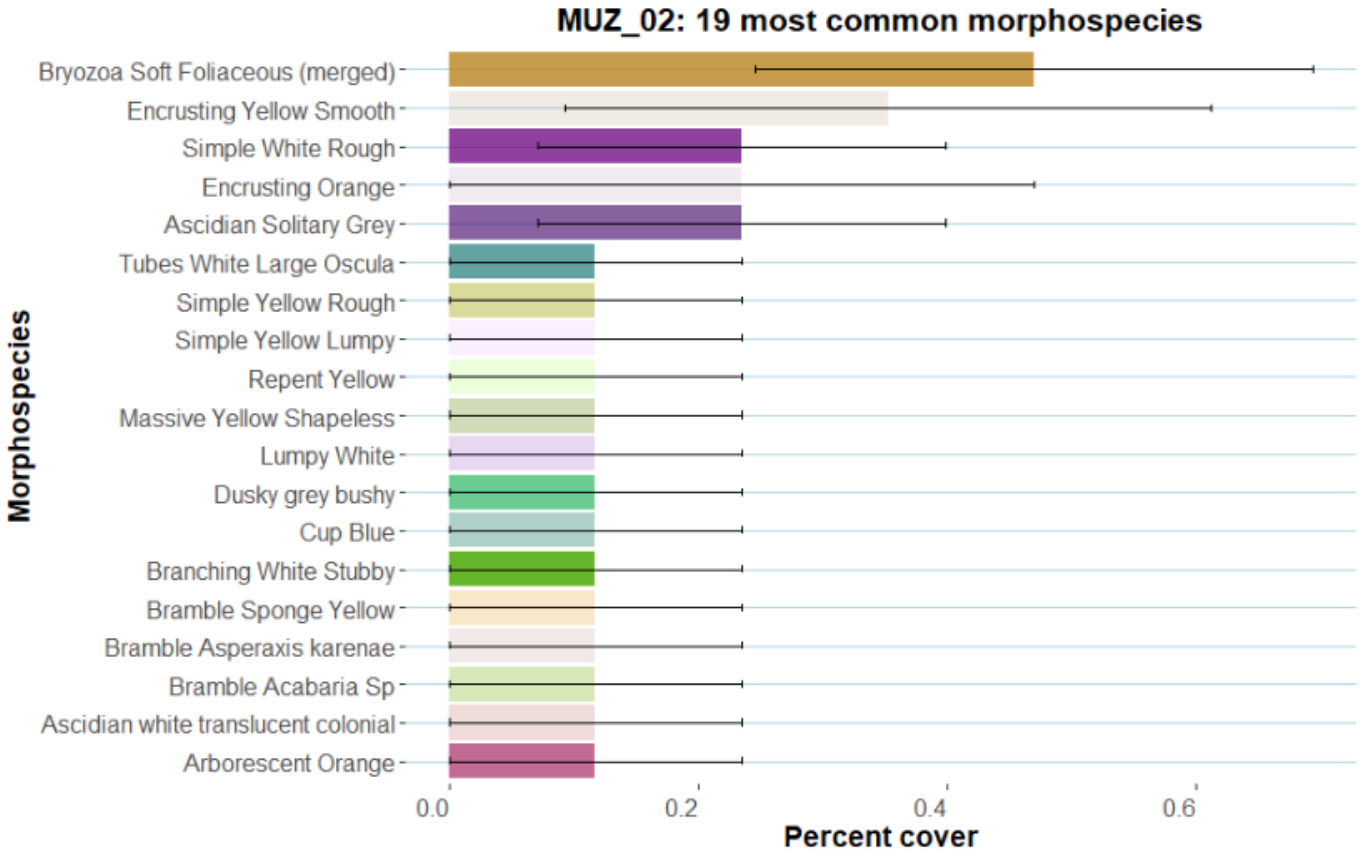

Figure 73. The 30 most dominant morphospecies across MUZ transect 2 in terms of percent cover. Error bars show standard error of percent cover estimates. Physical substrate categories, mobile species and biological matrix categories have been removed. Note that only 19 morphospecies were annotated in this transect.

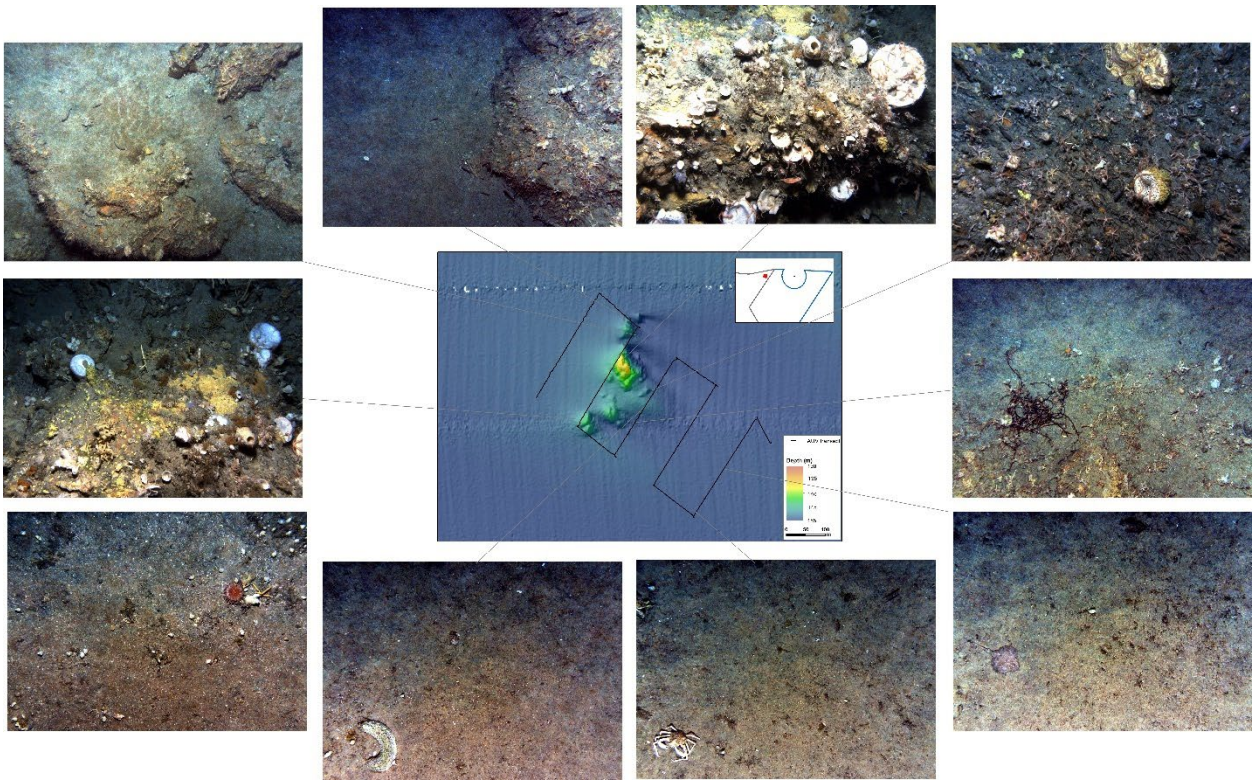

Figure 74. MUZ 2 transect and representative imagery. Showing key habitat features and common morphospecies. Common morphospecies include encrusting yellow smooth (top right and centre left images) and white cup sponges (top right and centre left images). Examples of morphospecies are shown in more detail in Figs 107-118 in the Appendix.

4.3.10 Northern reference transect (Ref_N_1)

The northern reference transect is located to the north of the MUZ approximately 3 km to the north-east of the MUZ_01 transect (Figure 54). The transect covers a mixture of large boulder/slab high-profile habitat interspersed with smaller patches of sediments that range in depth from ~63 to 114m, hence providing regional representation of reefs in the 65-100 m range that are not covered by transects within the TFMP (Figure 77). Examination of images with reef present indicated that overall biological cover was higher than any of the transects conducted inside the TFMP, with > 60% of annotated points landing on biological categories (Figure 55). Dominant species included soft bryozoans and the red *Pteronisis* gorgonian coral (Figure 76). A wide variety of sponge morphospecies were present including encrusting orange, yellow smooth, black, and beige smooth; massive forms such as lumpy white, simple beige shapeless, and massive grey laminar like; erect forms such as branching cream and yellow thick pointed; and white and red cup sponges. Hydroids, lace bryozoans, and octocorals were also present, such as bramble *Acabaria sp*., and sea whips.

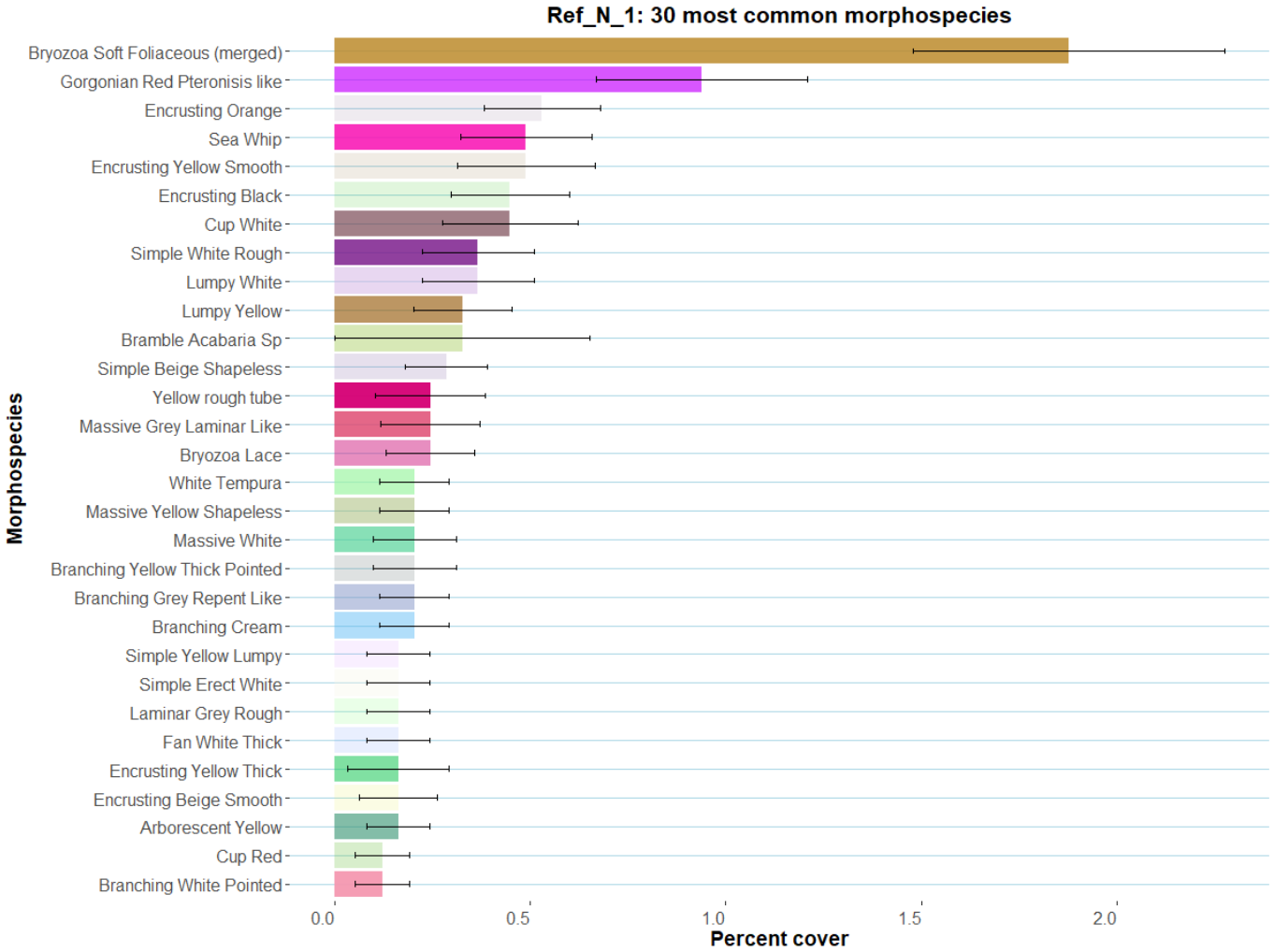

Figure 75. The 30 most dominant morphospecies across the northern reference transect in terms of percent cover. Error bars show standard error of percent cover estimates. Physical substrate categories, mobile species and biological matrix categories have been removed.

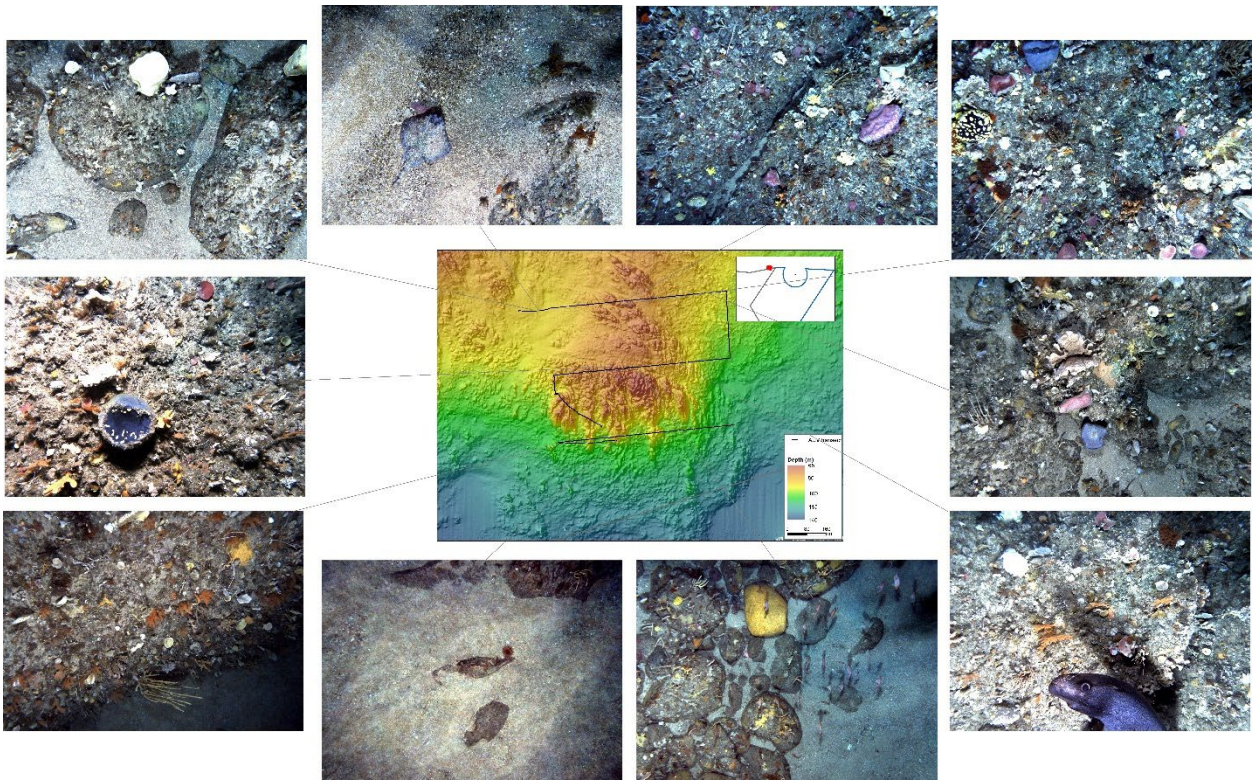

Figure 76. Northern reference transect and representative imagery showing key habitat features and examples of the more common morphospecies. Common morphospecies include encrusting yellow smooth (bottom right image), cup red (top right image), simple white rough sponge (bottom right), and encrusting orange sponge (bottom left image). Examples of morphospecies are shown in more detail in Figs 107-118 in the Appendix.

4.3.11 Central (Mewstone) reference transect (Ref_C_1)

The central reference transect is located ~1km directly south of the Mewstone (Figure 54). The transect was predominantly on reef and covers a mixture of large boulder/slab high-profile habitat interspersed with smaller patches of sediments and cobbles. The transect ranges in depth from ~39 to 69m and was intended as a regional representative of reef in the 40-65 m depth range, not adequately covered by other AUV-transects in this survey or region (Figure 79). Overall biological cover was the highest of any transect conducted, with > 75% of annotated points landing on biological categories (Figure 55). Dominant species included soft bryozoans, sea whips and the red *Pteronisis* gorgonian coral (Figure 78). Due to shallower depth of this transect, algal species were present, including encrusting calcareous red algae, which had ~2% cover across the transect (Figure 78). A wide variety of sponge morphospecies were present including encrusting orange, white lumpy, yellow thick, and white; massive forms such as lumpy white and simple white rough; erect forms such as palmate grey, and laminar peach irregular; and white and red cup sponges. Hydroids, parazoanthids, and lace bryozoans were also present, but octocorals (e.g., soft octocorals and *Acabaria sp*.) were notably not as abundant in this transect.

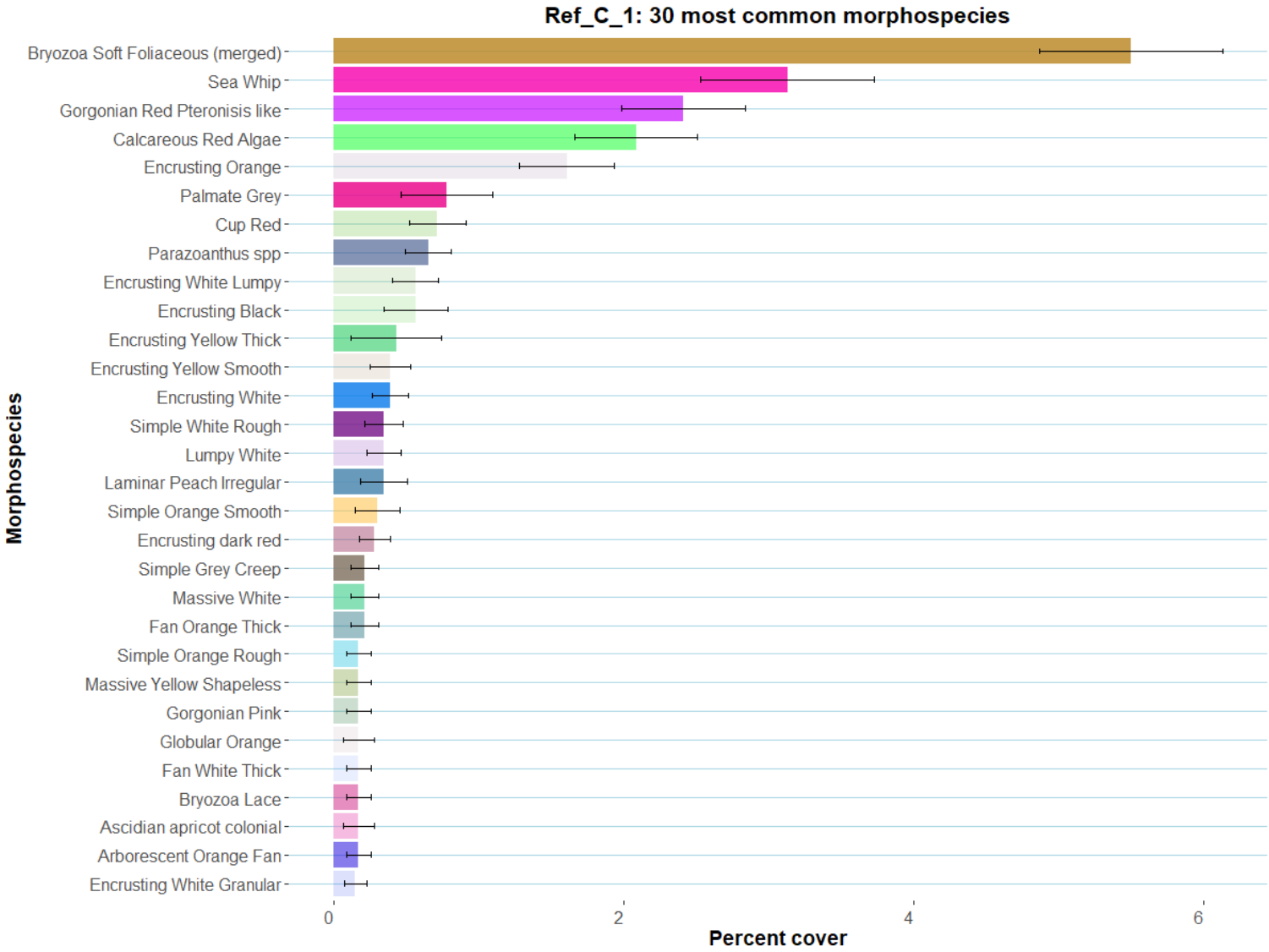

Figure 77. The 30 most dominant morphospecies across the central reference transect in terms of percent cover. Error bars show standard error of percent cover estimates. Physical substrate categories, mobile species and biological matrix categories have been removed.

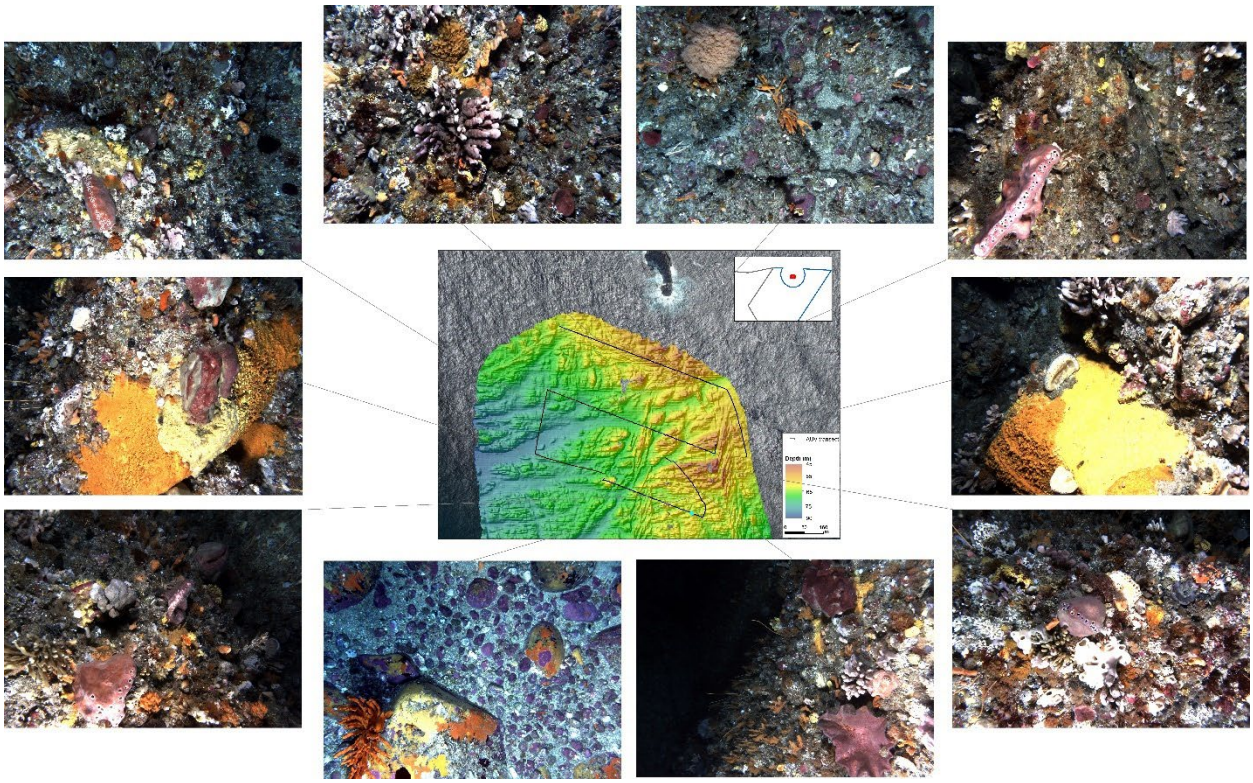

Figure 78. Central (Mewstone) reference transect and representative imagery showing examples of key habitat features and the more common morphospecies. Common morphospecies include palmate grey sponge (top left image), soft bryozoans (top right image), red cup sponges (bottom right image), encrusting orange and yellow smooth sponges (centre left and right images and bottom left images), and calcareous red algae (bottom left image). Examples of morphospecies are shown in more detail in Figs 107-118 in the Appendix.

4.4 Distribution maps for dominant seabed benthos

4.4.1 Soft bryozoans

Soft bryozoans were commonly found across all surveyed areas that contained rocky reef, and across all depths (Figure 80). The only transect where no soft bryozoans were observed was NPZ_08, which was a sand dominated transect with very little rocky reef. Despite the apparent high percentage cover per image shown in Figure 80, the average percentage cover of this grouped morphospecies (i.e. it includes all identified soft bryozoan morphospecies) in images including reef typically ranged from 0.1 to 2% across each of the transects in the survey. An example image and close-up is given in Appendix 6.1.

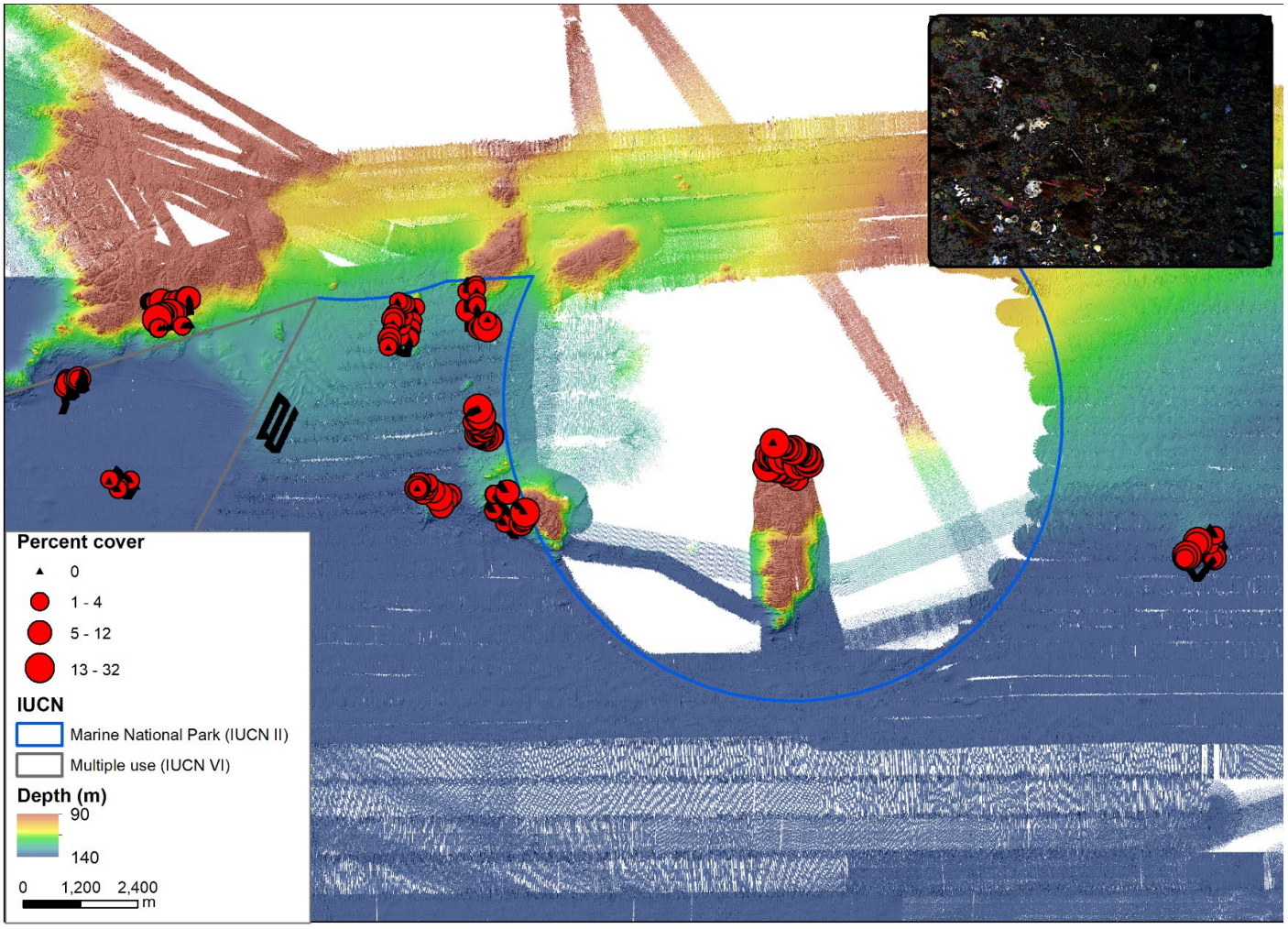

Figure 79. Distribution of soft bryozoans in AUV imagery across all annotated images

4.4.2 Red gorgonians (*Pteronisis* like)

Red gorgonians were common on rocky reefs across all transects, with the exception of the two transects in the MUZ (Figure 81). They were often found in high density within images, with cover of up to 24% within an image, and appear to be more dominant in shallower locations surveyed. Despite this apparent high cover in some imagery, the patchy nature of their distribution meant that the average cover of the red gorgonian morphospecies in images with any component of reef in them typically ranged from 0.1 to 1% cover for transects in this survey. An example image and close-up is given in Appendix 6.1.

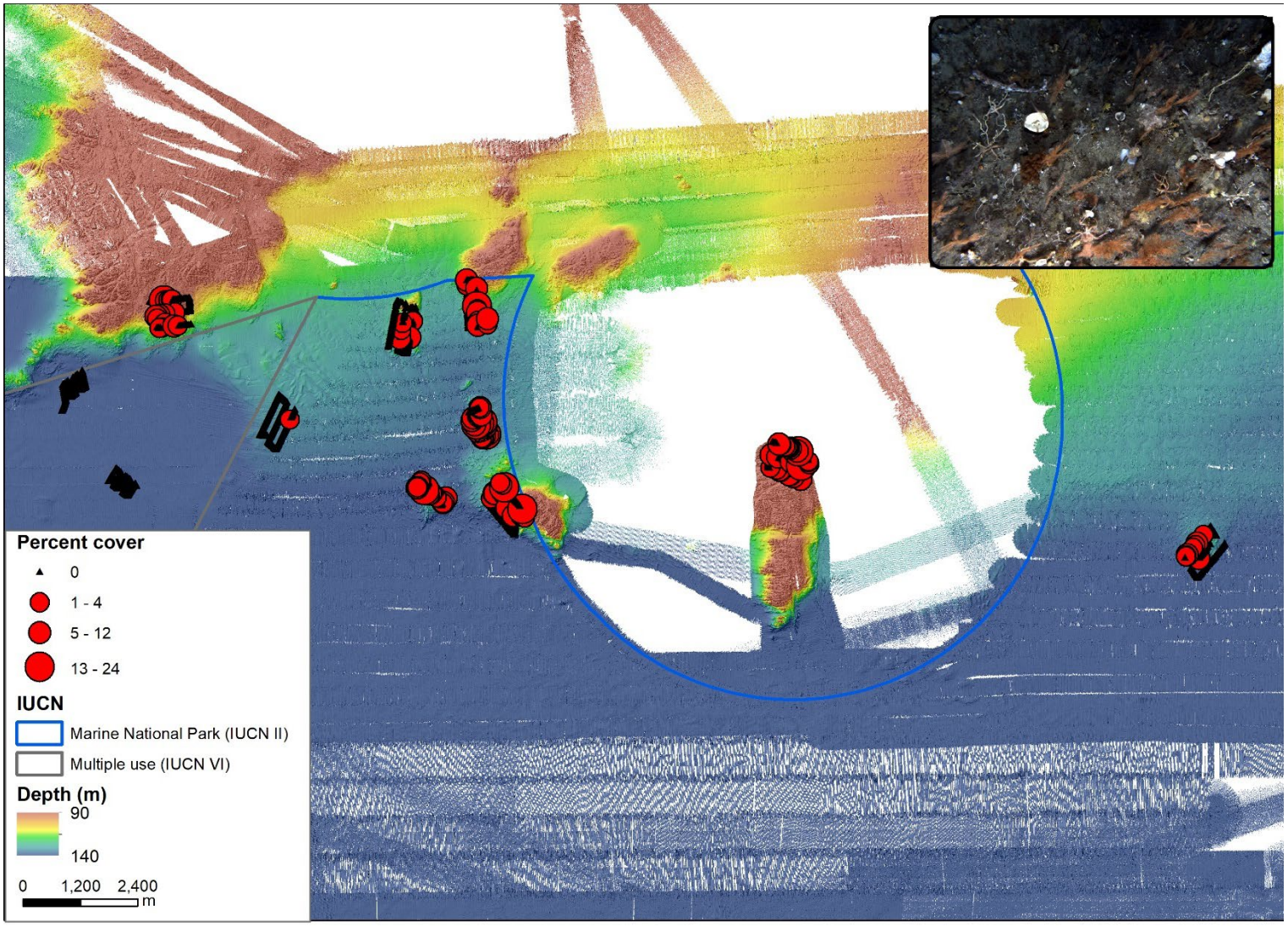

Figure 80. Distribution of red gorgonians (Pteronisis like) in AUV imagery across all annotated images

4.4.3 White cup sponge

White cup sponges are conspicuous and reasonably widespread across the surveyed area, but especially dominant on reefs within the NPZ, with the exception of NPZ_08 transect. White cups were abundant on the northern refence transect, but less dominant on the central reference transect and notably absent from the two transects in the MUZ (Figure 82). Despite this apparent moderate cover in some imagery, the patchy nature of their distribution meant that the average cover of the white cup sponge morphospecies in images with any component of reef in them typically ranged from 0.05% to 0.5% cover for transects in this survey where it was present. An example image and close-up is given in Appendix 6.1.

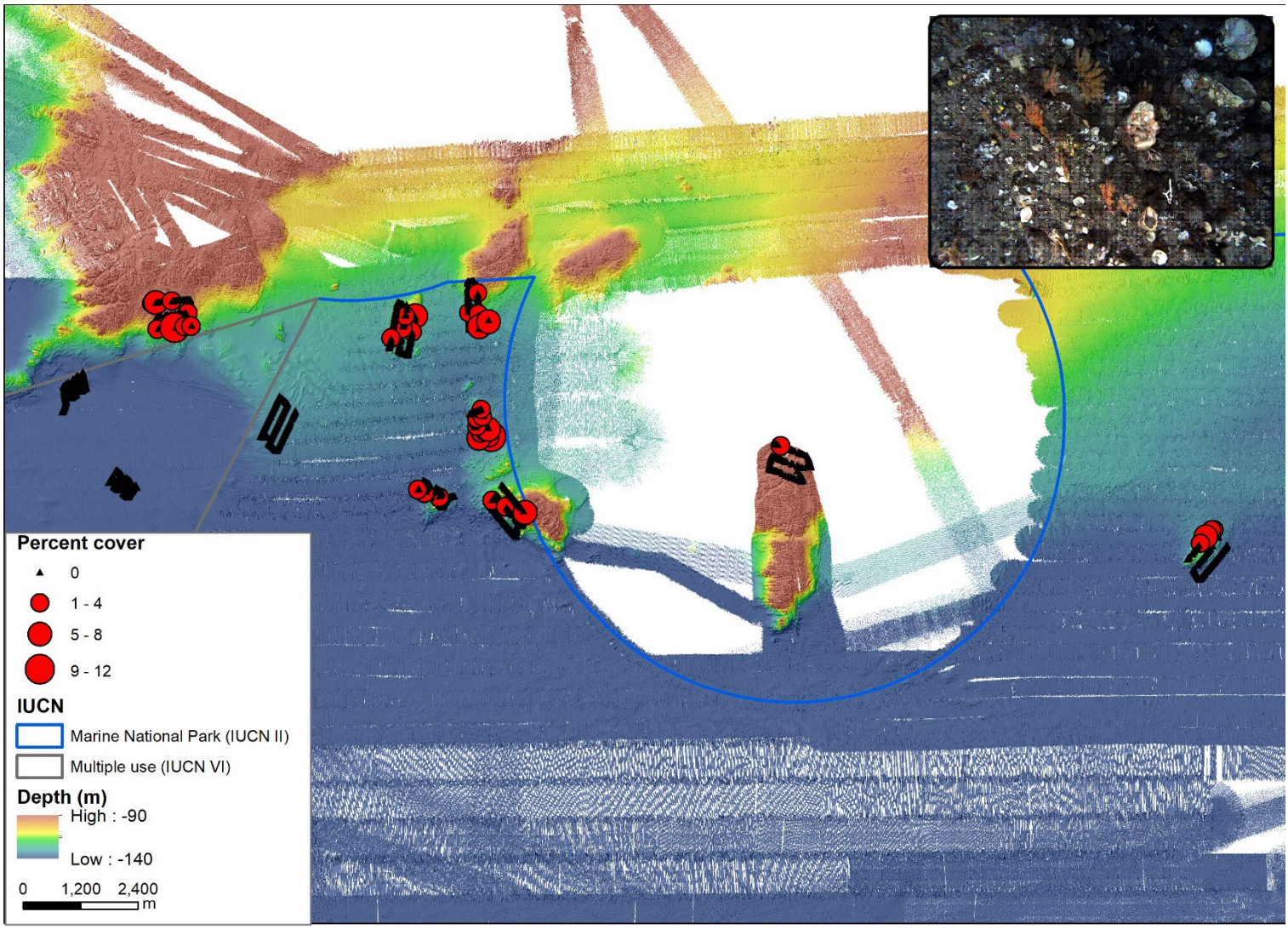

Figure 81. Distribution of white cup sponge in AUV imagery across all annotated images

4.4.4 Branching white pointed sponge

Branching white pointed sponge were more dominant in the western portion of the surveyed area, being found in all transects within the NPZ with the exception of NPZ_08 (Figure 83). This morphospecies was also found within the Northern reference transect, but not within the central reference transect. However, within the MUZ it was only found in within the MUZ_01 transect and not the MUZ_02 transect. It was found in lower abundance in the eastern NPZ_04 transect. Despite this apparent moderate cover in some imagery, the patchy nature of their distribution meant that the average cover of the branching white pointed sponge morphospecies in images with any component of reef in them typically ranged from 0.05 to 0.2% cover for transects in this survey where they were present. An example image and close-up is given in Appendix 6.1.

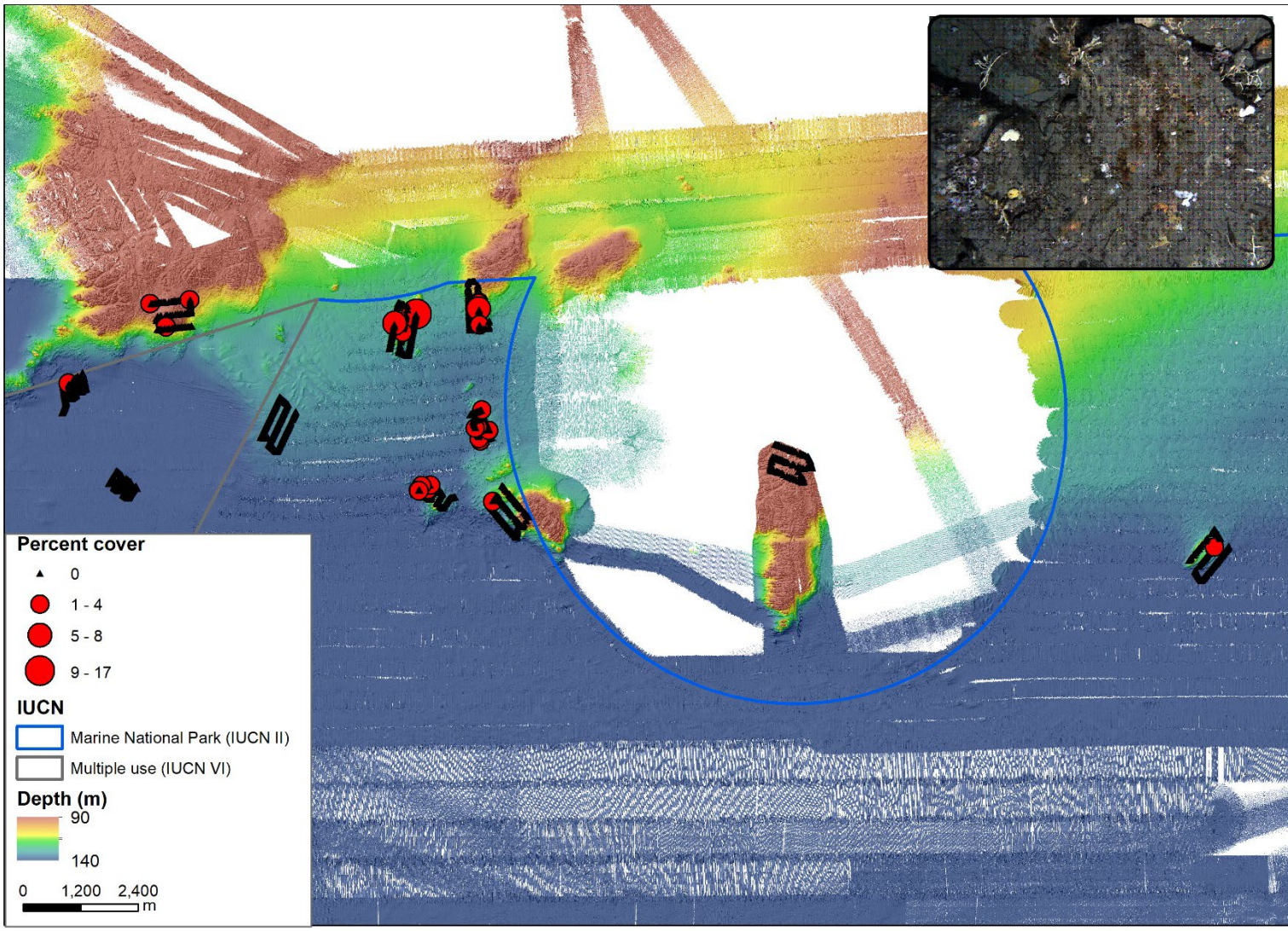

Figure 82. Distribution of branching white pointed sponge in AUV imagery across all annotated images

4.4.5 Encrusting yellow smooth sponge

Encrusting yellow smooth sponge was distributed widely, occurring across all transects in the surveyed area with the exception of NPZ_08 (Figure 84). Despite this apparent moderate cover in some imagery, the patchy nature of their distribution meant that the average cover of the encrusting yellow smooth sponge morphospecies in images with any component of reef in them typically ranged from 0.1 to 0.5% cover for transects in this survey. An example image and close-up is given in Appendix 6.1.

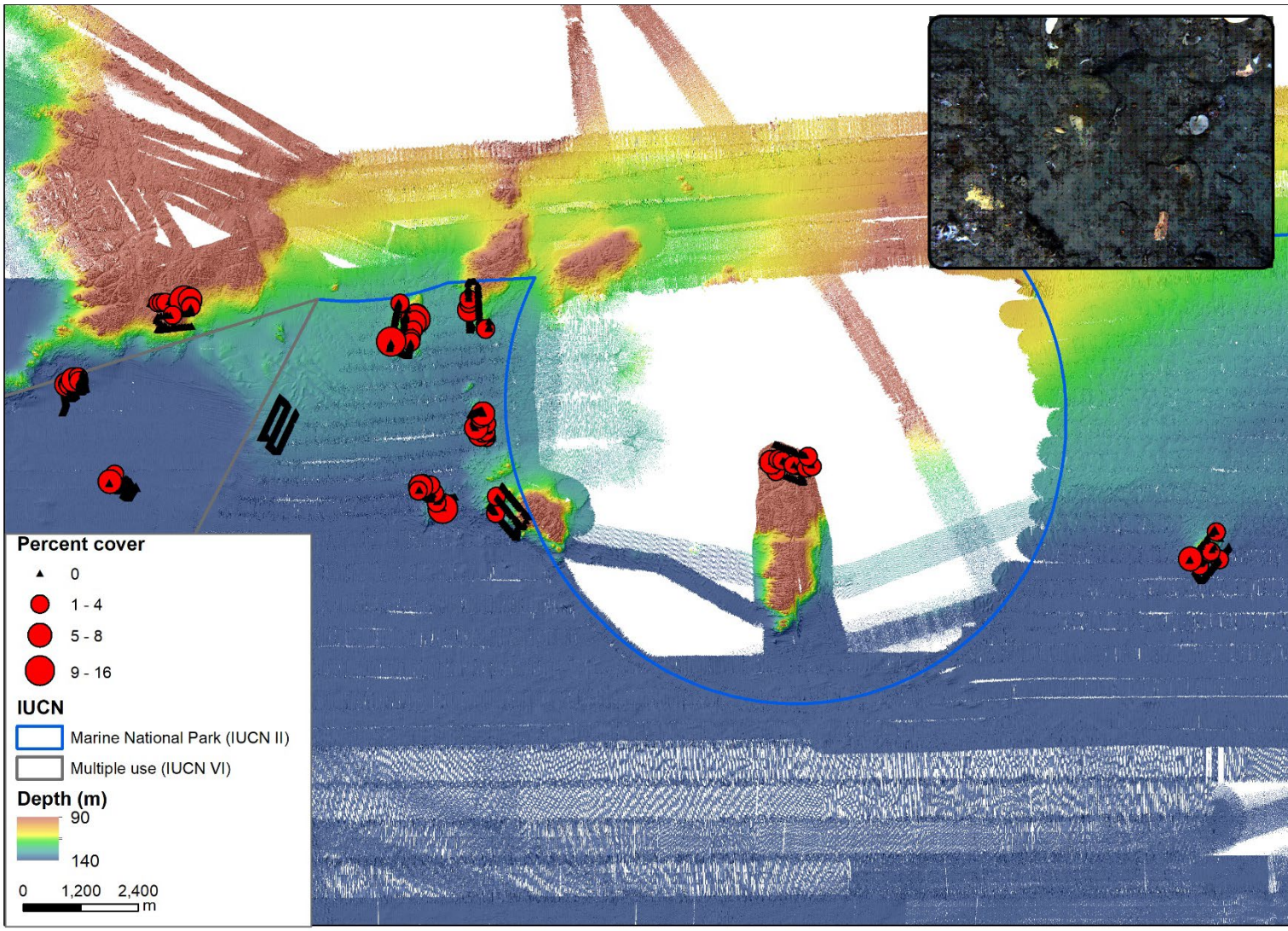

Figure 83. Distribution of encrusting yellow smooth sponge in AUV imagery across all annotated images

4.4.6 Encrusting orange sponge

Encrusting yellow smooth sponge was distributed widely, occurring across all transects in the surveyed area. It was especially dominant in the central reference transect, the northern transects in the NPZ (NPZ_01, NPZ_06, and NPZ_07; Figure 85). Despite this apparent high cover in some imagery, the patchy nature of their distribution meant that the average cover of the encrusting orange sponge morphospecies in images with any component of reef in them typically ranged from 0.1 to 1.2% cover for transects in this survey. An example image and close-up is given in Appendix 6.1.

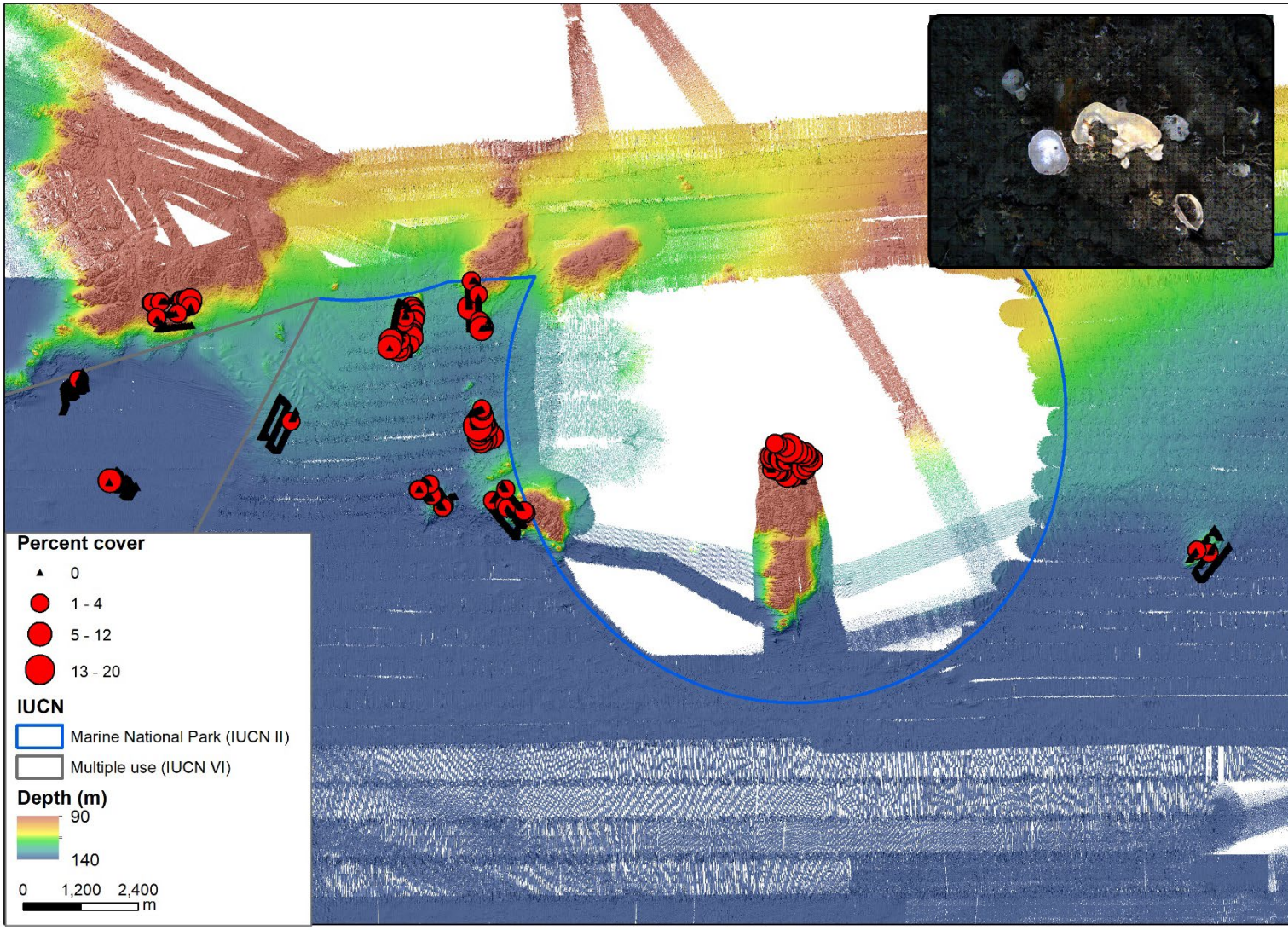

Figure 84. Distribution of encrusting orange sponges in AUV imagery across all annotated images

4.4.7 Lace bryozoans

Lace bryozoans were sparsely distributed across all transects except NPZ_08 and MUZ_02 (Figure 86). Despite this apparent high cover in some imagery from transects where they were found, the patchy nature of their distribution meant that the average cover of lace bryozoan morphospecies in images with any component of reef in them typically ranged from 0.1 to 0.5% cover for transects in this survey. An example image and close-up is given in Appendix 6.1.

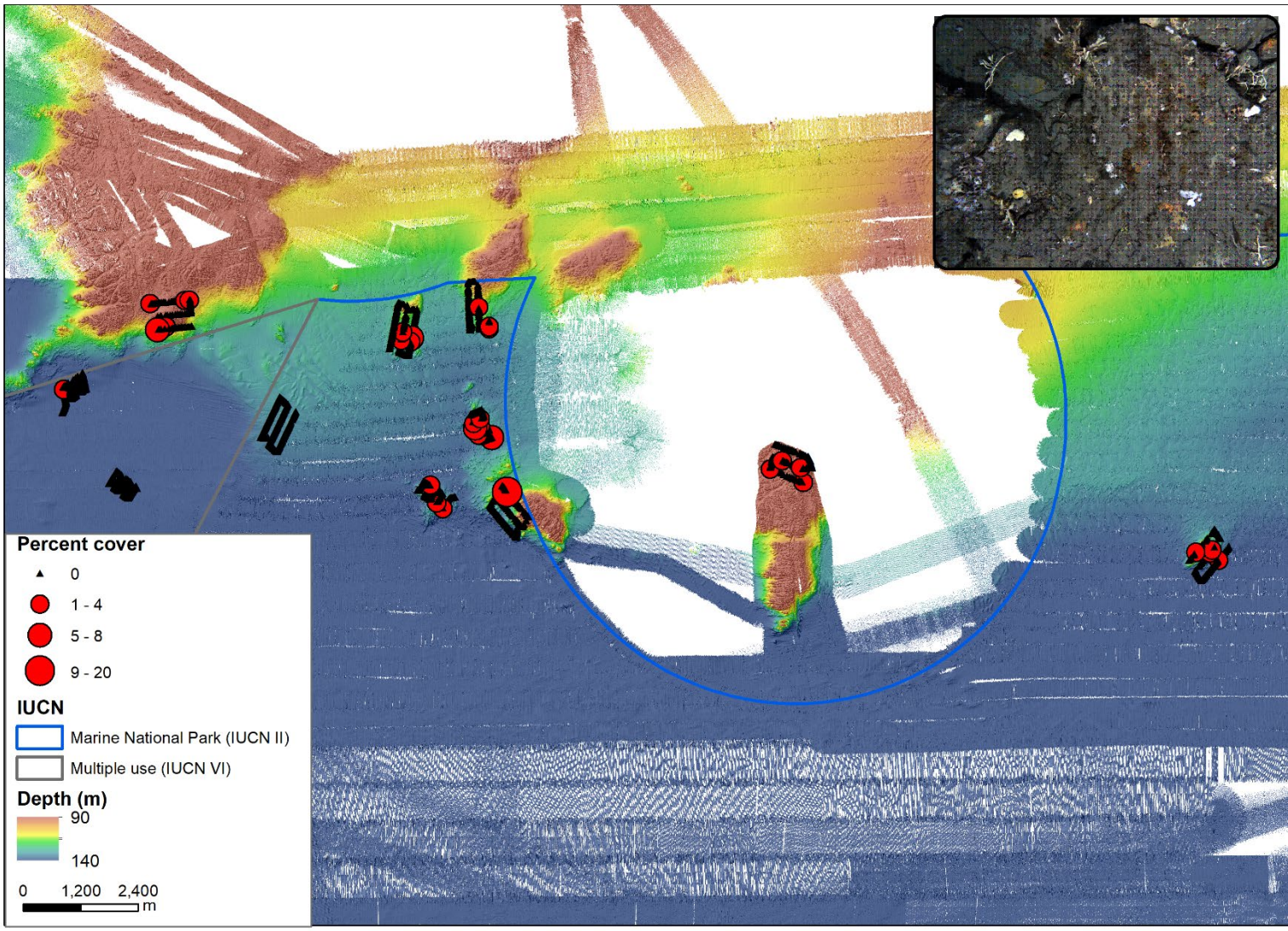

Figure 85. Distribution of lace bryozoan in AUV imagery across all annotated images

4.4.8 Simple white rough sponge

Simple white rough sponges were distributed relatively evenly across transects in the TFMP, occurring across all transects except NPZ_08 (Figure 87). Despite this apparent high cover in some imagery, the patchy nature of their distribution meant that the average cover of red gorgonians in images with any component of reef in them typically ranged from 0.1 to 1.2% cover for transects in this survey. An example image and close-up is given in Appendix 6.1.

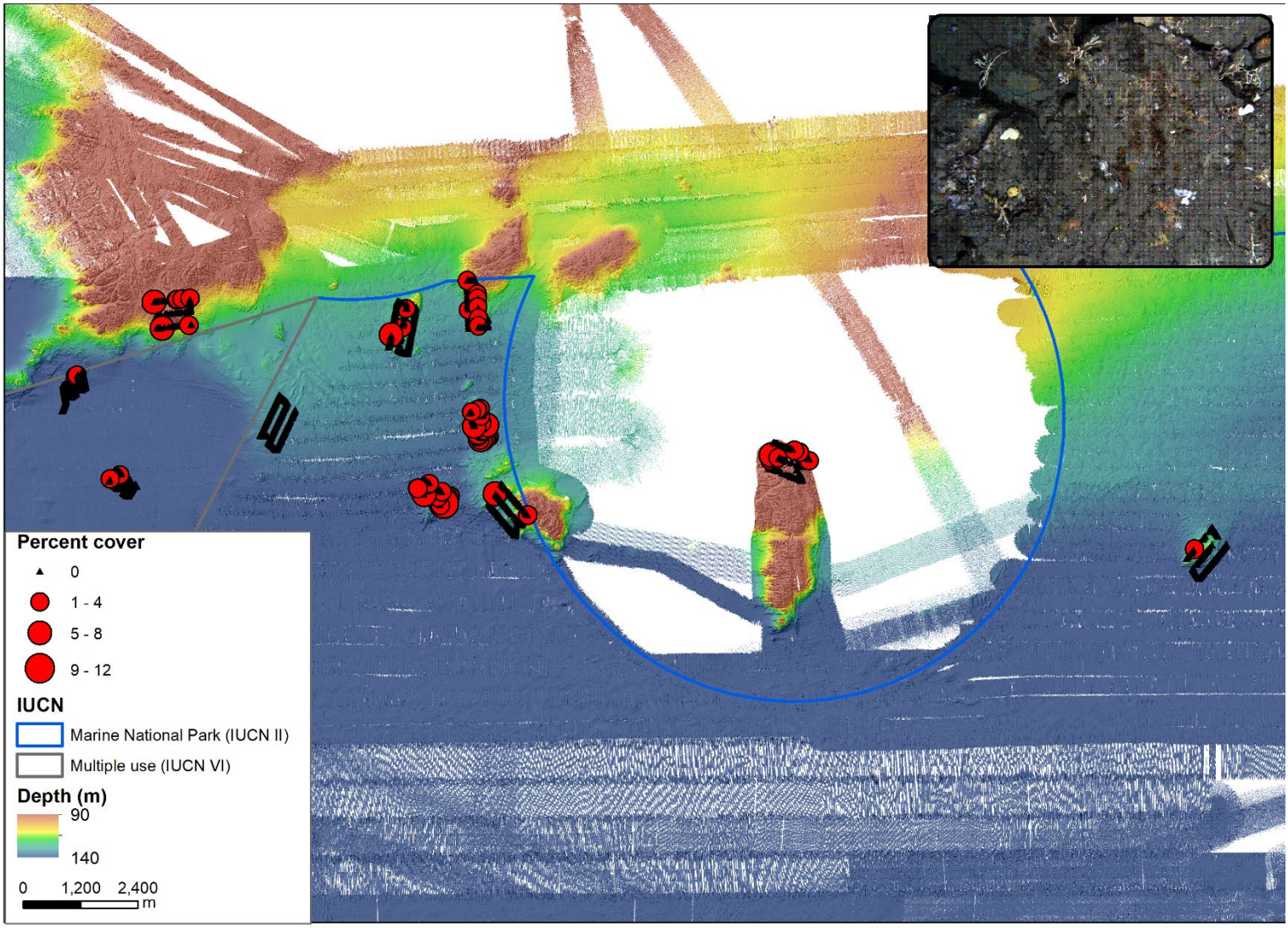

Figure 86. Distribution of simple white rough sponge in AUV imagery across all annotated images

4.5 Detailed analysis of changes across the time-series for dominant seabed benthos

4.5.1 Methods

Two AUV transects were completed within the NPZ in 2015 as part of a previous biodiversity survey that was unfortunately truncated by bad weather and gear failure before a larger number could be completed. These transects, NPZ_01 and NPZ_02 (Figure 54) were repeated in 2021 to gain an initial understanding of temporal variability in the sessile benthic biota of the deep reef systems in this region. The same annotation protocol was used across both data sets, with systematic image selection along each transect resulting in > 100 images sampled, with images overlain with 25 random points for annotation. A total of 261 images were scored in the 2015 survey and a total of 265 in the 2021 survey. However, images along a "transitory leg" between the two main transects was also scored in the 2015 data set. To make the data more spatially comparable between surveys, the imagery along this transitory leg (a total of 46 images) were first excluded from the 2015 data set, resulting in 215 images being available for analysis in the 2015 data. Both data sets were thoroughly checked for consistency in annotation across the surveys prior to data collation.

For analysis, images across the two transects were merged for each survey year. A spatial model-based approach was applied that treats images as samples and estimates the spatial autocorrelation between images for each morphospecies modelled. A similar modelling approach was used in the detailed modelling sections for the BRUV and rock lobster potting data in this report, and more details can be found there. A subset of "dominant" morphospecies was selected for detailed analysis. These morphospecies were those that had at least 0.25% cover in one of the surveys, resulting in a total of 19 morphospecies (Table 23). This is a conservative approach, as a 0.5% cut-off has been used previously (see Perkins et al. 2021), and therefore included a larger number of morphospecies than a 0.5% cut-off would have provided. The 19 morphospecies included soft bryozoans (grouped for analysis), octocorals (gorgonians, soft fleshy corals, and sea whips), a hydroid, and a variety of sponges including encrusting, massive, repent and cup morphospecies (Table 23). Brittle stars were also included in the detailed analysis. Despite being mobile species, which are typically excluded, they were particularly dominant across reefs in the region and are likely to be important in the trophic food web of the benthic ecosystem.

Table 23. Dominant morphospecies analysed across the two surveys (2015 and 2021) across the NPZ_01 and NPZ_02 transects

Taxonomic group	Morphospecies
Bryozoa	Bryozoa Soft (merged)
Echinoderms	Brittle / snake stars
Hydroids	Hydroid White
Octocorals	Soft White Octocoral
	Soft Capnella Like
	Sea Whip
	Gorgonian Red Pteronisis Like
	Bramble Acabaria Sp
Sponges	Simple White Rough
	Repent Yellow
	Massive White Shapeless
	Lumpy White
	Encrusting Yellow Smooth
	Encrusting Yellow Rough
	Encrusting White Lumpy
	Encrusting White
	Encrusting Orange
	Encrusting Black
	Cup White

Models treated the response variable for each morphospecies as a binomial variable. That is, the number of points used in an image (typically 25 but may be less where some points were unscorable) was treated as the number of trials, with the number of points falling on the morphospecies in each image being the number of 'successes'. Survey year (2015 or 2021) was treated as a categorical variable, so that the model intercept represents the estimate for the log-odds of a point landing on the specific morphospecies in the 2015 survey, and the 'temporal effect' tests whether the 2021 survey significantly differs from the 2015 survey. Depth was included a continuous covariate to account for any depth related effects and was scaled prior to analysis by centring on the mean and dividing by the standard deviation. As with detailed model outputs for BRUVs and rock lobster potting components, posterior distributions and the 95% credible intervals are provided in the output, with credible intervals that do not include zero being considered evidence of a "significant" effect in the frequentist sense. For ease of interpretation, coefficient estimates are highlighted red and green to indicate significant negative and positive effects.

The magnitude of the temporal change for morphospecies that displayed a significant result was estimated from the model coefficients by calculating the binomial probabilities at each time point. That is, the mean probability that a point lands on a given morphospecies for a specified survey year. For these calculations, the depth effect was set to zero. As depth was scaled, this calculation is therefore reflective of changes at the mean depth across the survey data (125 m). Probabilities were calculated by back-transforming from the log-odds scale both the intercept (representing the 2015 survey) and the linear combination of the intercept and the temporal term (representing the 2021 survey). The change in probability was then quantified as a percentage change.

4.5.2 Results

Raw percent cover for the dominant morphospecies indicated that some morphospecies have changed significantly between the 2015 and 2021 surveys (). This was supported by model outputs, with 13 of the 19 modelled morphospecies showing statistically significant changes between 2015 and 2021 (Table 24). Of particular note is a significant decline observed in 4 out of the 6 octocoral morphospecies. Large declines were observed in the cover of the Hydorid white, soft fleshy corals, soft white octocoral and soft *Capnella* like, but especially the latter which showed a 97% decrease in probability between 2015 and 2021 (Figure 89-Figure 92. The bramble *Acabaria* sp. octocoral also showed significant decline in cover between 2015 and 2021 (Figure 83; Figure 88), with an 87% decrease in probability. Sea whips showed no significant differences.

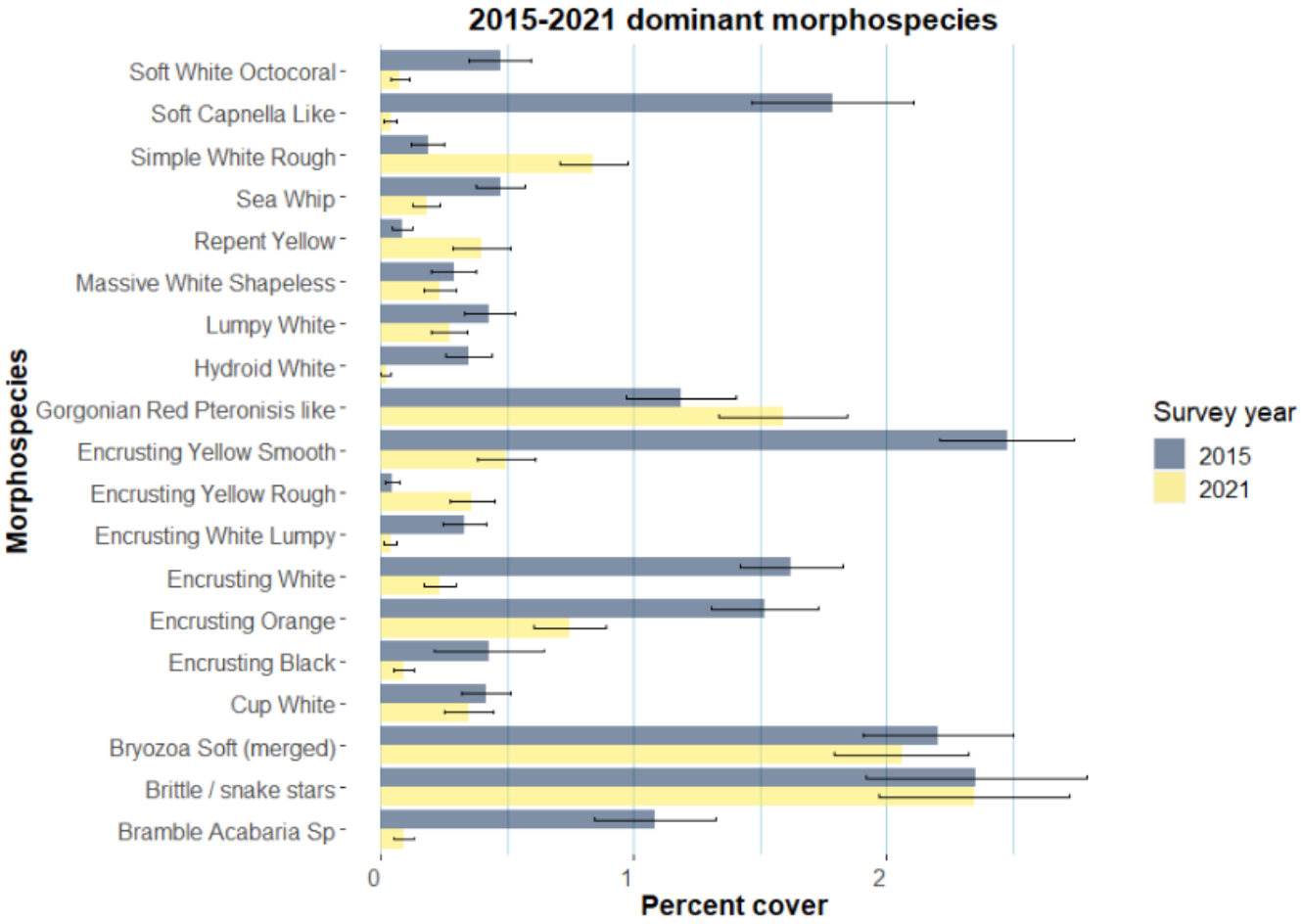

Figure 87. Raw percent covers (and standard errors) for the 19 dominant morphospecies analysed across the 2015-2021 surveys

Table 24. Model-based coefficient estimates of the temporal effect (change between 2015 and 2021) and depth effect for the 19 dominant morphospecies analysed. Effects highlighted red indicate a statistically significant decline (temporal effect) or negative association with depth, and green statistically significant increases (temporal effect).

Taxonomic group	Morphospecies	Temporal effect	Temporal effect size (% change in probability)	Depth effect
Bryozoa	Bryozoa Soft (merged)	0.018 (-0.292, 0.328)		-0.493 (-0.738, -0.246)
Echinoderms	Brittle / snake stars	0.044 (-0.313, 0.402)		-0.150 (-0.430, 0.131)
Hydroids	Hydroid White	-2.770 (-5.073, -1.031)	-94%	-0.442 (-0.813, -0.048)
Octocorals	Soft White Octocoral	-1.371 (-2.571, -0.347)	-75%	-0.758 (-1.152, -0.370)
	Soft *Capnella* Like	-3.354 (-4.955, -2.095)	-97%	-1.059 (-1.414, -0.710)
	Sea Whip	-0.638 (-1.439, 0.107)		-0.722 (-1.107, -0.334)
	Gorgonian Red *Pteronisis* Like	0.518 (0.100, 0.943)	68%	-0.999 (-1.308, -0.693)
	Bramble *Acabaria* Sp	-2.062 (-3.123, -1.156)	-87%	-0.543 (-0.978, -0.104)
Sponges	Simple White Rough	1.632 (0.930, 2.423)	409%	-0.271 (-0.583, 0.052)
	Repent Yellow	1.895 (0.862, 3.111)	564%	-0.601 (-1.067, -0.130)
	Massive White Shapeless	-0.212 (-1.011, 0.584)		0.014 (-0.394, 0.453)
	Lumpy White	-0.527 (-1.250, 0.177)		-0.098 (-0.444, 0.263)
	Encrusting Yellow Smooth	-1.538 (-2.008, -1.096)	-78%	-0.211 (-0.433, 0.015)
	Encrusting Yellow Rough	2.553 (1.226, 4.214)	1182%	-0.585 (-1.050, -0.108)
	Encrusting White Lumpy	-1.986 (-3.646, -0.656)	-86%	-0.480 (-0.878, -0.066)
	Encrusting White	-1.907 (-2.547, -1.331)	-85%	-0.168 (-0.374, 0.044)
	Encrusting Orange	-0.609 (-1.045, -0.183)	-46%	-0.400 (-0.614, -0.184)
	Encrusting Black	-1.396 (-2.579, -0.337)	-75%	0.045 (-0.464, 0.598)
	Cup White	-0.089 (-0.782, 0.603)		-0.531 (-0.842, -0.210)

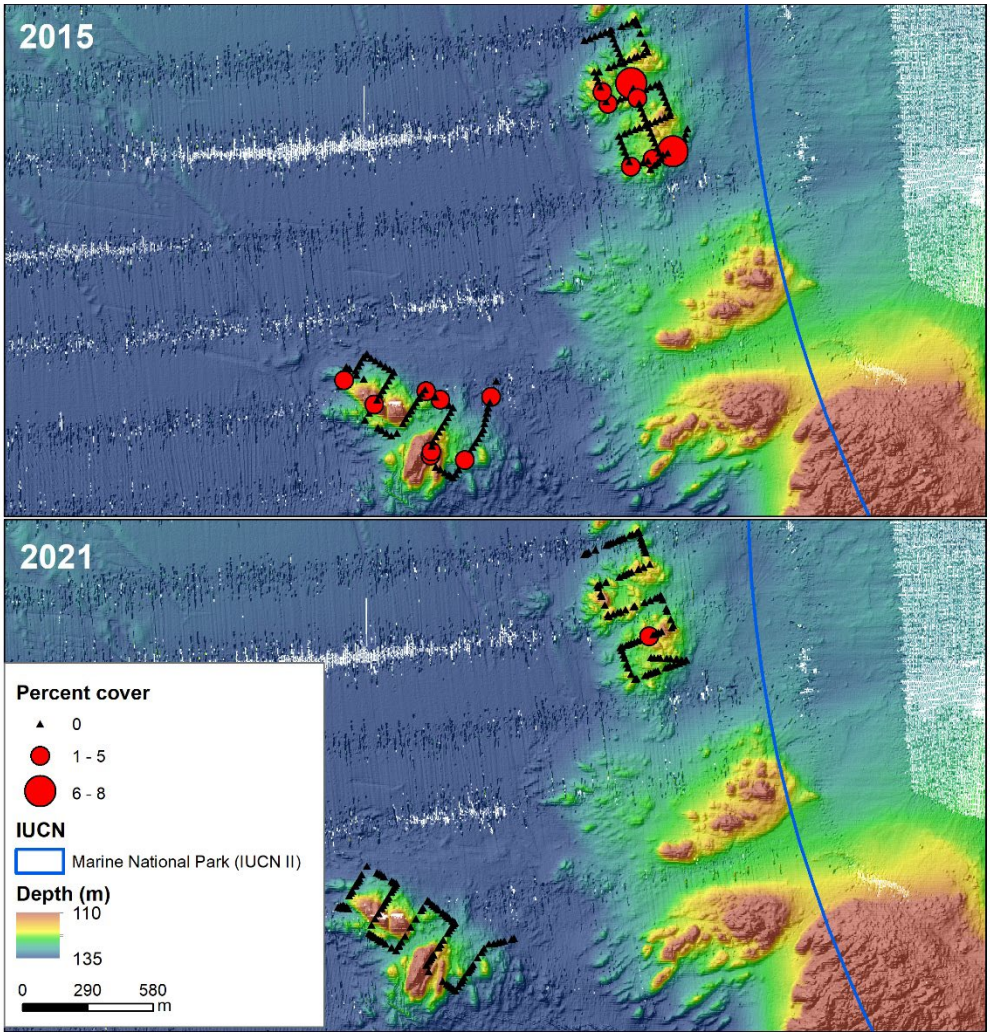

Figure 88. Change in cover between 2015 and 2021 for the Hydroid White morphospecies.

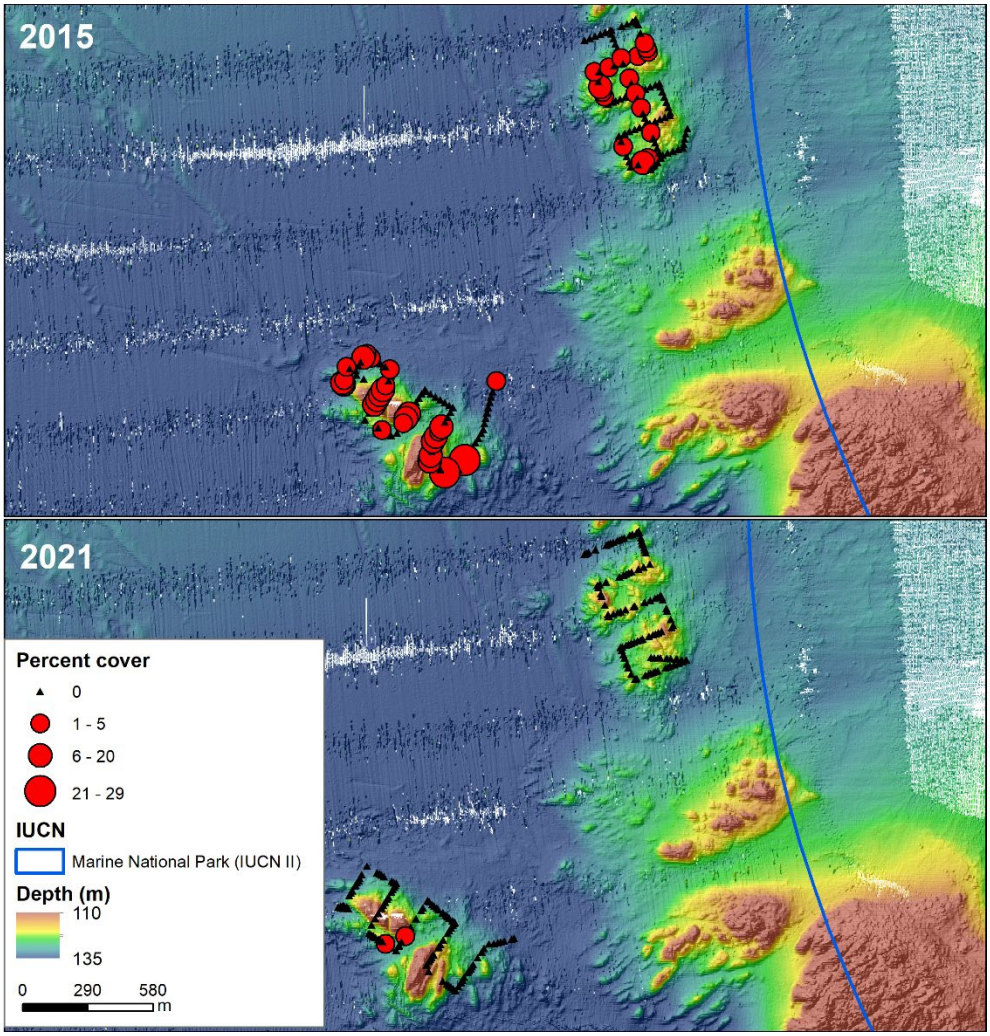

Figure 89. Change in cover between 2015 and 2021 for the Soft Capnella like morphospecies.

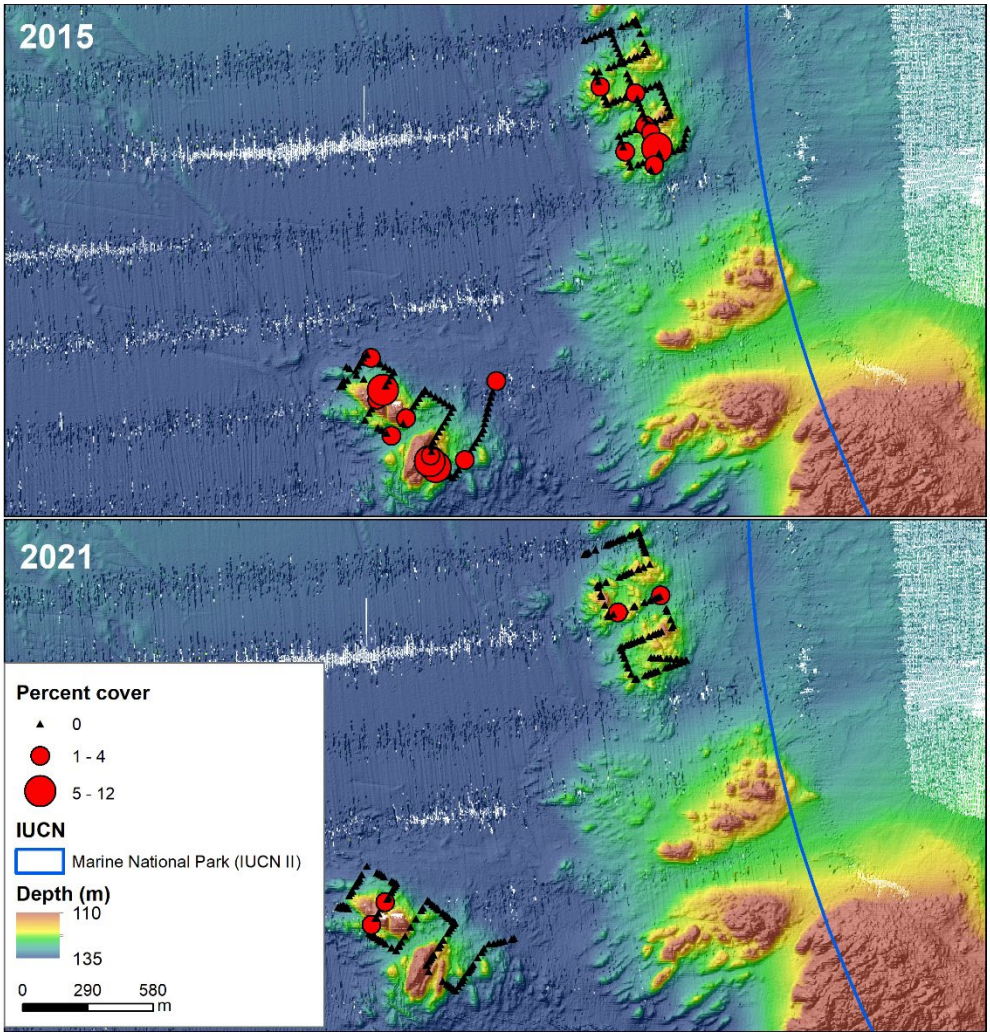

Figure 90. Change in cover between 2015 and 2021 for the Soft White Octocoral morphospecies.

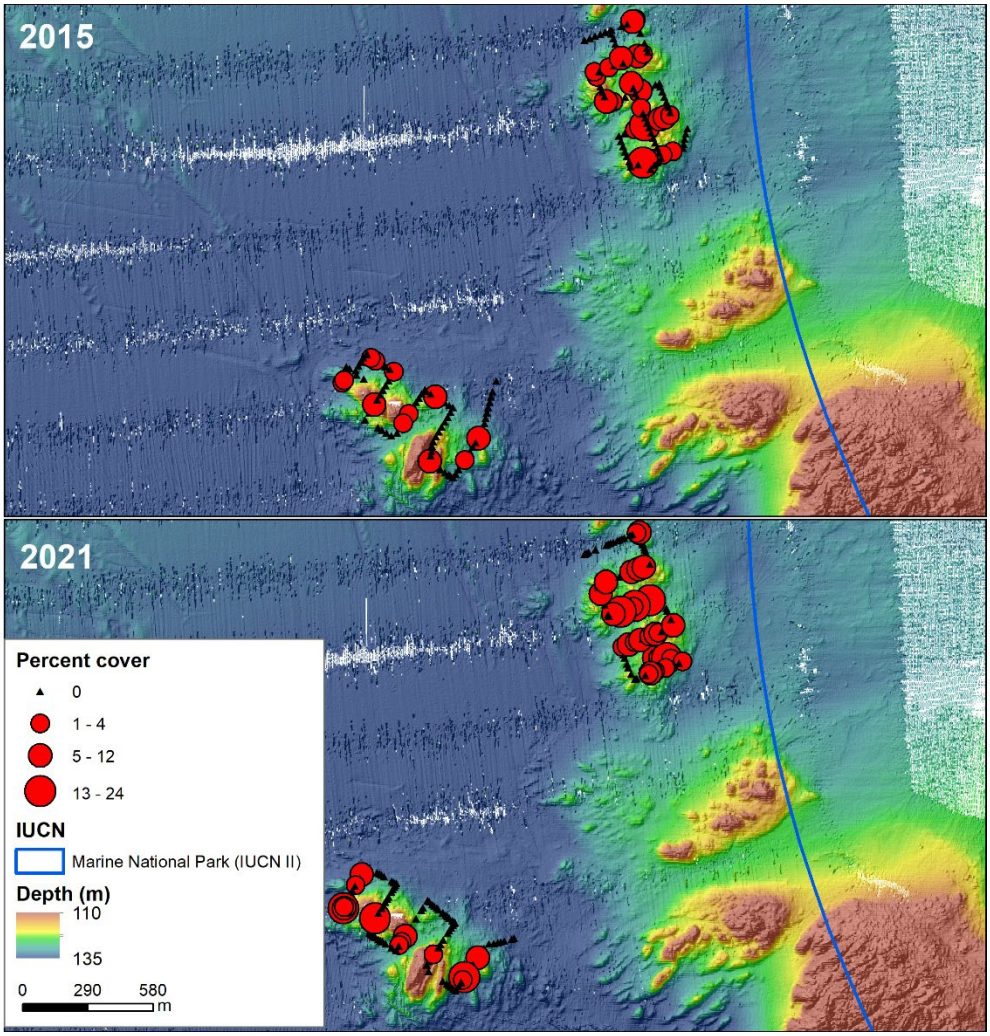

Figure 91. Change in cover between 2015 and 2021 for the Gorgonian Red Pteronisis Like morphospecies.

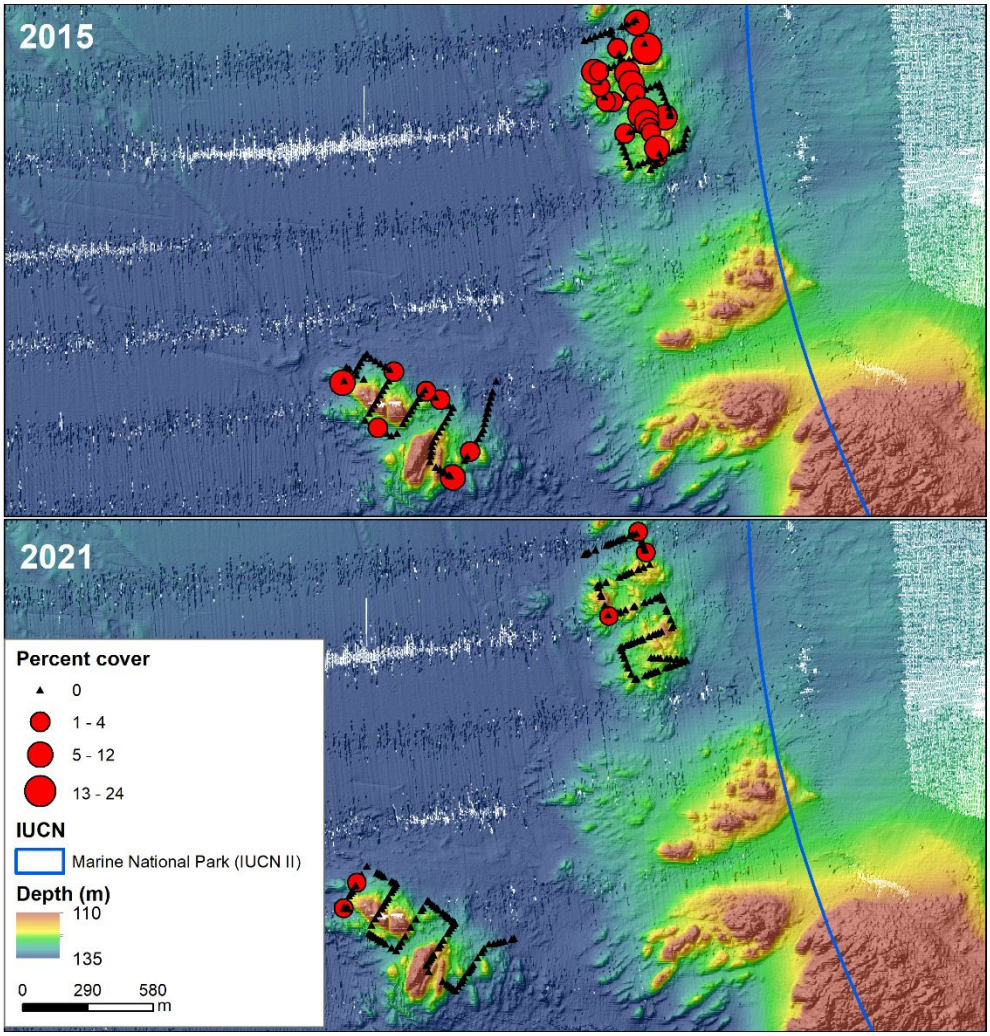

Figure 92. Change in cover between 2015 and 2021 for the Bramble Acabaria Sp morphospecies.

All the encrusting sponges analysed showed declines between 2015 and 2021, with the exception of encrusting yellow rough which showed a large significant increase from very low cover in 2015 (Table 24; Figure 89-Figure 93). Repent yellow and simple white rough sponges also showed a large increase from relatively low cover in 2015 (Figure 94; Figure 95). Massive white shapeless, lumpy white and cup white sponges did not display any significant changes.

Soft bryozoa had relatively high cover across both the 2015 and 2021 surveys () with no significant changes observed. Likewise, brittle stars, which were particularly conspicuous in much of the imagery, displayed no significant changes across the survey period.

Depth was found to be a significant factor for a number of morphospecies, with all significant effects being negative, indicating a preference towards the shallower depths surveyed. Depth varied across the survey images from 96 m to 139 m.

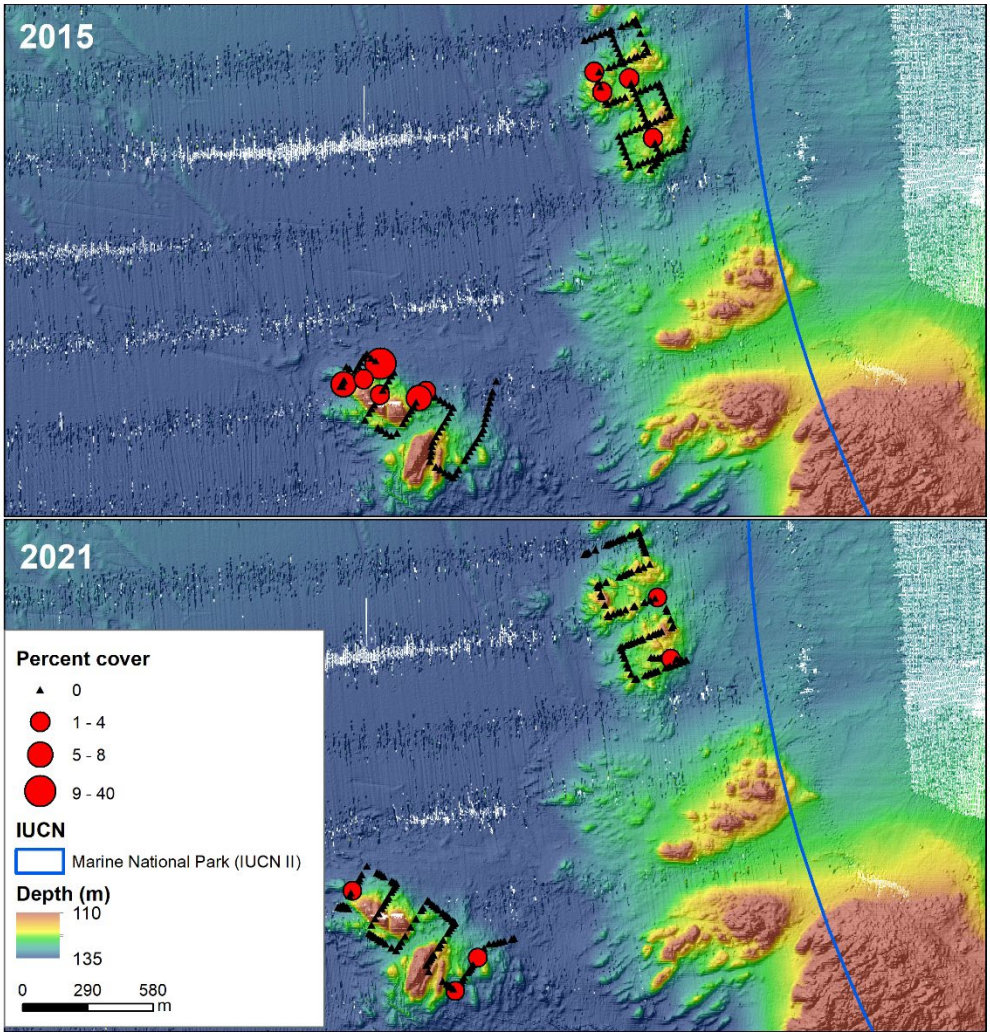

Figure 93. Change in cover between 2015 and 2021 for the Encrusting Black sponge morphospecies.

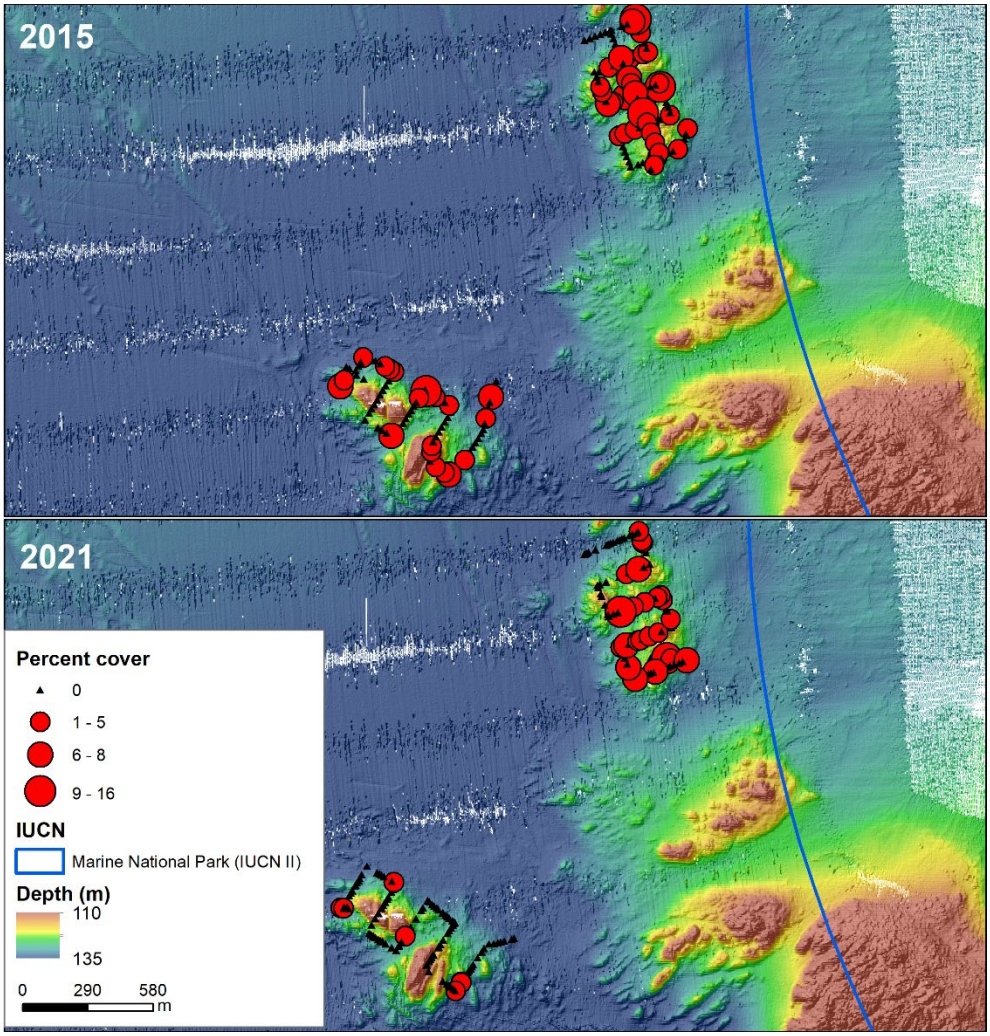

Figure 94. Change in cover between 2015 and 2021 for the Encrusting Orange sponge morphospecies.

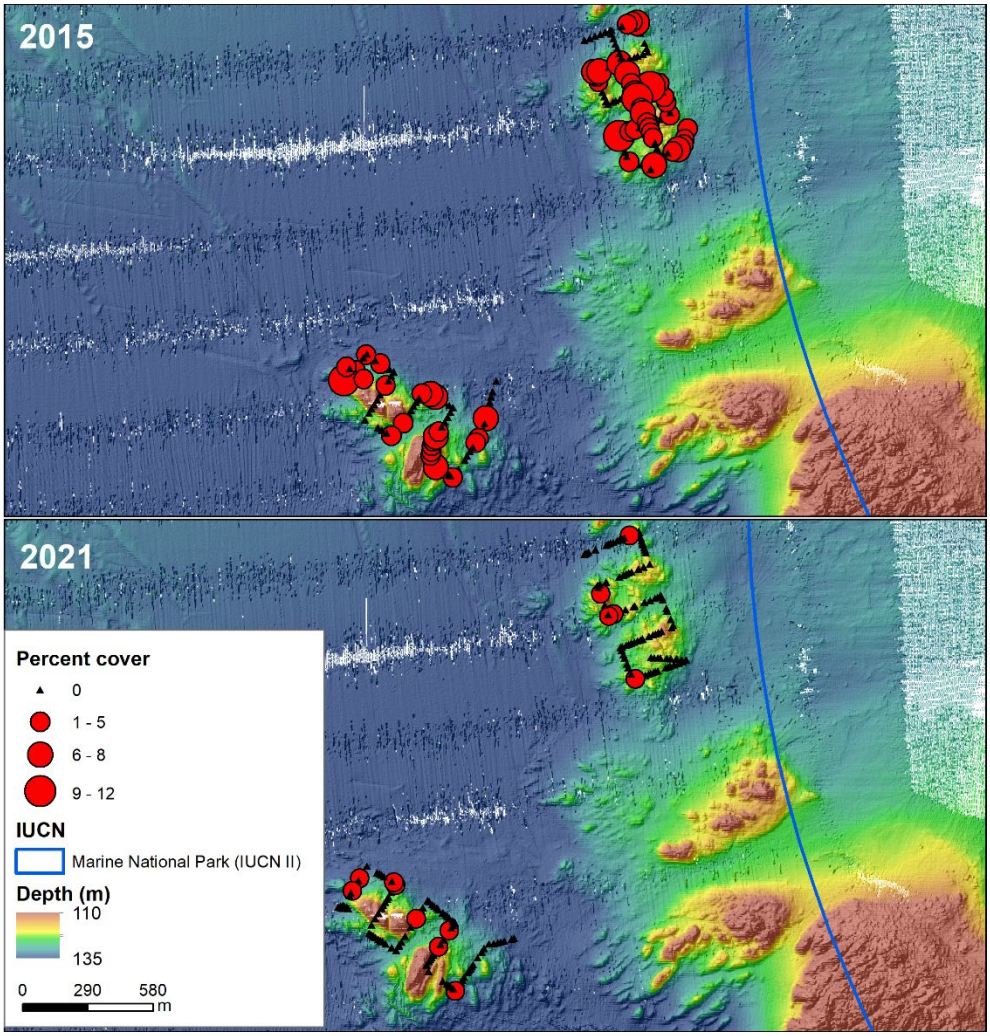

Figure 95. Change in cover between 2015 and 2021 for the Encrusting White sponge morphospecies.

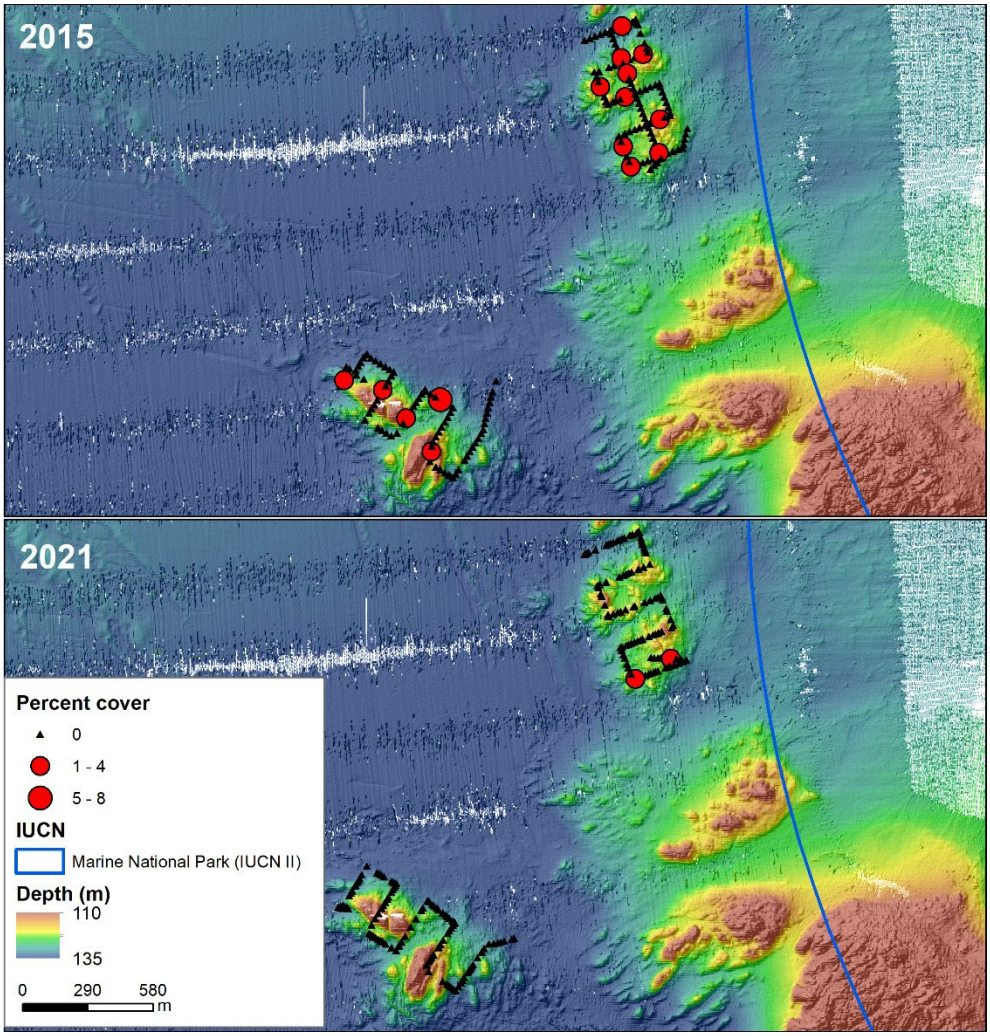

Figure 96. Change in cover between 2015 and 2021 for the Encrusting White Lumpy sponge morphospecies.

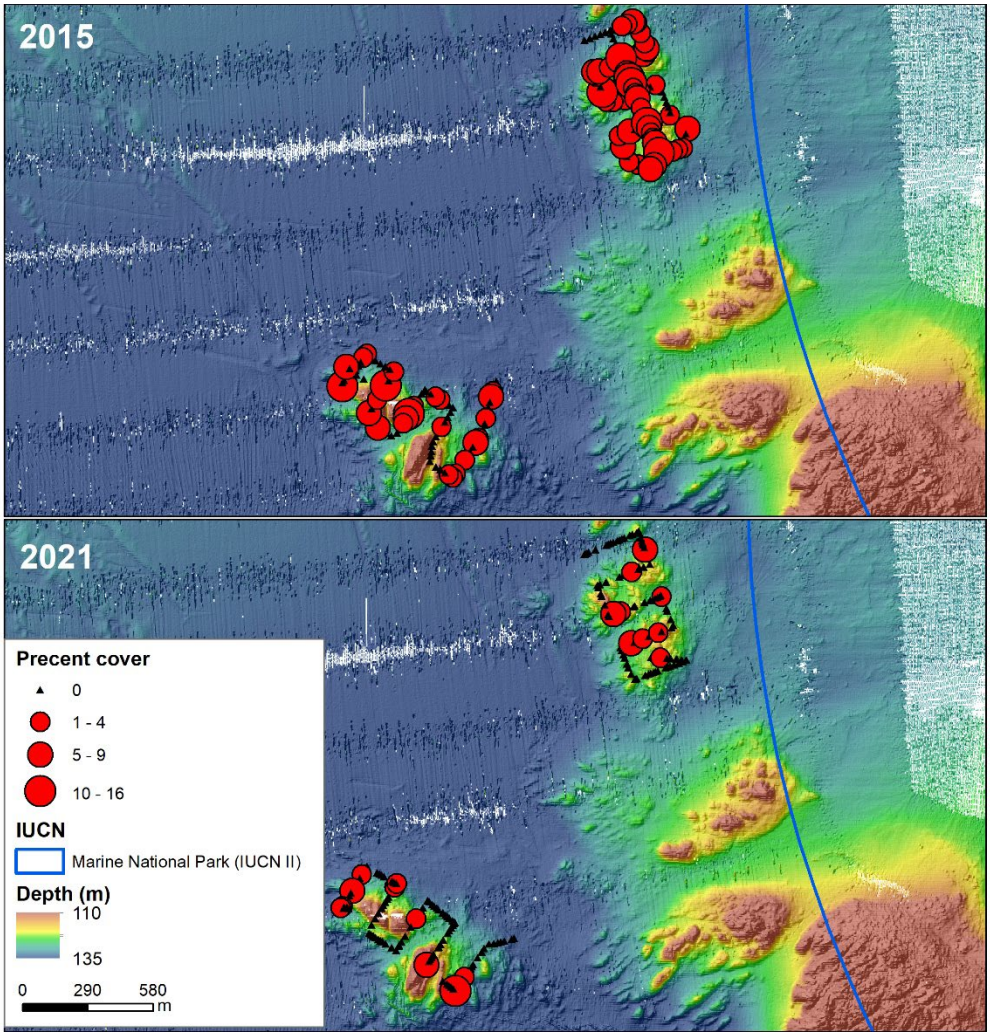

Figure 97. Change in cover between 2015 and 2021 for the Encrusting Yellow Smooth sponge morphospecies.

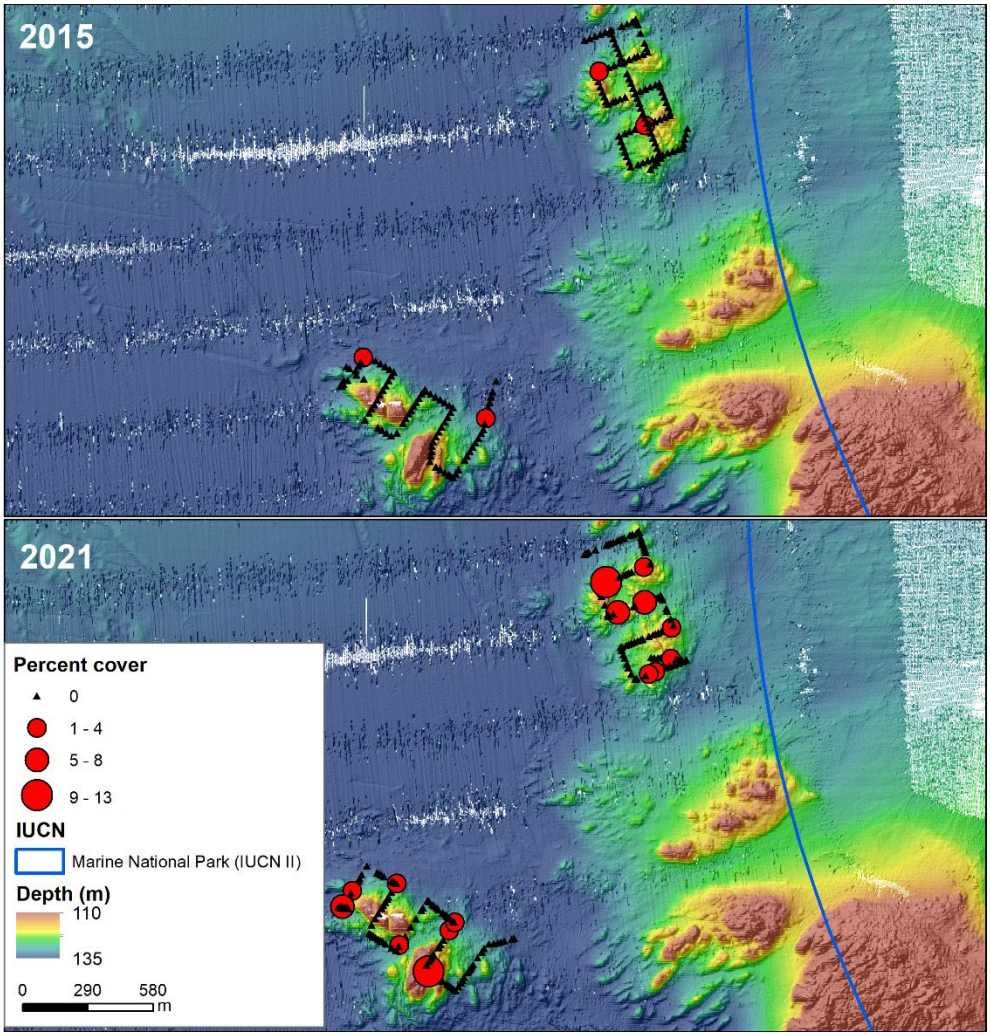

Figure 98. Change in cover between 2015 and 2021 for the Repent Yellow sponge morphospecies.

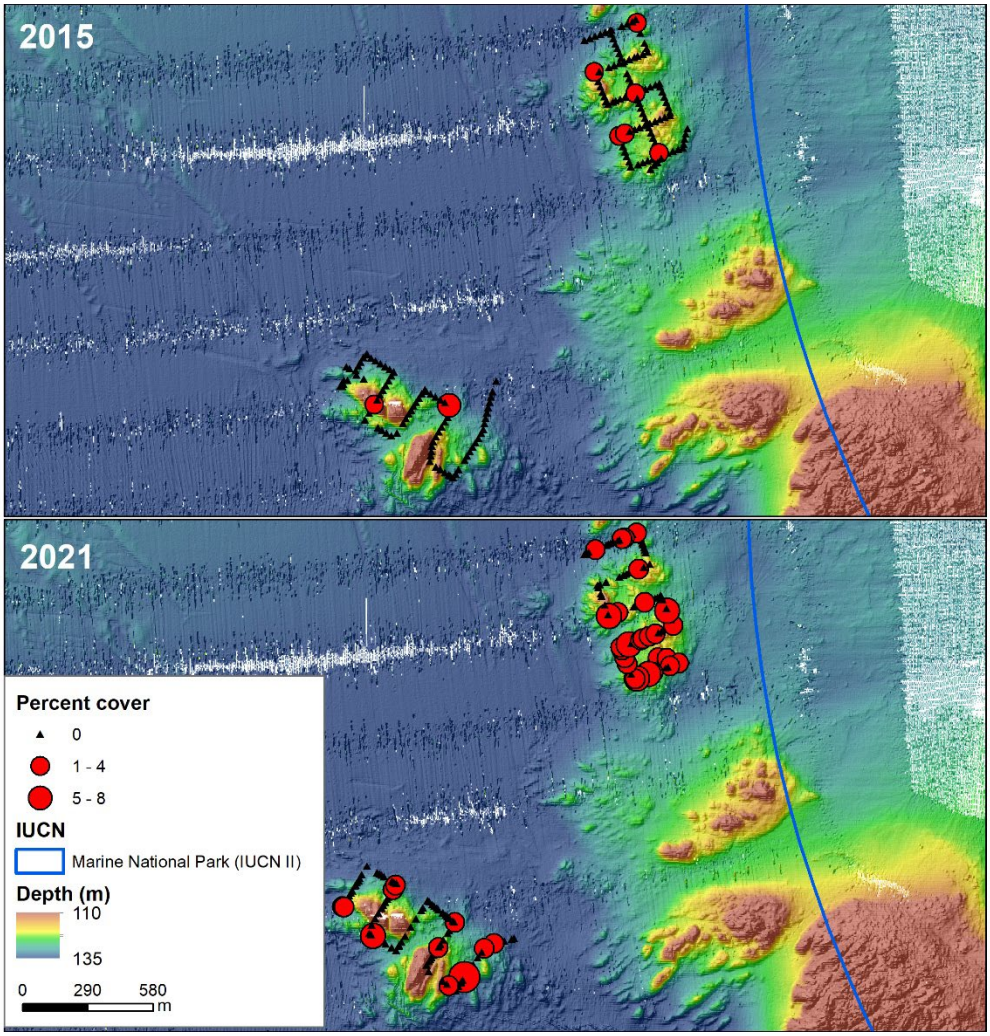

Figure 99. Change in cover between 2015 and 2021 for the Simple White Rough sponge morphospecies.

4.6 Conservation dependent species: quantifying handfish in AUV imagery

4.6.1 Background and methods

Following the observation of a pink handfish in the BRUV footage, a targeted effort was made to examine the AUV imagery to determine whether additional handfish could be found. The AUV imagery collected covers a much larger spatial extent than the individual BRUV drops, so it was reasoned that there was a good chance of finding additional individuals. Initially a dataset of all images was created, totally 115 334 images. The AUV captures overlapping images, with a spacing of approximately 4-5 images capturing non-overlapping sections of seafloor. Therefore, it was reasoned that exploring all images would give the best chance of finding additional handfish as they may occur close to the edges of an image and thus be missed in a subset of imagery. Progress was made scoring this data set, with two transects (NPZ_07 and NPZ_03) completed. However, scoring takes considerable time, particularly in reef images where the whole image needs to be scanned and handfish can often be camouflaged in amongst sponges and ascidians that may have similar colours and shapes. Therefore, other transects were subset to every fourth image to speed up annotation and allow a better initial description of the spatial distribution of handfish. The total number of images scored to date and the sampling procedure is outlined in Table 25. There are plans to do a more thorough scoring of imagery in the future, and to have different annotators score the same sets of imagery to check how often individual annotators are likely to miss handfish.

Post-annotation of the imagery, an expert in the identification of handfish (Peter Last, CSIRO) was consulted about the likely identity of observed species. The resolution of the imagery combined with the typically small number of biological samples and images of most handfish species makes identification problematic. Therefore, based on expert advice, different morphologies (colour, size, patterning) were classed into likely species groupings. However, it should be emphasized that these groupings are preliminary and are only likely ID's and not definitive ones. The potential species were: pink handfish (*Brachiopsilus cf. dianthus*), Australian handfish (*Brachionichthys cf. australis*), Ziebell's handfish (*Brachiopsilus cf. ziebelli*), and Warty handfish (*Thymichthys verrucosus var.*). For detailed description of these species including their known distribution see Last and Gledhill (2009). A further 3 morphologies were labelled as unknown: a pale morph, pink blotchy morph and yellowish dark banded morph. Examples of each potential species grouping is given in Appendix 6.2.

4.6.2 Results and map of handfish distribution

In the 9 out of 11 transects scored to-date, a total of 70 handfish have been found (Table 25). Handfish were found in all annotated transects except MUZ_02 (Figure 100). NPZ_03 had particularly high abundances, with almost half of all observed handfish (34 out of 70) being found on this transect.

Table 25. Targeted scoring of handfish in the TFMP, including the sampling strategy, number of images annotated to-date across each transect and number of individual handfish observed. TBC is To Be Counted.

Transect	Min. Depth (m)	Max. Depth (m)	Sampling	No. images scored	No. handfish	Depth range observed (m)
NPZ_01	109	133	Every 4th image	1755	6	118-126
NPZ_02	100	137	Every 4th image	1936	2	127-131
NPZ_03	90	148	Every image	10739	34	98-145
NPZ_04	95	142	Every 4th image	2697	4	123-130
NPZ_06	96	130	Every 4th image	2393	5	110-123
NPZ_07	90	127	Every image	9461	11	111-126
NPZ_08	123	134	Every 4th image	2598	3	130-132
MUZ_01	131	153	TBC	TBC	TBC	-
MUZ_02	135	157	Every 4th image	1795	0	-
Ref_C_1	39	69	TBC	TBC	TBC	-
Ref_N_1	63	114	Every 4th image	3829	5	92-106
			Total		70	

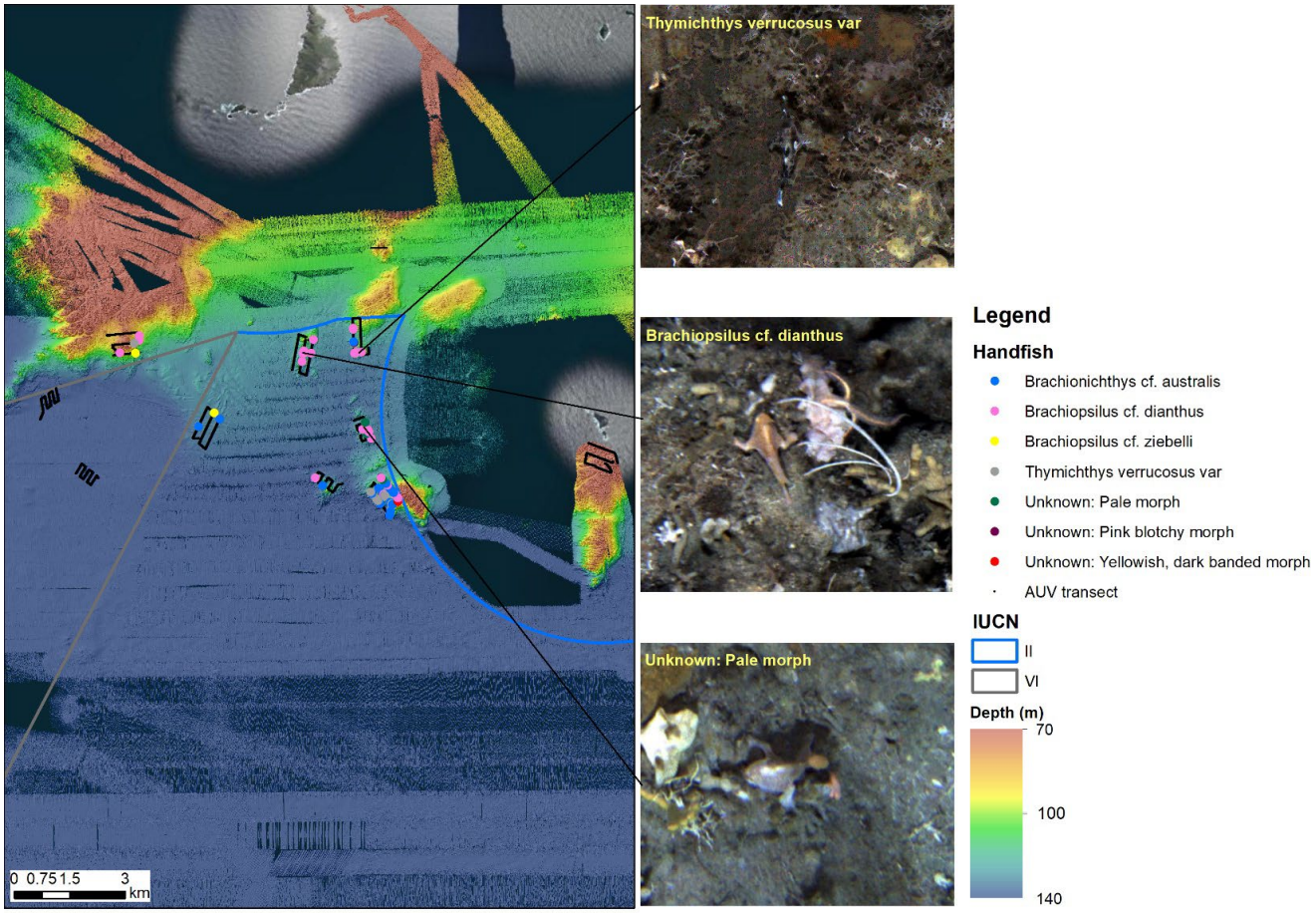

Figure 100. Map of handfish scored in AUV imagery with potential species groupings

Of the total 70 handfish found, 27 were placed in the *Brachiopsilus cf. dianthus* grouping, 22 in the *Brachionichthys cf. australis* grouping, 14 in the *Thymichthys cf. verrucosus var* grouping, 2 in the *Brachiopsilus cf. ziebelli* grouping, 3 in the unknown pale morph grouping, and 1 in each of the unknown pink blotchy and unknown yellowish dark banded grouping (Table 26). Of the 70 handfish found, 37 were found on sand and rubble dominated soft substrates and 33 on rocky reef, based on a visual assessment of habitat from the imagery. Handfish were observed in depth from 92 m (transect Ref_N1) to 145 m (transect NPZ_03). Detailed maps of handfish distributions are given in Appendix 6.3.

Table 26. Potential handfish species groupings, with numbers observed, habitats observations were made in and depth ranges

Potential species grouping	**Number observed**	**Habitats (and numbers) observed**	**Depth range (m)**
Brachiopsilus cf. dianthus (potentially pink handfish)	27	Reef (25) and rubble (2)	91 - 131
Brachionichthys cf. australis (potentially Australian handfish)	22	Sand (12), rubble (10)	121 - 150
Thymichthys cf. verrucosus var (potentially warty handfish)	14	Reef (3), sand (8), and rubble (3)	93 - 144
Brachiopsilus cf. ziebelli (potentially Ziebell's handfish)	2	Reef (1) and rubble (1)	106-130
Unknown: pale morph	3	Reef	116-120
Unknown: pink blotchy morph	1	Reef	124
Unknown: yellowish, dark banded morph	1	Rubble	119

5 Key findings and recommendations

5.1 Rock lobster

5.1.1 General trends and protection effects

Overall, the lobster potting surveys in the Tasman Fracture Park and surrounding areas continued to demonstrate that the reef habitats in this region support a significant lobster population. This was particularly the case on reefs shallower than 100 m that tend to be more highly structured than the deeper reefs found within the TFMP, hence offering more crevice structure for protection. Following on from the previous survey undertaken in 2014, there has been a considerable rebuilding in the abundance, biomass, and size structure of rock lobster populations in the time period until 2021. This rebuilding was not only in the NPZ of the TFMP but across the entire surveyed area, including the adjacent fished areas. Despite this general rebuilding, the NPZ displayed significantly larger increases in the average size of male rock lobsters when compared to the fished reference area and maintained a higher proportion of legal-sized rock lobsters. The shift in size structure was most evident in the largest size classes of rock lobsters which increased more noticeably in the NPZ, presumably due to ongoing survival and growth of the larger rock lobsters that had already accumulated in the NPZ between 2007 (when the NPZ became active) and 2014. While these metrics demonstrate evidence for the ongoing response of rock lobsters to protection in the NPZ, the effect size was not as evident as might be expected when compared to the fished reference area, based on historical trends. This appears primarily due to a decrease in fishing pressure in the fished reference area over the period from 2014-2020 in response to changes in market conditions (Figure A3, Appendix), resulting in significant stock-rebuilding within the offshore fishery off the south coast. This is particularly evident in the large increase in legal-sized rock lobsters in the fished reference area over this time. Over the period 2014-2021 the market shifted towards supplying live “red” rock lobsters to China, additional quota restrictions were implemented in the fishery, and in 2020, the Chinese market was essentially closed. All of which resulted in a marked shift from fishing in offshore areas such as found near the TFMP, to inshore waters, as rock lobsters from depths below 50 m tend to be “brindle” coloured (a whiter carapace), resulting in a lower market price than the “red” rock lobsters from inshore (Chandrapavan et al. 2009).

Significant increases in the abundance and size structure of *Jasus edwardsii* populations following establishment of protected areas are certainly expected when a significant fishery is operational and this has been reported elsewhere (Shears et al. 2006, Barrett et al. 2009b, McLeay et al. 2021). For example, McLeay et al. (2021) reported a 75% increase in abundance and 4.4 times greater relative abundance of legal-sized rock lobsters in a survey three years after protection was implemented for the Western Kangaroo Island Marine Park in South Australia. However, growth rates, the timing of recruitment events and the fishing effort in reference areas all play a key role in the magnitude and timing of a detectable effect of protection. The southwest of Tasmania is known to have extremely slow growth rates, particularly in deeper waters and for female rock lobsters. This means that detectable differences in the size structure are likely to take longer than other regions. Despite this, increases in the abundance of larger size classes were evident for both male and female rock lobsters in the 6.5 years between surveys. Also, an approximate doubling of abundance occurred over this time, indicating the likely influence of recruitment events and rebuilding of the population, although some contribution of year-to-year variation in catchability cannot be fully discounted.

Developing appropriate metrics for detecting the effects of protection in a scenario of reduced fishing pressure in reference areas is challenging and not commonly dealt with in MPA monitoring literature. In the case of the TFMP region, reduced fishing pressure combined with the marked

increase in abundances within smaller, sub-legal-size classes over the survey period decreased the strength of using the proportion of legal-sized rock lobsters (a widely used "indicator" in heavily fished populations) as a metric. Likewise, using direct counts of legal-sized rock lobsters or biomass to compare fished versus protected populations was also confounded by the large overall differences in abundance between the fished reference area and the NPZ. In the 2014 study, it was suggested that fishing pressure may alter the natural sex-ratio in this region, with lower abundances of females in fished reference areas, where sub-legal females are repeatedly caught and released before reaching legal size. Predation, both within pots and when rock lobsters are returned to the water, may therefore result in a lower female proportion in fished reference areas. However, by 2021 the strength of this pattern had declined, and differences were not statistically significant. It therefore appears likely that the reduced fishing pressure between 2014 and 2021 may have significantly reduced this female mortality in the fishery and hence the differences between fished and protected populations. These results highlight that in situations where there has been a reduction in fishing pressure outside of a no-take zone more sensitive metrics may be required to adequately describe/quantify the effectiveness of protection. Here, the clear "indicator" was the continuing progression of increases in rock lobsters in the largest size classes as the larger rock lobsters present in 2014 continued to survive and grow. Further exploration of metrics that better capture the transient responses (see White et al. 2013) of populations that are recovering from previous fishing mortality may prove useful and should be explored.

5.1.2 Physical factors driving rock lobster metrics

Spatial modelling revealed that several covariates, including depth, habitat complexity (as measured by rugosity from multibeam mapping) and the presence of predatory bycatch species in pots, all have an influence on catch rates of rock lobsters, thus providing a range of explanations for some of the observed differences. Notably, at the depths surveyed, despite the extended period of protection within the NPZ, there was an overall higher abundance of rock lobsters outside the NPZ across many of the size classes, that presumably is driven primarily by the availability of more suitable (complex reef) habitat outside the NPZ and the larger proportion of shallow reef habitat. As we scaled each of these covariates prior to modelling, the effects can be compared, with size related to a change in one standard deviation of the associated effect. So, for example, rock lobster abundance depth was found to be the strongest predictor of abundance, followed by rugosity (i.e., a metric of habitat complexity and therefore likely suitability) and finally bycatch of predators.

Depth was an important predictor for many of the metrics, with a strong trend of lower abundance in deeper areas of the offshore depth gradient found in the vicinity of the NPZ. Model estimates show an approximate three-fold increase in abundance in the shallowest depths surveyed (60-70 m) compared to the deepest depths (140-150 m). As the distribution of reef within the NPZ is heavily skewed towards depths below 100 m, catch rates in the zone are typically well below that found in adjacent areas where the fishery operates, as deep reef (below 100 m) is rare outside the NPZ. To compensate for this overall habitat difference, additional deeper reefs outside the NPZ were identified prior to the 2021 survey and included in that survey to ensure a more representative comparison between fished and protected habitats. However, due to time constraints and travel times to suitable comparable deep reefs in the fished reference areas, there remained a higher proportion of deeper reef surveyed in the NPZ relative to fished reference areas, requiring a model-based analysis to fully interpret overall trends. The model-based approach taken was able to account for residual differences in both depth and rugosity between deployment locations in the overall analysis. Furthermore, the spatial component of the model was able to account for differences that were not explained by the included covariates.

Habitat complexity is a known driver of species distributions and is particularly important for rock lobsters, which rely on refuge provided by complex habitat to avoid predation. Rugosity, a proxy for habitat complexity derived from multibeam mapping was an effective predictor of abundance, average male size and the sex-ratio (negatively correlated with the proportion of males). This implies that rugosity is a useful proxy for preferred habitat for rock lobsters, and that more rugose habitat is more likely to be occupied by larger male rock lobsters and female rock lobsters. This suggests that the preferred habitat is occupied by the largest male and female rock lobsters (which are generally lower in abundance), likely through competition for the best resources by larger males and their mating partners. The fifty metre buffer is likely to encompass the home range of rock lobsters (Barrett et al. 2009a), and it therefore makes ecological sense that there was stronger correlation at this scale rather than at the 500 m scale which was also included but not kept in best fitting models. Overall, habitat complexity was higher on a depth for depth basis in the fished reference areas relative of the NPZ, explaining one component of differences in abundance between areas surveyed.

Finally, the presence of conger eels and octopus as bycatch in pots, both predators of rock lobster, was also found to predict lower abundance of rock lobsters. The abundance of these bycatch species, particularly conger eels, was much higher in the NPZ, presumably in response to a lengthy period of protection, and therefore is likely to have influenced catch rates. It is likely that these predators were either harvested commercially as a by-product of rock lobster potting (e.g., Octopus) or kept and utilised as bait for rock lobsters, with their removal by the overall fishery resulting in increased catch rates through time. One possibility to be further explored is that increasing predator numbers within the NPZ result in less rock lobsters entering pots, particularly after a predator arrives, thus reducing overall catch rates despite rock lobsters being present.

5.1.3 Trends in bycatch

Overall, bycatch levels were relatively low in the survey region compared to elsewhere in South-east Australia (see Leon et al. 2019), presumably with the composition and abundance of species recorded here being driven in part by the deeper depth distribution of the reefs surveyed compared to those predominantly targeted in the fishery. As expected, bycatch of species likely to be impacted by fishing operations were higher in the NPZ. Conger eels were around twice as abundant inside the NPZ compared to outside, and roughly doubled in abundance between 2014 and 2021, both inside and outside the NPZ. Conger eels are often kept by fishermen to be used for bait. Therefore, recovering abundances of conger eels are an indicator of recovery from previous fishing pressure (inside the NPZ) and reduced fishing pressure (outside the NPZ).

5.1.4 Management implications

The two rock-lobster potting surveys inside the TFMP and in adjacent fished reference areas have provided a unique insight into offshore populations of rock lobsters in the region and demonstrate a rebuilding of the abundance and size structure of populations in recent years. The reduction in fishing pressure outside the NPZ between our 2014 and 2021 surveys has resulted in large increases in the proportion of larger rock lobsters outside the NPZ, making the effects of protection less apparent than would be expected under a scenario of more typical fishing pressure. Despite this, there were major differences observed between the overall rock lobster size structure seen in the NPZ and fished reference areas, with proportionally greater numbers of individuals in the largest size classes in the NPZ, indicative of an ongoing trajectory towards a size structure representative of an unfished population. It is unclear if this trajectory has yet to reach the natural end point of rock lobster growth in the region, with that likely to become more apparent in a future study at a similar time span. Overall, the knowledge gained through this project gives important insights into (1) the population dynamics of rock lobsters in the region, including the effects of protection in a NPZ,

major drivers of overall abundance of rock lobsters (habitat complexity, depth), the influence of predator numbers (Octopus and Conger eels) on catchability, (2) the effects of protection on bycatch species of rock lobster fishing, and (3) the influence of changing socio-economic drivers on regional rock lobster populations. Overall, the knowledge generated by this study is likely to be of equal value to conservation and fisheries management, by building an understanding around the key drivers of catch variation spatially and in time, as well as the influence of fishery behaviour on offshore stocks of rock lobsters in this region. Coupling these insights with data on past and future fishing pressure will be crucial in assessing future responses, and related studies on benthic habitats will allow further understanding of how rock lobsters, and protection may interact in wider ecosystem relationships.

Finally, the rebuilding of the abundance and size structure both inside and outside the NPZ in the survey area highlights potential successful recruitment events, perhaps prior to 2014, and the effect of reduced fishing pressure. The findings therefore have relevance to managers of the NPZ and fisheries managers interested in the status of stock in the region. While overall catch numbers between years may also be related to variation in rock lobster "catchability" between sampling events, the large changes in size structure, particularly larger, legal-sized individuals in fished reference areas, is clear evidence of changing fishing pressure and regional stock rebuilding.

5.2 Demersal fishes

Two surveys of fish populations inside the NPZ and in fished reference areas outside of the TFMP NPZ over a six-year period (in 2015 and 2021), and following initial no-take protection in 2007, have revealed that some potential effects of protection can be observed, with increasing abundances and sizes of targeted fish species in the NPZ. However, increases in abundance and size were also observed for most species in the fished reference area over the period 2015-2021, and in some cases these increases were more marked in the fished reference area than the NPZ. These observations indicate that fishing pressure is likely to have been low in this region between surveys, and potentially markedly lower than longer-term fishing in this region. This appears primarily driven by changes in the Tasmanian rock lobster fishery in response to changing market conditions and the effects of increased quota restrictions in this fishery, that together have driven effort towards inshore regions closer to ports, as well as reduced overall fishing effort. The response of the rock lobster stocks in the waters adjacent to the TFMP is discussed in the rock lobster section of this report. Concurrently, it is likely that the main direct pressure on finfish stocks, fishing for striped trumpeter (and its associated bycatch) has also declined over this period, as the fishery is based on rock lobster fishermen targeting their daily 200 kg target of striped trumpeter to supplement income from rock lobsters. Without rock lobster fishing, dedicated trips to catch striped trumpeter are sub-economic in this region due to the remote location.

Many of the typical metrics used to assess the "protection effect" from fishing in MPA's, such as increasing differences in abundance or larger size classes between protected and fished reference areas, are confounded when fishing effort is significantly reduced in the fished reference areas during such times. Hence, it is no surprise that in this study, trend-analysis methods based on detecting increasing differences show no overall effect, given fished reference areas currently appear to be mirroring no-take zones, albeit temporarily, due to a reduction in fishing effort. A similar observation was made in the rock lobster potting component of this report, where a large decrease in commercial rock lobster fishing effort between 2014 and 2020 resulted in contrasts between the NPZ and fished reference areas not being as large as might be expected. Unfortunately, spatial data on fishing effort for potential target finfish species in the region is not readily available to allow examination of long-term trends in effort. However, the remote location and often extreme

oceanic conditions make this region unlikely to receive a large amount of recreational fishing effort. During the 14 days of fieldwork undertaken in suitable weather in January-April 2021, only one recreational vessel was sighted fishing within the study area. Therefore, while recreational fishing effort likely remains low, and commercial effort declines, at least temporarily, protection effects will be small and difficult to detect. Nonetheless, these surveys provide a valuable baseline of demersal fish populations in deeper shelf waters in the region and will allow researchers and managers to better understand future changes. Also, significant correlations between depth and rugosity derived from multibeam mapping were found, increasing the knowledge of important environmental drivers for the distribution of key indicator species. This knowledge may allow future monitoring efforts to be more effectively targeted at habitats likely to return the highest abundance of chosen indicator species, if information needs are focussed on key indicator species rather than a broad ecosystem understanding.

Analysis of the initial survey data in 2015 found evidence for higher abundance and larger sizes of two targeted demersal fish species, jackass morwong and striped trumpeter in the NPZ relative to similar fished habitats, suggesting these species may act as indicators for protection from fishing (Monk et al. 2016). Analysis presented in this report, based on 2015 and 2021 data, and spanning a wider depth range in the 2021 survey, suggest that there is now currently little evidence of a protection effect for these species, at least relative to adjacent fished reference areas. The data suggests a lack of significant fishing pressure for finfish species in the fished reference area over the last 6 years at least, allowing fish stocks in these areas to resemble an unfished state. For jackass morwong, model results indicate an increase in mean size inside the NPZ between 2015 and 2021 and a slight decrease in mean size in the fished reference area. This could indicate some effect of protection. However, the abundance of legal-sized jackass morwong increased in both the NPZ and fished reference area through time, and there were a large number of juvenile jackass morwong present in the NPZ in 2015. Therefore, it appears that current trajectories are tracking the maturation of the cohort of juveniles observed in 2015 and little fishing mortality on larger individuals both inside and outside the NPZ. For striped trumpeter, an overall increase in the abundance of legal-sized individuals was detected between 2015 and 2021, but this appears to be driven by trends in the fished reference area more than the NPZ.

Another potential indicator of protection is the changes in abundance and size of important bycatch species in the rock lobster fishery. Draughtboard sharks, morid cods and ocean perch all increased in average size in the NPZ over the survey period. These species are all relatively abundant bycatch species in rock lobster pots, and cod and ocean perch are both susceptible to barotrauma resulting in higher post release mortality (Leon et al. 2019). Tracking ongoing trends in these species along with the rock lobster potting data may give further insights into how being caught as bycatch may be affecting their population dynamics in the area.

Depth and rugosity derived from multibeam mapping were both found to be useful predictors for most of the fish species for which detailed modelling was conducted. Interestingly, rugosity at a scale of 500 meters was more commonly found to be a useful predictor for fish species as opposed to at the 50-metre scale found for rock lobsters (see rock lobster section). This is likely to be related to home ranges of these species, with more highly mobile fish likely to move over preferred habitat in a larger range than less mobile rock lobsters. In the survey data there was slightly more mid-high rugosity habitat at the 500 m scale, suggesting there may be more preferred habitat in the fished reference area. These relationships should be investigated across other regions as they may help in future planning of key areas for protection and monitoring.

While we did not assess changes in metrics such as community thermal index, there appears to be no notable influence of climate-related range extending species in the assemblage present during either the 2015 or 2021 surveys, and no changes towards warmer affinity species in the community mix over the period 2015-2021. It appears that this region is primarily influenced by Southern Ocean water and potentially cold nutrient rich upwelling from a major shelf-incising canyon nearby, offshore from SW Cape, potentially providing greater stability than eastern Tasmanian waters subject to increasing influence of the East Australian Current (EAC), with associated warming.

In summary, the 2021 fish survey of shelf reefs in the TFMP and adjacent fished reference areas has provided the first time-step in an ongoing monitoring program, following an initial baseline survey in 2015. Rariphotic reefs within the TFMP were identified as a long-term priority under a recent monitoring prioritisation process by Parks Australia. At this point in time there are no marked differences in fish assemblages between fished and protected locations. It is likely that these patterns are the result of both the park being located in a remote region away from most recreational fishing pressures, and a low level of overall commercial fishing effort in recent years. The significant increase in rock lobster numbers and sizes outside the park between 2015 and 2021 that was recorded in our associated rock lobster study, suggests a major reduction in fishing effort occurred over that period in response to substantial market and quota changes. As rock lobster fishers also constitute the main line-fishing effort in this region, we can anticipate that there would be a corresponding increase in the abundance of target and bycatch species, and this pattern was seen here. While these trends in fishing effort can mask traditional analysis of MPA “effectiveness”, our overall results suggest general trends towards increases in abundance and sizes of target and bycatch species, in line with expectations of NPZ performance. Overall, the results show the benefit of establishing a marine park in remote areas in that there is currently little in the way of obvious pressure on park boundaries and via poaching and other enforcement issues. Finally, the southern location of this park means that it is likely the last cool water refuge for many shelf-associated species with cool-water affinity, and as such, provides a vital climate refuge for climate-threatened species such as the reef-associated pink handfish and the soft-sediment associated Australian handfish, found within this park. A dedicated survey of the regions that the handfish have been recorded is worthy of consideration to determine population size and status.

5.3 Seabed benthos

Extensive image-based surveys of the seafloor in TFMP using an AUV revealed a biodiverse benthic community, with a higher abundance of several groups of morphospecies than are found elsewhere in the South-east Network. In particular, a high abundance and diversity of octocoral morphospecies are found in the TFMP, including soft fleshy octocorals, gorgonian sea fans, sea whips, and bramble corals. While in many locations in SE Australia the sessile fauna on mesophotic/rariphotic reefs rarely has any morphospecies with greater than 2% overall cover, and the majority are often much less than 1% cover (e.g., Perkins et al. 2021), some of the AUV transects in the TFMP had cover of seawhips around 3% and red gorgonians at around 2.5% cover.

Important components of the benthic biota in TFMP include a high diversity of sponge morphospecies, soft bryozoans, hard bryozoans, hydroids, and a marked abundance of brittle stars. Analysis of the two repeated transects in the NPZ (NPZ_01 and NPZ_02) have revealed that these reef systems are also quite dynamic, with some significant changes having occurred over the six years between surveys. Declines in the cover of several octocoral morphospecies which are iconic to the TFMP were observed and should be followed up with future monitoring efforts.

Analysis of temporal changes in sessile benthic communities in the TFMP from mesophotic to rariphotic depths have shown that these systems are more dynamic than previously assumed, with significant changes occurring between surveys in 2015 and 2021. Of particular note is the decline in a number of octocoral species, which were noted to be characteristic of this region in the initial reporting of baseline surveys conducted in 2015 (Monk et al. 2016). Fleshy soft corals, such as the soft white octocoral and soft *Capnella*-like morphospecies, which were dominant in the 2015 survey displayed significant and dramatic declines between surveys, falling from 1.5% to 0.1% cover over this period Likewise, the bramble coral *Acabaria* sp. also showed significant declines, from 1.1% to 0.15% cover. The cause for these declines is currently unclear and may be related to natural cycles in recruitment and abundance of these morphospecies. For example, the red gorgonian *Pteronisis*-like was found to increase between surveys in the TFMP and has been shown to have large fluctuations in abundance over time periods of 5-10 years in other AMPs in the South-east Network (Perkins et al. 2017, Perkins et al. 2021). Likewise, another bramble octocoral species was found to have large fluctuations over a 6 year time period in Flinders Marine Park (Perkins et al. 2021). However, it is also possible that these octocoral morphospecies are susceptible to disturbances such as chronic warming, marine heatwave events or storms. There is a current lack of knowledge of the biology and life history of the majority of temperate octocoral species, making robust conclusions about the observed patterns problematic. Ongoing monitoring of the abundance of these species coupled with data on physical disturbances is recommended.

Other morphospecies that underwent significant changes included a number of sponge morphospecies and white hydroids, which have been noted to change significantly over similar time frames elsewhere across the South-east Network (Perkins et al. 2021). For example, encrusting yellow smooth (2.5% to 0.5%), white lumpy, white, orange, and black sponge morphospecies all declined in cover while encrusting yellow rough increased. Similar fluctuations in the cover of encrusting sponge morphospecies were seen elsewhere in the South-east Network (Perkins et al. 2021) and may be related to the opportunistic nature of encrusting sponges which colonise bare rock as it becomes available through natural mortality of other species or disturbance events. Similarly, repent yellow sponges showed a significant increase in the TFMP, and were noted to fluctuate considerably elsewhere in the South-east Network, displaying both increases and decreases over similar time frames. Conversely, the cup white and massive white shapeless sponge morphospecies remained relatively stable over the six years, reflecting similar patterns seen with other cup sponge and massive sponges elsewhere in the South-east Network which also tend to remain fairly stable over similar time periods. This suggests that these morphospecies with lower natural variability may prove to be better for tracking longer-term chronic impacts such as climate change due to lower natural variability and therefore have less 'noise' in their abundance through time. However, to be suitable indicators these morphospecies also need to respond to pressures of interest. Determining this will require a longer time series coupled with environmental data.

Depth was noted to be an important covariate for the majority of morphospecies when incorporated into models and the importance of depth is qualitatively evident when examining the distribution maps of a number of morphospecies. The two reference transects (central and north) included the shallowest habitats surveyed and had a much higher cover of biota than other transects. This is in part due to the higher proportion of rocky reef in these transects. However, some morphospecies more typically associated with shallower mesophotic depths such as coralline algae and red cup sponges were observed in the reference areas only. Analysis in the BRUV and rock lobster potting portions of this report also revealed that these areas are more rugose and therefore more likely to be important habitat for rock lobsters and some fish species. Essentially these shallower reference areas were sampled to give a better understanding of the depth distribution of key morphospecies

in this wider region, allowing for improved understanding of depth/rugosity relationships to underpin future model-based interpretation of species-habitat relationships as well as any assessment of protection-related habitat effects if suitable habitat is sampled outside the TFMP during future monitoring programs.

Ongoing surveys using AUVs across the South-east Network are providing valuable information about the spatial distribution of morphospecies as well as the temporal changes that have occurred. This information is crucial to underpinning effective long-term monitoring of mesophotic to rariphotic habitats and the biota within them across the region. Understanding where morphospecies occur, their natural variability and whether they may have responded to pressures helps with the selection of indicators for ongoing monitoring. Currently, only one repeat survey has been conducted in the TFMP, and therefore the monitoring program would still be considered in the early stages. However, surveys to date have revealed that these depths are biodiverse, contain rare and unique morphospecies such as octocorals and handfish, and are more dynamic than previously assumed. Trends observed between 2015 and 2021 show a marked decline in a number of iconic octocoral morphospecies in the TFMP. Whether this is the results of shorter-term natural variation, or a longer-term trajectory should be a focus of future survey work, to untangle our knowledge of natural variation vs that caused by a range of pressures, including storms and warming events.

5.4 Conservation-dependent species

An unexpected component of the visual (BRUV and AUV) surveys of the TFMP was the observation of a high density of conservation-dependent species including a large number of handfish, and a single Collar Seahorse (*Hippocampus jugumus*). The observation of the Collar Seahorse in BRUV imagery is the first sighting of this species in Australian continental waters, the only sighting of a live individual and only the third sighting of this species ever. The remaining records are from Lord Howe Island, and the Poor Knights Islands in New Zealand. The confirmed siting of a pink handfish in BRUV video footage along with a variety of other morphologically distinct handfish species in AUV imagery highlight the importance of deep reef and sediment habitats in the TFMP for handfish populations and the need for ongoing survey work to better quantify the species present and their population sizes.

A high abundance (> 70 individuals) of handfish were found in the AUV imagery as part of a separate process where images are searched specifically for the presence of handfish species, rather than the sub-sampled and random points percentage cover approached using for describing the remaining seabed benthos. This process revealed a variety of morphologically distinct groupings, with current evidence based on expert opinion indicating that these groupings may include a mix of pink handfish, warty handfish, Ziebell's handfish and Australian handfish, or potentially new undescribed species. However, the AUV-based imagery was not of sufficient resolution to definitively identify individuals to species level based on morphology and colour patterns, and there appears to be many intergrades between nominal "species-level" colour characteristics. Hence confirmation of the variety of species present is required with a mix of higher resolution imagery (for more accurate colour patterns and description of morphology) and eDNA sampling. We believe the density of handfish species is sufficiently high in this area, that with targeting based on positions from the current imagery, a reasonable chance exists for successful DNA collection and amplification based on recent developments in eDNA sampling for rare species. Genetic markers exist for Red, Spotted, Warty and the Australian handfish species, thus while any new species may be difficult to identify via eDNA methods, the approach would validate the presence of any of the above species, as well as any new but unidentified species.

In-situ observations of species such as pink and Ziebell's handfish are extremely rare, with less than 5 and 20 observations of these species ever being made respectively (Last and Gledhill 2009). Observations at depths beyond SCUBA diving limits, such as in TFMP, are even rarer with most deep-water observations coming from trawls as bycatch. In the cases of pink and Ziebell's handfish, both species have not been observed for > 15 years; and have not been recorded at depths greater that approximately 30 m previously. Also, the observation of the pink handfish is the most southern and western observation to date (Last and Gledhill 2009).

Due to the small size and often cryptic nature of handfish it is likely that current estimates of abundance in the imagery is an under-estimate. Furthermore, the footprint of the AUV survey in 2021 compared to the total area of potential habitat is small, indicating a high total abundance is likely across the TFMP. Future work could focus on targeted surveys of handfish in identified hotspots in this report with ROVs to gain better imagery for species identification. Also, the collection of eDNA samples in hotspot locations may further help with species-level identification.

The sighting of a Pink handfish, a cool-water species, may indicate the value of the shelf waters of the TFMP as a climate refuge for species no longer able to tolerate the increased temperatures in eastern Tasmanian waters. This species is one of a number of Tasmanian endemic handfishes that have been listed as threatened species on the basis of their declining populations, rarity, and suspected susceptibility to ocean warming. While this widespread distribution and wider thermal range of the Collar Seahorse indicates that this species may not be as vulnerable to warming as the handfish, its extreme rarity means that it is an almost automatic classification as a rare and endangered species on the basis of its rarity alone. Hence it ideally should be treated as such until a formal listing is prepared.

These observations lend support to the importance of protecting and monitoring deeper mesophotic to rariphotic habitats that are likely to contain rare or threatened species. The historic under-sampling of mesophotic and rariphotic ecosystems highlights that gathering quality data at these depths can fill in important knowledge gaps in conservation dependent species distributions.

References

Barrett, N., C. Buxton, and C. Gardner. 2009a. Rock lobster movement patterns and population structure within a Tasmanian Marine Protected Area inform fishery and conservation management. Marine and Freshwater Research **60**:417-425.

Barrett, N. S., C. D. Buxton, and G. J. Edgar. 2009b. Changes in invertebrate and macroalgal populations in Tasmanian marine reserves in the decade following protection. Journal of Experimental Marine Biology and Ecology **370**:104-119.

Chandrapavan, A., C. Gardner, A. Linnane, and D. Hobday. 2009. Colour variation in the southern rock lobsterJasus edwardsiiand its economic impact on the commercial industry. New Zealand Journal of Marine and Freshwater Research **43**:537-545.

Foster, S. D., J. Monk, E. Lawrence, K. R. Hayes, G. R. Hosack, T. J. Langlois, G. Hooper, and R. Przeslawski. 2020. Field Manuals for Marine Sampling to Monitor Australian Waters,Version 2. National Environmental Science Program.

Fuglstad, G.-A., D. Simpson, F. Lindgren, and H. Rue. 2018. Constructing Priors that Penalize the Complexity of Gaussian Random Fields. Journal of the American Statistical Association **114**:445-452.

Langlois, T. J., T. B. Jordan Goetze, Jacquomo Monk, Rene, J. A. Abesamis, Neville Barrett, Anthony Bernard, Phil, M. B. Bouchet, Mike Cappo, Leanne Currey-Randall, Damon, D. F. Driessen, Laura Fullwood, Brooke Gibbons, David, M. H. Harasti, Jamie Hicks, Thomas Holmes, Charlie, D. I. Huveneers, Alan Jordan, Nathan Knott, Hamish, D. M. Malcolm, Mark Meekan, David Miller, Peter Mitchell,, B. R. Stephen Newman, Fernanda Rolim , Benjamin, M. S. Saunders, Adam Smith, Michael Travers, Corey, and S. W. Wakefield, Joel Williams & Euan Harvey. 2020. A Field and Video-annotation Guide for Baited Remote Underwater stereo-video Surveys of Demersal Fish Assemblages. Marine Sampling Field Manuals for Monitoring Australia's Marine Waters. National Envirnomental Science Program.

Last, P. R., and D. C. Gledhill. 2009. A revision of the Australian handfishes (Lophiiformes: Brachionichthyidae), with descriptions of three new genera and nine new species Zootaxa **2252**:1-77.

Leon, R., N. R. Perkins, L. McLeay, D. Reilly, and S. J. Kennelly. 2019. Ensuring monitoring and management of bycatch in Southern Rock Lobster Fisheries is best practice. FRDC Project No 2017-082.

McLeay, L., A. Linnane, R. McGarvey, S. Bryars, and P. Hawthorne. 2021. Response of a southern rock lobster (Jasus edwardsii) population to three years of Marine Protected Area implementation within South Australia. Journal of the Marine Biological Association of the United Kingdom **101**:141-149.

Monk, J., N. Barrett, T. Bridge, A. Carroll, A. Friedman, D. Ierodiaconou, A. Jordan, G. A. Kendrick, and V. Lucieer. 2020. Marine sampling field manual for autonomous underwater vehicles (AUVs). National Environmental Science Program (NESP).

Monk, J., N. S. Barrett, J. Hulls, L. James, G. R. Hosack, E. Oh, T. Martin, S. Edwards, A. Nau, B. Heaney, and S. D. Foster. 2016. Seafloor biota, rock lobster and demersal fish assemblages of the Tasman Fracture Commonwealth Marine Reserve Region: Determining the influence of the shelf sanctuary zone on population demographics., A report to the National Environmental Research Program, Marine Biodiversity Hub.

Perkins, N. R., S. D. Foster, N. A. Hill, M. P. Marzloff, and N. S. Barrett. 2017. Temporal and spatial variability in the cover of deep reef species: Implications for monitoring. Ecological Indicators **77**:337-347.

Perkins, N. R., J. Monk, and N. Barrett. 2021. Analysis of a time-series of benthic imagery from the South-east Marine Parks Network Institute of Marine and Antarctic Sciences, University of Tasmania, Hobart, Tasmania.

Shears, N. T., R. V. Grace, N. R. Usmar, V. Kerr, and R. C. Babcock. 2006. Long-term trends in lobster populations in a partially protected vs. no-take Marine Park. Biological Conservation **132**:222-231.

White, J. W., L. W. Botsford, A. Hastings, M. L. Baskett, D. M. Kaplan, and L. A. K. Barnett. 2013. Transient responses of fished populations to marine reserve establishment. Conservation Letters **6**:180-191.

6 Appendix

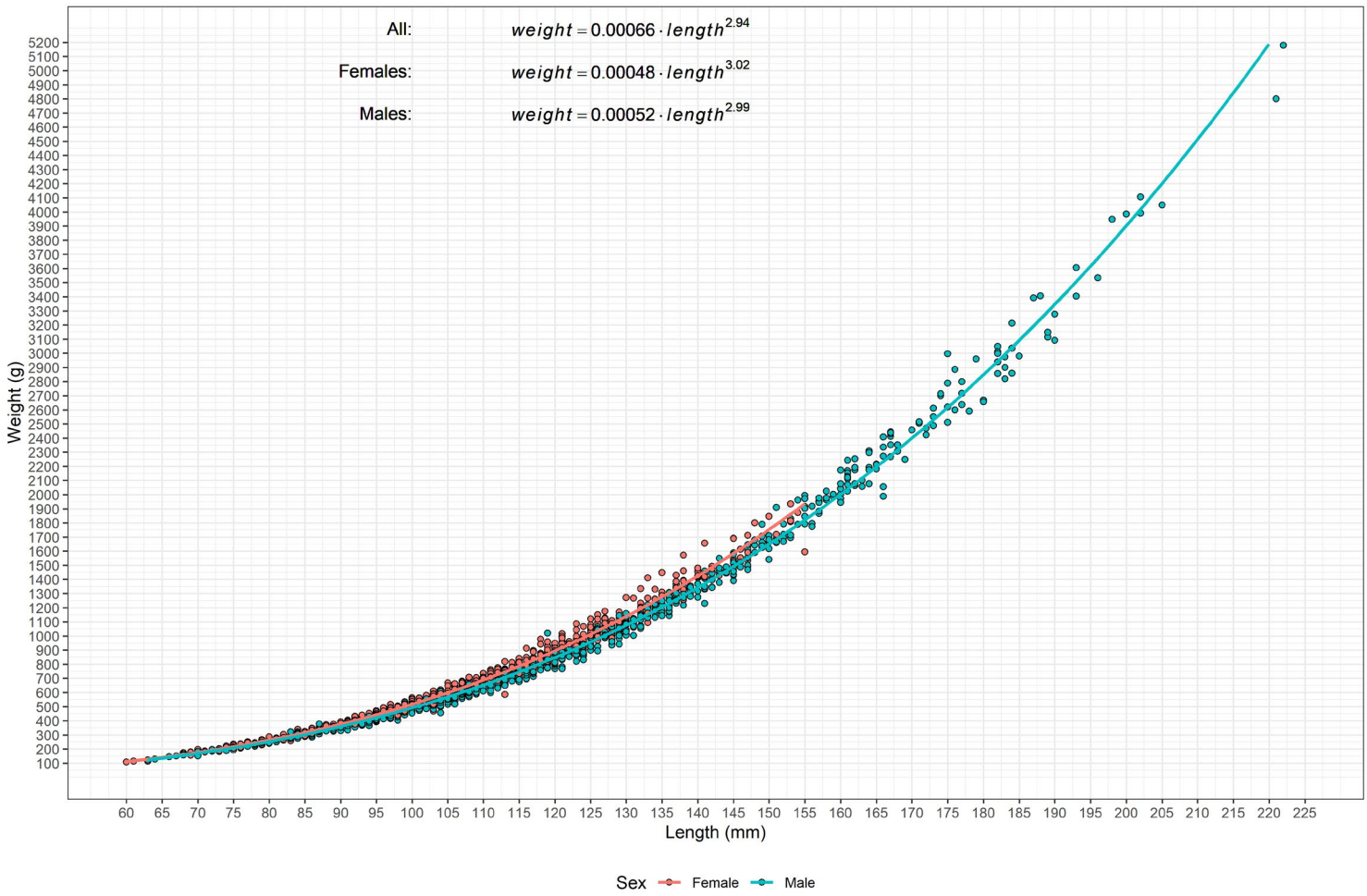

Figure 101. Length to weight relationship used to convert length frequency data to weight (biomass) for male and female rock lobsters. Data was sourced from the southwest of Tasmania. Data and modelled relationship provided by Rafael Leon, IMAS.

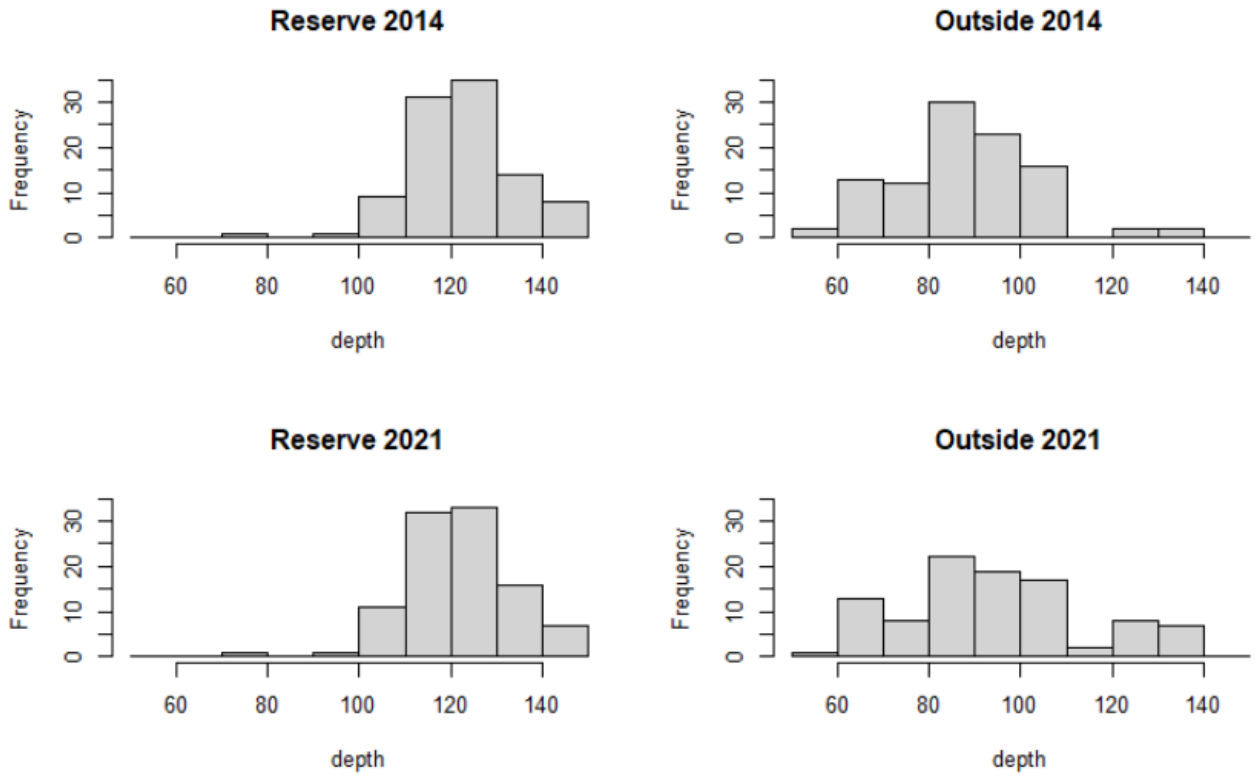

Figure 102. Depth distribution of sampled pot in the NPZ and outside areas for the 2014 and 2021 surveys.

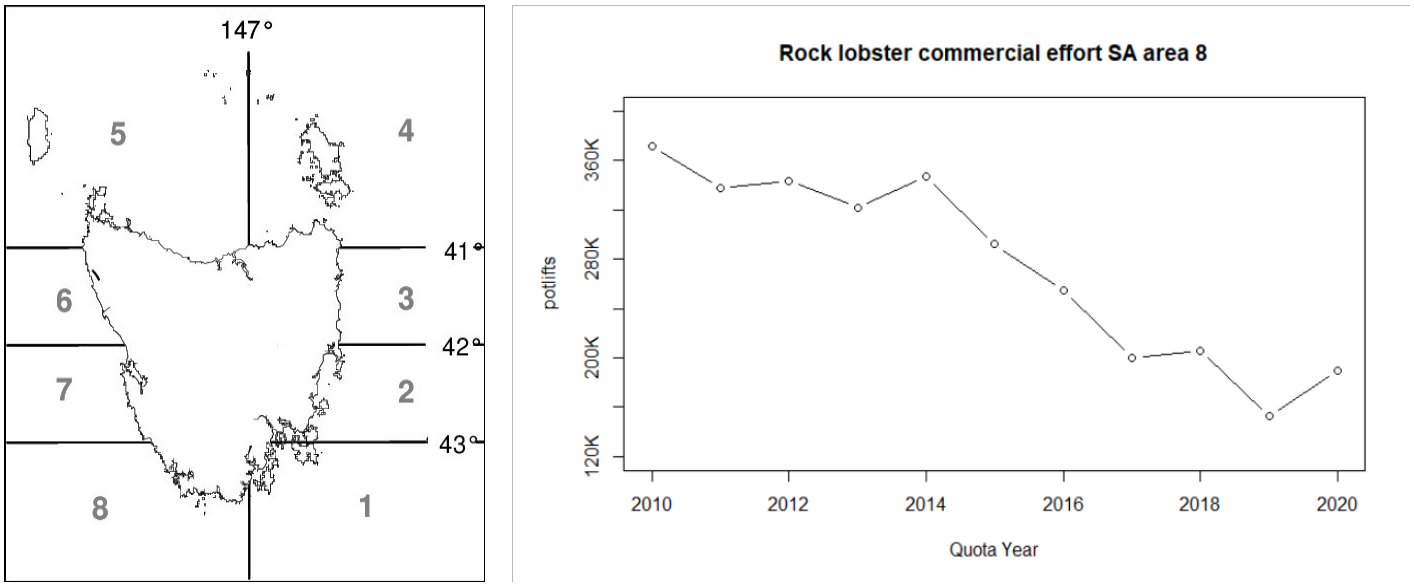

Figure 103. Commercial effort in stock assessment area 8, where Tasman Fracture Marine Park is located, between 2010 and 2020. Effort is shown in thousands (K) of potlifts. Map shows location of stock assessment area 8.

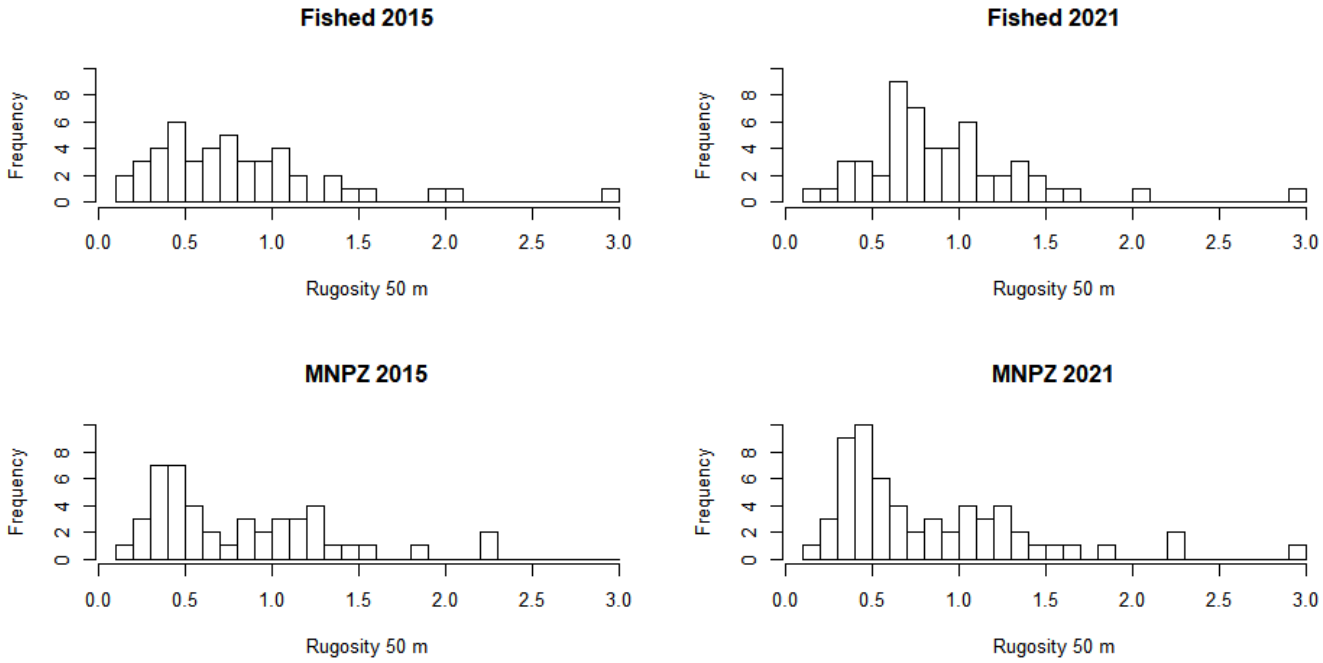

Figure 104. Distribution of rugosity at a 50 m scale across the NPZ and fished reference area and both the 2015 and 2021 surveys.

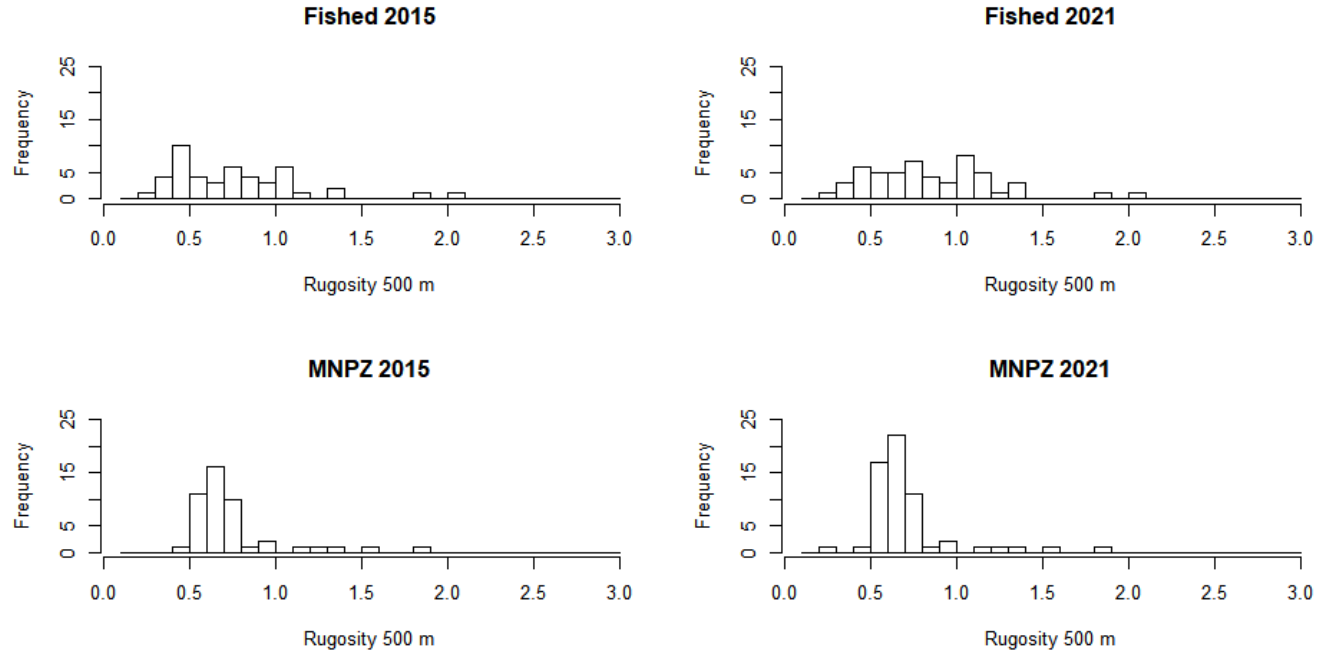

Figure 105. Distribution of rugosity at a 500 m scale across the NPZ and fished reference area and both the 2015 and 2021 surveys.

6.1 Example images of dominant and important benthic morphospecies

6.1.1 Brittle stars

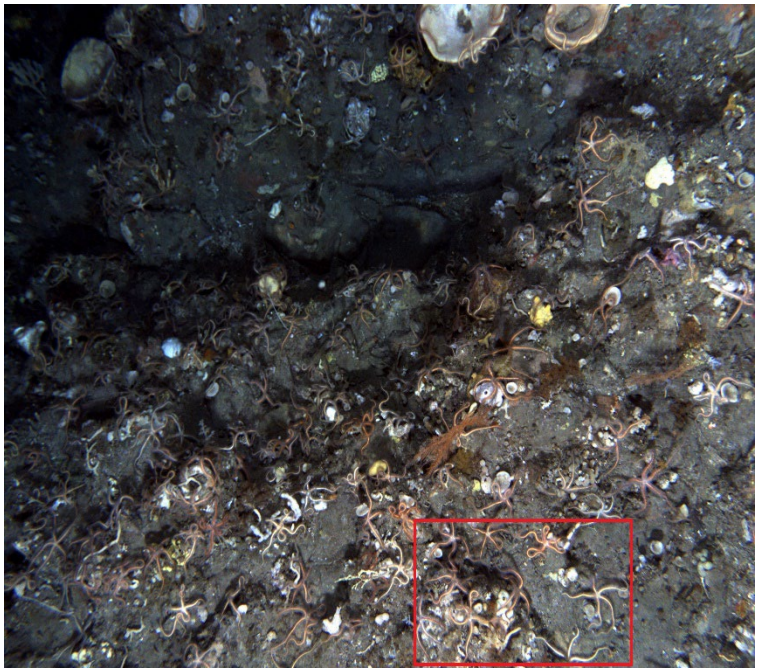

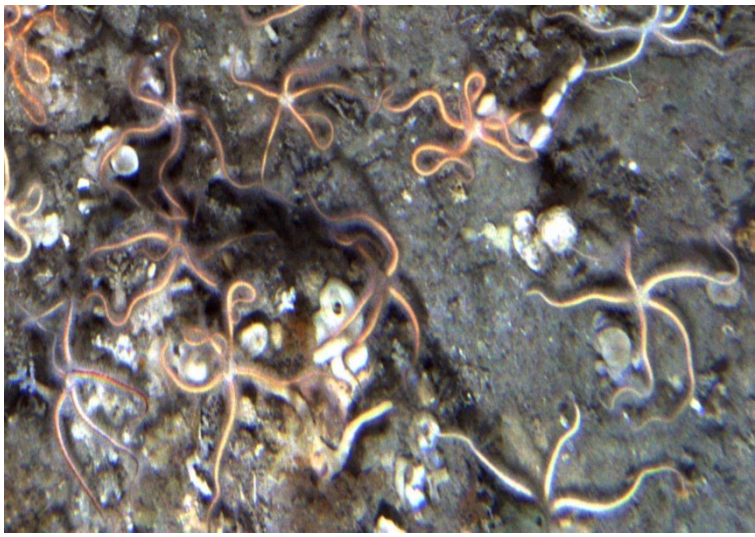

Figure 106. Example image and close up of brittle stars taken from the NPZ_01 transect. Red rectangle in full image on the left outlines area of close up on the right.

6.1.2 Branching white pointed sponge

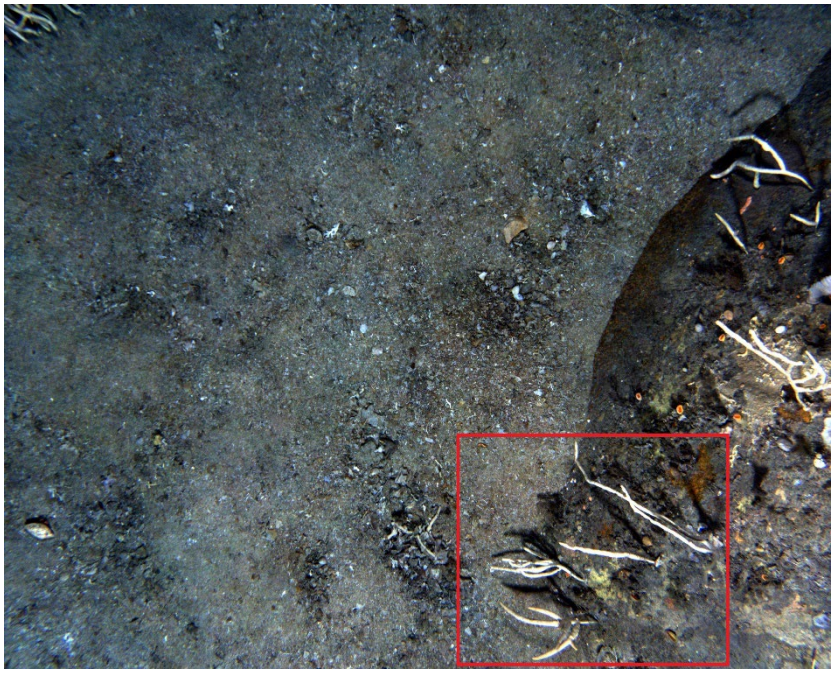

Figure 107. Example image and close up of branching white pointed sponge taken from the NPZ_06 transect. Red rectangle in full image on the left outlines area of close up on the right.

6.1.3 Encrusting orange sponge

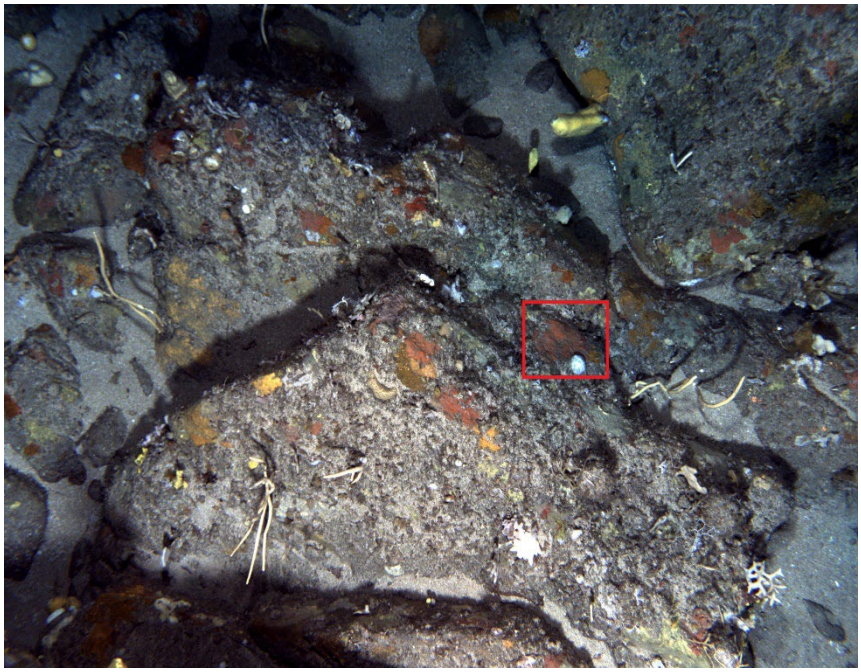

Figure 108. Example image and close up of encrusting orange sponge taken from the Ref_N1 transect. Red rectangle in full image on the left outlines area of close up on the right.

6.1.4 Encrusting yellow smooth sponge

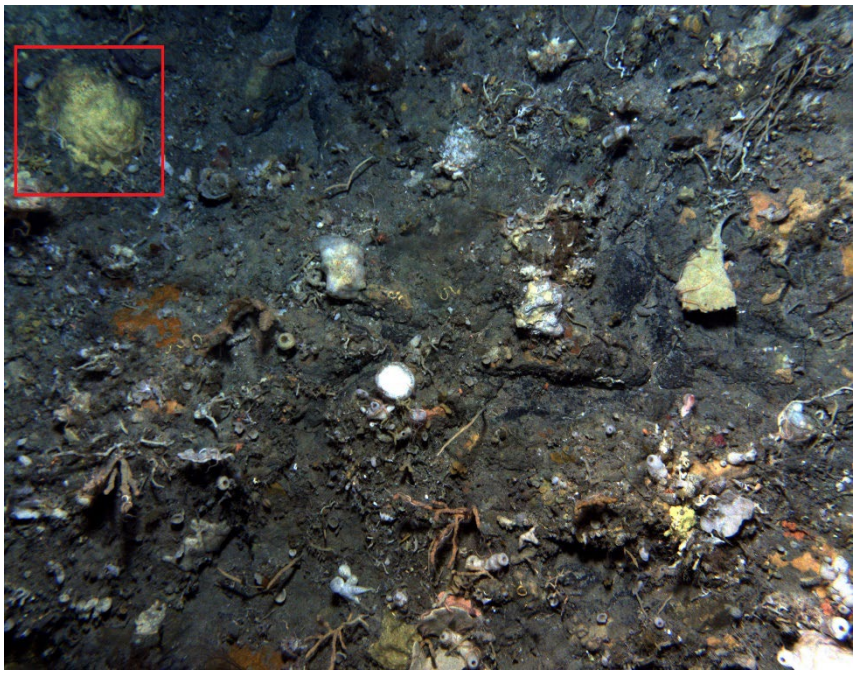

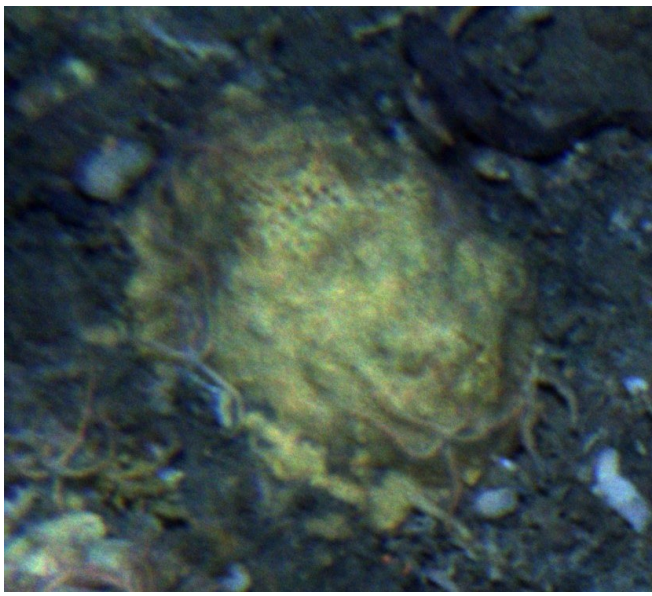

Figure 109. Example image and close up of encrusting yellow smooth sponge taken from the MUZ_01 transect. Red rectangle in full image on the left outlines area of close up on the right.

6.1.5 Gorgonian red Pteronisis like

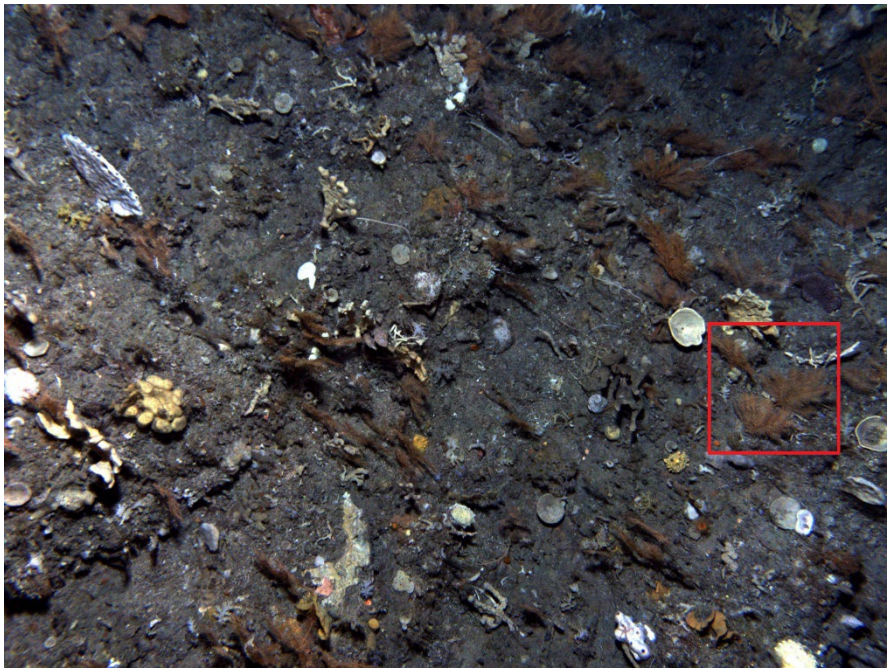

Figure 110. Example image and close up of gorgonian red Pteronisis like taken from the NPZ_02 transect. Red rectangle in full image on the left outlines area of close up on the right.

6.1.6 Lace bryozoan

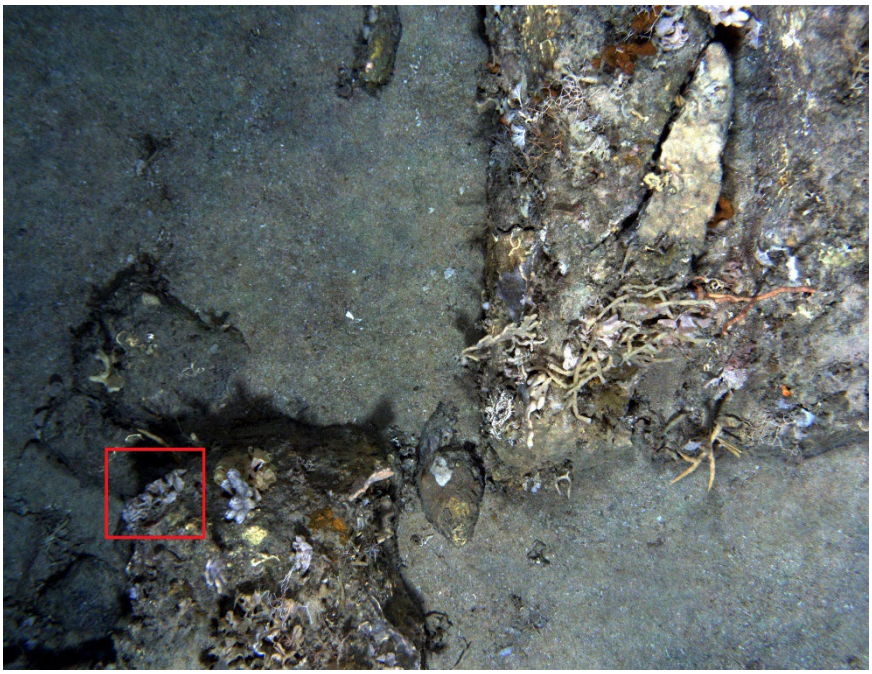

Figure 111. Example image and close up of lace bryozoan taken from the NPZ_04 transect. Red rectangle in full image on the left outlines area of close up on the right.

6.1.7 Sea whip

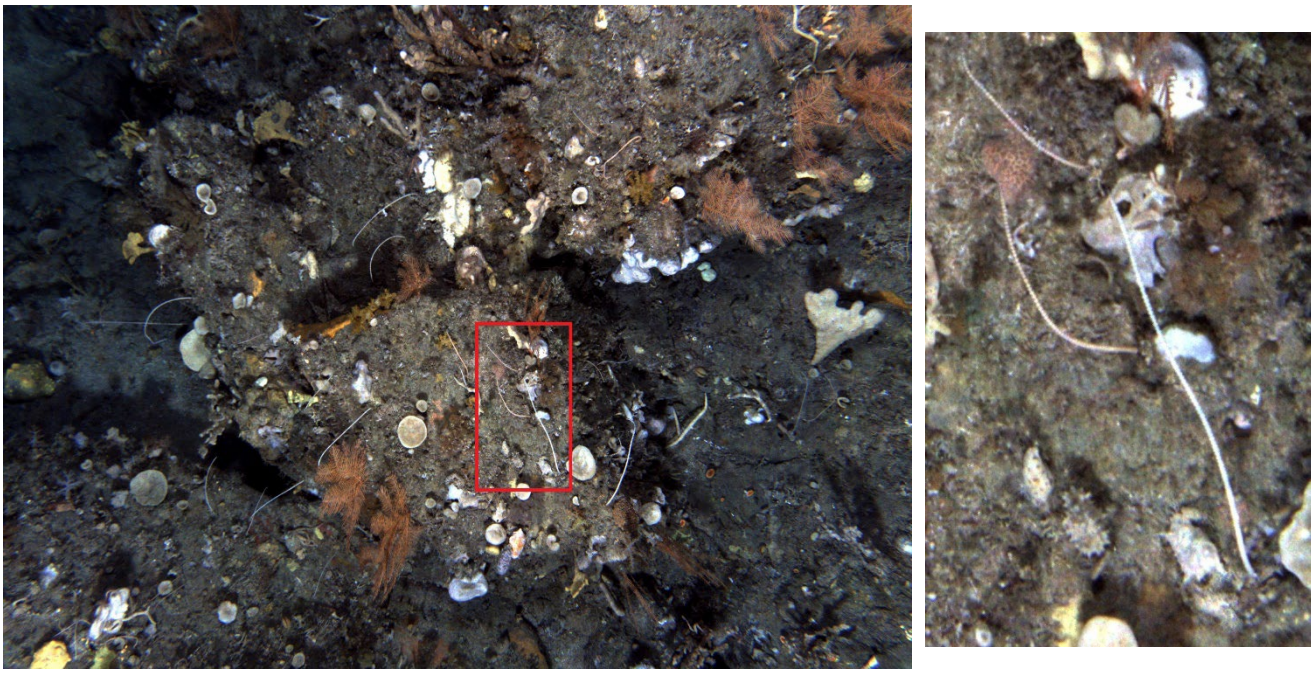

Figure 112. Example image and close up of sea whips taken from the NPZ_03 transect. Red rectangle in full image on the left outlines area of close up on the right.

6.1.8 Simple white rough sponge

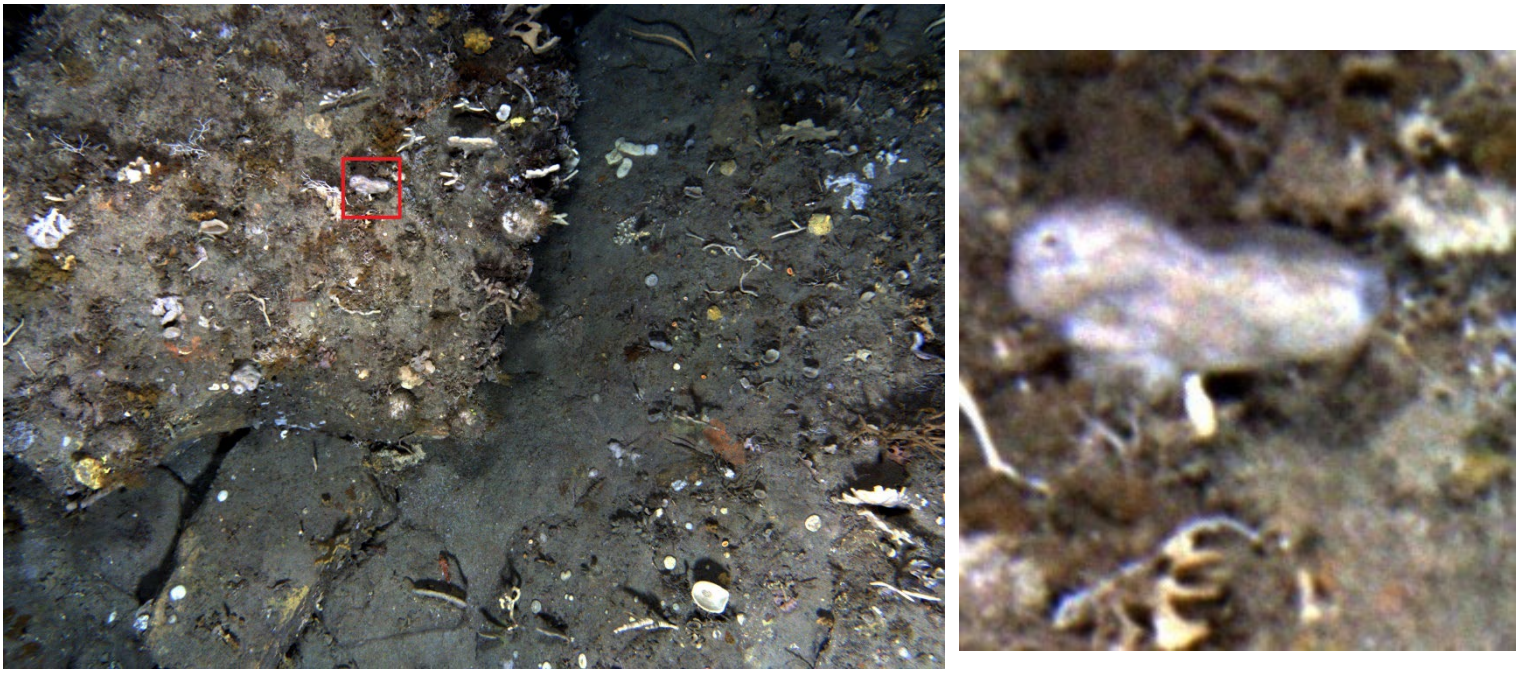

Figure 113. Example image and close up of simple white rough sponge taken from the NPZ_01 transect. Red rectangle in full image on the left outlines area of close up on the right.

6.1.9 Soft Capnella like octocoral

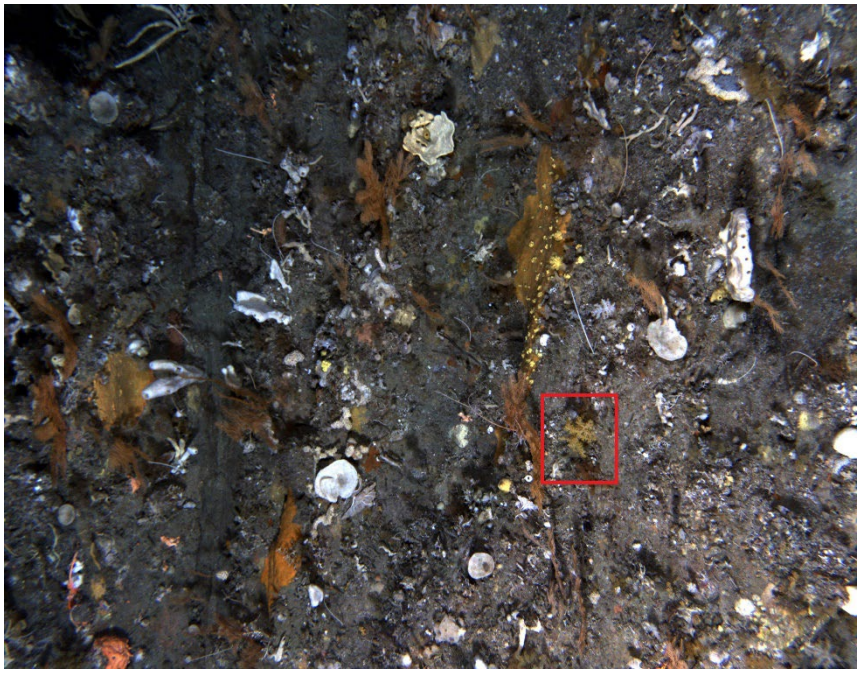

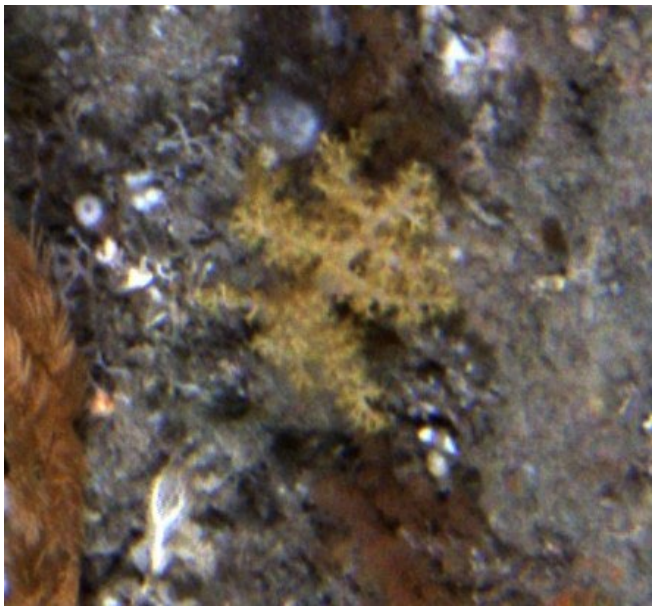

Figure 114. Example image and close up of soft Capnella like octocoral taken from the NPZ_07 transect. Red rectangle in full image on the left outlines area of close up on the right.

6.1.10 Soft orange bryozoan

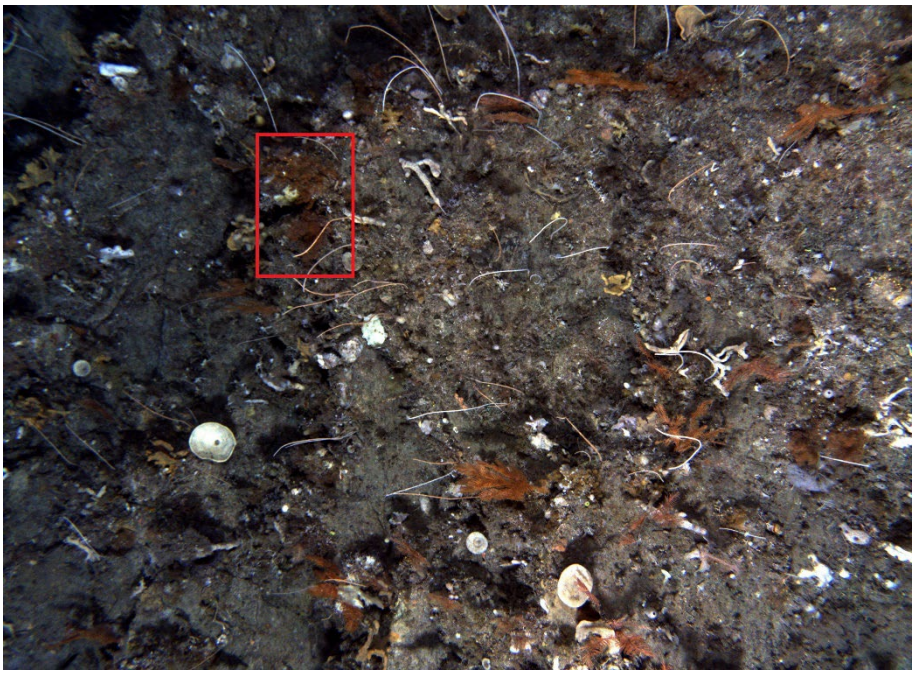

Figure 115. Example image and close up of soft orange bryozoan taken from the NPZ_03 transect. Red rectangle in full image on the left outlines area of close up on the right.

6.1.11 Soft white octocoral

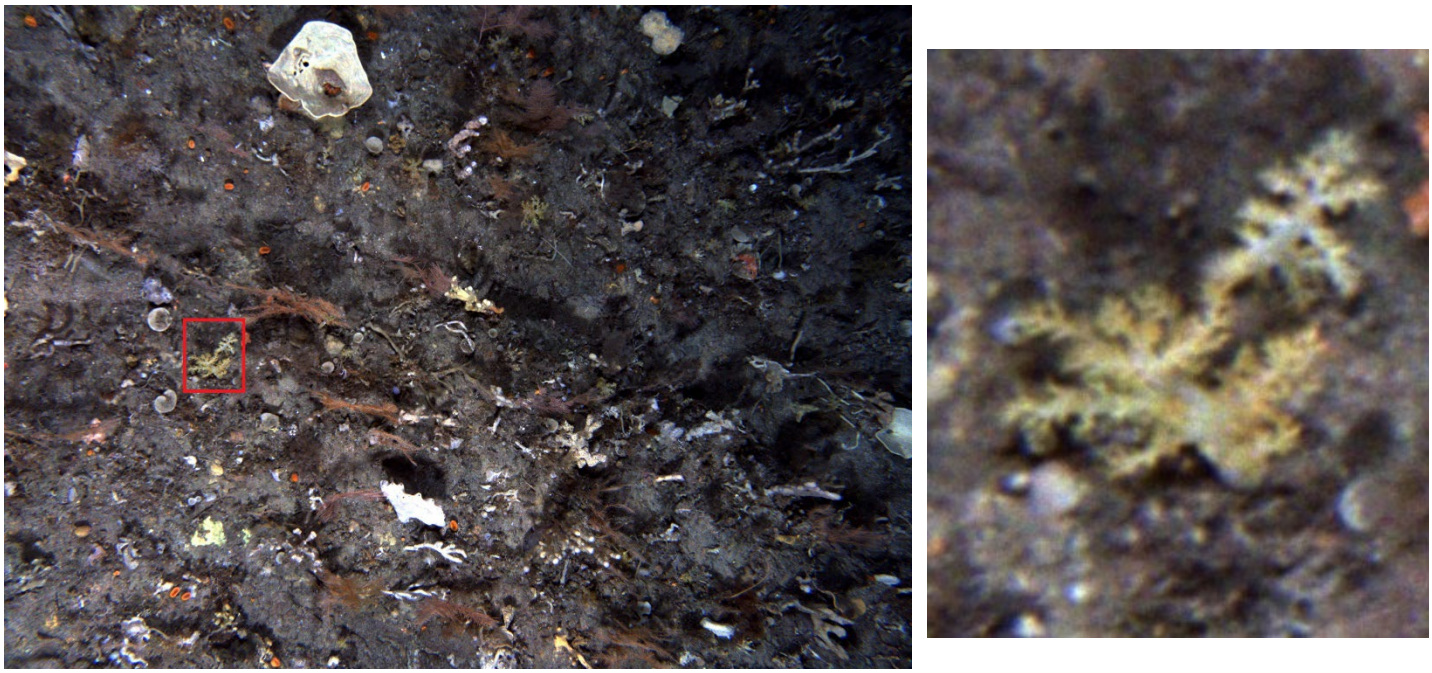

Figure 116. Example image and close up of soft white octocoral taken from the NPZ_01 transect. Red rectangle in full image on the left outlines area of close up on the right.

6.1.12White cup

Figure 117. Example image and close up of white cup sponge taken from the NPZ_01 transect. Red rectangle in full image on the left outlines area of close up on the right.

6.2 Example images of handfish species groupings observed in AUV imagery

Brachiopsilus cf. dianthus (potentially pink handfish)

Thymichthys verrucosus var.(potentially warty handfish variant)

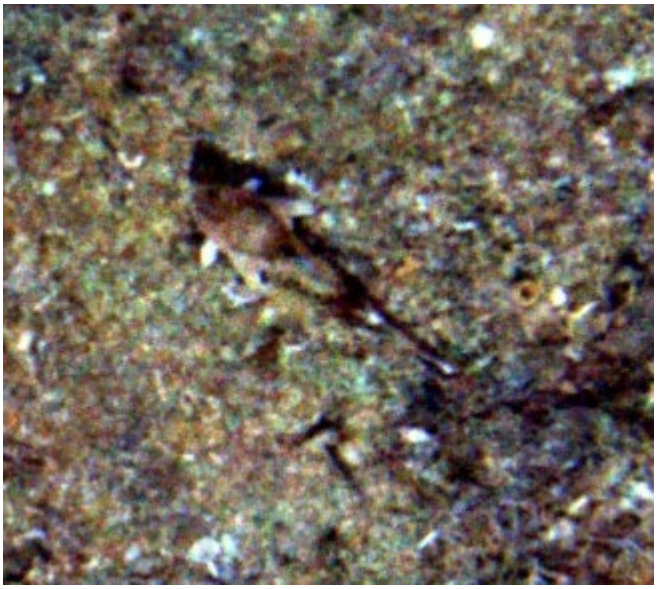

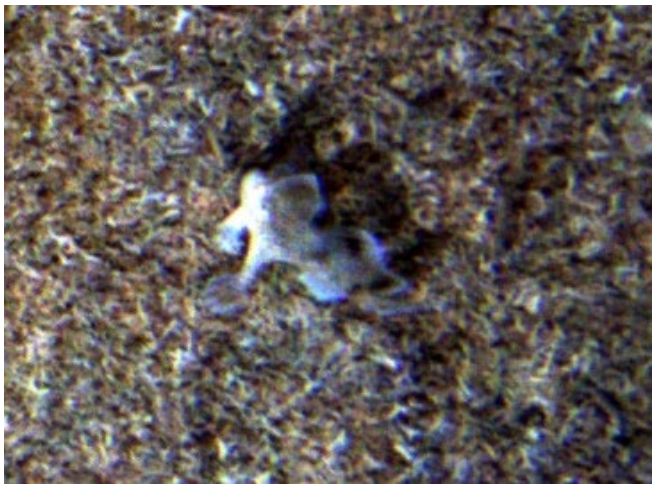

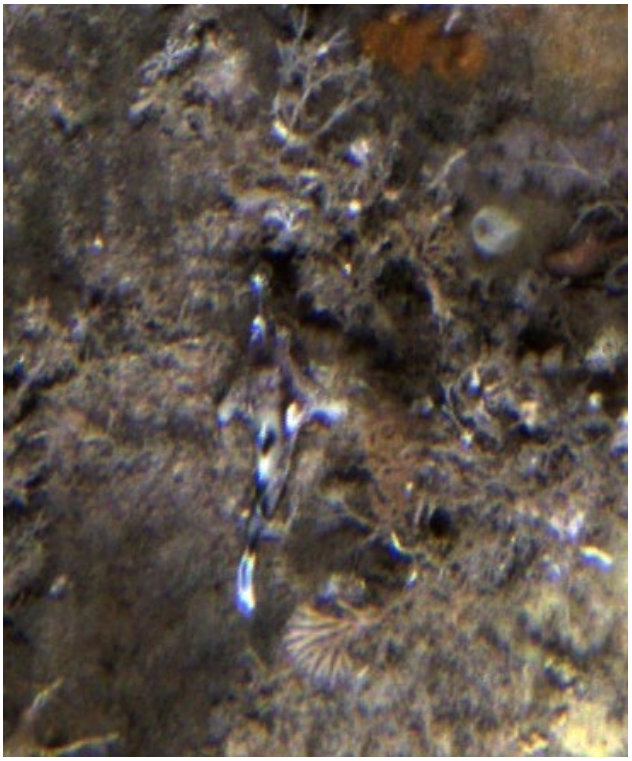

Brachionichthys cf. australis (potentially Australian Handfish)

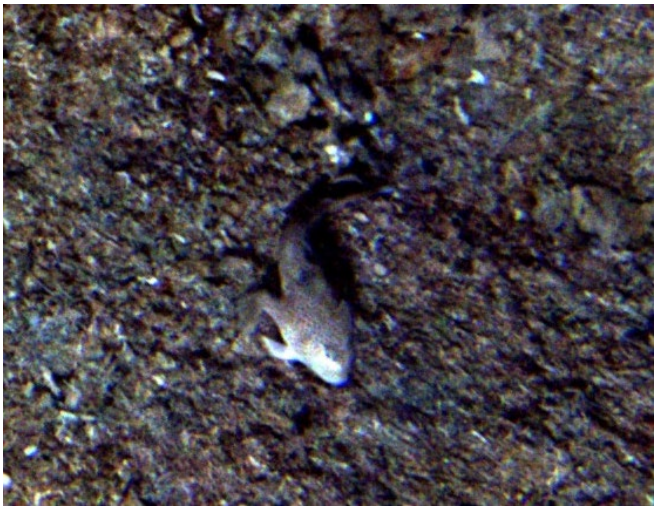

Brachiopsilus cf. ziebelli (potentially Ziebell's handfish)

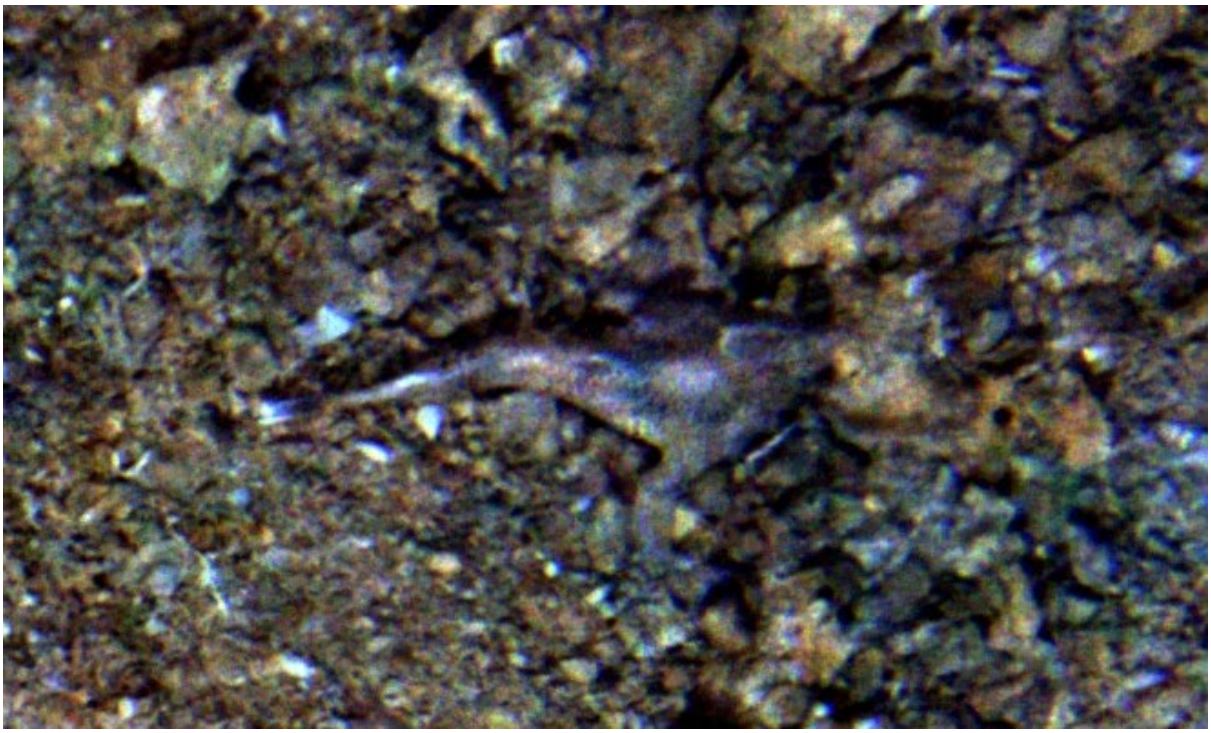

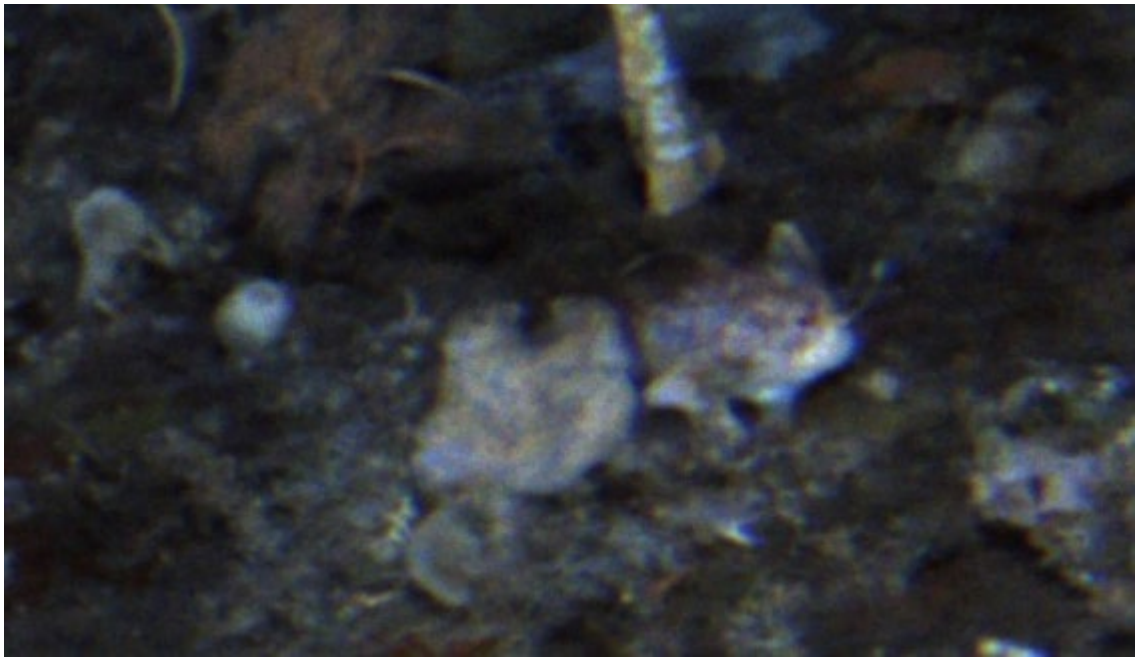

Unknown handfish species

Pale morph

Pink blotchy morph

Yellowish, dark banded morph

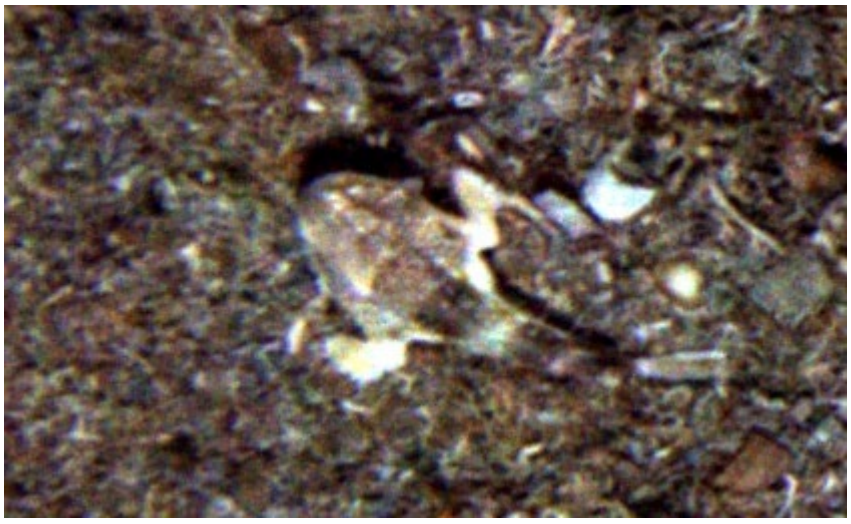

6.3 Detailed maps of handfish distributions across each scored transect

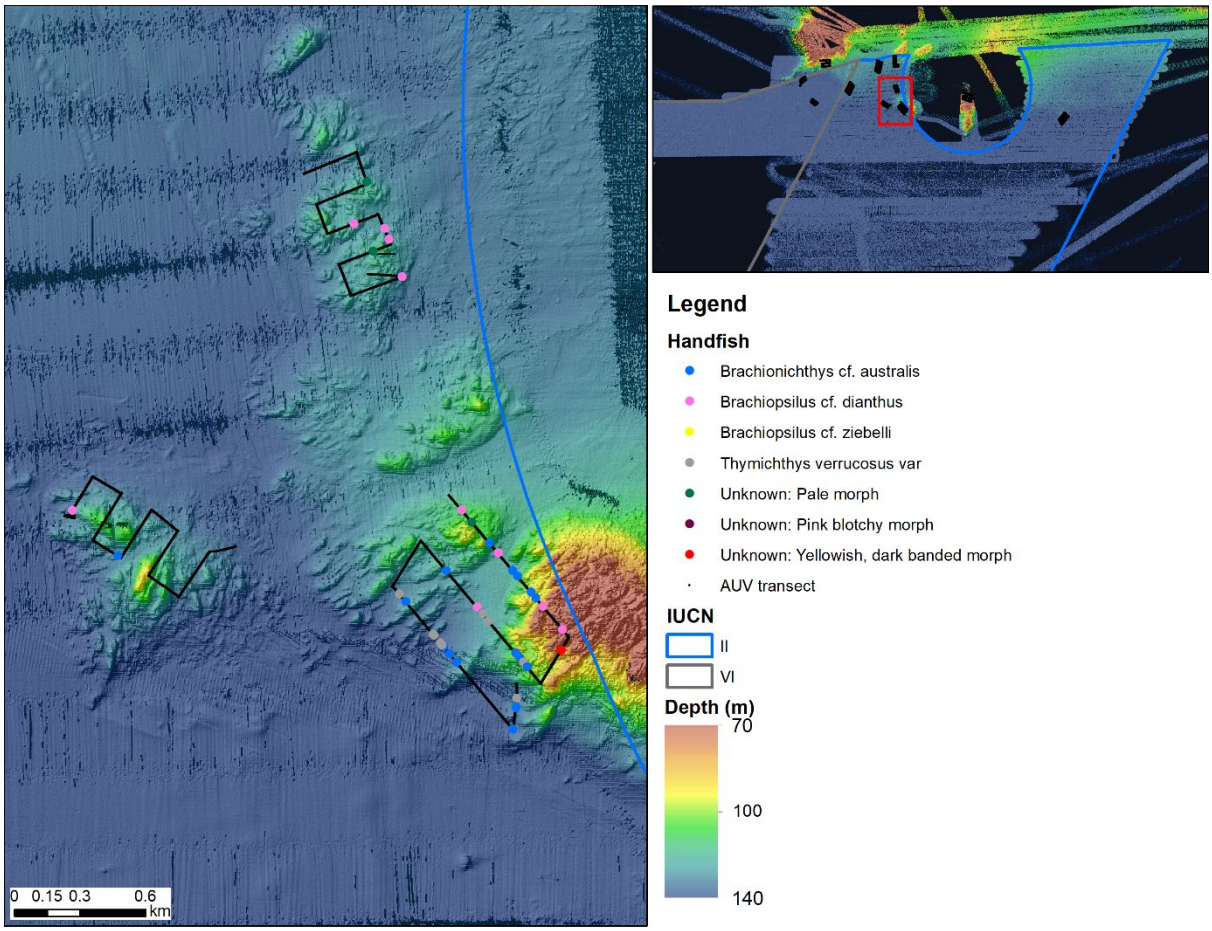

Figure 118. Map showing handfish scored in transects NPZ_01, NPZ_02 and NPZ_03 in the Tasman Fracture Marine Park.

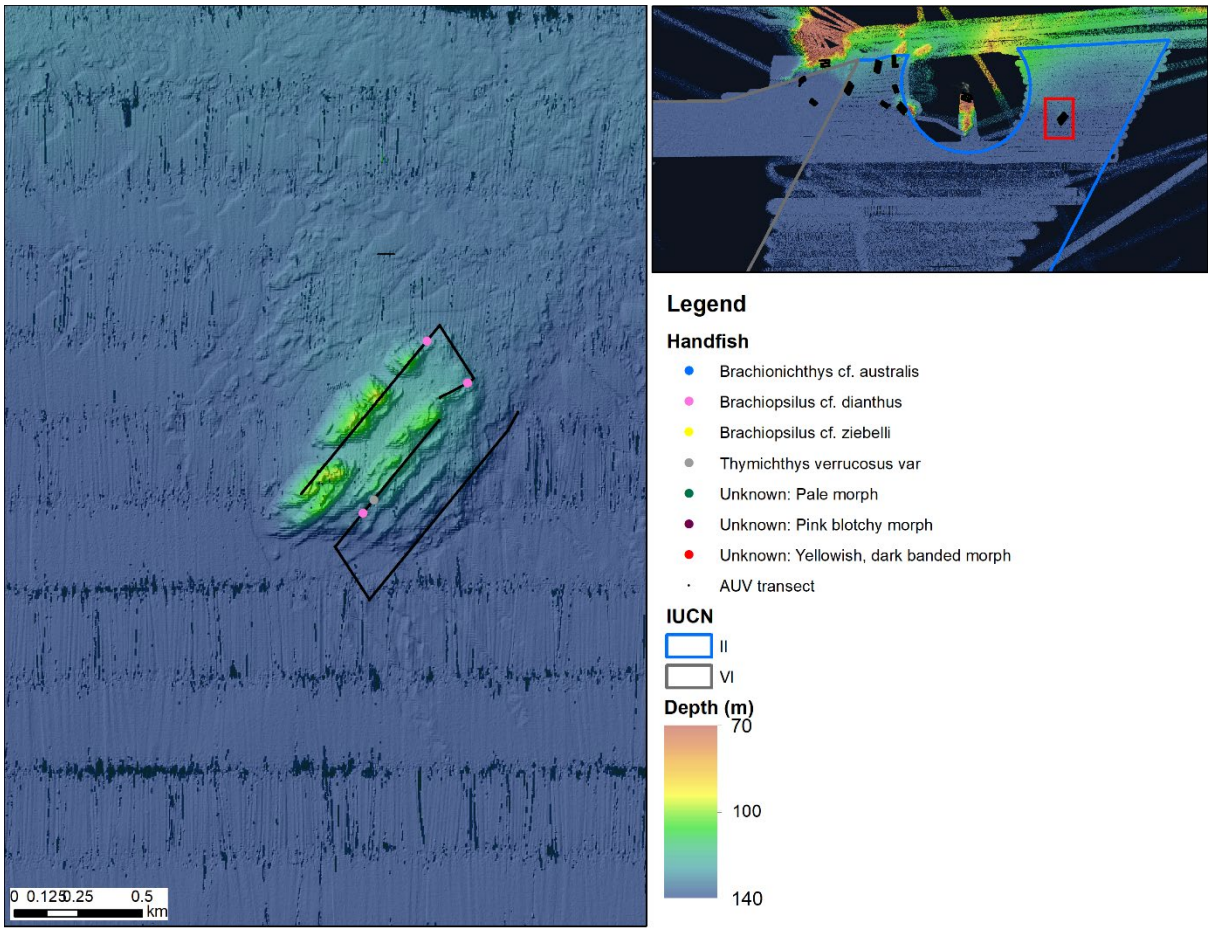

Figure 119. Map showing handfish scored in transect NPZ_04 in the Tasman Fracture Marine Park.

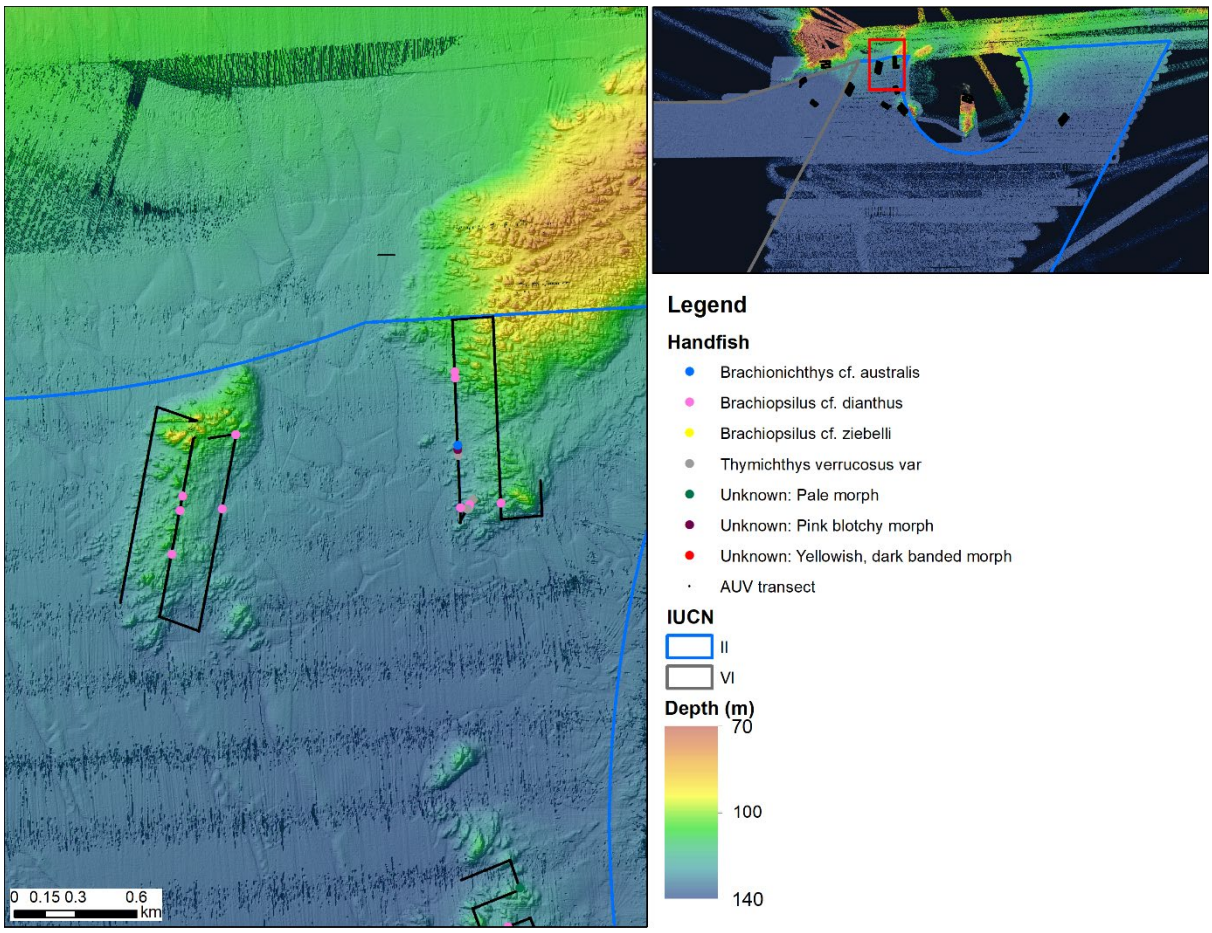

Figure 120. Map showing handfish scored in transects NPZ_06 and NPZ_07 in the Tasman Fracture Marine Park.

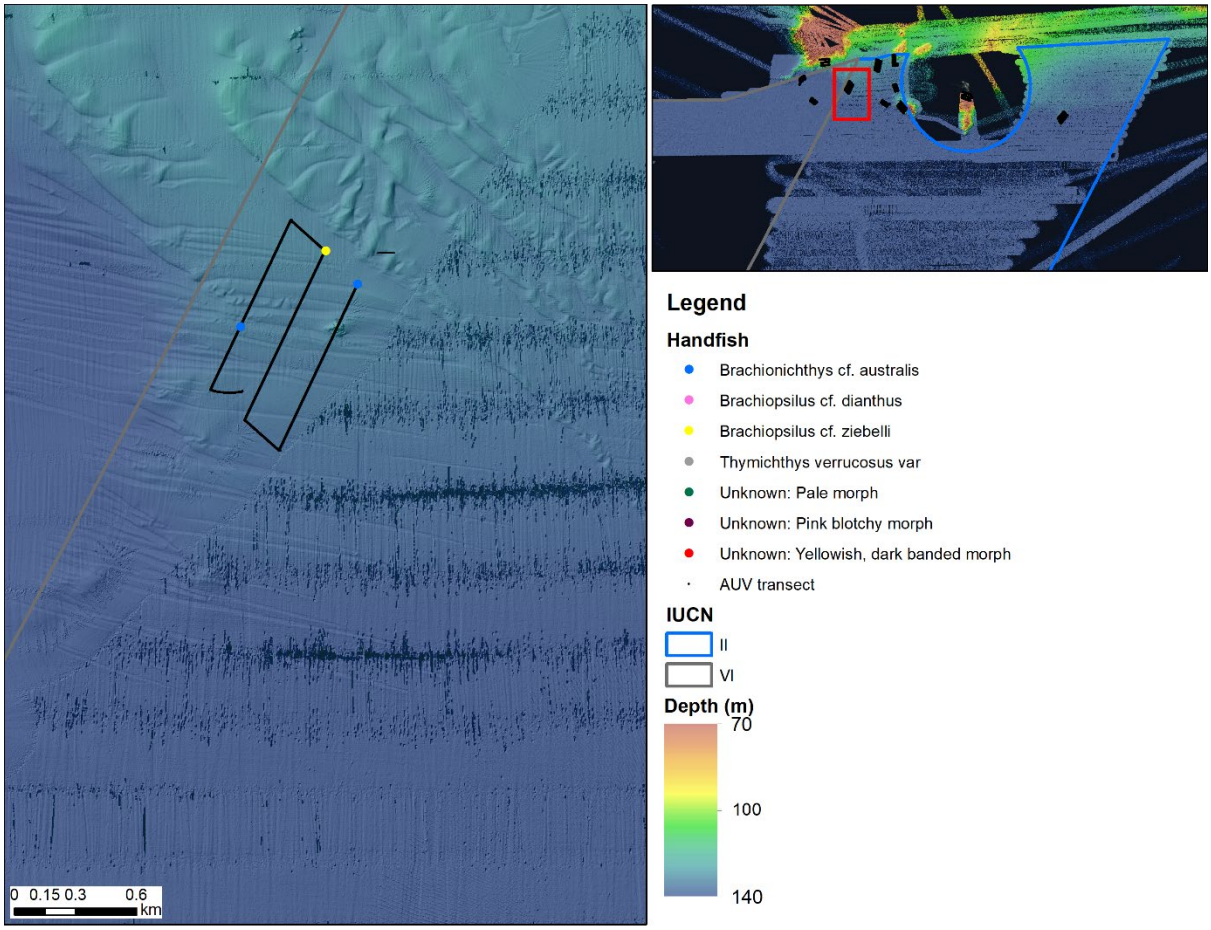

Figure 121. Map showing handfish scored in transect NPZ_08 in the Tasman Fracture Marine Park.

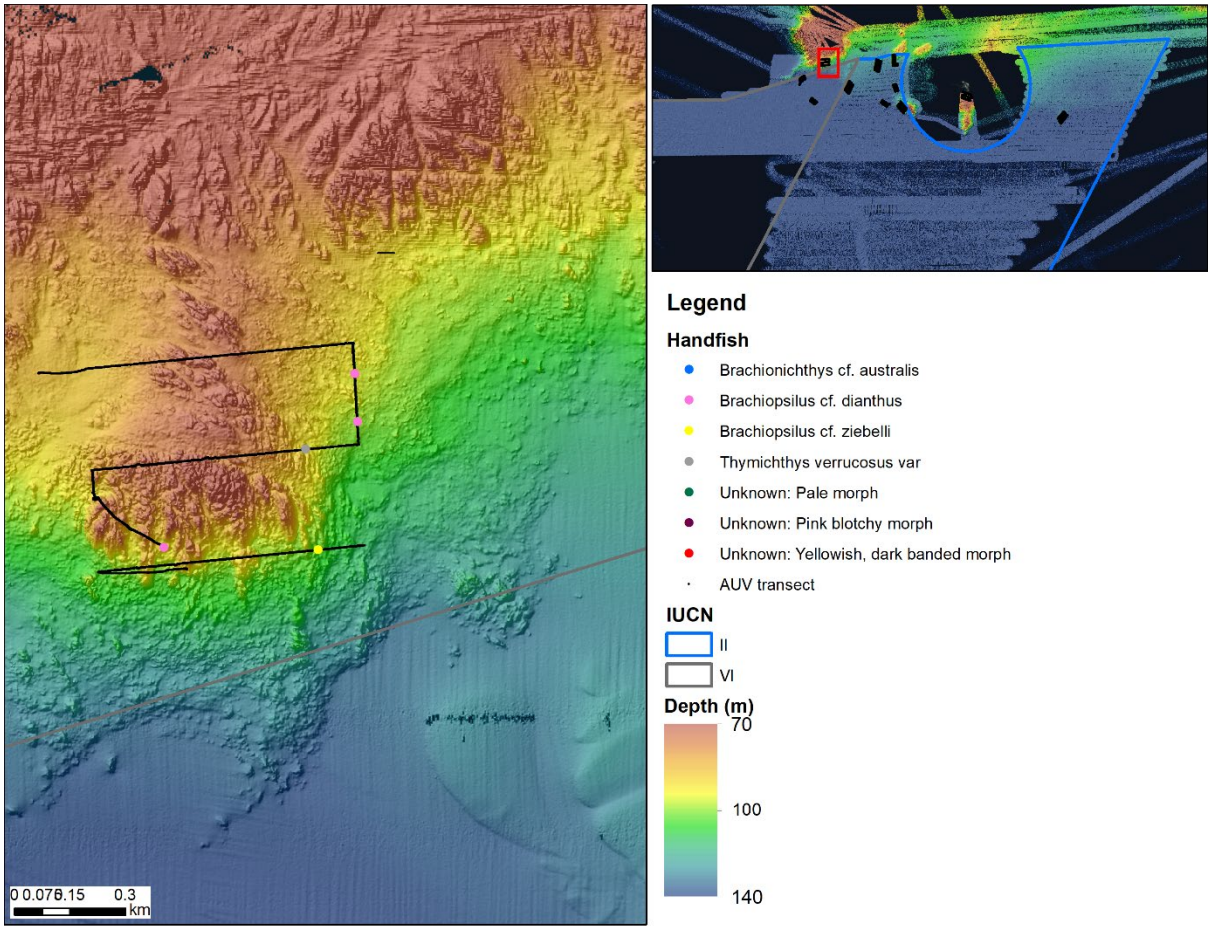

Figure 122. Map showing handfish scored in transect Ref_N1 in the Tasman Fracture Marine Park.